INVESTIGATION BY SOLID-PHASE FLUOROMETRY OF RHODAMINE B ADSORPTION ONTO SOIL SURFACES

BY

KENT P. KOLODZIEJ

Bachelor of Science

Purdue University

West Lafayette, Indiana

1980

Submitted to the Faculty of the
Graduate College of the
Oklahoma State University
in partial fulfillment of
the requirements for
the Degree of
MASTER OF SCIENCE
December, 1994

INVESTIGATION BY SOLID-PHASE FLUOROMETRY

OF RHODAMINE B ADSORPTION

ONTO SOIL SURFACES

Thesis Approved:

William F. McTernan

Thesis Adviser

Dean of Graduate College

PREFACE

The original purpose of this study was to perform experimental work at Amoco Production Company in Tulsa, Oklahoma, on a fluorescently labeled monoclonal immunoassay specific to soil bound polycyclic aromatic hydrocarbons. However, unexpected delays in the production of antibodies by the manufacturer postponed the immunoassay work. As a result, the study's focus shifted from one of soil/immunoassay reactivity research to one of investigating soil parameters that may affect the prospective immunoassay's fluorescent label. Data compiled from this research will be used in the development of a fluoroimmunoassay for field analysis of contaminated soils.

I wish to express my sincere appreciation to Dr. J. B. Fisher for his constant encouragement and guidance throughout the preparation of this thesis. I extend special thanks to Dr. N. P. Kemp and the Amoco Environmental Group who also have provided valuable guidance and consultation. Many thanks are extended to all ancillary support personnel at the Amoco facility who, without question, responded to each and every request. The financial assistance of Amoco Production Company is gratefully acknowledged.

I wish to thank the Oklahoma State University professors who make the masters program within The University Center At Tulsa possible. I extend

special thanks to Dr. W. F. McTernan whose constant help and guidance proved to be invaluable throughout the program. I wish to thank Dr. J. N. Veenstra for his guidance, suggestions, and support.

Finally, I wish to thank all the friends and family members who have encouraged and supported me throughout the entire research process. I extend sincere thanks to Rebecca Brandon for her patience and understanding along the way. I wish to acknowledge the help of my colleagues Karl Kriegh and Galen King who have acted as sounding boards for a broad spectrum of new thoughts and ideas.

TABLE OF CONTENTS

Chapter		Page
I.	INTRODUCTION	1
II.	LITERATURE REVIEW	4
	Introduction	4
	Fluorescence	5
	Theory of Fluorescence	5
	Fluorescent Spectra	7
	Quantum Yield	10
	Fluorescent Intensity and Solution Concentrations	10
	Light Scattering Interferences	11
	Adsorption of Chemicals Onto Soils	13
	Types of Isotherm Models	16
III.	EXPERIMENTAL APPARATUS	22
	Introduction	22
	Equipment	22
	FL-750 Spectrofluorometer	22
	Centrifuge	29
	Eppendorf Pipettes	29
	Ovens	30
	Vials	30
	Tyler Rotap Sieve Shaker	30
	Malvern Laser Optics Particle Sizer	31
	Millipore Water Purification	31
	Ultrasonic Mixer	31
	Scanning Electron Microscope	31
	Miscellaneous Equipment	32
	Computer Equipment and Software	32
IV.	EXPERIMENTAL MATERIALS AND METHODS	33
	Introduction	33
	Adsorbents	35
	Selection	35
	Preparation and Characterization	37
	Adsorbates	40
	Selection	40
	Characterization	40
	Preparation	44
	Isotherm Development Using Fluorometric Methods	45
	Selection and Characterization	45
	Preparation	45

Chapter Page

Equilibrium 47
Liquids Measurement 48
Solids Measurement 49
Blanks and Control Solutions 49
Data Handling 50
Integration of Response Curve Area 50
Isotherm Model Selection 53
Miscellaneous 53
Gas Chromatography (GC) Analysis 53
Surface Area Measurement 55
Mineralogy 55

V. RESULTS AND DISCUSSION 56

Introduction 56
Liquid-Phase Fluorescence 57
Fluorescent Absorption and Emission Spectra 57
Calibration Curves 61
Adsorption Isotherms Using Liquid-Phase Fluorescence 65
Hydrocarbon Isotherms 70
Rhodamine Isotherms 79
Solid-Phase Fluorescence 82
Adsorbent Physical Characteristics 83
Equipment Influences on Soil Fluorescence 91
Grain Size Influences 93
Surface Geometry of Soil Particles 94
Moisture Content 102
Fluorescence Quenching 112

VI. SUMMARY AND CONCLUSIONS 117

BIBLIOGRAPHY 123

APPENDIXES 127

APPENDIX A - EXAMPLE CALCULATIONS 127

APPENDIX B - EXPERIMENTAL DATA 132

APPENDIX C - EXAMPLE FLUORESCENT SCANS 161

APPENDIX D - COMPUTER PROGRAM TO CALCULATE FLUORESCENT RESPONSE AREAS 168

APPENDIX E - SURFACE CONTOURS AND FILTERING EFFECTS ON FL-750 SIGNAL RESPONSE 176

APPENDIX F - EQUIPMENT DETECTION LIMITS OF FLUORESCENT DYES IN AQUEOUS SOLUTIONS 182

APPENDIX G - EQUIPMENT DETECTION LIMITS OF FLUORESCENT MATERIAL IN SOILS 189

APPENDIX H - OPTIMIZATION TECHNIQUES OF THE FL-750 FOR THE DETECTION OF FLUORESCENT MATERIAL IN SOILS 193

APPENDIX I - FL-750 DETECTION LIMITS BASED UPON OPTIMUM EQUIPMENT SETTINGS 203

APPENDIX J - SOLUBILITY OF KODAK DYES 208

APPENDIX K - SDI SOIL DESCRIPTIONS 211

APPENDIX L - ARKANSAS RIVER SAND CHARACTERIZATION 218

APPENDIX M - IMMUNOASSAY DEVELOPMENT 229

LIST OF TABLES

Table Page

1. Materials Used in Study 34

2. Adsorbate Physical Constants 41

3. Stock Solution Concentrations 54

4. Isotherm Model Selection Based on R^2 Values 69

5. FRVC Model Accuracy 76

6. Fluorometric Analysis Vs. GC Analysis of Naphthalene 77

7. B.E.T. Measured Soil Surface Areas 88

8. Soil Mineralogy 89

9. Adsorbent Characterization 90

10. Illuminated Window Geometry 93

11. Grain Size Sensitivity 96

12. Moisture Effects 107

13. Fluorescent Intensity Responding to Changes in Moisture 109

14. Supernatant Fluorescent Responses Used in Variable Mass Experiment 133

15. Isotherm Values - Variable Mass Method (VM) 137

16. Isotherm Values - Variable Concentration Method (VC) 140

17. Summary of Coefficients and Errors for Various Isotherm Models 144

18. Isotherm Derived Values Vs. Observed Data 147

19. Grain Size Influences on Solid Surface Scans in ARS 153

20. Moisture and Organics Influences on Solid Surface Scans in ARS 154

Table Page

21. Calibration Curve Data 155

LIST OF FIGURES

Figure		Page
1.	Jablonski Potential Energy Diagram	6
2.	Quinine Sulfate Absorption Bands at Variable Concentrations	9
3.	Quinine Sulfate Emission Bands at Variable Concentrations	9
4.	Fluorometer Primary Measurement Unit	23
5.	Solid Sample Changer and Holder Assembly	27
6.	Effective Illuminated Area on Solid Sample Holder	29
7.	Experimental Procedure Logic Diagram	35
8.	Rhodamine B Molecular Configuration	43
9.	Naphthalene Molecular Configuration	43
10.	*p*-Xylene Molecular Configuration	44
11.	Rhodamine Fluorescence Response Area With Soil Background Compensation	52
12.	Rhodamine Absorption and Emission Spectra	58
13.	Naphthalene Absorption and Emission Spectra	60
14.	*p*-Xylene Absorption and Emission Spectra	60
15.	Naphthalene Calibration Curve	63
16.	*p*-Xylene Calibration Curve	63
17.	Rhodamine Calibration Curve	64
18.	Equilibrium Results for Arkansas River Sand	67
19.	Equilibrium Results for Shelbyville Sand	67
20.	Naphthalene in Arkansas River Sand Isotherm	71
21.	Naphthalene in Shelbyville Sand Isotherm	71

Figure Page

22. *p*-Xylene in Arkansas River Sand Isotherm 72

23. *p*-Xylene in Shelbyville Sand Isotherm 73

24. Adsorptive Intensity of ARS and SS 74

25. Adsorptive Capacity of ARS and SS 74

26. Rhodamine in Arkansas River Sand Isotherm 81

27. Rhodamine in Shelbyville Sand Isotherm 81

28. Fluorescent Chemical Preferentially Bound to Small Quantities of Fines and Organics Surrounding a Single Sand Grain 83

29. Arkansas River Sand Dry Sieve Analysis 85

30. Arkansas River Sand Wet Sieve Analysis 85

31. Shelbyville Sand Dry Sieve Analysis 86

32. Shelbyville Sand Wet Sieve Analysis 87

33. SEM of Clean Arkansas River Sand 101

34. Moisture Coating and Effective Surface Area 104

35. High Rhodamine Soil Concentrations, Wet & Dry Conditions 106

36. Low Rhodamine Soil Concentrations, Wet & Dry Conditions 106

37. Moisture Effect on Rhodamine's Detectability in Soil 108

38. SEM of ARSPAN Demonstrating Reduced Visible Surface Roughness 111

39. Kevex™ Scan of an Arkansas River Sand Grain 113

40. Dry Soil Fluorescence in No Organic and High Organic Soil ... 114

41. Fluorescence Quenching Effect Resulting from Large Quantities of Soil Organic Matter 115

42. Computer Simulation of Rhodamine on Silica Surface at Lowest Binding Energy 116

NOMENCLATURE

λ Wavelength of Light

Φ Quantum Yield of Fluorescent Chemicals

ν Frequency of a Light Wave

S_1 Singlet State Energy Level

G Ground State Energy Level

ARS Arkansas River sand

SS Shelbyville sand

INVESTIGATION BY SOLID-PHASE FLUOROMETRY OF RHODAMINE B ADSORPTION ONTO SOIL SURFACES

CHAPTER I

INTRODUCTION

The testing of soils which are suspected of hazardous chemical contamination requires time-consuming and costly laboratory procedures. Traditional analytical methods are hampered by cumbersome protocols and procedures; weeks may pass before results are attained (Carter, 1992). In an effort to reduce laboratory analysis time and to accelerate the site evaluation process, research is being focused toward on-site and *in-situ* soil analytical tools. Lieberman *et al.* (1992), for example, have reported success with *in-situ* aromatic hydrocarbon detection using the combined technology of a cone penetrometer and pulsed N_2 laser. The data supplied by these types of new devices provide a quick and efficient means of directing remediation procedures for environmental engineers while on location.

Contaminant specific fluoroimmunoassays (FIAs) applied directly to soils are an example of another such research effort now under development. An

FIA is a special form of immunochemical assay which has proven to be very specific and sensitive by targeting a single chemical for measurement in the soil. Biologically engineered antibodies with fluorescent labels emit photons under ultraviolet stimulation when attached to a soil-bound analyte. The photons are measured by a hand held photometer and subsequently converted to soil concentrations (Stave, 1992).

Fluoroimmunoassays have proven to be a viable field measurement technique for analyzing chemicals with large molecular weights within extraction solutions. The focus of environmental immunoassay research now has turned to the smaller, less complex molecules such as polycyclic aromatic hydrocarbons (PAHs). Because of their size, PAHs once were thought unable to produce immunological responses in laboratory animals. Recent successes with PAHs, however, have produced antibody responses in mice by covalently linking large protein molecules, called Bovine Serum Albumin, with naphthalene (Stave, 1993).

The stage is set to begin the development of a PAH-specific fluoroimmunoassay which can be applied directly to soils. This type of fluoroimmunoassay relies upon the direct measurement of soil contamination without a need for solvent extractions. The success of a direct FIA hinges upon the ability to separate the background interferences from the fluorescent signals of the FIA bound to the target analyte.

The primary objective of the present investigation is to approximate the fluorescent emissions of an FIA in soil through the adsorption of Rhodamine B onto soil surfaces. In essence, this study simulates the fluorescent label attached to the antibody and identifies how soil parameters influence fluorescent signals from surfaces.

Data were obtained on fluorescent emissions from rhodamine-coated soils under variable conditions (e.g., moisture, grain size, and organics). The experimental data and results were analyzed to determine the feasibility of directly measuring fluorescent emissions from soil surfaces. A complete fluoroimmunoassay capable of detecting PAH surface contamination was not available at the time of this study.

It should be pointed out that the data and results presented herein are applicable only to rhodamine and the two selected soils. The extension of this data to fluoroimmunoassays in other soils should be substantiated by further experimental studies.

CHAPTER II

LITERATURE REVIEW

Introduction

Physical adsorption is described as the accumulation of a given chemical at the interface of two phases, whether it be a gas-solid, gas-liquid, liquid-solid, or a liquid-liquid interface. Such processes are considered in great detail within the reported literature. In the present study, only liquid-solid adsorption is considered. A review of the literature revealed that little information is available on direct measurement of fluorescent chemicals adsorbed onto soil surfaces using solid-phase fluorometry.

Solid-phase fluorometry is characterized as a surface phenomenon well suited to measure fluorescence directly from solids if light scattering interferences are eliminated (Wolfbeis, 1993). Elimination of scattered light from soil surfaces is very difficult and may explain the absence of soil fluorescence data in the literature. Only recently Lieberman *et al.* (1993) have published a paper which describes a pulsed laser device capable of measuring fluorescent chemicals directly from soils. A review of fluorescence theory

uncovers properties which are exploited in the present study to enhance the sensitivity of direct soil measurements.

Fluorescence

Guilbault (1973) reports that luminescence is a well established analytical technique first observed in 1565 by Monardes from the extract of Ligirium Nephiticiem. In 1852, Sir G. G. Stokes described the mechanism of absorption and emission. Stokes coined the word "fluorescence" from the mineral fluorspar which emits a light blue fluorescence. In 1935, Jablonski proposed the electronic energy level scheme which has become the basis for the interpretation of luminescence phenomena.

Luminescence spectroscopy is one of analytical chemistry's most sensitive methods available for quantification and identification of chemicals (Harris *et al.*, 1988). Photoluminescence occurs when molecules are excited by interactions with photons of electromagnetic radiation. Fluorescence is described as the re-emission of photons which are less energetic than the absorbed photons (Guilbault, 1973).

Theory of Fluorescence

The following review provided by Guilbault (1973) concerning the theory of fluorescence is presented in a condensed format based upon information relevant to this study.

The Jablonski diagram in Figure 1 illustrates how the absorption of energy can be transferred into vibrational and potential energy then re-released as fluorescence or phosphorescence. Every molecule possesses a series of closely-spaced energy levels and transfers from a lower to a higher energy level by the absorption of a discrete quantum of light equal in energy to the difference between the two energy states.

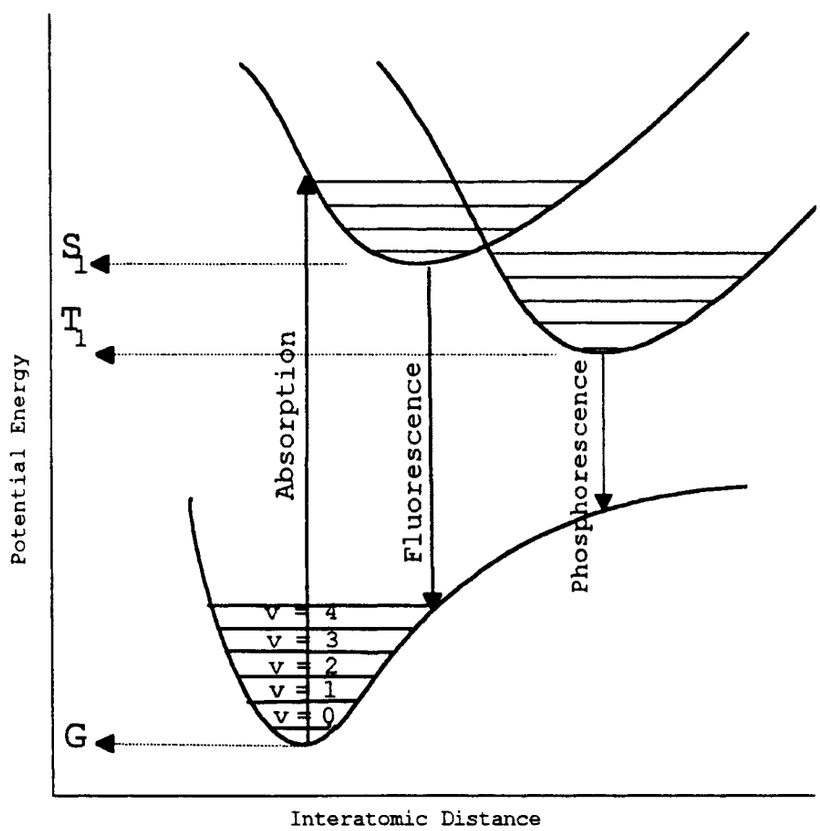

Figure 1. Jablonski Potential Energy Diagram
(recreated from Undefriend, 1962)

Guilbault (1973) reports that when a quanta of light strikes a molecule, absorption occurs in 10^{-15} sec which causes a transition in the molecule to a higher energy state. An electron then rises to an upper excited singlet state (S_1) from the ground state (G). Ground-to-Singlet transitions are responsible for the visible and ultraviolet absorption spectra. During the time the molecule spends in the excited state (10^{-4} sec) some energy in excess of the lowest vibrational energy level is rapidly lost. Once the lowest vibrational level (v=0) of the excited singlet state (S_1) is reached, the electron must return to the ground state. In returning to the ground state, the electron releases energy in the form of a photon. This phenomenon is referred to as fluorescence. Because some energy is lost in a brief instant before emission occurs, the emission photon is less energetic and therefore has a longer wavelength than the absorbed photon.

Fluorescent Spectra

Every fluorescent molecule has two distinct spectra: the absorption spectrum and the emission spectrum. The absorption spectrum represents the relative efficiency of various excitation wavelengths in causing fluorescence. The emission spectrum represents the relative intensity of radiation emitted at different wavelengths.

The fluorescence normally observed in solutions, termed Stokes fluorescence, is characterized by the re-emission of less energetic photons than

the absorbed photons (Guilbault, 1973). The difference between these two wavelengths is termed the Stokes loss. The Stokes loss is an indication of the energy dissipated during the lifetime of the excited state before returning to the ground state. Larger Stokes losses are of particular interest in this study because they can be used to reduce direct light scatter. A smaller Stokes loss results in the absorption spectrum overlapping and interfering with the emission spectrum.

A very useful phenomenon of fluorescent absorption and emission spectra is exploited in this investigation. Excitation in any portion of the absorption spectrum produces a fluorescent emission peak at a constant wavelength. Therefore, the fluorescent peaks generally occur at the same wavelength regardless of the excitation wavelength as long as the excitation remains in the absorption band (Guilbault, 1988). The intensity of the fluorescence, however, vary with the relative strength of the absorption intensity, i.e., concentration.

Figures 2 and 3 (generated by the author) demonstrate the phenomenon of a fluorescent emission peak occurring at the same wavelength regardless of the excitation wavelength. Quinine sulfate at various concentrations are used to illustrate this point. Wherever the excitation wavelength is placed along the adsorption curve (Figure 2) the emission peaks (Figure 3) always occurr at the same wavelength. Guilbault reminds us this is because fluorescent emissions always take place from the lowest excited singlet state (S_1). However, the

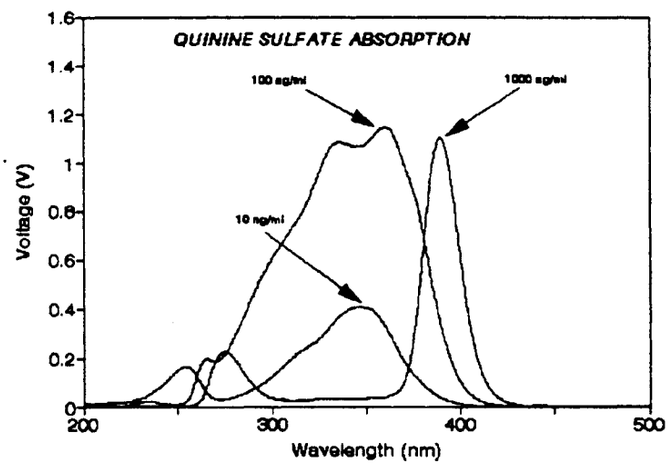

Figure 2. Quinine Sulfate Absorption Bands at Variable Concentrations

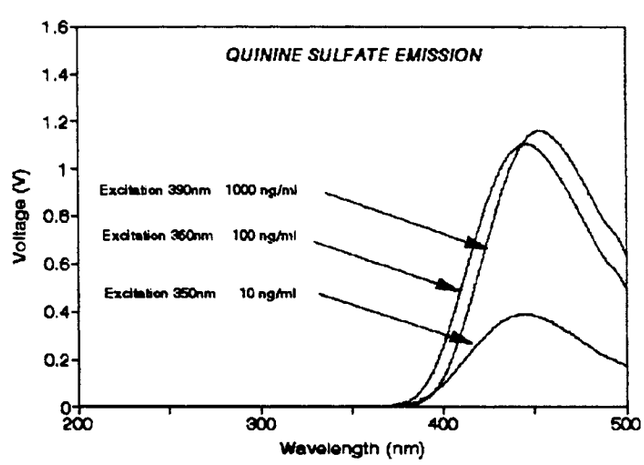

Figure 3. Quinine Sulfate Emission Bands at Variable Concentrations

intensity of the emission peak changes with changing solution concentrations. It is therefore possible to identify a fluorescent compound by exciting (anywhere along its absorption band) and measuring the emission at its characteristic peak.

Quantum Yield

Fluorescent responses from changing solution concentrations are sometimes difficult to predict. Every molecule has a characteristic property that is described by a number called the quantum yield. Quantum yield (Φ) represents the ratio of the total energy emitted per quantum of energy absorbed. Quantum yield is analogous to variable wattages between light bulbs. Guilbault defines quantum yield as the ratio of photons emitted to those absorbed. Increasing values of the quantum yield represent increasing fluorescence potential of a compound. Nonfluorescent molecules are those whose quantum yield is zero. Energy absorbed by nonfluorescent molecules is lost by collisional deactivation.

Fluorescent Intensity and Solution Concentrations

Fluorescent intensity responses are dependent upon several factors, one of which is the quantum yield. Another influential factor is the solution concentration. The general form of the relationship between fluorescence

intensity and solution concentration is represented by the equation (Harris *et al.*, 1988):

$$F = \Phi I_o(1 - e^{-\epsilon bc}) \quad (1)$$

For very dilute solutions, the observed fluorescence intensity is directly proportional to concentration:

$$F = 2.3\ (I_o\ \epsilon bc)(\Phi) \quad (2)$$

where I_o is incident light intensity, ϵ is the molar absorptivity, b is the cuvette cell thickness, c is the concentration and Φ is the quantum yield. Equation 1 is more likely to apply to the fluorescent responses in this study because of the broad range of concentrations utilized for the isotherm experiments.

Light Scattering Interferences

Several interferences are capable of affecting the intensity of fluorescent responses which are independent of solution concentrations and therefore must be accounted for in the measurement process. Scattered light refers to light emerging from the sample which is of the same or longer wavelengths as that of the excitation wavelength but not part of fluorescence. In solutions, scattering of light can be composed of Rayleigh scattering from solvents, Raman scatter from Rayleigh satellites, Tyndall scattering from the colloidal

particles, and light scattering from the surface of the cuvette (Harris, 1988; and Undefriend, 1962). When fluorescence emissions and excitation wavelengths are close together, the distortion to the signal due to light scattering severely limits instrumental sensitivity. At sensitive equipment settings, efforts must be made to eliminate the effects of scattering. Light cutoff filters maximize the signal while minimizing scattered light (Harris, 1988).

Similar scattering can be expected in solid-phase fluorometry. The strongest scattering is due to direct reflectance of the excitation wavelength from the soil's surface. This type of light scattering resembles Tyndall and Rayleigh scattering that must be carefully filtered.

Rayleigh Scatter. The reemission of a photon from matter at the same energy level it was absorbed (within 10^{-15} sec) is called Rayleigh scatter. The intensity of the scattered light is lessened at longer wavelengths. Rayleigh scatter interferes with the sample response when Stokes losses are low and fluorescence intensity are also low in comparison to the excitation radiation (Guilbault, 1973).

Raman Scatter. Related to Rayleigh scatter, Raman scatter appears in fluorescence scatter at both higher and lower wavelengths relative to the excitation wavelength. Raman scatter at higher wavelengths is of the most concern by potentially affecting the fluorescent emission spectra of a sample.

Raman scatter peaks are satellites of Rayleigh peaks and occur at constant frequency differences from the excitation wavelength (~50 nm). Raman peaks are weaker than Rayleigh peaks but become significant at high equipment sensitivity settings. Raman peaks are due to vibrational energy being added to the excitation photon (Guilbault, 1973).

Tyndall Scatter. The Tyndall effect is caused by colloids in suspension (Osipow, 1962). When a beam of light passes through an emulsion, light is scattered in a sideways direction at the boundary of the dispersed particles. If the beam of light is monochromatic, the scattered light is also monochromatic and of the same wavelength.

Adsorption of Chemicals onto Soils

Adsorption is defined as the accumulation of a chemical (adsorbate) from solution onto the surface of soil particles (adsorbent). Freundlich and Langmuir isotherm equations (see nonlinear isotherms this chapter) can be used as empirical models to predict the overall adsorption process (Fetter, 1988).

Weber (1992) cautions that the sorption capacity for solutes varies widely among different soils with ostensibly similar properties. He goes on to report that adsorption of chemicals onto soils is dependent upon mineralogy, particle size, surface area, soil moisture and pH. The magnitude of adsorption reportedly is proportional to the adsorbing chemical's activity. Karickhoff

(1979) reports that clays tend to be strong adsorbers, since they have both a high surface area per unit volume and a significant electrical charge at the mineral surfaces. Most clay minerals have an excess of imbalanced negative charges in their crystal lattice system. Therefore, adsorptive processes in soils favor the adsorption of cations from solution.

Completely mixed batch reactors (CMBR), miscible displacement (MD), and gas purge (GP) are three different experimental procedures which can be used to derive empirical constants from the isotherm models. CMBRs are batch reactors (usually vials) representing a closed system where soil and solution concentrations are determined after a period of mechanical mixing (Karickhoff, 1979; Briggs, 1981). MD experiments measure effluent concentrations of displaced fluids in column studies (Abdul, 1987; Brusseau, 1990). In a similar purging manner, GP experiments measure headspace gas concentrations (Brusseau, 1990). Each of these experimental techniques have practical limitations. These limitations have a direct effect on the empirical constants they derive and, in turn, add variability to the predictive results obtained by the mathematical models they create.

Brusseau *et al.* (1990) compares two experimental methods and reports that results from MD experiments breakdown for highly adsorptive soils and the viability of the GP technique is strongly dependent upon chemicals with Henry's constants of sufficient magnitude for detection. Karickhoff *et al.* (1979) in a series of batch experiments reports that the applicability of

normalizing partitioning coefficients to soil organic matter is unreliable for soils containing less than 0.1% organic matter. Chin *et al.* (1988) and Lick (1991) suggest that the "solid effect" may be responsible for such a breakdown in the correlation between the organic carbon coefficient (K_{oc}) and the partitioning coefficient (K) for soils low in organics. The solids effect is defined as an apparent decrease in the partition coefficient with increasing solids to water ratios. McKinley *et al.* (1991) observes that, as a result of ineffectively accounting for the solids effect, incorrect data reduction in many experiments have yielded faulty results. Rutherford *et al.* (1992) also reports greater variability in the organic matter coefficient (K_{om}) for soils with low organic content and comments on the need for further study of factors affecting adsorption other than soil organic matter.

The combination of these experimental uncertainties result in variability among published sorptive parameters for like soils. The absence of a good explanation for the wide variation in partitioning values is not caused by lack of research on the subject but can be traced to the model construction and verification process itself. The best technology over the past decade includes a host of very sensitive measurement devices which demand sophisticated laboratory techniques. The one common denominator for almost all of these techniques is that an extraction step is required to bring the target analyte off soil surfaces and into dilute solutions before a measurement can be taken. Extractions are subject to removal efficiency losses, but generally 95%

is the opposite process, described as the rate at which the organic chemical transfers from the adsorbed state into water. At true equilibrium these rates should be equal, but the organic chemical concentrations in the water and in the soil are different from the initial conditions. A common linear expression is used to describe the distribution of an organic chemical between soil surfaces and water. The distribution coefficient (K_d) is used to express chemical partitioning between soil and water concentrations:

$$K_d = C_s/C_w \tag{3}$$

where C_s is concentration absorbed on soil surface (mg/kg soil) and C_w is concentration in water (mg/l water).

K_d can be normalized on the basis of soil's organic matter or organic carbon content. These normalized soil adsorption coefficients, K_{om} and K_{oc}, are expressed as:

$$K_{om} = K_d/om \quad \text{and} \quad K_{oc} = K_d/oc \tag{4}$$

where K_{om} is the soil adsorption coefficient normalized for soil organic matter content, K_{oc} is the soil adsorption coefficient normalized for soil organic carbon content, om is soil organic matter content (mg organic matter/mg soil), and oc is soil organic carbon content (mg organic carbon/mg soil).

Values of K_{oc} and K_{om} have been measured for a large number of organic chemicals. A direct relationship, developed by Dragun (1988), between K_{oc} and K_{om} based upon a wide range of chemicals is expressed as:

$$K_{oc} = 1.724\ K_{om} \tag{5}$$

The parameters required to predict sorption behavior reduces to a few readily obtainable numbers if a linear model is employed. Numerous empirical relationships have been derived relating a characteristic of the soil to a characteristic of the solute. Dragun (1988) compiled a list of several predictive linear equations based upon the solubilities and soil organic make-up. The solubility of a solute, S, is related to the organic carbon partitioning coefficient , K_{oc}, through the expression:

$$\text{Log } K_{oc} = -0.55 \log S + 3.64 \tag{6}$$

where S is the solute concentration measured in mg/l.

The octanol water partitioning coefficient, K_{ow}, is related to the organic carbon partitioning coefficient, $K_{oc,}$, through the expression:

$$\text{Log } K_{oc} = 0.544 \log K_{ow} + 1.377 \tag{7}$$

The octanol water partitioning coefficient, K_{ow}, is related to the organic matter partitioning coefficient, K_{om}, through the expression :

$$\text{Log } K_{om} = 0.52 \log K_{ow} + 0.64 \qquad (8)$$

Many of these empirically derived expressions generally describe the summation of results for many chemicals (including naphthalene and p-xylene) over concentrations representing one or two orders of magnitude. Karickhoff *et al.* (1979) reports that the high degree of variability in soil compositional factors contributes to a wide range of empirically derived vales for seemingly like soils.

Nonlinear Isotherms

Evidence suggests that subsurface soils tend to exhibit nonlinear adsorption behavior (Weber *et al.*, 1992). Nonlinearity should be expected for surface adsorption when solution concentrations span large concentration ranges. Freundlich and Langmuir are two of the most popular nonlinear predictive sorptive models. Weber *et al.* (1992) suggests that Freundlich isotherms result from the overlapping several Langmuir sorptive processes. This implies that several nonlinear (as well as linear) adsorption reactions are present in heterogeneous soils causing deviations from a linear isotherm model.

Freundlich Isotherm. A Freundlich isotherm can be applied to chemisorption adsorption processes (Veenstra, 1992). If soil/chemical equilibrium data, when plotted on log-log paper, form a straight line, the results can be represented by the equation:

$$\log q = b \log C_r + \log K \tag{9}$$

where b is the slope and an indication of adsorption intensity, K is a distribution coefficient and the Y intercept, q is the mass of sorbate per mass of sorbent (mg/g), and C_r is the equilibrium concentration of solute in contact with the soil (mg/l). K and b are coefficients that are a function of the solute, soil type, and equilibrium conditions in the solute/soil system. If the value of b equals 1.0, the isotherm is linear and the data plots on a straight line.

Langmuir Isotherm. The Langmuir isotherm can be applied to monolayering sorptive processes (Veenstra, 1992). The Langmuir isotherm has two forms which describe either high or low solute adsorption onto soil. The low Langmuir adsorption isotherm is developed by plotting C_r/q versus C_r on arithmetic paper. If the data points fall in a straight line, a Langmuir isotherm can be expressed for low solute concentrations as:

$$\frac{C_r}{q} = \frac{1}{\beta_1\beta_2} + \frac{C_r}{\beta_2} \tag{10}$$

where C_r is the equilibrium concentration of the solute in contact with the soil (mg/l), q is the amount of chemical adsorbed per unit weight of soil (mg/g), β_1 is an adsorption constant related to the binding energy (slope/intercept), and β_2 is the adsorption maximum or reciprocal of the slope (Fetter, 1988).

It is possible for this model to yield two straight lines indicating high and low concentration forms. The same parameters for the low Langmuir are used in the development of the high Langmuir for high concentration solutions:

$$\frac{1}{q} = \frac{1}{\beta_2} + \frac{1}{\beta_1 \beta_2 C_r} \tag{11}$$

CHAPTER III

EXPERIMENTAL APPARATUS

Introduction

A McPherson Instrument FL-750 HPLC spectrofluorometer was modified to measure both aqueous and solid phase fluorescence. A great deal of care was taken to determine the optimum equipment settings necessary to detect solid phase fluorescence at ambient conditions (Appendixes E-I). Special adaptations provided by the manufacturer permitted solid phase fluorescence investigations. Further adaptations and refinements were necessary to enhance the signal output. The development of these adaptations was critical to this study and is discussed in detail.

Equipment

FL-750 Spectrofluorometer

The McPherson Instrument FL-750 Spectrofluorescence Detector consisted of a focused 150W xenon arc ultraviolet (and visible) light source , double monochromator optical unit, photomultiplier tube (PMT), power

supply, analog to digital converter, and data file capture system. An assortment of filters, slits and sample holders also were available.

The xenon light source was located in the upper left corner of the FL-750 fluorescence detection unit (Figure 4). Light from the source passed through an adjustable bandwidth slit (0, 2, 4, 8, and 16 nm), struck a mirror and reflected onto the excitation grating. The reflected light then passed through another interchangeable slit held by the cuvette changer. This lights focal point was centered in the cuvette which was held in place by the cuvette changer. The apparatus had a focal length of 200 cm converging at the center of the cuvette in the changer.

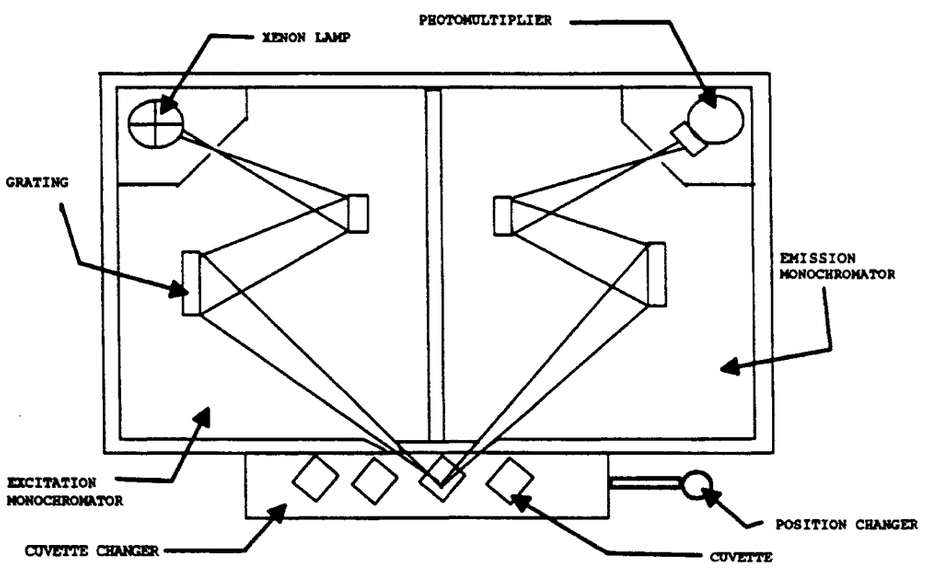

Figure 4. Fluorometer Primary Measurement Unit

The emission light left the center of the cuvette 90° to the excitation beam, passed through the interchangeable exit slit, struck the emission monochromator, reflected off a focusing mirror, passed through the final adjustable slit, and finally struck the PMT.

Principles of Operation

Radiation from the xenon lamp source was dispersed by the grating on the excitation monochromator into monochromatic radiation. The definition of radiation (in this sense) encompassed both UV and visible light photons. Fluorescent emissions from the sample were dispersed by a similar monochromator into monochromatic radiation which was detected by the PMT. The emission photons created a cascading effect within the PMT which transformed into a weak electrical signal. The signal from the PMT was amplified by a photometer. The photometer output was viewed on an external meter. The voltage, once amplified, then was passed to the analog-to-digital converter, and the digitized signal with its corresponding wavelength was stored in an ASCII data file for future recall.

The scanning wavelengths of this instruments ranged from 100 to 800 nanometers (nm) and the resulting signal voltage outputs ranged from 0 to 1 volt in normal setup mode. The instrument, however, was modified to operate within a linear dynamic range from 0 to 4 volts. In this modified voltage output configuration, the instrument was capable of accurately

measuring emittances over a broader range of intensities. The requirement for sensitivity changes or gain adjustments between measurements therefore was eliminated. This modification allowed consistency in output among greater solution concentration ranges.

The instrument contained two independent scanning monochromators. It was possible to hold either constant while the other scanned for the sample's response. The instrument therefore was capable of independently scanning both the emission and the absorbence spectra. Both of these options were used to gather the absorbence and emission spectra.

An assortment of interchangeable slit widths were provided by the manufacturer for use in the cuvette changer. It was possible to change slits in the cuvette changer for both the entrance and the exit of the monochromatic light passing through the sample. The proper selection of slit sizes was based upon the objectives of the experiment. Wider slit openings provided enhanced sensitivities while smaller slit openings increased resolution but decreased sensitivity. Available slit widths allowed 2, 4, 8, or 16 nm bandwidth (.5, 1, 2, or 4 mm) of light to be transmitted through the sample port.

Xenon Lamp

The xenon lamp was superior to a xenon-mercury lamp for the purposes of this investigation. The xenon lamp's capacity to maintain relatively even intensities over a broad spectrum of excitation wavelengths was advantageous.

A xenon-mercury lamp could deliver much more intense spikes of light but over a limited number of band widths. These band widths included 370 nm, 405 nm, and 440 nm, but did not necessarily correspond to optimum excitation wavelengths in the present study.

It was anticipated that several fluorescent chemicals would be reviewed to model fluorescence in soils. The lamp type for the FL-750 was selected to eliminate light source intensity as a variable. The location of the intense peaks generated by the xenon-mercury lamp were eliminated as a major variable by the selection of the xenon lamp as the light source.

Sample Changers

Cuvette Changer for Liquids. Fused silica cuvettes (1X1 cm) were used in all solution investigations. These silica cuvettes held approximately 5 ml of liquid. The cuvette changer illustrated by Figure 4 consisted of four cuvette holders, each with interchangeable slits. A removable cover plate was provided to replace cuvettes once scanned. An external handle was available to slide new cuvettes into position without removing the cover plate.

Solids Changer for Soils. A specially manufactured (McPherson Instruments) solid sample changer was designed to hold soils for surface investigations (Figure 5). The solid sample changer was adapted to be attached to the FL-750 by the same fittings as the cuvette changer. A solid sample holder was designed (by author) to accommodate soils with variable

properties. The soil holder had an adjustable soil surface height and was able to hold an antireflective quartz window to retain loose soils. The solid sample changer was designed to achieve the optimum focal length on the sample holder's surface by adjusting a screw to raise or lower the surface relative to the xenon source. Minor adjustments to the solid's surface location with respect to the focal length then could be made by the operator. In this manner, the fluorescent properties of the spiking compound could be optimized by reducing background reflectance of the soil itself, thereby increasing fluorescent intensity available to the PMT.

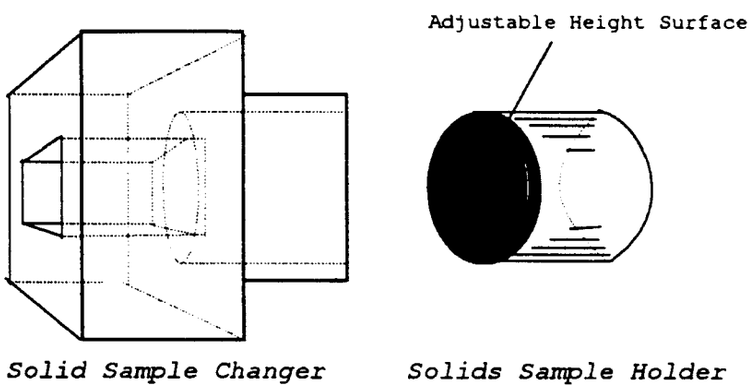

Figure 5. Solids Sample Changer and Holder Assembly

Optimizing the sample holder's properties included minor changes to the fluorometer's focal length. Placing the sample 1 or 2 mm closer to the light

source (relative to the focal point) decreased surface scattering and increased fluorescent detectability. Once the optimum setting for the soil holder was determined, all future experiments on soil surfaces were run at this setting.

Sample Holder Surface. In contrast with solutions where fluorescence originated from the center of a cuvette, solid phase fluorescence came from soil surfaces. An adjustment of the excitation beam's focal length was necessary to force termination on the solid surface instead of at the cuvette's center (see focal length optimization procedure in Appendix H).

Dimensions of the slit windows (which allow excitation radiation in and emission radiation out) were fixed which provided a rectangular area of light on the surface of the sample holder that measured 0.48 cm x 1.11 cm. The impact of this rectangle on fluorescent readings was important. The "window," illustrated in Figure 6, was depicted as the bright rectangle on the soil holder. It exposed a small portion of the solids sample holder to the excitation radiation. This illuminated rectangular area on the sample holder was the area on which excitation radiation struck the soil sample and the resultant emission radiation emanated. The remaining area on the sample holder's surface did not contribute to the signal intensity.

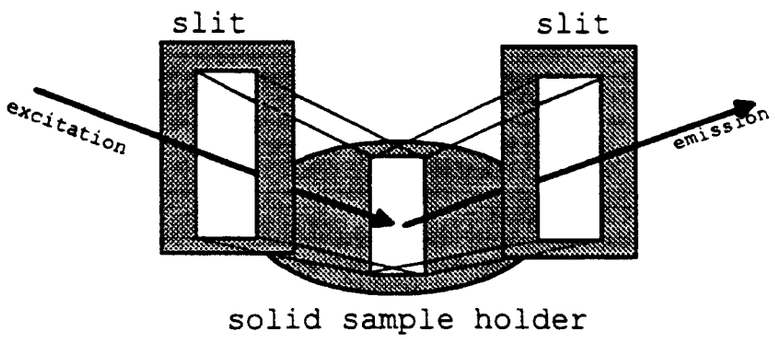

Figure 6. Effective Illuminated Area on Solid Sample Holder

Centrifuge

A Baxter Scientific Products Omnifuge model RT centrifuge was utilized to settle colloids out of solution before fluorometric measurements. The centrifuge also was used to extract spiking fluids from soil pore space as a means to simulate field capacity soil moisture conditions.

Eppendorf Pipettes

A 1000 μL Eppendorf positive displacement pipette with disposable tips was used to transfer liquids into the cuvettes. Pipette tips were discarded after each transfer to eliminate cross contamination of spiking fluids between transfers.

Ovens

A General Signal Blue M constant temperature cabinet oven was used in drying soils at 105°C to drive off moisture without affecting the organics in the soil. A General Signal Blue M box-type muffle furnace was used to burn off organics in the soil at a temperature of 550°C .

Vials

Borosilicate vials (25 ml) were used as completely mixed batch reactors (CMBRs) for test samples, controls and blanks. Each vial was sealed with a Teflon-lined screw cap. I-Chem open-port (40 ml) vials with Teflon lined screw tops were used as CMBRs for the GC analysis. Each of these vials was wrapped in foil to avoid photodegradation.

Tyler Rotap Sieve Shaker

Dry sieve particle sizing was performed by a Tyler Manufacturing Rotap model RX-29 soil shaker. A 20 minute shaking time was performed according to the manufacturer's recommendations. The Tyler nest of sieves Nos. 40, 60, 140, 200, 270, and pan material used in the experiments corresponded to 2 μm, 425 μm, 250 μm, 106 μm, 75 μm, 53 μm, and pan material, respectively.

Malvern Laser Optics Particle Sizer

The Malvern Laser Optic Particle sizer evaluated all gradations for mean particle sizes. The output of the machine provided detailed information concerning percentage of particles within size ranges.

Millipore Water Purification

A Millipore Ultra Pure Water System provided all deionized water. The system contained carbon filters, an ion exchange unit and a .22 μm rated pore filter. Deionized water was used as a solvent in all chemical mixtures and cleaning procedures.

Ultrasonic Mixer

The ultrasonic mixer was used in conjunction with a sodium hexametasulfate 24-hour bath to disagglomerate soils before performing the wet sieve analysis. This allowed accurate particle sizing during the wet sieve analysis.

Scanning Electron Microscope

The scanning electron microscope (SEM) was used to investigate surface geometry of individual particles. A Kevex™ analysis also was provided in conjunction with the SEM as a tool to determine elemental composition. The

Kevex™ provided an energy dispersive x-ray analysis as a means for determining the presence of various elements.

Miscellaneous Equipment

The following apparatus were standard laboratory equipment routinely used throughout the study:

- Associated Design sample tumbler #1317
- Beckman pH Meter, model Pi45
- Cole-Palmer Magnetic Stir Plate, model 4810
- Denver Instrument moisture analyzer, model IR-100
- Mettler AT261 scales
- Type 1600 Maxi Mixer

Computer Equipment and Software

Software spreadsheets by Quattro Pro (Version 4.1) and Lotus 1-2-3 (Version 3.1) were utilized for graphics conversion of ASCII files generated by the FL-750. Paradox (Version 4.0) was used as a database manipulator. Its PAL™ script language was utilized to write an area integration program. Statistica™ was used as a statistical data manipulation program.

TABLE 1

MATERIALS USED IN STUDY

Material	Source
Soil	
Arkansas River Sand (Tulsa, Oklahoma)	[a]36-19n-12e SE NW [a]Kiomatia series [a]pH 7.9-8.4 [a]Fine sand [a]Well drained Low in organics
Shelbyville Sand (Georgetown, Delaware)	[b]Pocomoke series [b]Slightly acid [b]Sandy loam (black dirt) [b]Poorly drained High in organics
Chemicals	
Naphthalene	Fluka Chemika, Flakes
p-Xylene	Janssen Chemica, Reagent
Rhodamine B	Eastman Kodak, Powder
Deionized water	Milipore Ultrapure System
Methanol	Fisher Scientific, HPLC

a US Soil Conservation Service, Tulsa County , OK

b US Soil Conservation Service, Sussex County, DE

were first spiked, tumbled, and allowed to reach equilibrium. The adsorbents were then separated from adsorbates, scanned, signals processed, and referenced to calibration curves which estimated residual solution concentrations. Once residual solution concentrations were determined, solids concentrations were calculated from a mass balance. Soil surfaces were scanned with the fluorometer and their responses were compared to the calculated solids concentrations. This procedure served to link a known solids concentration to the soil surface scan generated by the fluorometer.

Adsorbents

Selection

The environmental engineering thrust of this study required that the selected soils have a ubiquitous presence in the environment. Therefore the

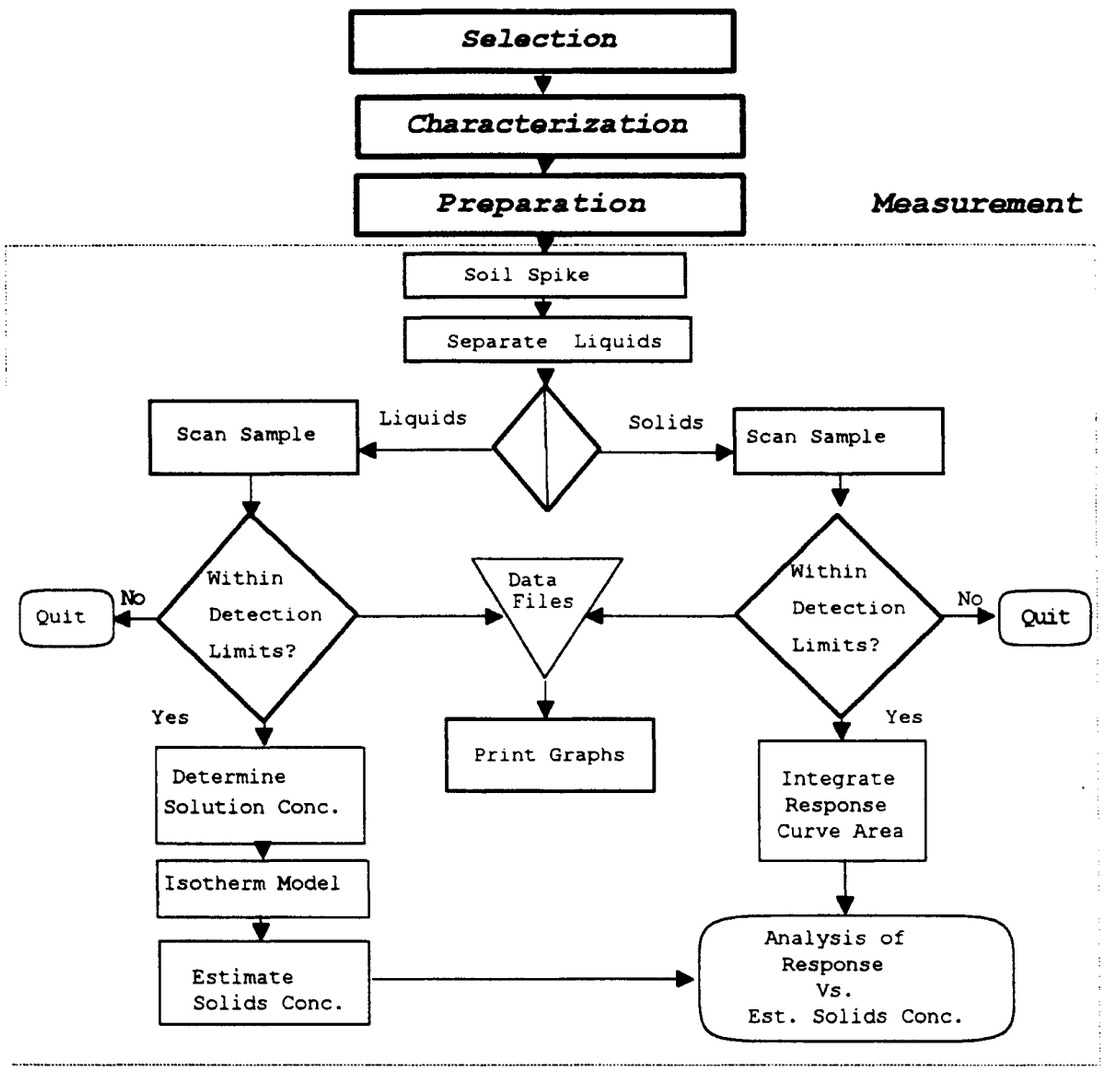

Figure 7. Experimental Procedure Logic Diagram

soils were selected to represent a general range of organic content, particle size, and surface area typical of aquifer materials. A clean aquifer sand (Arkansas River sand) and a sand high in organics (Shlebyville sand) were chosen as these representative soil types.

A variety of different soils, ranging from 100% clays to humic sands, were initially provided by Strategic Diagnostics, Inc. (SDI) of Newark, DE. Appendix K provides a complete evaluation for each of the soil candidates from SDI. Soils selected from the SDI lot were available in a limited supply of approximately 1 kilogram. Local soils offered an alternative but were limited in diversity. The final two selections were a compromise between available quantity and aquifer soil representation.

Arkansas River sand (ARS) was selected because it was abundantly available as a clean aquifer sand. ARS is characterized by it's low organic content and relatively broad range of gradations. A sample (approximately 25 kilograms) was collected from the banks of the Arkansas River in Tulsa, Oklahoma, in SE SE NW 36-19N-12E from the Kiomatia horizon. The sample was stored at its original moisture content in a large sealed container.

Shelbyville sand (SS) was selected from the many soils made available by SDI. SS was characterized by its high organic content. Based upon results from Karickhoff *et al.* (1979), it was anticipated that SS organics would provide alternative sorption sites for the accumulation of hydrophobic chemicals.

Preparation and Characterization

Arkansas River Sand (ARS)

The primary reason for the selection of ARS was to conduct adsorption experimentation (of fluorescent chemicals) upon soil surfaces free from the influences of organics but not necessarily free from the influences of grain size, surface features, or moisture content. Preparation of ARS included stripping the sand of organics and separating gradations into discrete homogeneous sizes without damaging the natural surface irregularities.

Several 1 Kilogram portions of ARS were dried at 105°C for 24 hours then sieved into six gradations. These six gradations include sand fractions retained on Tyler sieves numbered 40, 60, 140, 200, 270 and pan material. In a dry sieve analysis, each fraction's mass was measured as a percentage of the total beginning mass. The wet sieving procedure required washing a sample of ARS through a nest of sieves. Each fraction retained by a sieve was dried and its dry mass was recorded as a percentage of the total beginning dry mass.

Stock ARS sand fractions were carefully prepared. To eliminate organics individual fractions were sterilized in a continuously mixed 3% sodium hypochlorite bath for 24 hours (Mikhail *et al.*, 1978). In a sample preparation similar to Karickhoff *et al.* (1979), each fraction was drained, washed and exposed to gravity settling in a deionized water bath. The settling procedure consisted of individual fractions being placed in 4-liter beakers and subjected

to a continuously agitating flow of deionized water. This created a particle separation environment that removed residual colloids through the effluent stream. The inflow of the deionized water was carefully controlled, allowing primary settling of the main sand fraction while simultaneously flushing undesirable colloids into the effluent stream. The procedure continued (2-4 hrs) until the effluent was visually perceived to be clear of colloids.

The homogeneous clean fractions of soil were then oven dried at 105°C for 24 hours. Each fraction was further characterized by identifying average grain size, particle diameter, grain density, number of grains per gram of sample, surface area, and moisture content. The detailed method of analysis is explained in Appendix L and summarized within the results and discussion chapter. The moisture content within each fraction was described by three ranges paralleling field moisture conditions described by Fetter (1988). These moisture conditions are saturated (maximum), field capacity (medium) and wilting point (minimum).

Through the addition of fluid to the soil, a saturated moisture condition was approximated. Saturated soil moisture is a condition analogous to soils within an aquifer where 100% of the soil's void spaces are filled with fluid. Simulated field capacity was achieved by extracting liquids from void spaces through centrifugation. In this procedure, residual spiking fluids were drained, stainless steel screens were placed at the mouth of the sample vial, and placed upside down within the centrifuge vial holders for 1 hour at

1500 rpm. As a result of the centrifuge settings the field capacity values matched ranges supplied by Fetter (1988) in similar soils. Simulated wilting point moistures were achieved by wetting each fraction of sand past field capacity and allowing them to air dry (under a vented hood) for 24 hours. All fractions were stored in bulk at wilting point conditions in polyethylene bottles.

Shelbyville Sand (SS)

The work provided by Abdul *et al.* (1987) and Webber *et al.* (1992) made it clear that the organics in SS would provide alternative binding sites for the chemicals used in this study. Subsequently, results from spiking experiments offered a good contrast between the organic dominated adsorption sites of SS and the mineral surface adsorption sites of ARS.

Preparation of SS involved a less complicated procedure than ARS. Dry and wet sieve analyses were performed on SS using a similar techniques as in the ARS sieve analyses. In preparation for the dry sieve analysis, a portion of SS was oven dried at 105° C for 24 hours. Approximately 1 kilogram of the dried soil was placed in a Rotap sieve shaker for 20 minutes. The dry sieve analysis was immediately performed on fractions retained on Tyler sieves numbered 40, 60, 140, 200, 270 and pan.

An organic content evaluation was performed on each fraction after the completion of the dry sieve analysis. The method used to evaluate organic

content of each gradation involved ignition in a muffle furnace at 550° C for 1 hour. After ignition, fractions were allowed to cool in a desiccater before being weighed. The percentage difference in weight before ignition and after ignition determined the organic content (Clesceri, 1988).

Adsorbates

Selection

Adsorbates used in this study were required to be fluorescent, available in spectrofluorometric grades, and soluble in water. Naphthalene was chosen as an adsorbate to represent PAH's of low volatility which, for purposes of comparison, paralleled some of rhodamines chemical properties (low vapor pressure and large Stokes loss). The selection of naphthalene was particularly significant when experimental results from this study are coupled with Strategic Diagnostics Inc. data on naphthalene antibody production. A more volatile adsorbate, *p*-Xylene, was chosen to represent a constituent of the BTEX group. Rhodamine B as an adsorbate, demonstrates an affinity for soil mineral surfaces and, because of this property, has been used as a tracer dye in aquifer and sand migration studies (Ingle, 1966).

Characterization

Physical constants for each of the selected adsorbates are summarized in Table 2. The table lists molecular weights, density, aqueous solubility, vapor

pressure, quantum yield, and organic carbon partition coefficients (K_{oc}) for each adsorbate.

TABLE 2

ADSORBATE PHYSICAL CONSTANTS

Chemical	[a]M.W. (g/mol)	[a]Density	Solubility (mg/l)	[a]Vap. Pr. (mmHg@ °C)	Quantum Yield	Log K_{oc}
Rhodamine	479.02	1.31	[b]50,000	N/A	[e]0.97	[h]3.57
Naphthalene	128.18	0.96	[c]34	1@52	[f]0.23	[g]3.11
p-Xylene	106.17	0.86	[c]156	10@27	[f]0.40	[g]2.31
Water	18.00	1.00	N/A	19@21	N/A	N/A

a Weast (1992)
b Aldrich Chemical (1992)
c Mackay (1992)
d Baker Chemical (1992)
e Berlman (1971)
f Guilbault (1973)
g Abdul *et al.* (1987)
h Everts *et al.* (1989), Rhodamine WT

Naphthalene, abundant in coal tar, is a minor component of refined petroleum products. Its environmental fate is partially governed by a moderate aqueous solubility (34 mg/l), an organic carbon partition coefficient (3.11). A minor component of refined petroleum, *p*-Xylene's environmental fate is partially governed by a higher solubility (156 mg/l) and a lower organic carbon partition coefficient (2.31). Rhodamine has the greatest aqueous

solubility (50,000 mg/l) and the largest organic carbon partition coefficient (3.57).

Abdul *et al.* (1987) and Guerin *et al.* (1992) reported that naphthalene and *p*-xylene were considered nonionic organic contaminants. Nonionic organics have shown little tendency to adsorb to mineral surfaces which are polar and/or electrostaticly charged. The preferential adsorption of water by soil minerals ostensibly inhibits nonionic organics from interacting with these surfaces. Rhodamine's polar nature (Wolfbeis, 1993) and low vapor pressure enhances its adsorption potential to anionic mineral surfaces compared to the nonionic adsorbates.

The molecular configuration of the adsorbates (Figures 8, 9, and 10) are important to understanding the fluorescent characteristics each posses. These illustrations help to clarify the relative orientation of the various ringed structures in the molecule. Guilbault (1967) reported that most intensely fluorescent aromatic molecules are characterized by rigid, planar structures. Increasing molecular rigidity decreases vibrational amplitudes and reduces energy conversion mechanisms that compete with fluorescence.

Rhodamine B

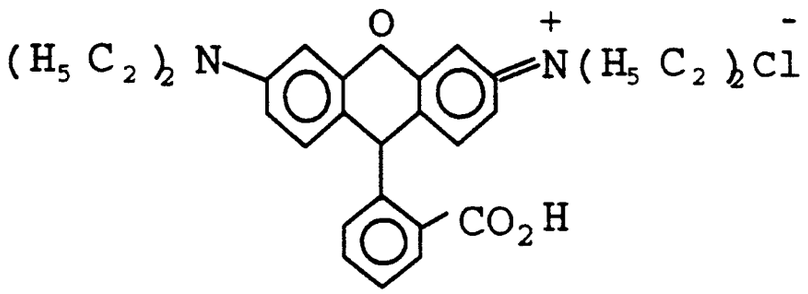

$C_{26}H_{30}N_2O_3HCl$

Figure 8. Rhodamine B Molecular Configuration (Reproduced from Kodak Catalog No. 51, 1981)

Naphthalene

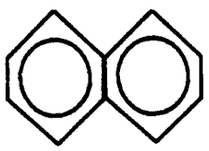

$C_{10}H_8$

Figure 9. Naphthalene Molecular Configuration (Reproduced from Weast,1992)

p-Xylene

$1,4\text{-}(CH_3)_2C_6H_4$

Figure 10. *p*-Xylene Molecular Configuration
(Reproduced from Weast, 1992)

Preparation

Stock Solutions

The procedure for making stock solutions began by adding a predetermined weight of chemical into 100 ml of deionized water. The solution was diluted further with deionized water until the target concentration was reached. This mixture was placed on a stir plate and vigorously stirred for approximately 15 minutes. Stock solutions of rhodamine and naphthalene were stored in 1000 ml glass bottles sealed with a Teflon screw-top lid. All glass bottles were kept in a light-proof storage container until needed to avoid photodegradation. Stock solutions of *p*-xylene

were mixed as needed under similar mixing conditions to avoid concentration fluctuations due to head space losses as the stock was consumed.

Working Solutions

Working solutions used in the soil spiking experiments were prepared from aliquots of the stock solutions. Target spiking concentrations were achieved in a series of dilutions with the aid of a computer spread sheet based upon the original stock solution concentration. Target concentrations were determined gravimetricly on the basis of a gram chemical per liter of solution.

Isotherm Development Using Fluorometric Methods

Selection and Characterization

Nonlinear Freundlich and Langmuir isotherms were used to model the adsorption of fluorescent chemicals onto soil surfaces based upon the work of Karickhoff *et al.* (1979) and Fetter (1988). A more complete discussion of the isotherms is offered in chapter V.

Preparation

Adsorption isotherm experiments, were carried out using 25 milliliter screw-top, borosilicate vials as individual completely mixed batch reactors (CMBRs) in bottle-point experiments. Each point on the adsorption isotherm

line was determined from an individual CMBR by equilibrating a given concentration of adsorbate with a given mass of adsorbent (Chin *et al*, 1987).

Two methods of isotherm construction were investigated as a means to estimate soil partitioning. The first method mixed a constant spike concentration with three soil masses from each soil gradation. The second method mixed a constant soil mass with variable solution concentrations.

Nonvolatile Spiking Liquids

In the variable mass adsorption experiments, an aliquot from the stock solution was diluted with deionized water in a glass beaker to the target spiking concentration. The beaker was stirred for several minutes on a magnetic stir plate. Two, four, and eight grams of each soil grade were added to individual vials. Approximately eight grams of the spiking solution was added to each vial. The vials were sealed with a Teflon lined screw caps and wrapped in foil to reduce photodegradation. The batch mixtures then were placed in a rotary tumbler for 24 hours (based upon equilibrium results in Chapter V) allowing equilibrium to take place.

In the variable concentration adsorption experiments, eight grams of soil were mixed with solution concentrations which ranged over six orders of magnitude. Similar mixing and tumbling procedures from the variable mass experiment were applied to achieve equilibrium.

Volatile Spiking Liquid

Isotherm experiments which involved the more volatile chemical *p*-Xylene were performed leaving no head space in the vial. This practice reduced volatile losses. Appropriate soil masses were placed in each vial according to the above protocols. The spiking solution was rapidly transferred by pipette into the vial until full. The vial was sealed and vibrated for 60 seconds to remove trapped air bubbles. The cap was removed and more solution (range from 0 to 0.25 ml) was added to completely fill the vial. The vial was tightly sealed after the addition of the makeup fluid. The remainder of the experiment was executed in the same manner as the nonvolatile liquids proceedure.

Equilibrium

Adsorption rate studies were conducted over a five day period to determine the time required to reach equilibrium. Equal masses of soil were added to a series of 24 vials which represented 4 test periods for 2 adsorbents and 3 adsorbates. Equivalent concentration solutions representing the three adsorbates were added to each vial prior to agitation in the rotary tumbler. Vials were wrapped in foil to ensure protection from photodegradation during the tumbling process. Then, at predetermined intervals (1 hour, 1 day, 2 days, and 5 days), the tumbler was stopped. One vial representing each

centrifuged at 1500 rpm for 1 hour to separated the solid and liquid phases. The supernatant was transferred by pipette to cuvettes and the residual concentrations were measured fluorometrically (see Chapter V, Figures 18 and 19 for results).

Liquids Measurement

In the adsorption isotherm experiments, sealed vials were centrifuged at 1500 rpm for 1 hour following equilibrium, to force colloids out of the liquid phase (Smettem *et al.*, 1983). Supernantant tests revealed that the colloids left in solution represented less than 0.1% of the total dry sorbent mass. A portion of the supernatant was transferred by pipette from the vials directly into the cuvette. The emission spectrum of the sample then was scanned at ambient temperatures.

The 4 ml samples placed in the cuvettes eliminated any meniscus effects on fluorescence discussed by Harris *et al.* (1988). Cuvettes were washed with soap after each run then rinsed five times with deionized water. Cuvettes then were dried with low lint Kimwipes™ EX-L before scanning. Latex gloves were worn at all times during the scanning procedure to eliminate fingerprints on the cuvettes as a source of fluorescence.

Solids Measurement

Direct soil scans were conducted using the specially designed soil holder described in Chapter III. Approximately one third of a gram of soil was placed onto the holder for each scan. Soil samples were scanned at various moisture contents and compared to the estimated soil concentrations (see Chapter V). Background interferences due to direct light scattering from particle surfaces were compensated for through an area integration process (see Integration of Response Curve Areas, this chapter).

Blanks and Control Solutions

Soil/water blank CMBRs and calibration samples were run concurrently with the test CMBRs. Blanks contained the same soil types and weights as the test samples. However, each blank was spiked with deionized water in place of the chemical solutions. Sample blank extraction liquids were used to confirm fluorometric background response. Sample blank soils were used in a similar manner to confirm background fluorometric response.

Controls containing a spiking solution but no soil were run simultaneously with the isotherm CMBRs to determine whether any significant losses of the solute had occurred in the system. Results verified no noticeable losses had occurred due to volatilization, photodegradation, or interaction within the CMBR surfaces. Experiments proceeded in batch mode with test samples, blanks, and controls being prepared simultaneously. Approximately

samples, blanks, and controls being prepared simultaneously. Approximately 10-20 vials were prepared for an individual experiment. The contents of each vial (solid or liquid) were scanned three times. Vials were removed from service after scanning, not to be used again.

Data Handling

Data generated by the scanning procedures were imported into a Paradox base file. The area integration program written in Paradox PAL™ language (see Appendix D) reduced the data to volt-nanometer units (v-nm).

All response curves, liquid or solid, were converted to this single value where the magnitude represented the amount of fluorescence detected by the FL-750 PMT. The areas generated by the integration of the response curves were converted to apparent solution concentrations using the standard calibration curves. Calibration curves built for each chemical represented a range of fluorescent responses (areas) produced at known solution concentrations (see calibration curves in chapter V).

Integration of the Responses Curve Area

The values for the response area described by the preceding paragraph were calculated from a trapezoidal integration of the intensity-wavelength response curves (Ebert *et al.*, 1989). Figure 11 illustrates an area which was computed by the integration program. The integration program

mathematically subtracts the background responses from the fluorescent response before integration occurs.

Background responses can take several forms and the primary response graph must compensate for their presence. The most important form of background response originated from soil reflectance (Rayleigh scatter). Direct reflectance from the soil interfered with the ability to quantify fluorescent responses. Light filtration as well as setting the excitation wavelength as far away as possible from the emission maxima helped reduce scattering effects but did not eliminate it. A tradeoff existed between the excitation/emission offsets and the intensity of fluorescent responses.

Shown in Figure 11 is a response curve from a rhodamine spiked soil superimposed on the response curve from a clean sand at the same moisture conditions. The background soil scan was subtracted from the rhodamine soil scan leaving a background corrected composite curve represented by the shaded region. The area of the shaded region represents a single volt-nanometer value used in the computations.

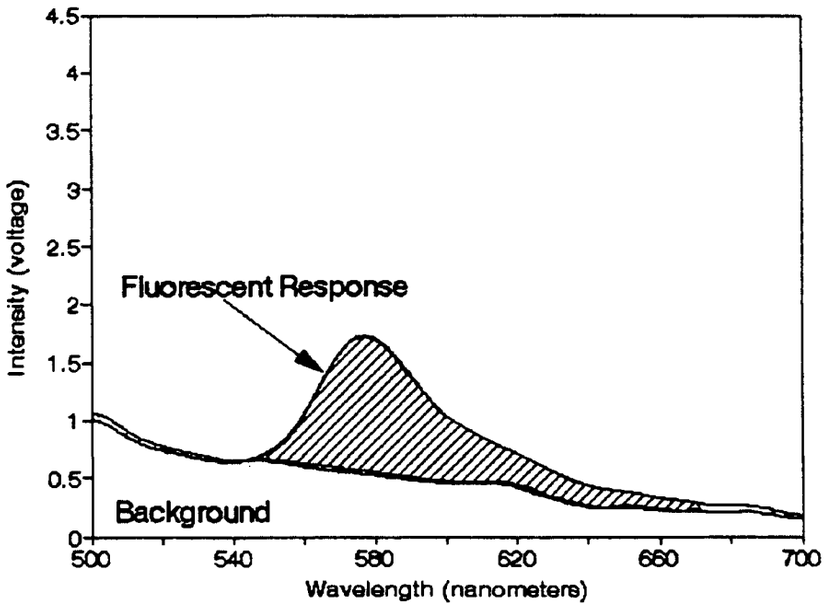

Figure 11. Rhodamine Fluorescence Response Area
With Soil Background Compensation

Additional background compensation was required when low concentration solutions necessitated high equipment sensitivities. A significant contribution from a Raman peak was produced under these conditions which was not part of a fluorescent response and therefore had to be compensated for in a similar manner. Generally, solutions at higher concentrations needed little background compensation because the Raman peak was small in comparison to the magnitude of the fluorescent peak.

Isotherm Model Selection

Twelve separate isotherms were constructed to evaluate the sorptive properties of the various soil/chemical combinations. The six basic isotherm mathematical models included: Freundlich variable mass (FRVM), Freundlich variable concentration (FRVC), Langmuir-low concentration variable mass (LLVM), Langmuir-low variable concentration (LLVC), Langmuir-high variable mass (LHVM), and Langmuir-high variable concentration (LHVC). Each of these isotherms were further evaluated based upon sorbent masses and sorbent surface areas. As a result, a total of total of twelve separate isotherm models were constructed for comparison on the basis of a regression analysis.

Miscellaneous

Gas Chromatography Analysis

Standard stock solutions were submitted to National Analytical Laboratory of Tulsa, Oklahoma, for gas chromatography analysis to verify estimated dilution concentrations. The results listed in Table 3 served as a basis for the hydrocarbon stock solution concentrations. Values for all subsequent dilutions prepared from stock solutions relied upon these GC verified concentrations with the exception of rhodamine which was quantified through gravimetric methods.

TABLE 3

STOCK SOLUTION CONCENTRATIONS

Chemical	Concentration (mg/l)
Rhodamine	[a]1039.51
Naphthalene	[b]44.48
p-Xylene	[b]165.97

a gravimetric analysis
b GC analysis

Gas chromatography analyses were also performed on vials containing one fraction of each soil type mixed with approximately 10 mg/l naphthalene. Duplicate vials were prepared for simultaneous fluorometric analysis. One set of vials were delivered to National Analytical Services of Tulsa, Oklahoma, for GC analysis. A parallel vial set was measured fluorometrically at the same time the GC analysis was conducted. In the gas chromatography method (EPA 8260), two values were obtained from the same vial. One concentration measurement was taken from the fluids and another from the solids. The fluorometric analysis measured only the residual solution concentrations then calculated the solids concentration from a mass balance of the system. The results from the GC analyses were compared to fluorometric results. This comparison was considered a measure of accuracy for the fluorometric method of analysis (see Chapter V).

Surface Area Measurements

The Braunauer-Emmett-Teller (B.E.T) method for surface area measurements was performed by Micromeritics Inc. of Norcross, Georgia. An ASAP 2400 surface area analyzer used the single point method at liquid nitrogen temperatures. Surface area measurement were performed on six gradations of the stock Arkansas River sand and the three gradations of stock Shelbyville sand used in the experiment.

Mineralogy

Mineral compositions were determined through X-ray diffraction performed on both ARS and SS soil by Mineralogy, Inc. of Tulsa, Oklahoma.

CHAPTER V

RESULTS AND DISCUSSION

Introduction

Rhodamine B was used to determine the soil factors that influence solid-phase fluorescence measurements. Naphthalene, *p*-xylene, and rhodamine isotherms were developed to predict solids concentrations from residual liquid concentrations using a fluorometric method of analysis. These isotherms were tested for sensitivity, precision, and accuracy. The evaluation of rhodamine spiked solid-phase fluorescence data relied upon the correlation between isotherm-derived solids concentrations and fluorometric readings from soil surfaces.

The discussion of results incorporates two different data types that were obtained from the equipment and procedures described in Chapters III and IV. The first set of data, liquid-phase fluorescence, was used in the creation of adsorption isotherms. The second set of data, solid-phase fluorescence, was obtained directly from the surfaces of rhodamine spiked soils then correlated to surface concentrations derived from the rhodamine isotherms. Soil

moisture, grain size, and organic content were found to be significant influences on solid-phase fluorescence measurements.

Liquid-Phase Fluorescence

Fluorescent Absorption and Emission Spectra

Liquid phase absorption spectrums helped to identify characteristics useful in obtaining solid-phase fluorescence measurements. Emission scans for each of the adsorbates (Figures 12, 13 and 14) serve to illustrate typical fluorescence responses produced by both the calibration fluids and the supernatant fluids used within the isotherm experiments. The magnitude of each peak fluctuated with changing solution concentrations. In the isotherm experiments, the magnitude of the response depended on specific soil adsorption.

Rhodamine

Rhodamine had a relatively large absorption spectrum that from beginning to end spanned almost 400 nm (Figure 12). Rhodamine was characterized by an absorption maximum of 540 nm and two small absorption peaks at 300 nm and 350 nm. Absorption began at 225 nm and ended at 590 nm. The emission spectrum was much narrower in width and had its greatest intensity at 580 nm. The Stokes shift, measured from absorption peak to emission peak, was 40 nm.

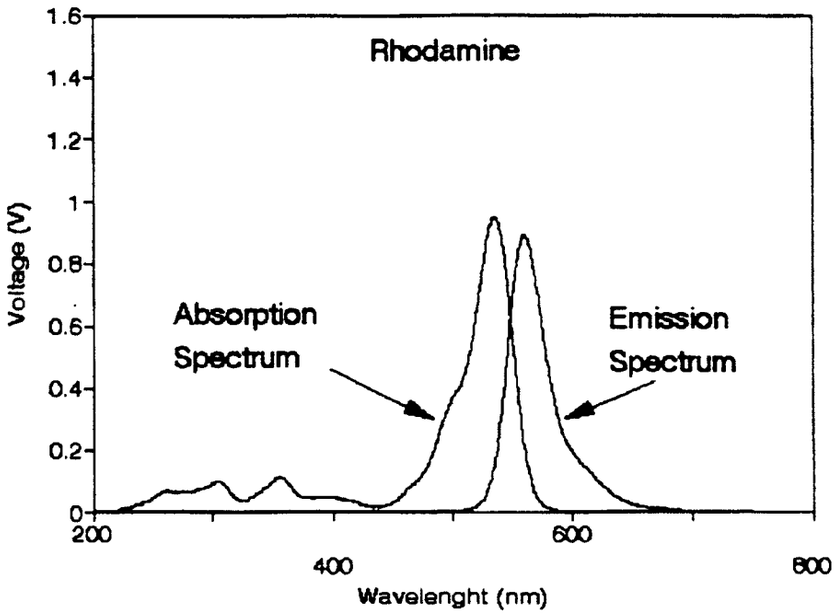

Figure 12. Rhodamine Absorption and Emission Spectra

In the present solid-phase fluorescence study, a lowering of the excitation wavelength actually improved rhodamine detectability by reducing Rayleigh, Raman, and Tyndall interference. Since excitation anywhere in the rhodamine absorption band produced an emission at 580 nm, decoupling the excitation further from the emission maximum served to reduce light scattering interference. A lowering of the excitation wavelength from the maximum (but within the adsorption band width) reduced absorptivity, which in turn reduced the intensity of the fluorescent response. Increased equipment sensitivity settings compensated for these reductions in fluorescent responses. In this

manner, masking of fluorescent responses by background soil emissions was reduced.

The combination of rhodamine's high quantum yield (0.97) and wide absorption band width provided a fluorescent dye which, when adsorbed to soil surfaces, was detectable but difficult to quantify. Optimization procedures outlined in Appendix H indicated that an excitation wavelength of 350 nm produced the best fluorescent soil readings and at the same time kept light scattering to a minimum.

Naphthalene and *p*-Xylene

Naphthalene and *p*-xylene spectra (Figures 13 and 14), unlike rhodamine, were characterized by small Stokes losses and relatively narrow absorption bands. The combination of lower quantum yields and the inability to decouple the excitation far from the emission maximum made naphthalene and *p*-xylene virtually impossible to detect on solid surfaces using the FL-750. The effects of Tyndall light scattering from soil surfaces saturated the photomultiplier tube masking fluorescent readings. Large Raman interference's were also common in *p*-xylene solution measurements. In future experimentation, a time-gated diode laser (Lieberman, 1993) will eliminate these problems by totally decoupling the excitation from the emission radiation making it possible to detect PAHs in soils.

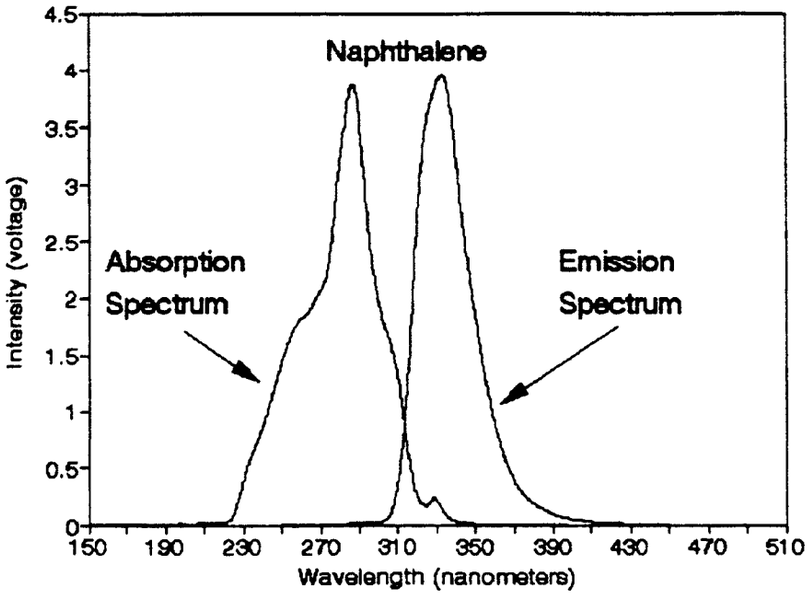

Figure 13. Naphthalene Absorption and Emission Spectra

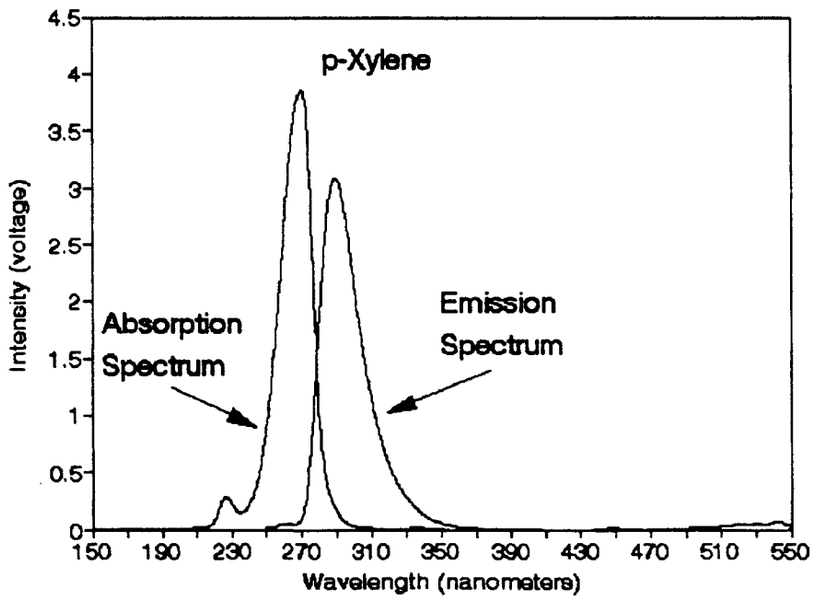

Figure 14. *p*-Xylene Absorption and Emission Spectra

Calibration Curves

Prior to the isotherm experiments, aqueous phase calibration curves were established for each adsorbate in aqueous dilutions (Figures 15, 16, and 17). Fluorometric response curves were recorded at measured concentrations and integrated into areas. The values of these areas were plotted against their corresponding concentrations (in triplicate) on semi-log paper to build solute calibration curves. Fluorescence response values (v-nm) from the batch isotherm experiments were referenced to their respective calibration curve and converted to a residual concentration (mg/l).

Relatively low aqueous solubilities for naphthalene and *p*-xylene limited the maximum concentration responses on the X-axis; while chemical-specific quantum yields limited the maximum intensity responses on the Y-axis. A broad range of concentrations yielded nonlinear calibration curves primarily due to fluorescence inner filter effects. The inner filter effect (or the effects of concentration) resulted in a significant amount of fluorescent radiation being reabsorbed into the solution, reducing the signal response (Guilbault, 1973). Inner filter effects due to the high aqueous solubility of Rhodamine B caused the peak of its calibration curve (maximum area) to fall far below its maximum aqueous solubility concentration. Hydrocarbon peak areas fell near their respective maximum solubility concentrations.

Naphthalene and *p*-Xylene

The calibration curves generated by naphthalene and *p*-xylene in aqueous concentrations spanned six orders of magnitude. The naphthalene maximum response area reached 113 v-nm and corresponded to a concentration of 47 mg/l (Figure 15). The *p*-xylene maximum response area reached 100 v-nm and corresponded to a concentration of 120 mg/l (Figure 16). The minimum response area for either solute occurred at less than 1 ug/l which reflected the equipment's detection limit.

A maximum sensitivity setting of 12 (0.01) was selected for all solutions based upon the fluorometer's 4 volt linear dynamic operating range. Further increases in sensitivity settings resulted in large signal fluctuations that saturated the PMT rendering the measurements useless.

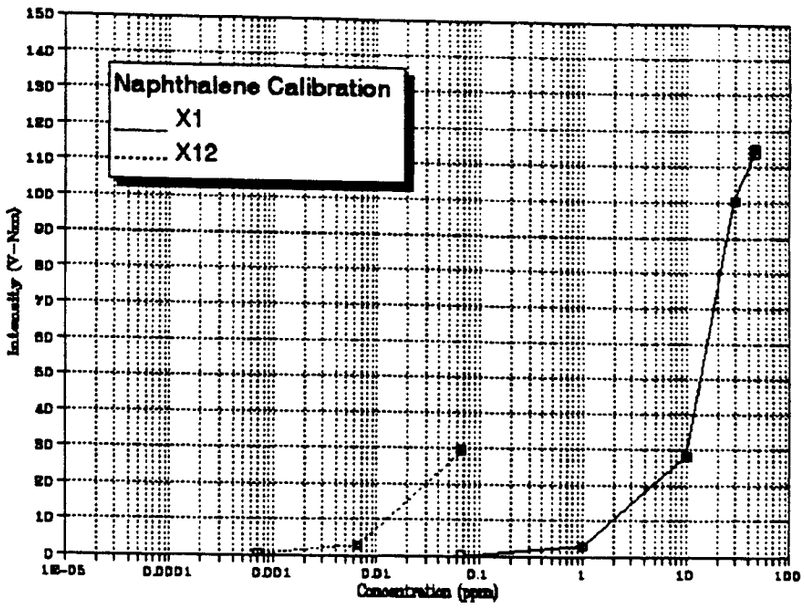

Figure 15. Naphthalene Calibration Curve

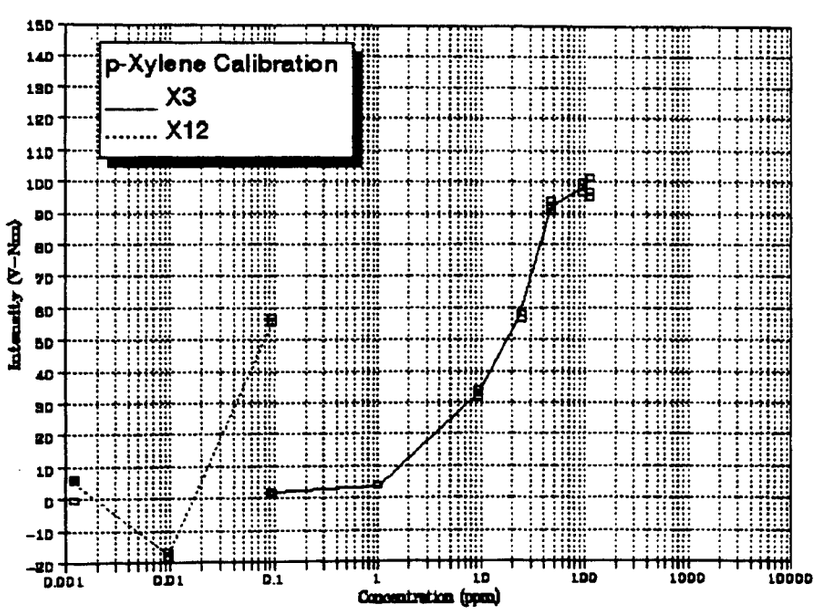

Figure 16. *p*-Xylene Calibration Curve

Rhodamine B

The high aqueous solubility of rhodamine resulted in high solute concentrations that produced a Gaussian shaped calibration curve (Figure 17). Fluorescence intensity increased as concentrations increased. Once the peak fluorescent intensity was reached (180 v-nm), inner filter effects obscured the photons returning to the detector and reduced the signal intensity. As a result, even though concentrations continued to increase past the peak intensity, the signal response decreased regardless of the equipment settings.

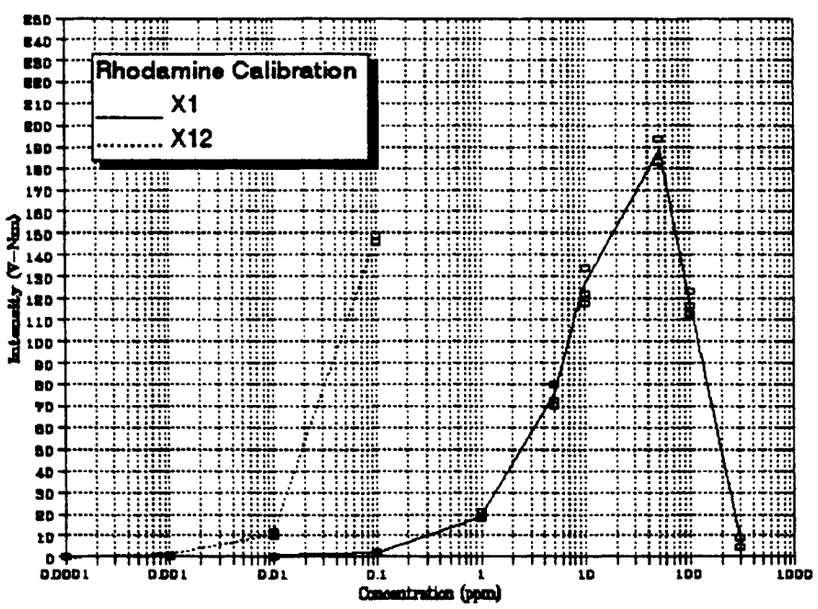

Figure 17. Rhodamine Calibration Curve

The limit of detection in liquid fluorometry at high solute concentrations was affected by self absorbency of the photons from the solute itself (inner filter effects). The limit of detection at a low solute concentration was affected by interferences from solvent photon emissions (Raman scatter). Although the selection of water as a solvent limited the range of hydrocarbon detectability in this study to a small degree at very high sensitivity settings, it was established early in the experimental procedures that modeling natural systems took priority over detectability limits.

Adsorption Isotherms Using Liquid-Phase Fluorescence

Karickhoff *et al.* (1979) was effective in linking the organic partitioning coefficient's sorptive predictabilities to grain size distribution and organic content. The organic carbon partitioning coefficient ($K_{oc,}$) was found to be dependent upon soil grain size distributions. It was determined that silt sized particles possessed the maximum K_{oc} while sand fractions had the lowest K_{oc} values. This indicated that adsorbates tended to accumulate in the smaller particles.

The affinity some materials have for certain soil fractions will likely create a baseline adsorption in soil fluoroimmunoassays which quite possibly will change with grain size distribution. In the present study, this baseline was quantified through adsorption isotherms.

In an effort to quantify a baseline adsorption under variable soil conditions, methods to determine the degree of soil/solute partitioning were carefully considered. Lick (1991) reported that the "solids concentration effect" may have an influence upon the accurate determination of partitioning coefficients for hydrophobic chemicals. The chemical mass transfer rates from the solution to the solids decreased adsorption rates with increased solids concentrations if the equilibration time was too short. In this study, the solids concentration effect was reflected in a lower coefficient of determination from regression analyses under the variable mass method of isotherm construction. However, batch experiments were conducted to eliminate the solids concentration effect by holding the soil masses constant while varying the solute concentrations. The results were higher regression correlations for a variable concentration method of isotherm construction. It was also discovered that colloids from completely mixed batch reactor supernatants affected the accuracy of the fluorometric method of analysis, but they did not affect the methods precision (see GC analysis section).

Equilibrium

Measurements of equilibration times for the materials used in this study indicated a rapid adsorption rate within the first hour (Figures 18 and 19). Organic chemicals have been found to exhibit a two-stage equilibrium behavior: (1) a short period (minutes to hours) of rapid mass transfer, and

(2) an extended period (days to months) of slow mass transfer for the remaining adsorbate (Brusseau, 1990).

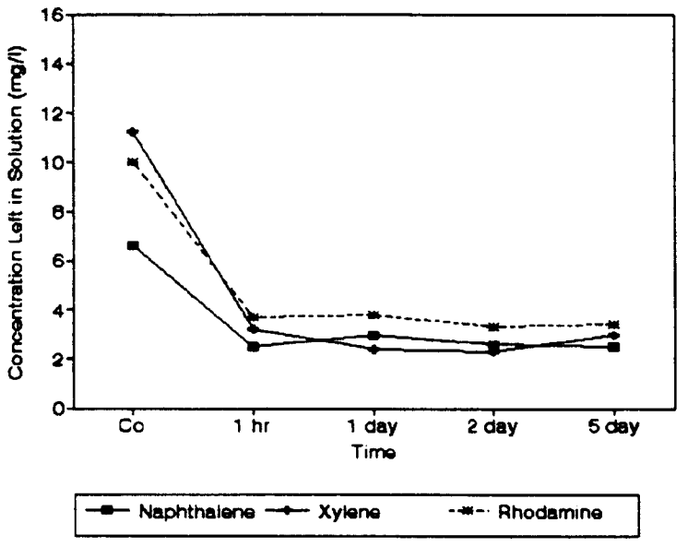

Figure 18. Equilibrium Results for Arkansas River Sand

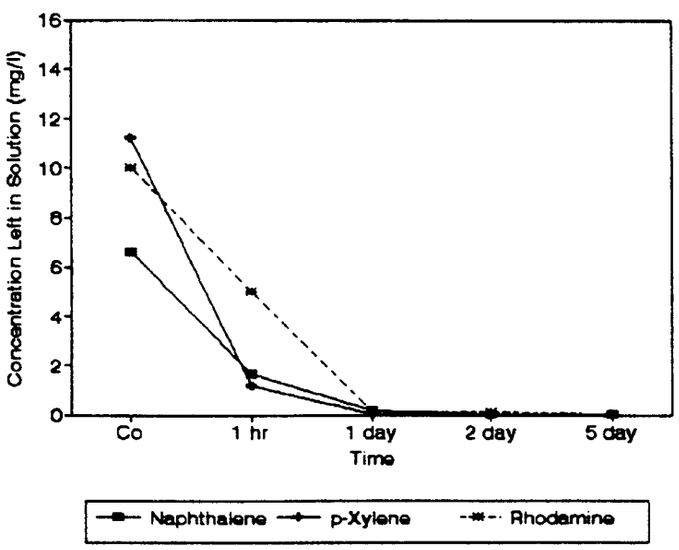

Figure 19. Equilibrium Results for Shelbyville Sand

These results indicated that greater than 95% of chemical adsorption occurred within 24 hours of mixing in either soil. A comparison of the two graphs indicated that Shelbyville sand adsorbed with greater efficiency than the Arkansas River sand, leaving only trace amounts of solute in the residual solutions. A 24-hour period was determined to be adequate time for the batch adsorption isotherms to reach equilibrium.

Regression Analysis for Optimum Isotherm Model Selection

Results from a regression analysis of 6 possible isotherms described in Chapter IV (Freundlich, high-Langmuir, low-Langmuir for variable mass and variable concentration measurements) are reported in Table 4. This table was compiled to aid in the selection of an isotherm model which best fit the observed data. The numbers in the table represent the coefficient of determination (R^2) which are an objective measure of the predictive value of the regression equations when applied to each soil/solute combination. Wadsworth (1990) defined R^2 as the percentage of the total variability in Y (soil concentrations) that was accounted for by using X (liquid residual concentrations) to predict Y. If the regression line fell on all the data points, R^2 will equal 1.

Starting from the left column in the first row of the table and searching to the right, the isotherm model that had the highest value of R^2 best fit the regression line to the data (see Appendix B Table 17). In this example of

naphthalene in Arkansas River sand, the Freundlich Variable Concentration isotherm model (FRVC) had the highest value (0.98) compared to any other model within that soil/solute combination. The Freundlich variable concentration isotherm model was therefore selected as the model which best fit the trend of the data.

The R^2 values in Table 4 indicated that the Freundlich isotherm solution generally favored the hydrocarbons with higher coefficients. It was also better modeled through a variable concentration batch method of experimentation thus eliminating the solids effect. Naphthalene demonstrated higher R^2 values in both soils than *p*-xylene, probably as a result of its lower volatility and stronger fluorescent properties. *p*-Xylene demonstrated lower R^2 values in the Arkansas River sand than in the Shelbyville sand.

TABLE 4

ISOTHERM MODEL SELECTION BASED ON COEFFICIENT OF DETERMINATION (R^2) VALUES

	LLVM	LLVC	LHVM	LHVC	FRVM	FRVC
			Hydrocarbons			
Naph. in ARS	0.32	0.00	0.49	0.96	0.68	**0.98**
Naph. in SS	0.95	0.82	0.83	0.94	0.82	**0.99**
p-Xy. in ARS	0.39	0.16	0.06	0.63	0.09	**0.85**
p-Xy. in SS	0.99	0.00	0.97	0.98	0.89	**0.93**
			Rh. Dye			
Rhod. in ARS	0.60	**0.99**	0.69	0.97	0.71	0.93
Rhod. in SS	0.68	**0.99**	0.29	0.40	0.66	0.93

It should be noted that the model which exhibited the lowest R^2 values for nonionic hydrocarbons (LLVC) exhibited the highest R^2 values for rhodamine (FRVC). This difference suggested that rhodamine adsorption proceeded via a mechanism which differed from that driving hydrocarbon adsorption.

Hydrocarbon Isotherms

Use of Freundlich isotherms were based upon the higher coefficient of determinations from Table 4. The relatively high degree of correlation between the data and the selected model provided a means to predict surface concentrations if beginning and ending solution concentrations were known. The Freundlich isotherm developed by the variable concentration method of analysis (FRVC) on a surface area basis was selected as the best hydrocarbon model with a 0.94 average coefficient of determination.

Naphthalene

Naphthalene data from Table 4 demonstrated the highest R^2 values. This translated into tight 95% confidence intervals around the plotted data points of the isotherm. Naphthalene in Arkansas river sand (Figure 20) had a slightly lower coefficient of 0.98 than the Shelbyville sand of 0.99 (Figure 21).

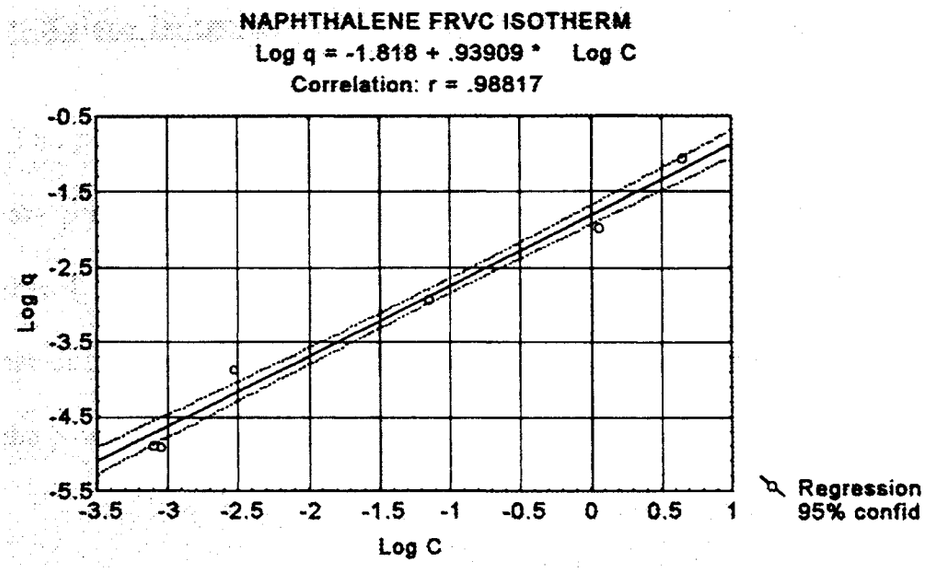

Figure 20. Naphthalene in Arkansas River Sand Isotherm

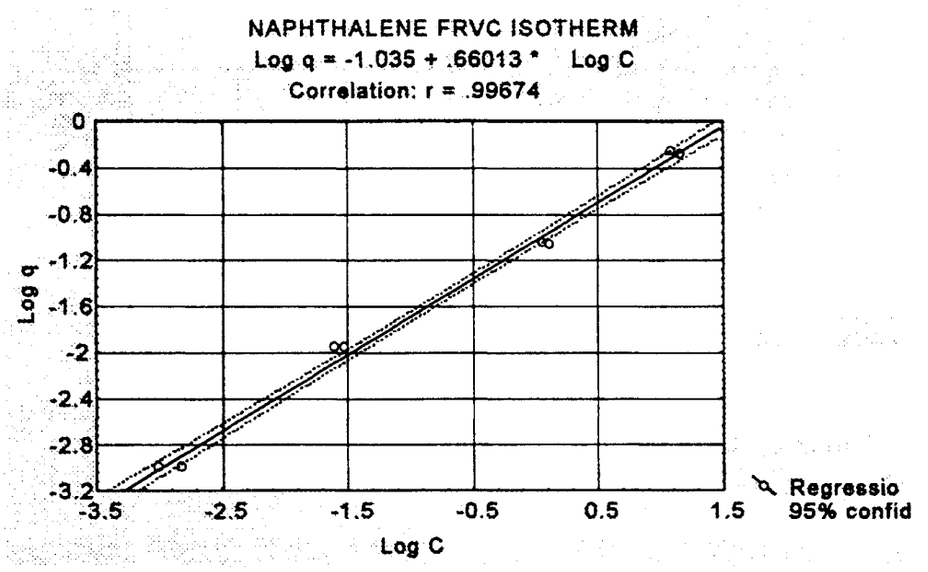

Figure 21. Naphthalene in Shelbyville Sand Isotherm

p-Xylene Isotherm

The *p*-xylene data demonstrated wider 95% confidence intervals around the data points that reflected lower values for the coefficients of determination in Table 4. Of the *p*-xylene data, the Shelbyville sand (Figure 22) had the highest coefficient at 0.93. While the Arkansas river sand (Figure 23) data had the lowest at 0.85.

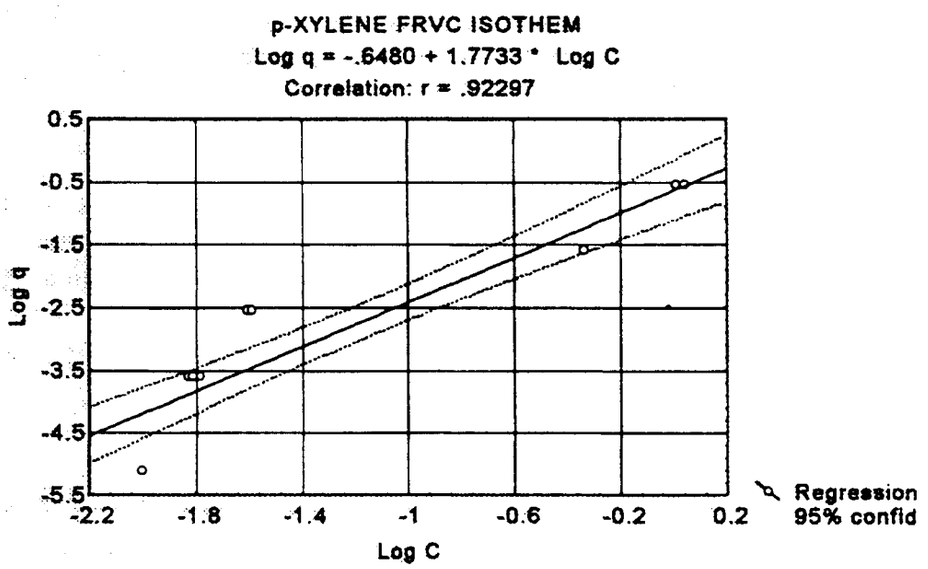

Figure 22. *p*-Xylene in Arkansas River Sand Isotherm

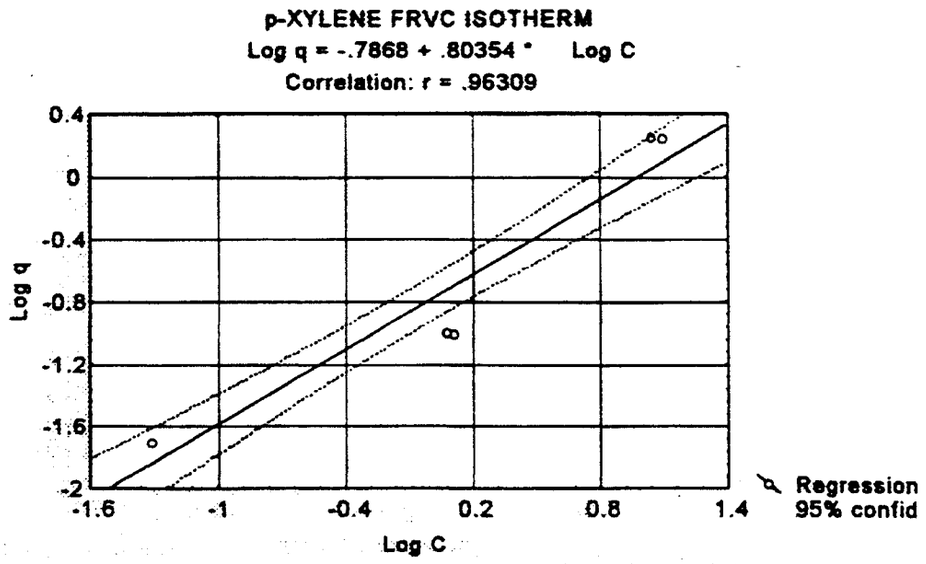

Figure 23. *p*-Xylene in Shelbyville Sand Isotherm

The Freundlich equation (Equation 9) yielded information about the adsorptive capacity (log K=intercept) and intensity (1/n=slope) of each soil. The adsorptive intensity of the Shelbyville sand was greater than the Arkansas River sand for all adsorbates (Figure 24). Rhodamine spiked Shelbyville sand demonstrated the greatest adsorptive intensity of 2.15. The regression line solutions indicated that there was also a greater adsorptive capacity within the Shelbyville sand (Figure 25). Among the hydrocarbons, naphthalene had the greater adsorptive intensity while *p*-xylene demonstrated greater adsorptive capacity especially in the Arkansas River sand.

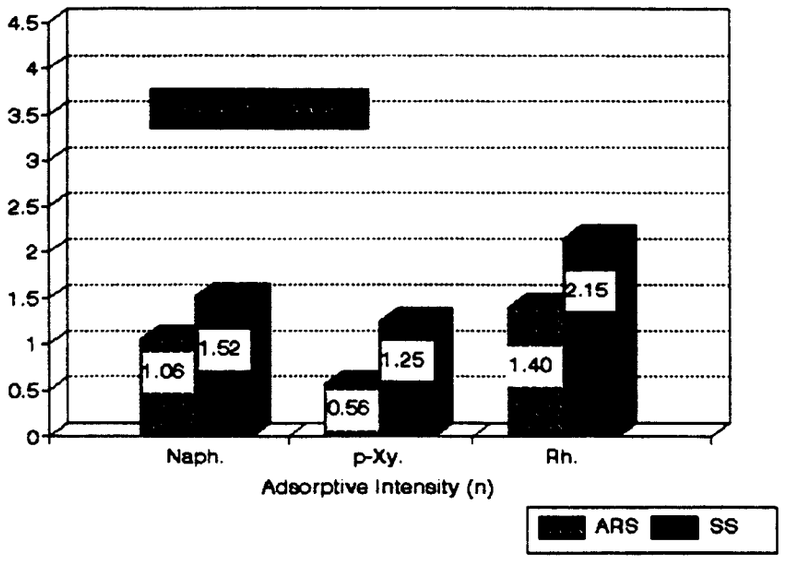

Figure 24. Adsorptive Intensity of ARS and SS

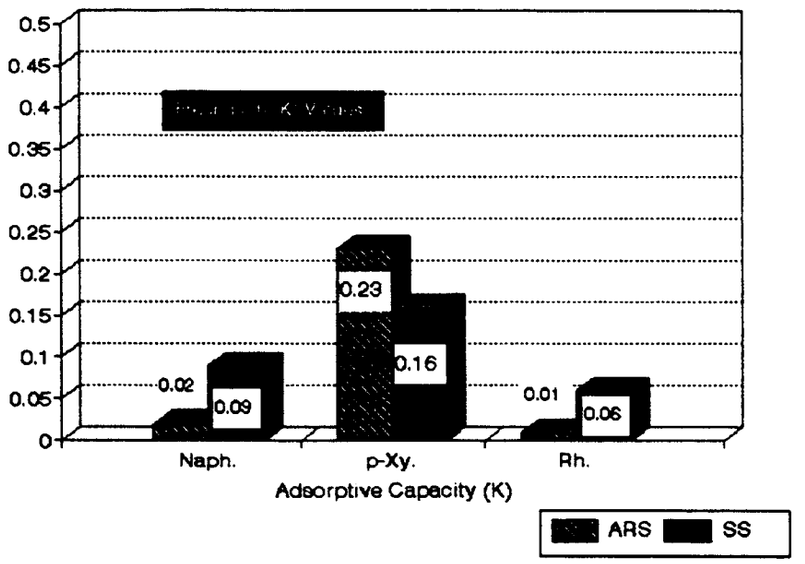

Figure 25. Adsorptive Capacity of ARS and SS

Isotherm Sensitivity Analysis

Model-derived concentrations are compared to fluorometricly measured concentrations in Table 5 (Appendix B, Table 18). Errors between modeled and measured values were an indication of the predictive accuracy of the FRVC model. When the initial concentrations were used in the isotherm equations (Appendix A for example calculation), cumulative errors between the measured and modeled results were found to be low (11%) for the residual solution concentration and still lower (3%) for the solids surface concentration.

An initial concentration of 47.22 mg/l resulted in a residual concentration (measured fluorometricly) of 4.4 mg/l and a soil surface concentration of 86.37 ug/m^2. The FRVC model predicted a residual concentration of 6.1 mg/l and a soil concentration of 83.07 ug/m^2 based upon the same initial concentration of 47.22 mg/l. The residual concentration from the model was 35.56% greater than the measured data, while the surface concentration for the modeled data was 3.60% lower than the measured data.

TABLE 5

FRVC MODEL ACCURACY [a]

	MEASURED DATA		MODEL RESULTS		% ERROR	
Co (mg/l)	[b]Cr (mg/l)	q (ug/m2)	Cr (mg/l)	q (ug/m2)	Cr %	q %
47.224	4.400	86.370	6.100	83.070	35.560	-3.600
6.620	1.117	10.390	0.717	11.130	-37.650	7.780
0.664	0.071	1.160	0.065	1.170	-9.720	1.170
0.072	0.003	0.130	0.006	0.130	106.670	-2.440
0.007	0.001	0.010	0.001	0.010	-38.890	-16.050
				Total	11.190	-2.630

a For Naphthalene in Arkansas River Sand, gradation 60

b Average of three measurements

Other isotherm models that produced lower coefficients of determinations generated higher cumulative errors. It was reasoned that because the FRVC model produced relatively low cumulative errors, the FRVC empirical solution was the better model. This model was capable of predicting hydrocarbon adsorption using the data supplied by fluorometric measurements.

Correlations Between Fluorometric, Empirical and GC Analyses

A comparison of the fluorometricly derived values to gas chromatography values produced conflicting results. The results in Table 6 demonstrated a general agreement between the FRVC model and the fluorometric data. While the GC values showed poor correlation to either the FRVC model or the fluorometric values until an optical density correction was applied. Small

errors in the measurement of residual concentrations (Cr) were found to cause large errors in surface concentrations when checked against the GC values.

TABLE 6

[a]FLUOROMETRIC vs.GC ANALYSIS OF NAPHTHALENE

	FLUORO DATA [b]			FRVC MODEL			GC DATA [c]		
Soil	Co (mg/l)	Cr (mg/l)	q' (mg/kg)	Co (mg/l)	Cr (mg/l)	q' (mg/kg)	Co (mg/l)	Cr (mg/l)	q' (mg/kg)
				UNCORRECTED FOR COLLOIDS					
ARS60	10.500	2.800	9.260	9.920	2.800	8.560	6.500	6.000	0.710
				CORRECTED FOR COLLOIDS					
ARS60				6.800	6.000	0.853			

a Naphthalene in ARS60
b 8.09 g sand, 9.72 g sol.
c 8.24 g sand, 8.75 g sol.

The uncorrected fluorometric data at first glance suggested greater soil adsorption when compared to the fluorometric data. The GC spiking concentration (Co) measured 6.50 mg/l while the fluorometricly determined spiking concentration (using the same soil and spiking solution) calculated as 10.50 mg/l, a 61% increase. Further comparing the two measurement methods, the GC residual concentration (Cr) measured 6.00 mg/l while the fluorometric value measured 2.80 mg/l, a 47% decrease. Finally, the soil

concentration (q') measured 0.71 mg/kg while the fluorometric value (based upon Cr) calculated as 9.26 mg/kg, an increase by a factor of 12.

Calculated soil concentrations derived by fluorometric analysis were shown to be very sensitive to slight changes in measured residual solution concentrations using the current Freundlich solution. In fact, a 50% change in Cr resulted in at least an order of magnitude change in q' when compared to the GC-derived data.

Wolfbeis (1993) reported that corrections must be made for changes in fluorescent intensity due to differences in optical densities between the standards and sample measurements. The presence of colloids in the batch reactor supernatants attenuate the intensity of the excitation light (I_o) thereby creating a source for measurement error by reducing fluorescent intensity responses. The effect is an apparent increase in soil adsorption, which may account for the observed data. If the amount of obscurity can be estimated, a more accurate isotherm solution can be constructed which compensates for the increase in optical density.

The application of a constant to the fluorescent readings was shown to compensate for the obscurity cause by the colloids in the supernatants. A factor of 5.6 was determined to be the correction, which when applied to the fluorometric readings (Cr) in the FRVC model, provided results that correlated more closely to the GC-derived values. This factor estimated the reduction in excitation light intensity through the equation:

$$\frac{I_o}{I} = 5.6 \qquad (12)$$

where I_o is the original light intensity and I is the colloid obscured intensity. When this factor was applied to the existing fluorescent data, a new FRVC model was constructed (1/n=0.871, log K=-3.077). As a result, in Table 6, when the new FRVC-derived values are compared to GC-derived values the models accuracy greatly increases (Co = 6.80 mg/l and q' = 0.85 mg/kg). A 4.62% difference between initial concentrations was observed and only a 20.14% difference in soil concentrations occurred.

The experimental results from the GC analysis demonstrated that the fluorometric method of analysis was not an accurate method for estimating solids concentration without first compensating for optical density changes in the supernatant. The fluorometric method of analysis did exhibit good precision by providing data for the Freundlich model which required only the multiplication of a single factor (over six orders of magnitude) to make the model both accurate and precise.

Rhodamine Isotherms

Since the hydrocarbon experimental results showed good empirical correlations, and the fluorometric method to determine surface concentrations demonstrated a degree of accuracy, the method to estimate soil partitioning for rhodamine proceeded in a similar manner. However, based upon the R^2

values for rhodamine in Table 6 the Langmuir (low concentration) isotherm was chosen as the better empirical model over the Freundlich isotherm.

The Langmuir model offered the opportunity to discover information about the binding energies and adsorption maximum that rhodamine demonstrated in the presence of different adsorbents. The binding energy of Shelbyville sand was found to be slightly higher than the Arkansas River sand, however Shelbyville sands adsorptive capacity was much greater.

The Langmuir isotherm for rhodamine in Arkansas River sand (Figure 26) relates the slope of the plot to the adsorption maximum and calculated as 544 ($1/B_2 = 0.00184$). The Y intercept, related to the binding energy, calculated as 0.056 ($1/B_1B_2 = .03257$). The Langmuir isotherm for rhodamine in Shelbyville sand (Figure 27) had an adsorption maximum of 625 ($1/B_2 = 0.0016$). Its binding energy calculated as 0.06 ($1/B_1B_2 = 0.00265$). Therefor Shelbyville sand had a higher adsorption maximum but almost the same binding energy as the Arkansas River sand.

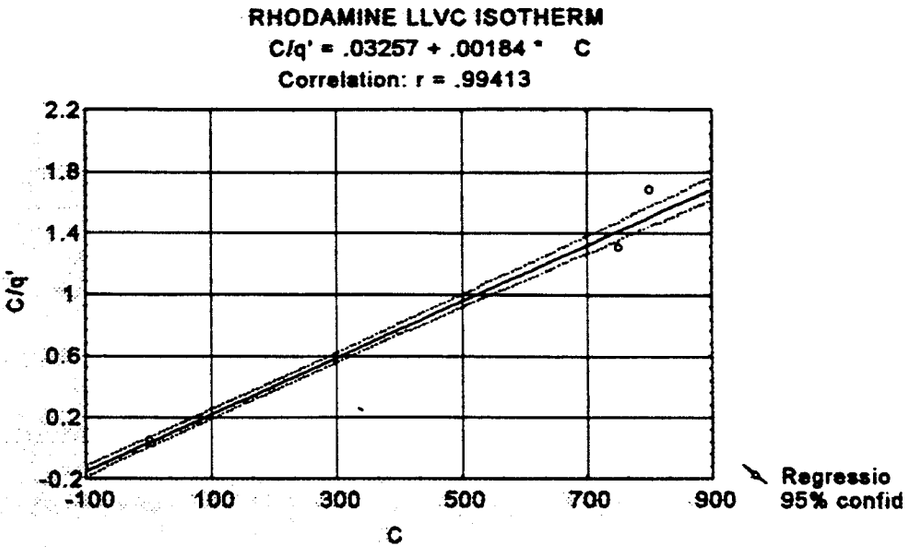

Figure 26. Rhodamine in Arkansas River Sand Isotherm

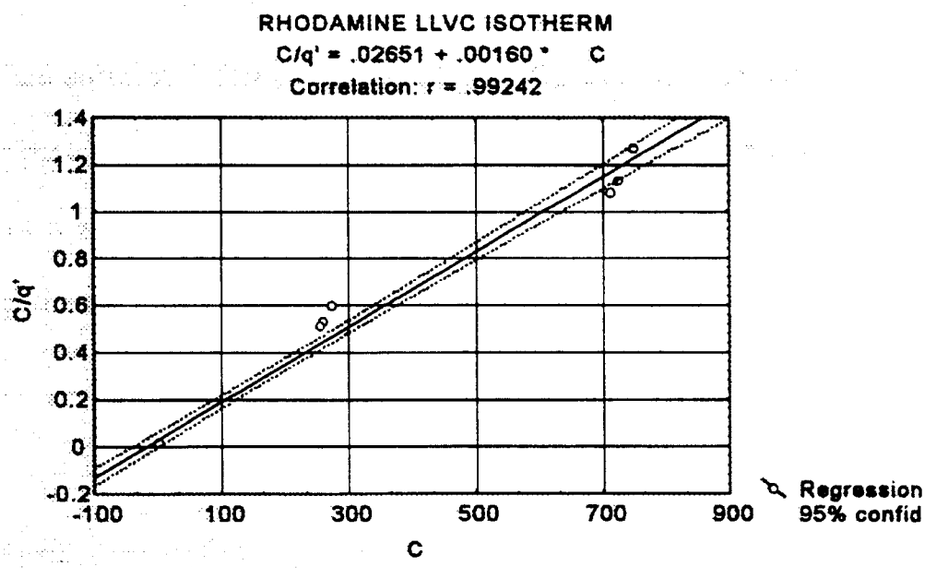

Figure 27. Rhodamine in Shelbyville Sand Isotherm

SOLID-PHASE FLUORESCENCE

One of the main objectives of the present study was to determine the influence that adsorbent physical properties had on the surface responses of a fluorescent adsorbate. The liquid-phase data served to verify the methods used to estimate rhodamine surface concentrations which could not otherwise be determined by conventional methods of analysis (i.e., GC analysis).

Karickhoff *et al.* (1979) reported that a higher concentration of solute will partition in order of preference onto soil's: (1) organic fraction, (2) fines, and (3) mineral surfaces. The photograph in Figure 28 illustrates solid-phase fluorescence under ultraviolet stimulate. It demonstrates variable fluorescent intensities on adsorption sites surrounding a single Shelbyville sand grain in an ethoxylate solution. The fines are brightly fluorescent. Small amounts of organic material which coat portions of the particle surface emit a dull yellow fluorescence and exhibit a quenching effect. The lowest levels of fluorescence exist on the particles surface.

Soil Analysis

Sieve analyses provided particle size distributions within each soil type. The dry sieve analysis of Arkansas River sand (Figure 29) represents the percentage that each fraction retained on the corresponding sieve. A wet sieve analysis (Figure 30) was performed on the same sand to characterize each fraction more accurately. Differences between the wet and dry sieve analyses provided additional information that indicated the quantity of mobile grains made available by the flushing action of a wet sieve procedure. A comparison of the two sieve analyses indicated that the wet sieve fractions passing sieve No. 200 (< .08 mm) had increased 26% (from 19% to 45%) over the dry sieve analysis; while the wet mass retained on larger than sieve No. 60 (> 0.25 mm) decreased 18% (from 24% to 6%). An increase of the pan material percentages after wet sieving demonstrated that a large percentage of the fines were available to move off the surfaces of larger particles. This indicated that the wet sieved fractions were more homogeneous within each gradation by eliminating the finer fractions.

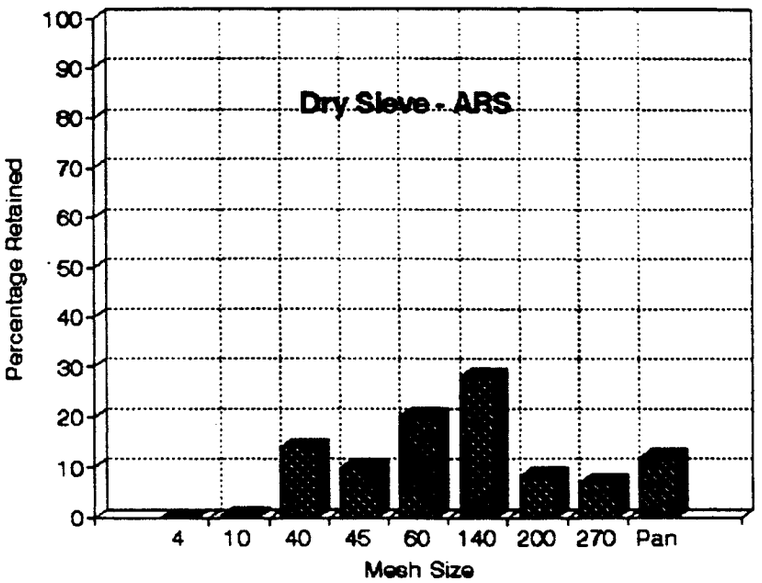

Figure 29. Arkansas River Sand Dry Sieve Analysis

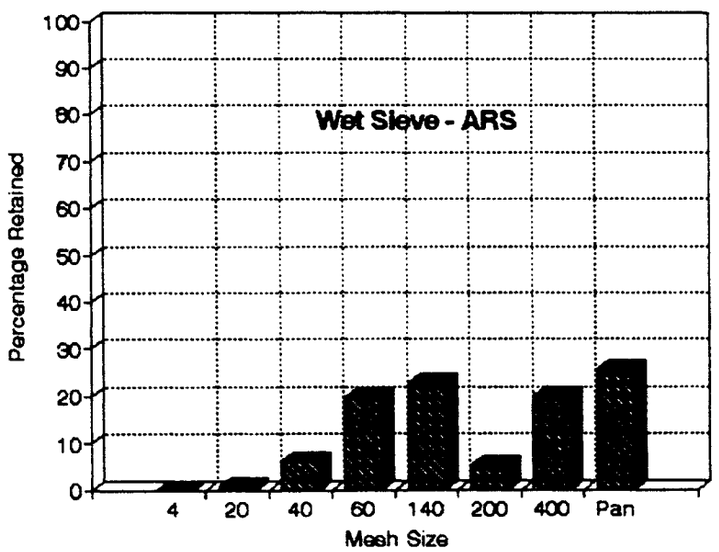

Figure 30. Arkansas River Sand Wet Sieve Analysis

In the dry sieve analysis of Shelbyville sand (Figure 31), over 40% of the soil was shown to be retained on Tyler sieve No. 140 (0.106 mm) and 22% was retained on sieve No. 60 (0.250 mm). A wet sieve analysis performed on the same sand (Figure 32) demonstrated that the largest portion (> 60%) of the soil was retained between Tyler sieves No. 60 and No. 140, while the percentage of particles smaller than sieve No. 200 (< .08) increased from 10% to 21%. Thus a similar migration of fines was consistent for both the Arkansas River sand and the Shelbyville sand.

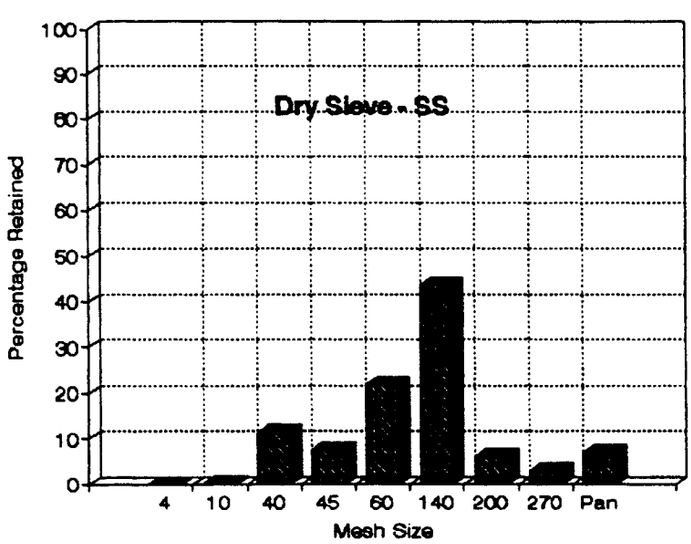

Figure 31. Shelbyville Sand Dry Sieve Analysis

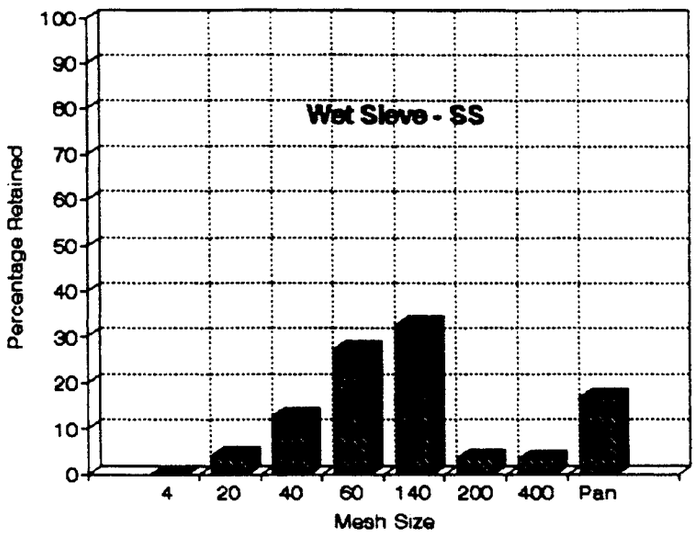

Figure 32. Shelbyville Sand Wet Sieve Analysis

Table 7 lists the surface areas for each soil and each gradation as determined by Micromeritics. Surface areas increased with decreasing grain sizes on a per gram basis. The pan sized material possessed the greatest surface area per gram of material.

TABLE 7

B.E.T. MEASURED SOIL SURFACE AREAS

	Soil Type	
Gradation	ARS (m2/g)	SS (m2/g)
40	0.410	0.700
60	0.210	0.530
140	1.000	0.630
200	1.430	1.430
270	1.790	NA
Pan	2.250	NA

Mineralogy Inc.'s soil mineralogy analysis is provided in Table 8. The mineralogy of the two soils were very similar. Both were quartz dominated. ARS however, had more than twice the total feldspar (14%) of SS (5%), while most other minerals were found to be present at less than 1%.

TABLE 8

SOIL MINERALOGY (%)

Mineral	ARS	SS
Quartz	79.000	92.000
Plagioclase Feldspar	6.000	2.000
K-Feldspar	8.000	3.000
Calcite	1.000	
Dolomite	1.000	1.000
Siderite	1.000	Trace
Gypsum	Trace	
Magnetite		1.000
Hematite		Trace
Kaolintite	1.000	Trace
Illite	1.000	Trace
Illite/Smectite	2.000	1.000
Total	100.000	100.000

Table 9 list adsorbent characteristics. Average grain size diameters and number of grains per gram of soil are listed under the "General" heading. The table lists the organic content for Arkansas River sand and Shelbyville sand over six gradations. Finally, three moisture conditions as well as pH values are also listed in the table.

The accumulation of organic content in the smaller gradations of the Shelbyville sand correlated with the findings of Karickhoff *et al.* (1979) who demonstrated K_{oc} increased in the silt sized gradations. The finest fractions of Shelbyville sand also contained the greatest percentages of organics. Tyler

sieve No. 270, for example, retained particles that contained 38% organics, while particles from sieve No. 60 contained only 4% organics. An increase in moisture holding capacity was also consistent with an increase in organics which suggested the organics held most of the water.

TABLE 9

ADSORBENT CHARACTERIZATION

	Sieve #					
	40	60	140	200	270	<270
			GENERAL			
Sieve size (mm)	0.430	0.250	0.110	0.080	0.053	<0.05
[a]Avg. Dia (mm)	0.900	0.380	0.120	0.110	0.070	0.050
[b]# Part. / gram	1,006	19,066	404,459	635,672	1,871,878	8,106,169
			ARS			
Organics (%)	0.000	0.000	0.000	0.000	0.000	0.000
Max. Moist. (%)	17.330	18.500	17.930	19.730	18.000	22.070
Med. Moist. (%)	1.020	3.160	3.650	5.200	5.430	8.410
Min. Moist. (%)	0.490	0.180	1.190	0.290	1.550	1.270
[c]pH (2:1)	7.770	7.570	7.760	7.820	7.620	7.560
			SS			
Organics (%)	13.400	3.580	8.130	26.830	38.020	43.640
Max. Moist. (%)	32.430	24.560	23.630	49.910	59.730	62.370
Med. Moist. (%)	13.730	7.320	12.670	31.560	46.780	50.340
Min. Moist. (%)	1.210	1.160	2.330	2.250	3.870	4.260
[c]pH (2:1)	7.300	7.530	7.670	7.700	7.400	7.800

a Malvern Particle Sizer

b Appendix L

c 2 parts liquid to 1 part soil

Equipment Influences on Soil Fluorescence

Knowledge of the soil characteristics coupled with the equipment's mechanical properties provided a truer picture of fluorescent measurements from soils. The key to an accurate measurement of surface fluorescence was to first determine the quantity of soil surface area exposed in the illuminated rectangle on the sample holder (see Figure 6, Chapter III).

Three assumptions were necessary to estimate the exposed surface area of the soil: (1) only a single particle layer was assumed to be detectable while on the sample holder, (2) the number of particles which fit into the illuminated rectangle were estimated by assuming each had a spherical shape, and (3) the spherical particles within the illuminated rectangle were assumed to be packed neatly in rows and columns. Once the surface area of a single particle was established in a gradation, the total soil surface area exposure in the illuminated rectangle then was estimated.

One further assumption addressed particle orientation relative to the lamp source. Portions of the soil surfaces were immediately eliminated as contributing to fluorescence because of shielding from the lamp source. The bottom half, or 50% of each particle, were out of the excitation radiation's path and considered dead area. Another 25% was eliminated because of the 90° orientation between the excitation radiation and the emission radiation. Any rhodamine which was on the remaining 25% soil surface, but not in the direct path of the excitation radiation, also did not contribute to fluorescent

intensity responses. Chemicals adsorbed within interior adsorption sites on granular surfaces, for example, most likely did not contribute to the overall fluorescent intensity response. It was reasoned that on a gross scale less than 25% of the total surface area measured can actually be labeled as "effective" soil surface area (ESA) in soil fluorometry. Therefore 25% of the measured surface area was considered a possible source for fluorescent signal contributions from rhodamine adsorbed to soil surfaces.

Table 10 demonstrates how the exposed surface areas changed through different gradations based upon the above assumptions. As grain sizes decreased the number of grains-per-gram and the surface area-per-gram increased. The surface area-per-grain decreased, however, with decreased grain sizes. This created an optimum surface area in the ARS200 gradation. This was the grain size which fit the most granular surface area into the fixed area of the illuminated rectangle.

The ARS200 gradation fit 4,768 particles in the illuminated window, had 10,728 mm^2 of total surface area and exposed 2,682 mm^2 of effective surface area. As a result of particle packing, ARS60 exposed the least amount of effective surface area at 1,290 mm^2, even though it retained the highest surface area per grain at 11.22 mm^2.

TABLE 10

ILLUMINATED WINDOW GEOMETRY[a]

Gradation	Grain (Grain/g)	Bet SA (m^2/g)	SA/grain (mm^2)	Grains (Grain/Win)	SA/Window (mm^2/Win)	ESA/Window (mm^2/Win)	Measured[b] (v-nm)
ARS60	19,066	0.210	11.22	460	5,161	1,290	25.26
ARS140	40,445	1.003	2.48	3,532	8,759	2,189	26.39
ARS200	635,782	1.429	2.25	4,768	10,728	2,682	36.67
ARS270	1,871,878	1.793	0.96	9,864	9,469	2,367	8.68
ARSPAN	8,106,169	2.251	0.28	25,958	7,268	1,817	6.08

a Appendix A

b Co 5mg/l rhodamine spike, 8g soil, @ field cap.

Grain Size Influences

Soil grain sizes and their corresponding effective surface areas were found to be significant factors in solid-phase fluorometry. The results from Table 10 suggested that if the FL-750 were truly a surface measurement device, the largest fluorescent responses should come from the gradation with the largest effective surface area i.e., ARS200. The "measured" fluorescent intensities do indeed peak at the ARS200 gradation. These measurements verified a direct correlation between surface area and measured intensity responses. It can be said that medium grain sizes fit together to form an optimum packing within the illuminated rectangle of the sample holder by exposing the greatest amount of surface which resulted in maximum responses from the adsorbed rhodamine. However, the differences in measured

intensities between gradations did not correlate directly with the differences in effective surface areas between gradations.

Surface Geometry of Soil Particles

On a gram-per-gram basis smaller particles were more efficient at removing rhodamine from the solution when organics are not present. Results in Table 11 indicate that the ARS60 gradation in a 2 gram CMBR experiment removed 10 ug rhodamine/kg soil while the ARS270 gradation removed 19 ug rhodamine/kg soil. However, on an available surface area basis the larger grains are more efficient at attracting rhodamine out of solution. The ARS60 gradation in the 2 gram CMBR experiment removed 48 ug rhodamine/m^2 of surface area while the ARS270 gradation removed just 11 ug rhodamine/m^2 of surface area. This implied that the smaller grains removed more rhodamine from solution simply because surface areas were greater per gram of soil. If equal amounts of surface area were made available between the two gradations, rhodamine would have partitioned preferentially onto ARS60 because it offered more attractive adsorptive sites.

The data supports the notion that changes in surface concentrations between gradations did not correlate directly with the changes in measured intensity responses. For example, the results in Table 11 demonstrate that in the 2 gram CMBR experiment, the greatest measured intensity response came from the ARS140 gradation (47.79 v-nm) but did not correspond to the

highest surface concentration from the ARS60 gradation (48 ug/m^2) as one might expect. High surface concentrations did not always mean high fluorescent responses. Surface responses depended upon where the rhodamine adsorption sites were located. Also noteworthy in the data from Table 11 was the relationship between soil concentrations on a surface area basis (q) versus a mass basis (q'). ARS60 had the highest surface concentration of rhodamine at 48 ug/m^2 but the lowest soil mass concentration at 10 ug/kg.

As a means to quantify some of these discrepancies between the calculated surface concentrations (q and q') and the measured fluorescent responses, the terms "fitting factor" and "apparent" rhodamine mass are introduced in Table 11. The fitting factor was employed as a method to quantify the percentage of rhodamine that partitioned onto surfaces shielded from the excitation radiation (and therefore not detectable). An apparent mass was calculated to normalize surface concentrations by removing the effects of grain size and the soil particle arrangement within the illuminated window. The "apparent" mass was characterized as the mass of rhodamine adsorbed onto the effective surface area (25% of total area) as if the particle surface were a smooth sphere.

TABLE 11

GRAIN SIZE SENSITIVITY[a]

Gradation	q (ug/m²)	q' (ug/kg)	Measured (v-nm)	Apparent (ug)	Fitting Factor	Undetect. (%)
			2 g of Soil			
ARS60	48.000	10.000	18.690	0.062	0.191	80.900
ARS140	14.000	14.000	47.790	0.031	1.000	0.000
ARS200	12.000	18.000	44.490	0.032	0.921	7.900
ARS270	11.000	19.000	29.760	0.026	0.724	27.600
ARSPAN	8.000	18.000	15.090	0.015	0.658	34.200
			8g of Soil			
ARS60	16.000	3.000	25.260	0.021	0.267	73.300
ARS140	5.000	5.000	26.390	0.011	0.533	46.700
ARS200	3.000	5.000	36.670	0.008	1.000	0.000
ARS270	3.000	5.000	8.680	0.007	0.267	73.300
ARSPAN	2.000	5.000	6.080	0.004	0.356	64.400

a Co 5 mg/l rhodamine spike @ Field capacity

The fitting factor essentially reduced the effective surface area used to estimate the apparent adsorbed rhodamine mass. It forced the apparent mass to match the trends in the measured fluorescent responses. A deviation between the apparent surface mass and the measured intensity response (utilizing a surface measurement device) signified that a portion of the rhodamine had adsorbed onto areas not available for detection, i.e., dead space in the effective surface area. Dead space was characterized as shadows cast by surface irregularities, etch pits, porosity or even the effects of

multilayering. In this manner, the fitting factor was an indication of the surface area where rhodamine had adsorbed but was not detectable.

In the calculations, the fitting factor was considered unity at the gradation with the highest measured fluorescence. This gradation was considered the standard gradation containing smooth spheres where 25% of the adsorbed mass was available for detection. Fitting factors for all other gradations became a fraction of the standard gradation's and an indirect measure of the adsorbed yet unmeasurable rhodamine mass. Comparisons of fitting factors were made between gradations as a means to estimate the mass of rhodamine adsorbed but obscured from detection.

The fitting factor was determined from the following equation:

$$FF = \frac{I_i C_s}{I_s C_i} \tag{13}$$

where FF equals the fitting factor, I_i equals the fluorescent intensity of gradation of interest (v-nm), I_s equals the fluorescent intensity of the standard gradation (v-nm), C_s equals the apparent concentration of the standard gradation (ug), and C_i equals the apparent concentration of the gradation of interest (ug).

From the 8 gram batch experiment in Table 11, the fitting factor was determined as follows:

$C_s = 0.008$ ug

C_i = 0.021 ug

I_t = 36.67 v-nm

and I_i = 25.26 v-nm

therefore $FF = \frac{25.26 \bullet 0.008}{36.67 \bullet 0.021} = 0.267$

When the fitting factor was multiplied by the apparent surface mass, a detectable surface mass was calculated. For example in the ARS60 gradation:

0.267 x 0.021 (ug) = .0056 (ug)

or 0.0056 ug rhodamine was the exposed mass available for detection which resulted in 73% (0.021-0.0056/0.021) of the adsorbed rhodamine mass left unmeasurable on surfaces not reachable by the excitation light.

If the majority of the adsorption of rhodamine took place within unmeasurable surface locations, the fitting factor was low. A low fitting factor indicated a large adjustment was necessary to bring the apparent (calculated) surface concentrations in line with the measured results. As an example, from Table 11, the ARS60 had double (0.062 ug) the apparent concentration of the ARS140 (0.031 ug). Yet, at the same time, ARS60 responded with less than half of the fluorescent intensity (18.69 v-nm) of ARS140 (47.79 v-nm). Based upon the apparent concentrations however, the expected intensity responses from ARS60 should have been double ARS140's.

Application of a 0.19 fitting factor meant that 81% (1-0.19) of the available rhodamine mass on the surface of ARS60 was not detectable. By design, high fitting factors that approached unity indicated a small adjustment was necessary to the effective surface area to emulate the measured fluorescent intensities.

In a comparison between variable adsorbate mass batch experiments using the fitting factor, additional information about preferential adsorption sites was gathered. In the 2 gram ARS60 batch experiment 81% of the adsorbed rhodamine mass was not detected. While in the 8 gram ARS60 batch experiment 73% of the adsorbed rhodamine mass was not detected. It can be said that in high or low solids concentrations rhodamine appeared to migrate to interior adsorption sites within the grains regardless of the mass of the adsorbent.

From Table 11, a comparison between the smaller grains of the ARS270 gradation resulted in a different observation. The data indicates that in the 2 gram CMBR only 28% of the rhodamine mass was unmeasurable. However, in the 8 gram CMBR, 73% of the rhodamine mass was unmeasurable. A decrease in measurable adsorbed rhodamine with increasing adsorbate mass measured over the same surface area indicated that preferential adsorption occurred mostly on interior sites of the 8 gram CMBR experiment. When fewer interior adsorption sites were available (2 gram CMBR) other less favorable sites on the particle surfaces became filled and resulted in higher

surface fluorescence. On the contrary, when more interior site were available (8 gram CMBR) the interior sites had the capacity to adsorb most of the rhodamine which resulted in lower surface fluorescence. As a result of these observations, surface fluorometry became a method to estimate surface roughness and the location of adsorption sites based upon the differences between the measured fluorescence and calculated surface concentrations. Rough, pitted, etched or porous surfaces resulted in less fluorescence if preferential adsorption sites were located on the interior surfaces they created.

A large degree of surface pitting in the ARS140 gradation (Figure 33) contained preferential intragranular adsorption sites. It was hypothesized that interior adsorption sites within the pitted surfaces caused a measured decrease in fluorescent responses by shielding excitation light from the adsorbed rhodamine. The overall effective surface area was high for ARS140 particles but the actual detectable surface areas (that which was outwardly visible) was reduced by the presence of the etch pits.

Figure 33. SEM of Clean Arkansas River Sand at Gradation 140

The data supplied here could further explain the solids concentration effect reported by Lick (1992) and McKinley (1991). Lick (1992) attributed the solids effect to the lessening of the interior surface areas of cohesive sediments when exposed to the spiked solutions. Lick (1992) suggested that an individual grain had the highest adsorption rate. Adsorption rates decrease with increasing particle cohesion, thereby denying available surface area to the solute for solids partitioning. A decreasing adsorption rate with increasing solids concentration was dependent upon the availability of preferential adsorption sites and their corresponding locations within the cohesive mass.

The same logic can be applied to grains on an individual basis and therefore, gradations within a heterogeneous soil. The rate of adsorption was dependent upon the location of preferential adsorption sites on the soil

surfaces (internal and external). At high solids concentrations in a homogeneous soil such as ARS140, an abundance of preferential sites were available. However, if these abundant adsorption sites exist within the interior of the grains (or organics), adsorption becomes a function of longer solute mass transfer rates from solution to solid surfaces. Therefore, if equilibrium had not been reached before measurement, the solute would not have had the time to adsorb onto the preferential internal sites. Rhodamine, in this situation, would have been in the process of migrating to these interior sites at the time of measurement and would demonstrate a lower rate of adsorption. Evidence of this was provided by the equilibrium rate study (see Figure 19). Rhodamine in SS demonstrated a slower adsorption rate in the first 24 hours than rhodamine in ARS. The organics in SS not only provided a higher adsorption capacity but also offered higher internal resistance to rhodamine migrating to the preferential interior adsorption sites. In a conventional GC measurement, a solute extraction before equilibrium had been reached would capture the system in an incomplete mass transfer resulting in an apparent lower adsorption rate.

Moisture Content

Fluorescent intensity responses from soils were strongly dependent upon moisture content. Effective surface area exposure to the excitation light was dominated by either the soil's wetting fluid, or in dry conditions, the particles

surface features. The concentration of interstitial moisture had a large impact on fluorescent responses under wet conditions, particularly within the smaller gradations. Moisture held within the soil's pore space increased the effective surface area and made moisture itself the dominant source of fluorescence, not the rhodamine coated soil surfaces.

Effective surface area had been calculated as a function of the BET surface areas. However, in terms of surface area actually available to the detector, it should be amended to compensate for the dead surfaces housed within intragranular surface roughness. The application of a fitting factor was an attempt to account for these cryptic areas. Moisture added to dry soils, however, increase effective surface area by smoothing roughened surfaces with fluids and filling in the gaps created by pitting. The resultant fluorescent intensities became mostly dependent upon the wetting fluid's concentration as opposed to the concentration of the rhodamine adsorbed surfaces.

As an example to illustrate moistures gross effect on effective surface area, assigning spherical particles a diameters of 0.122 mm (ARS140) and 3,532 particles (rows and columns, one particle deep) in the illuminated window with 25% (definition of ESA) maximum surface exposure, 41.28 mm^2 of surface area was available to the detector. If moisture were added to coat the grains and fill void spaces between particles, the effective surface area increases to at least that of the entire illuminated rectangle or 52.88 mm^2, a 21% increase. Therefore, the presence of a wetting fluid not only adds to the

detectable area within the illuminated rectangle but also could change the dominant source of fluorescence, from that of a solid surface, to that of the liquid wetting the solid surface.

Changes in soil moisture influence the effective surface area of individual soil grains (Figure 34). In dry soil conditions, the effective surface area is reduced. Fluorescent responses in this case are entirely due to rhodamine adsorbed to the soil surfaces. In dry conditions, soil surface concentrations became the controlling factor influencing fluorescent intensity responses.

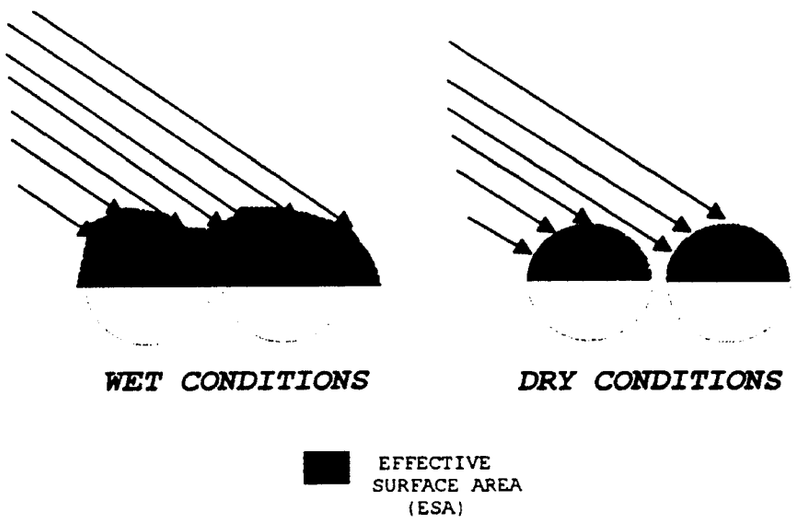

Figure 34. Moisture Coating and Effective Surface Area

Wet soils created two possible cases that influenced the fluorescent response from the effective surface area. The first case involves high residual

solution concentrations acting as the soil wetting fluids. In this case, soil adsorption of rhodamine has maximized yet left high residual concentrations of rhodamine within the wetting fluid. Wet soil measurements in this condition exhibited high fluorescent intensities primarily in response to the wetting fluid.

This notion is supported in Figure 35 which illustrates intensity response curves for soil containing high rhodamine surface concentrations estimated to be 247 ug/m^2 (490 mg/kg) under both saturated and dry soil moistures. The highest overall response at 580 nm originated from the fluorescence of the high concentration of rhodamine in the wetting fluid. As the moisture content was reduced and the high concentration soil surfaces were exposed to the detector, the fluorescent response lowered. Lower moisture contents had a quenching effect on the soil's fluorescent response. Another noticeable feature was that the fluorescent response of dry soil from 540 to 600 nm was totally eliminated, shifting the location of the peak intensity response from 580 nm to 620 nm.

Low residual concentrations of rhodamine in the wetting fluid masked the potential responses of the higher surface concentrations. In this case, the initial concentration of rhodamine was sufficiently low and the affinity for soil was sufficiently high that most of the rhodamine had partitioned onto the soil, leaving behind a low concentration wetting fluid. Figure 36 illustrates the composite response to wetting fluid around a soil (ARS140) with low surface concentrations estimated to be 1 ug/m^2. Increases in moisture reduced the

fluorescent response due to the dominance of the low concentration wetting fluid. A fluorescent scan of the wet soil in this case exhibited low measured intensities. The larger effective surface area created by low concentration moisture overshadowed the surface responses making them unmeasurable. Measurement of the soil after drying revealed a slight increase in intensities which resulted from the exposure of adsorbed rhodamine on the surfaces.

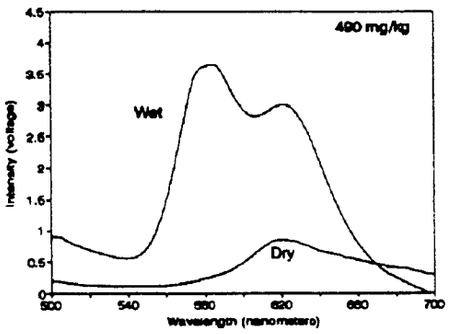

Figure 35. High Rhodamine Soil Concentration, Wet & Dry Conditions

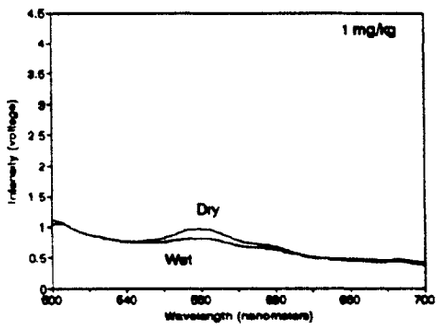

Figure 36. Low Rhodamine Soil Concentration, Wet & Dry Conditions

Results in Table 12 demonstrate that high moisture and high residual wetting fluid concentrations combined to result in the highest fluorescent responses. In addition, low wetting fluid concentrations coupled with moderate soil adsorption in high soil moistures attenuated fluorescent responses from soil surfaces. At saturated soil moisture conditions, a high

residual wetting fluid concentration of 792,000 ug/l and a high surface concentration of 1,069 pg resulted in the highest measured intensity response (238 v-nm). As moisture was lost, the measured fluorescent intensity reduced significantly (29.99 v-nm). When the wetting fluid concentration lowered to 352 ug/l (surface concentration of 22.80 pg), a fluorescent intensity of 21 v-nm was measured, while the dry soil measured a higher intensity of 39 v-nm. Removal of the low concentration wetting fluid increased the measured fluorescent intensity responses from a low concentration soil.

TABLE 12

MOISTURE EFFECTS[a]

Cr (ug/l)	Surface (pg)	Moisture		
		Saturated	Field Cap.	Dry
792,000.000	1,069.323	238.213	98.030	29.990
7,600.000	344.239	137.277	48.180	62.837
352.000	22.801	21.350	40.450	39.210
33.000	2.179	3.497	17.900	8.233
3.000	0.218	1.383	0.900	0.223
0.450	ND	ND	ND	ND

a Rhodamine in ARS140 gradation

When detectable rhodamine masses are plotted against measured intensity responses in dry soils (Figure 37), a quenching effect was observed at high adsorbed rhodamine masses (> 0.40 ug). This type of behavior demonstrated

that elements of liquid phase fluorometry are also applicable to solid phase fluorometry. Much like liquid fluorometry, inner filter effects were observed to influence surface fluorometry as well. This meant that increased surface concentrations did not necessarily mean a more intense fluorescent response.

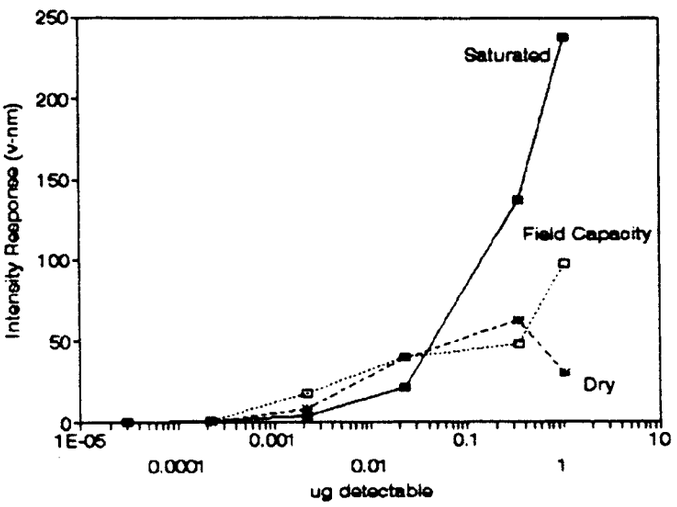

Figure 37. Moisture Effect on Rhodamines Detectability in Soil

Table 13 provides the results from spiking variable soil gradations with a single concentration (5 mg/l) rhodamine solution. Measured fluorescent intensities under wet and dry soil conditions were compared to unmeasurable percentages of adsorbed rhodamine. These results offered further evidence of low concentration wetting fluids attenuating fluorescence. In addition, the

data offered insight into how a wetting fluid coated grains differently according to their size.

TABLE 13

FLUORESCENT INTENSITY RESPONDING TO CHANGES IN MOISTURE

Gradation	[a]Cr (mg/l)	Field Cap. (v-nm)	Dry (v-nm)	Undetectable[b] Field Cap. (%)	Dry (%)	Change (%)
ARS60	1.550	25.260	33.240	73.330	77.140	-3.810
ARS140	0.193	26.390	38.380	46.670	50.000	-3.330
ARS200	0.047	36.670	48.750	0.000	14.290	-14.290
ARS270	0.122	8.680	49.200	73.330	0.000	73.330
ARSPAN	0.019	6.080	22.870	64.440	14.286	50.150

a Co = 5 mg/l

b Estimated by fitting factors

A comparison of the undetectable portions of rhodamine surface concentrations in Table 13 revealed significant fluorescent increases after drying in the smaller gradations. The change of undetectable rhodamine in the larger gradations (ARS60, ARS140 and ARS200), under wet or dry conditions, remained fairly constant. After drying the smaller gradations (ARS270 and ARSPAN) however, the percentage of detectable rhodamine increased significantly. A wet ARS270 gradation emitted 8.68 v-nm. The same dry gradation increased six fold emitting 49.20 v-nm. These results

suggested that the presence of moisture attenuated surface responses the most within the smallest gradations. Once the wetting fluid surrounding the smaller grains was removed, rhodamine adsorbed to the soil's surface significantly increased the measurable intensity.

This data demonstrated that the larger grain sizes retained a constant percentage of undetectable rhodamine in wet or dry soil conditions. This also suggested that in the larger gradations granular surface features were the controlling soil characteristic that influenced fluorescent responses, not moisture. The data indicated that the larger grains at field capacity (wet) were coated with a thin layer of moisture that left the excitation light less impeded in its path to the adsorbed rhodamine surfaces.

Within the smallest gradations, experimental results indicated that moisture had a larger impact on measured fluorescent responses. Significant increases in fluorescent intensities associated with the exposure of more surface area upon drying suggested that etch pits did not exist where rhodamine could adsorb and remain undetected. These increased intensities indicated adsorption sites remained on the particle surface for easy detection after drying. Therefore, indirect evidence was provided to indicate the absence of pitting and surface roughness within the smaller particle gradations. As evidence of this, an SEM of the ARSPAN gradation (Figure 38) demonstrates the absence of the surface pitting.

The overriding factor that controlled fluorescent responses within the smaller gradations was found to be moisture, not the surface roughness associated with the larger grains. Wetting fluids created a thicker boundary layer relative to grain size around these smaller grains. By virtue of its thickness and low concentration, this fluid attenuated fluorescent responses more on the smaller grains than that same wetting fluid around the larger grains.

Figure 38. SEM of ARSPAN Demonstrating Reduced Visible Surface Roughness

The BET measured surface areas of the smaller gradations were therefore more representative of the effective surface area as defined in this study. Adsorption of any fluorescent chemical onto the surface of these smaller gradations had a higher likelihood of being detected as long as the soil was dry. Surface roughness, etch pits, and granular porosity lowered effective surface area and also offered favorable interior adsorption sites for rhodamine. In surface fluorometry, the more porous surfaces observed in the larger gradations created by etch pits resulted in an undetectable portion of rhodamine that could not be recovered through drying.

Fluorescence Quenching

Metal Ions

The mechanisms which cause quenching in solutions have been well documented; inner filter effect, metal ions, oxygen, impurities, and temperature (Guilbault, 1973). Some of the same quenching mechanisms for solutions were found to be at work on mineral surfaces. Rhodamine is ionic and demonstrates sizable fluorescence quenching in highly polar environments (Wolfbeis, 1993). The results from a Kevex™ scan (Figure 39) was used to detect the presence of quenching elements on particle surfaces. Metal quenching ions of iron, aluminum, potassium and calcium, were all found to be present in the soils that were investigated.

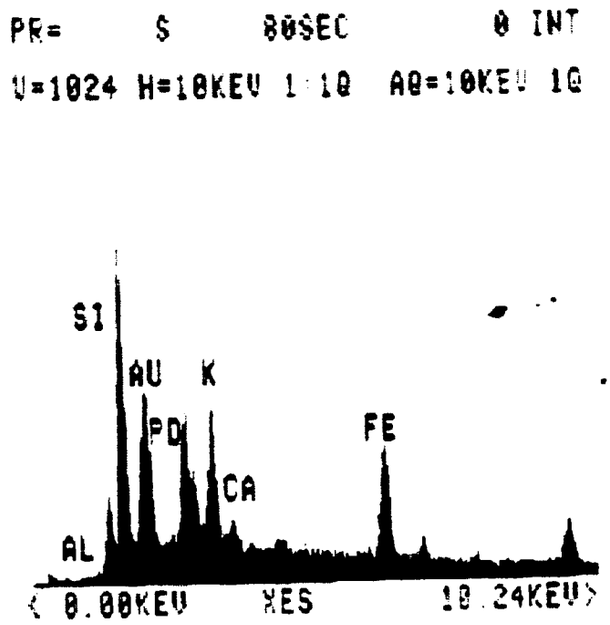

Figure 39. Kevex™ Scan of an Arkansas River Sand Grain

Organics

Fayahd (1990) reported that organics had a quenching effect on fluorescence in soil/hydrocarbon extracts as well. In a comparison between fluorescent rhodamine responses from Arkansas River sand (no organics) and the fluorescent responses from Shelbyville sand (high organics), the quenching effect reported by Fayahd was observed (Figure 40). A definite quenching of rhodamine responses was detected within the high organic soil (SS). In the most extreme case Arkansas River sand produced 65 v-nm at a surface

concentration. A reduction in fluorescence by a factor of 13 due to the presence of organics.

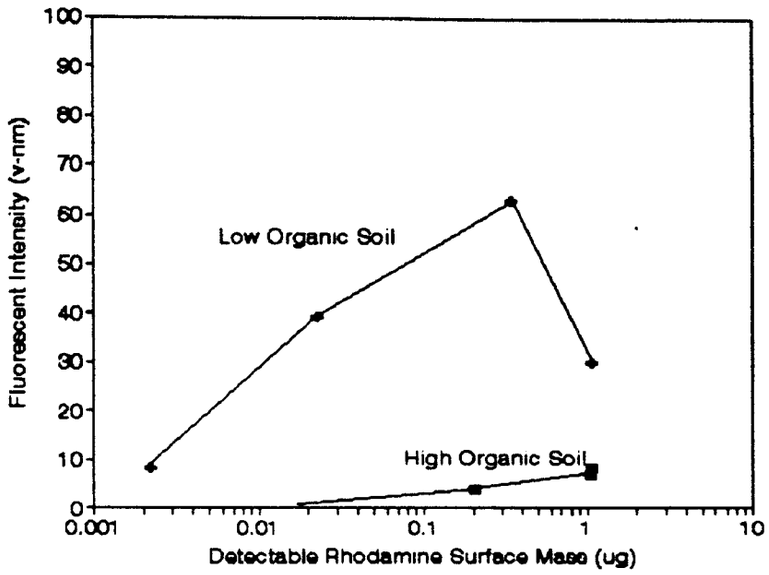

Figure 40. Dry Soil Fluorescence in Sands with Low and High Organics

Further evidence for quenching in the presence of organics is provided by the photograph in Figure 41. Soil grains present in the picture have what appear to be a dull fluorescence compared to the bright fluorescence from the free phase solution. Significant quenching is observed in the dark areas which corresponds to clumps of organic matter scattered among sand grains.

CHAPTER VI

SUMMARY AND CONCLUSIONS

Simulation of a direct fluoroimmunoassay was achieved through the adsorption of a fluorescent dye (Rhodamine B) onto soil surfaces. The fluorescent readings from these soils were found to be highly dependent upon changing soil conditions. Several of theses findings are important to the selection of the fluorescent (or phosphorescent) label which will be covalently bound to antibodies during the development of a direct soil fluoroimmunoassay.

Examination of the experimental data resulted in the following solid-phase fluorometry observations:

- Moisture content

  Fluorometric readings were most sensitive to the concentration of the soil's wetting fluids. In the absence of wetting fluids (or dry soil conditions), the fluorometer was sensitive to granular surface features and soil packing arrangements on the sample holder.

High moisture content in the form of wetting fluids containing high concentrations of rhodamine amplified signal responses. The moisture essentially wrapped each grain in an envelope of high concentration fluid and dominated the fluorescent signals returning to the detector. Wetting fluids containing low concentrations of rhodamine dampened signal responses. This condition actually contributed to light scattering interferences which added to a fluorescent-surface masking effect. The excitation light simply could not penetrate the shroud of liquid coating the grains to reach the adsorbed rhodamine.

In dry soil conditions, the measurement of rhodamine was quenched at high surface concentrations much like the inner filter effect observed in liquid-phase fluorescence. A limiting surface concentration was reached after which further concentration did not add to the fluorescent intensity response. In dry soil conditions where rhodamine surface concentrations were below the upper saturation levels, the intensity of the signal return was dependent upon the location of the soil adsorption sites. Cryptic or hidden rhodamine adsorbed to sites within etch pits were shielded from the excitation light and did not contribute to the fluorescent signal. In this sense the fluorometer became a way to estimate surface roughness. Smaller grains were discovered to contain fewer etch pits and therefore displayed more of the adsorb rhodamine from the surface when dry.

- Grain Size and Surface Area

Solid-phase fluorometry measures fluorescence from the surfaces of the adsorbent being investigated. It was observed that as total surface area under measurement increased with decreasing particle size, the signal responses decreased. This was because, on a gram-per-gram basis, rhodamine had adsorbed onto the finer particles in greater quantity. However, on a gram-per-m^2 basis, rhodamine concentration had actually decreased. A fixed sampling area and surface concentrations spread over a wider area combined to decrease signal responses as grain size decreased.

It was discovered that an optimum grain size packing in the measurement window occurred in grain sizes of 0.08 mm (sieve No. 200). This resulted in the maximum exposure of surface area by a single homogeneous gradation. The effective surface area exposed to the detector was however, reduced by the presence of irregular surface features found on the larger grains. This in effect, reduced outward (detectable) surface area and created the appearance of less adsorption when in fact they housed adsorption sites which were attractive to rhodamine.

- Quenching of Fluorescence

The primary source of fluorescence quenching came from the presence of organic matter in the soil. The combination of the adsorptive powers of organics and their quenching effects create areas for further research in how they will affect direct fluoroimmunoassays. Other sources of quenching included the orientation of the adsorbed rhodamine on the mineral surfaces. Rhodamine was modeled as a loosely attached molecule on a silica surface, adding to the quenching effect.

- Accuracy of Fluorometric Measurements

The accuracy of a fluorometric method for the estimation of surface concentrations was found to be dependent upon optical clarity of the supernatant solution (residual) with respect to the standard solution. Standard solutions are prepared in the absence of colloids. Therefore referencing supernatant fluid responses to their respective calibration curves required a correction for optical obscurity. Initially, results from a Gas Chromatography test of supernatant fluids did not correlate with fluorometric results performed in a parallel study. Being an optical method of analysis, corrections in the fluorometric readings were necessary to compensate for colloids in the supernatant fluids.

A method was discussed to compensate for the changes in optical density of the supernatant fluids. An iterative approach using the Freundlich isotherm parameters compensated for this potential source of error. The fluorescent response of residual solution concentrations were found to be attenuated by a factor of 5.6 due to the presence of colloids in solution. If corrections to the fluorescent responses for colloids are not made, an error by a factor of three in residual concentrations could result in an order of magnitude error in surface concentrations

- Adsorption

A comparison of adsorptive properties for Arkansas River sand and Shelbyville sand based upon Langmuir coefficients revealed that the binding energies were similar. However, the adsorptive capacity of organic rich Shelbyville sand was greatly enhanced.

Preferential adsorption sites in soils free of organics were found to be dependent upon surface features such as etch pits, surface roughness and intragranular porosity. Rhodamine was found to be attracted to the interior of these surface features and possibly subject to mass transfer rates controlled by internal resistance. Since the larger gradations contained more of these sites, mass transfer rates became grain size

dependent. Smaller gradation had fewer internal adsorption sites and therefore were only subject to external resistances in a mass transfer.

- Isotherms

Freundlich and Langmuir isotherms demonstrated good empirical correlation with the adsorption data measured by a fluorometer. The Freundlich isotherm, a chemisorption model, favored the nonionic nature of hydrocarbons. The Langmuir isotherm, a monolayering model, favored the ionic nature of Rhodamine B.

BIBLIOGRAPHY

Abdul, A. S.; Gibson, T. L.; and Rai, D. N. (1987). Statistical Correlations for Predicting the Partitioning Coefficient for Nonpolar Organic Contaminants Between Aquifer Organic Carbon and Water. *Hazardous Waste and Hazardous Materials, 4* (3), 211-222.

Aldrich Chemicals (1993). Personal Communication with Technical Support Service (FAX).

Berlman, I. S. (1971). *Handbook of Fluorescence Spectra of Aromatic Molecules.* 2nd ed., Academic Press, New York:, N.Y.

Briggs, G. G. (1981). Theoretical and Experimental Relationships between Soil Adsorption, Octanol-Water Partition Coefficients, Water Solubilities, Bioconcentration Factors, and the Parachor. *Journal of Agricultural Food Chemistry, 29,* 1050-1059.

Brown, D. S. and Flagg, E. W. (1981). Empirical Prediction of Organic Pollutant Sorption in Natural Sediments. *Journal of Environmental Quality, 10* (3), 382-385.

Brusseau, M. L.; Jessup, R. E.; and Rao, P. S. (1990). Sorption Kenitics of Organic Chemicals: Evaluation of Gas-Purge and Miscible-Displacement Techniques. *Environmental Science and Technology, 25* (5), 727-735.

Brusseau, M. L. and Rao, P. S. (1991). Influence of Sorbate on Nonequilibrium Sorption of Organic Compounds. *Environmental Science and Technology, 25* (8), 1501-1506.

Cheung, P. K.; Gee, S. J.; and Hammock, B. D. (1988). Pesticide Immunoassay as A Biotechnology. *American Chemical Society Symposium: Impact of Chemistry on Biotechnology*, Series 362. American Chemical Society, 217-229.

Chin, Y.; Peven, C. S.; and Weber, W. J., Jr. (1988). Estimating Soil/Sediment Partition Coefficients for Organic Compounds By High Performance Reverse Phase Liquid Chromatography. *Water Research, 22* (7), 873-881.

Chiou, C. T.; Porter, P. E.; and Schmedding, D. W. (1983). Partition Equilibria of Nonionic Organic Compounds between Soil Organic Matter and Water. *Environmental Science and Technology, 17* (4), 227-231.

Clesceri, L. S.; Greenberg, A. E.; and Trussell, R. R. (1989). *Standard Methods For the Examination of Water and Wasetwater*. 17th ed., American Publich Health Association, Washington, D.C.

Dragun, J. (1988). *The Soil Chemistry of Hazardous Materials*. Harzardous Materials Control Research Institute, Silver Springs, MD.

Ebert, K.; Ederer, H.; and Isenhour, T. L. (1989). *Computer Applications in Chemistry*. VCH Publishers, New York, N.Y.

Everts, C. J.; Kanwar, R. S.; Alexander, E. C., Jr.; and Alexander, S. C. (1989). Comparison of Tracer Mobilities under Laboratory and Field Conditions. *Journal of Environmental Quality*, 18, 491-498.

Fetter, C. W. (1988). *Applied Hydrogeology*. Merrill Publishing Co., Columbus OH.

Goodman, M. (1993). Molecular Probes, Inc. Personal Communication.

Guerin, W. F. and Boyd, S. F. (1992). Differential Bioavailability of Soil-Sorbed Naphthalene to Two Bacterial Species. *Applied and Environmental Microbiology*, 1142-1152.

Guilbault, G. G. (1973). *Practical Fluorescence: Theory, Methods and Techniques*. Marcel Dekker, Inc., New York, N.Y.

Guilbault, G. G. (1967). *Fluorescence: Theory, Instrumentation, and Practice*. Marcel Dekker, Inc., New York, N.Y.

Hall, C. H.; Deschamps, R. J.; and McDermott, M. R. (1990). Immunoassay to Detect and Quantitate Herbicides in the Environment. *Weed Technology*, 4, 226-234.

Hammock, B. D.; and Mumma, R. O. (1980). Pesticide Immunochemical Technology for Pesticide Analysis. *American Chemical Society Symposium: Advances in Pesticide Analytical Methodology*, Series 136. American Chemical Society, 321-352.

Harris, D. A.; and Bashford, C. L. (1988). *Spectrophotometry and Spectrofluorimetry*. IRL Press, Washington, D.C.

Haugland, R. P. (1993). Handbook of Fluorescent Probes and Research Chemicals. *Molecular Probes*. Molecular Probes, Inc., Eugene, Oregon.

Howard, P. H.; Boethling, R. S.; Jarvis, W. F.; Meylan, W. M.; and Michalenko, E. M. (1991). *Book of Environmental Degradation Rates*. Lewis Publishers, Inc., Chelsea, Michigan.

Howard, P. H. (1991). *Handbook of Environmental Fate and Exposure Data For Organic Chemicals*. Lewis Publishers, Inc., Chelsea, Michigan.

Hemmilia, I. A. (1991). Applications of Fluorescence in Immunoassays. John Wiley & Sons, Inc., New York, N.Y.

Hurtubise, R. J. (1990). *Phosphorimetry: Theory, Instrumentation, and Applications*. VCH Publishers, Inc., New York, N.Y.

Ingle, J. C., Jr. (1966). *The Movement of Beach Sand: An analysis using fluorescent grains*, American Elsevier Publishing Company, New York, N.Y.

Karickhoff, S. W.; Brown, D. S.; and Scott, T. S. (1979). Sorption of Hydrophobic Pollutants on Natural Sediments. *Water Research, 13*, 241-248.

Karickhoff, S. W. and Bailey, G. W. (1973). Optical Absorption Spectra of Clay Minerals. *Clays and Clay Minerals*, 21, 59-70.

Kodak Laboratory Chemicals Catalog No. 51 (1981). Eastman Kodak Co., Rochester, N.Y.

Lick, W. (1991). Physical Parameters and the Solids Concentration Effect in the Sorption of Hydrophobic Chemicals from Water. An unpublished paper. University of California.

Lieberman, S. H. (1993). Personal Communication.

Lieberman, S. H. and Apitz, S. E. (In press 1993). Real-Time *In Situ* Measurements of Fuels in Soil: Comparison of Fluorescence and Soil Gas Measurements. *Field Screen Methods for Hazardous Wastes and Toxic Chemicals*.

Mackay, D.; Shiu, W. Y.; and Ma, K. C. (1992). *Illustrated Handbook of Physical-Chemical Properties and Environmental Fate for Organic Chemicals*. Lewis Publishers, Inc., Chelsea, Michigan.

McKinley, J. P. and Everett, A. J. (1991). Experimental Investigation and Review of the "Solids Concentration" Effect in Adsorption Studies. *Environmental Science and Technology, 25* (12), 2082-2087.

Mikhail, E. H. and Briner, G. P. (1978). Routine Particle Size Analysis of Soils Using Sodium Hypochlorite and Ultrasonic Dispersion. *Journal of Soil Resourse*, 16 (2), 241-244.

Neff, J. M.; Langseth, D. E.; Graham, E. M.; and Smyth, A. H. (1992). Subsurface Transport of Non-BTEX Petroleum Constituents: Candidate Compounds. *Technical Report*. Arthur D. Little, Cambridge, MA.

Osipow, L. I. (1962). *Surface Chemistry*. Reinhold Publishing Corporation, New York, N.Y.

Rutherford, D. W.; Chiou, G. T.; and Kile, D. E. (1992). Influence of Soil Organic Matter Composition on the Partition of Organic Compounds. *Environmental Science and Technology, 26* (2), 336-340.

Rutherford, D. W. and Chiou, C. T. (1992). Effect of Soil Organic Matter on the Partition of Organic Compounds. *Environmental Science and Technology, 26* (5), 965-970.

Smettem, K. R. J. and Trudgill, S. T. (1983). An Evaluation of Some Fluorescent and Non-Fluorescent Dyes in the Identification of Water Transmission Routes in Soils. *Journal of Soil Science.* 34, 45-56.

Stave, J. (1992). Personal Communication Resulting from Trip to Stratigic Diagnostic Offices.

Schwalbe, M.; Dorn, E.; and Beyermann, K. (1984). Enzyme Immunoassay and Fluoroimmunoassay for the Herbicide Diclofop-methyl. *Jorunal of Agricultural Food Chemistry. 32*, 734-741.

Undefriend, S. (1962). *Fluorescence Assay in Biology and Medicine.* 3rd ed., Academic Press, New York, N.Y.

Van Emon, J. M. and Mumma, R. O. (1990). *Immunochemical Methods for Environmental Analysis.* American Chemical Society Symposium Series 442. American Chemical Society, Washington D.C.

Veenstra, J. N. (1992). Advanced Unit Operations. Class Notes.

Wadsworth, H. M., Jr. (1990). *Handbook of Statitical Methods for Engineers and Scientists.* McGraw Hill Publishing Company, New York, N.Y.

Weast, R. C. (1992). *CRC Handbook of Chemistry and Physics.* 70th ed., CRC Press, Boca Raton, FL.

Weber, W. J., Jr.; McGinley P. M.; and Katz, L. E. (1992). A Distributed Reactivity Model for Sorption by Soils and Sediments. *Environmental Science and Technology, 26* (10), 1955-1962.

Willard, H. H.; Merritt L. L., Jr.; Dean, J. A.; and Settle, F. A., Jr. (1981). *Instrumental Methods of Analysis.* 6th ed., D. Van Nostrand Company, New York, N.Y.

Wolfbeis, O. S. (1993). *Fluorescence Spectroscopy.* Springer-Verlag, Berlin, Germany.

APPENDIX A

EXAMPLE CALCULATIONS

EXAMPLE CALCULATIONS

Direct Measurements

Isotherm Construction

An example calculation of the soil concentration, q', is provided on a mass-per-mass basis directly from fluorometric readings utilizing the following eqaution:

$$q' = \frac{(C_o - C_r)(\text{mg/l}) \bullet \text{spike wt (g)} \bullet 1/1000\ (\text{l/g})}{\text{Sand wt. (g)}} \qquad \text{(units)}$$

therefore: $q' = \frac{\text{mg solute}}{\text{g sand}}$

From Table 16, in the ARS60 gradeand 2 grams sand, q' is computed as:

$$q' = \frac{(6.655 - 3.237) \bullet 8.077}{2.263 \bullet 1000} = 0.012 \text{ mg naphthalene / gram sand}$$

Substituting area for the 2.263 grams of sand, q becomes the soil concentration on a mass-per-m^2 basis

$$q = \frac{(6.655 - 3.237) \bullet 8.077}{0.485 \bullet 1000} = 0.057 \text{ mg naphthalene / m}^2 \text{ sand surface area.}$$

Indirect Measurements

FRVC Model (Hydrocarbon Adsorption)

An example calculation is provided utilizing the FRVC mathematical constants to determine predictability of the isotherm modeled versus measured values. If the CMBR is mass balanced, Co becomes a function of the solid (q) and residual solution concentrations (Cr) in the following equation:

$$C_o = \left[\frac{q\left(\frac{mg}{m^2}\right) \bullet \text{Tot. SA (m}^2)}{\text{Wt. Spike Sol. (g)}} \bullet 1000\left(\frac{g}{l}\right) \right] + Cr\left(\frac{mg}{l}\right) \qquad \text{(units)}$$

Equation 12 is used in conjuction with the optimum constants from Table 9 to estimate q from Cr:

$$\log q = b \log C_r + \log K$$

or

$$q = KC_r^b$$

Substituting the naphthalene constants, log K = -1.818 and b = 0.939 into the equation , Co is rewritten as a function of Cr only:

$$Co = \left[\frac{0.0152 \bullet C_r^{0.939}\left(\frac{mg}{m^2}\right) \bullet \text{tot.SA}\,(m^2)}{\text{Spike Sol. Wt. (g)}} \bullet 1000\left(\frac{g}{l}\right) \right] + C_r\left(\frac{mg}{l}\right)$$

Values from Table 17 for spike solution weight (8.46 g) and total surface area (4.19 m^2) are plugged into the equation while Cr is manipulated until the original Co has been reached:

$$Co = \left[\frac{0.0152 \bullet 6.10^{0.939} \bullet 4.19}{8.46} \bullet 1000 \right] \bullet + 6.10$$

therefore q = 0.086 mg/m2 and Co = 47.22 mg/l.

LLVC Model (Rhodamine Adsorption)

An example calculation utilizing the LLVC solution constants to determine predictability of the isotherm model is provided. If the CMBR is mass balanced, Co becomes a function of the solid (q') and residual solution concentrations (Cr) in the following equation:

$$C_o = \left[\frac{q'\left(\frac{mg}{kg}\right) \bullet \text{Wt. Soil (g)} \bullet \left(\frac{kg}{1000\,g}\right)}{\text{Wt. Spike Sol. (g)}} \bullet 1000\left(\frac{g}{l}\right) \right] + Cr\left(\frac{mg}{l}\right) \qquad \text{(units)}$$

Equation 13 is used in conjuction with the optimum constants from Table 9 to estimate q from Cr:

$$\frac{Cr}{q} = \frac{1}{\beta_1\beta_2} + \frac{Cr}{\beta_2}$$

or

$$\frac{1}{q'} = \frac{1}{\beta_1\beta_2 Cr} + \frac{1}{\beta_2}$$

Substituting the rhodamine constants where $\frac{1}{\beta_1\beta_2} = 0.033$ and $\frac{1}{\beta_2} = 0.002$ into the equation , Co is rewritten as a function of Cr only:

$$Co = \left[\frac{\left(\frac{1}{\frac{0.033}{Cr} + 0.002} \right) \left(\frac{mg}{kg} \right) \bullet \text{Wt. Soil (kg)}}{\text{Spike Sol. Wt. (g)}} \bullet 1000 \left(\frac{g}{l} \right) \right] + C_r \left(\frac{mg}{l} \right)$$

Values from Table 17 for spike solution weight (8.00 g) and soil weight (4.045 g) are plugged into the equation while Cr is manipulated until the original Co has been reached (see also Table 19).

$$Co = \left[\frac{\left(\frac{1}{\frac{0.033}{791} + 0.002} \right) \bullet 4.045}{8.00} \right] + 791.00$$

Therefore q' = 489.78 mg/kg and Co = 1039.58 mg/l.

Surface Area Estimations

Illuminated Window Calculations

The calculations necessary for the determination of "apparent" surface concentrations required knowlege of the number of particles that will fit into the illuminated window. If the average surface area of one particle at each gradation is know the total exposed surface area can be estimated (see Table 10).

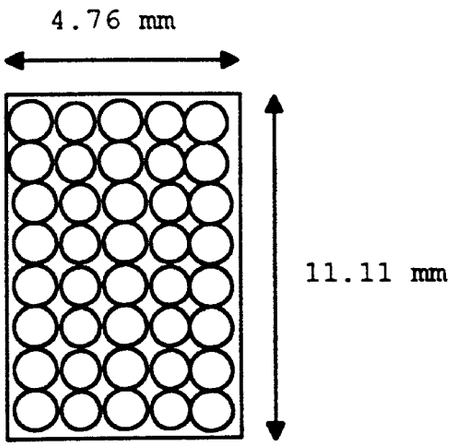

Number of ARS60 particles with average diameters of 0.338 mm which fit in the illuminated rectangle is caculated as:

$$\frac{4.763\ \text{mm}}{0.338\ \text{mm}} = 14.09 \text{ particles in width}$$

$$\frac{11.113\ \text{mm}}{0.338\ \text{mm}} = 32.88 \text{ particles in length}$$

therefore 14.09 X 32.88 = 463.28 ARS60 particles fit into illuminated rectangle.

Surface area of Particles

$$\frac{1}{\#\ \text{particles/gram}} \bullet SA\left(\frac{m^2}{g}\right) \bullet \frac{1X10^6\ mm^2}{m^2} = \frac{mm^2}{\text{particle}} \qquad \text{(units)}$$

$$\frac{1}{19{,}066.00} \bullet 0.21 \bullet 1x10^6 = 11.11\ \frac{mm^2}{\text{particle}}$$

Total Surface Area in Illuminated Rectangle

$$\#\ \text{particles} \bullet \frac{mm^2}{\text{particle}} = mm^2 \text{ apparent surface area} \qquad \text{(units)}$$

or $463.28 \bullet 11.11 = 5147.03\ mm^2$

Effective Surface Area (ESA)

Effective surface area is estimated to be 25% of the Total surface area:

or $0.25 \bullet 5147.03 = 1286.76\ mm^2$

Detectable Surface Mass

The "apparent" surface mass of the ARS60 gradation from Table 12 is estimated by multiplying the ESA (mm^2) by q (mg/m^2):

$$q\left(\frac{mg}{m^2}\right) \bullet ESA\ (mm^2) \bullet \left(\frac{m^2}{1x10^6\ mm^2}\right) = \text{ mg of apparent rhodamine} \qquad \text{(units)}$$

or $0.048 \bullet 1286.76 \bullet \frac{1}{1x10^6} = 0.000062$ mg

or 0.062 ug of apparent surface adsorbed rhodamine.

APPENDIX B

EXPERIMENTAL DATA

TABLE 14

SUPERNATANT FLUORESCENT RESPONSE VALUES USED IN VARIABLE MASS EXPERIMENT

Soil Gradation	Intensity			Wt. Sample			Residual Solution Conc. (Cr)			BET Area	Total SA			Estimated Solution Conc./Gram			Estimated Solution Conc./m2		
	2 gram (v-sm)	4 gram (v-sm)	8 gram (v-sm)	2 gram (g)	4 gram (g)	8 gram (g)	2 gram (mg/l)	4 gram (mg/l)	8 gram (mg/l)	(m2/g)	2 gram (m2)	4 gram (m2)	8 gram (m2)	2 gram (mg/g-l)	4 gram (mg/g-l)	8 gram (mg/g-l)	2 gram (mg/g-l)	4 gram (mg/g-l)	8 gram (mg/g-l)
NAPHTHALENE IN ARS Co = 6.655 mg/l																			
ARS60-1	16.130	11.560	8.370	2.263	4.087	8.088	3.200	2.100	1.800	0.214	0.485	0.876	1.733	1.414	0.514	0.223	6.599	2.398	1.039
ARS60-2	16.310	11.820	8.650	2.263	4.087	8.088	3.210	2.150	1.900	0.214	0.485	0.876	1.733	1.419	0.526	0.235	6.620	2.455	1.096
ARS60-3	16.600	12.010	8.750	2.263	4.087	8.088	3.300	2.200	1.920	0.214	0.485	0.876	1.733	1.458	0.538	0.237	6.804	2.512	1.108
Avg	16.347	11.797	8.590	2.263	4.087	8.088	3.237	2.150	1.873	0.214	0.485	0.876	1.733	1.430	0.526	0.232	6.675	2.455	1.081
ARS140-1	5.820	1.430	0.340	2.156	4.383	8.158	1.450	0.250	0.060	1.003	2.164	4.398	8.186	0.672	0.057	0.007	0.670	0.057	0.007
ARS140-2	5.890	1.440	0.350	2.156	4.383	8.158	1.460	0.250	0.060	1.003	2.164	4.398	8.186	0.677	0.057	0.007	0.675	0.057	0.007
ARS140-3	0.000	1.450	0.410	2.156	4.383	8.158	0.000	0.260	0.065	1.003	2.164	4.398	8.186	0.000	0.059	0.008	0.000	0.059	0.008
Avg	5.855	1.435	0.367	2.156	4.383	8.158	1.455	0.250	0.062	1.003	2.164	4.398	8.186	0.675	0.056	0.008	0.672	0.058	0.008
ARS200-1	2.790	0.880	8.100	2.089	4.043	8.001	1.050	0.150	0.010	1.429	2.986	5.777	11.434	0.503	0.037	0.001	0.352	0.026	0.001
ARS200-2	2.910	0.880	8.230	2.089	4.043	8.001	1.100	0.150	0.011	1.429	2.986	5.777	11.434	0.526	0.037	0.001	0.368	0.026	0.001
ARS200-3	2.950	0.910	8.260	2.089	4.043	8.001	1.110	0.160	0.012	1.429	2.986	5.777	11.434	0.531	0.040	0.001	0.372	0.028	0.001
Avg	2.883	0.890	8.197	2.089	4.043	8.001	1.087	0.153	0.011	1.429	2.986	5.777	11.434	0.520	0.038	0.001	0.364	0.027	0.001
ARS270-1	3.790	2.610	33.960	2.039	4.013	8.041	1.200	0.950	0.088	1.793	3.655	7.195	14.414	0.589	0.237	0.011	0.328	0.132	0.006
ARS270-2	4.930	2.700	33.960	2.039	4.013	8.041	1.300	1.000	0.088	1.793	3.655	7.195	14.414	0.638	0.249	0.011	0.356	0.139	0.006
ARS270-3	5.120	2.710	34.010	2.039	4.013	8.041	1.350	1.000	0.089	1.793	3.655	7.195	14.414	0.662	0.249	0.011	0.369	0.139	0.006
Avg	4.613	2.673	33.983	2.039	4.013	8.041	1.283	0.983	0.088	1.793	3.655	7.195	14.414	0.629	0.245	0.011	0.351	0.137	0.006
ARSPAN	0.640	12.460	0.530	2.091	4.005	8.178	0.100	0.015	0.001	2.251	4.708	9.017	18.411	0.048	0.004	0.000	0.021	0.002	0.000
ARSPAN	0.670	12.490	0.690	2.091	4.005	8.178	0.101	0.016	0.001	2.251	4.708	9.017	18.411	0.048	0.004	0.000	0.021	0.002	0.000
ARSPAN	0.680	12.730	0.490	2.091	4.005	8.178	0.102	0.016	0.001	2.251	4.708	9.017	18.411	0.049	0.004	0.000	0.022	0.002	0.000
Avg	0.663	12.560	0.570	2.091	4.005	8.178	0.101	0.016	0.001	2.251	4.708	9.017	18.411	0.048	0.004	0.000	0.021	0.002	0.000
p-XYLENE in ARS Co = 2.000 mg/l																			
ARS60-1	8.530	6.950	3.080	2.033	4.054	8.098	1.720	1.400	0.950	0.214	0.436	0.869	1.735	0.846	0.345	0.117	3.947	1.611	0.547
ARS60-2	8.170	6.730	3.040	2.033	4.054	8.098	1.710	1.350	0.940	0.214	0.436	0.869	1.735	0.841	0.333	0.116	3.924	1.554	0.542
ARS60-3	8.110	6.330	2.710	2.033	4.054	8.098	1.700	1.320	0.900	0.214	0.436	0.869	1.735	0.836	0.326	0.111	3.901	1.519	0.519
Avg	8.270	6.670	2.943	2.033	4.054	8.098	1.710	1.357	0.930	0.214	0.436	0.869	1.735	0.841	0.335	0.115	3.924	1.562	0.536
ARS140-1	6.100	2.340	-5.220	2.333	4.024	8.374	1.300	0.250	0.015	1.003	2.340	4.037	8.403	0.557	0.062	0.002	0.555	0.062	0.002
ARS140-2	5.820	2.340	-6.290	2.333	4.024	8.374	1.250	0.260	0.014	1.003	2.340	4.037	8.403	0.536	0.065	0.002	0.534	0.064	0.002
ARS140-3	5.930	0.000	-6.510	2.333	4.024	8.374	1.200	0.000	0.010	1.003	2.340	4.037	8.403	0.514	0.000	0.002	0.513	0.000	0.002
Avg	5.977	2.440	-5.340	2.333	4.024	8.374	1.250	0.255	0.016	1.003	2.340	4.037	8.403	0.536	0.042	0.002	0.534	0.042	0.002

TABLE 14 (continued)

SUPERNATANT FLUORESCENT RESPONSE VALUES USED IN VARIABLE MASS EXPERIMENT

Soil Gradation	Intensity			Wt. Sample			Residual Solution Conc. (Cr)			BET Area	Total SA			Estimated Solution Conc./Gram			Estimated Solution Conc./ml		
	2 gram (v-sec)	4 gram (v-sec)	8 gram (v-sec)	2 gram (g)	4 gram (g)	8 gram (g)	2 gram (mg/l)	4 gram (mg/l)	8 gram (mg/l)	(m2/g)	2 gram (m2)	4 gram (m2)	8 gram (m2)	2 gram (mg/g-l)	4 gram (mg/g-l)	8 gram (mg/g-l)	2 gram (mg/g-l)	4 gram (mg/g-l)	8 gram (mg/g-l)
ARS200-1	7.300	7.620	0.700	2.133	4.096	8.134	1.550	1.600	0.090	1.429	3.049	5.853	11.625	0.727	0.391	0.011	0.508	0.273	0.008
ARS200-2	7.660	7.820	0.780	2.133	4.096	8.134	1.600	1.610	0.095	1.429	3.049	5.853	11.625	0.750	0.393	0.012	0.525	0.275	0.008
ARS200-3	7.810	8.660	0.810	2.133	4.096	8.134	1.610	1.750	0.096	1.429	3.049	5.853	11.625	0.755	0.427	0.012	0.528	0.299	0.008
Avg	7.590	8.033	0.777	2.133	4.096	8.134	1.587	1.653	0.094	1.429	3.049	5.853	11.625	0.744	0.404	0.012	0.520	0.282	0.008
ARS270-1	4.240	1.920	-0.430	2.116	4.169	8.090	1.110	0.099	0.017	1.793	3.794	7.473	14.504	0.525	0.024	0.002	0.293	0.013	0.001
ARS270-2	4.160	1.820	-0.550	2.116	4.169	8.090	1.110	0.098	0.018	1.793	3.794	7.473	14.504	0.525	0.024	0.002	0.293	0.013	0.001
ARS270-3	4.360	1.890	-0.550	2.116	4.169	8.090	1.120	0.098	0.018	1.793	3.794	7.473	14.504	0.529	0.024	0.002	0.295	0.013	0.001
Avg	4.253	1.877	-0.510	2.116	4.169	8.090	1.113	0.098	0.018	1.793	3.794	7.473	14.504	0.526	0.024	0.002	0.293	0.013	0.001
ARSPAN	0.200	0.550	-21.510	2.037	4.119	8.112	0.030	0.020	0.011	2.251	4.585	9.273	18.262	0.015	0.005	0.001	0.007	0.002	0.001
ARSPAN	0.210	0.480	-21.000	2.037	4.119	8.112	0.032	0.021	0.012	2.251	4.585	9.273	18.262	0.016	0.005	0.001	0.007	0.002	0.001
ARSPAN	0.000	-0.440	-20.900	2.037	4.119	8.112	0.020	0.022	0.012	2.251	4.585	9.273	18.262	0.010	0.005	0.001	0.004	0.002	0.001
Avg	0.157	0.490	-21.163	2.037	4.119	8.112	0.027	0.021	0.012	2.251	4.585	9.273	18.262	0.013	0.005	0.001	0.006	0.002	0.001
NAPHTHALENE IN SS Co = 6.670 mg/l																			
SS60-1	3.960	1.310	29.240	2.135	4.097	8.417	1.290	0.100	0.065	0.533	1.138	2.183	4.486	0.562	0.044	0.008	1.054	0.082	0.014
SS60-2	4.060	1.360	29.810	2.135	4.097	8.417	1.300	0.100	0.066	0.533	1.138	2.183	4.486	0.609	0.044	0.008	1.142	0.082	0.015
SS60-3	4.100	1.370	30.900	2.135	4.097	8.417	1.300	0.190	0.070	0.533	1.138	2.183	4.486	0.609	0.046	0.008	1.142	0.087	0.016
Avg	4.040	1.347	30.010	2.135	4.097	8.417	1.267	0.103	0.067	0.533	1.138	2.183	4.486	0.593	0.045	0.008	1.113	0.084	0.015
SS140-1	2.960	1.140	45.500	2.468	4.072	8.076	1.100	0.150	0.090	0.626	1.545	2.549	5.056	0.446	0.037	0.011	0.712	0.059	0.018
SS140-2	2.960	1.190	47.010	2.468	4.072	8.076	1.100	0.150	0.095	0.626	1.545	2.549	5.056	0.446	0.037	0.012	0.712	0.059	0.019
SS140-3	2.970	1.270	47.140	2.468	4.072	8.076	1.100	0.160	0.095	0.626	1.545	2.549	5.056	0.446	0.039	0.012	0.712	0.063	0.019
Avg	2.963	1.200	46.577	2.468	4.072	8.076	1.100	0.153	0.093	0.626	1.545	2.549	5.056	0.446	0.038	0.012	0.712	0.060	0.018
p-XYLENE IN SS Co = 11.349 mg/l																			
SS60-1	5.590	33.330	2.000	2.011	4.100	8.006	1.350	0.045	0.015	0.533	1.072	2.186	4.267	0.671	0.011	0.002	1.260	0.021	0.004
SS60-2	5.800	34.200	2.040	2.011	4.100	8.006	1.400	0.046	0.015	0.533	1.072	2.186	4.267	0.696	0.011	0.002	1.306	0.021	0.004
SS60-3	6.090	35.390	2.080	2.011	4.100	8.006	1.450	0.047	0.015	0.533	1.072	2.186	4.267	0.721	0.011	0.002	1.353	0.022	0.004
Avg	5.853	34.307	2.053	2.011	4.100	8.006	1.400	0.046	0.015	0.533	1.072	2.186	4.267	0.696	0.011	0.002	1.306	0.021	0.004
SS140-1	4.030	34.010	1.370	2.207	4.018	8.050	1.200	0.049	0.014	0.626	1.382	2.515	5.040	0.544	0.013	0.002	0.860	0.019	0.003
SS140-2	4.370	36.150	1.430	2.207	4.018	8.050	1.210	0.051	0.014	0.626	1.382	2.515	5.040	0.548	0.013	0.002	0.876	0.020	0.003
SS140-3	5.590	36.200	2.000	2.207	4.018	8.050	0.852	0.052	0.014	0.626	1.382	2.515	5.040	0.386	0.013	0.002	0.616	0.021	0.003
Avg	4.663	35.120	1.597	2.207	4.018	8.050	0.821	0.051	0.014	0.626	1.382	2.515	5.040	0.372	0.013	0.002	0.594	0.020	0.003

TABLE 14 (continued)

SUPERNATANT FLUORESCENT RESPONSE VALUES USED IN VARIABLE MASS EXPERIMENT

Soil Gradation	Intensity 2 gram (v-nm)	Intensity 4 gram (v-nm)	Intensity 8 gram (v-nm)	Wt. Sample 2 gram (g)	Wt. Sample 4 gram (g)	Wt. Sample 8 gram (g)	Residual Solution Conc. (Cr) 2 gram (mg/l)	Residual Solution Conc. (Cr) 4 gram (mg/l)	Residual Solution Conc. (Cr) 8 gram (mg/l)	BET Area (m2/g)	Total SA 2 gram (m2)	Total SA 4 gram (m2)	Total SA 8 gram (m2)	Estimated Solution Conc./Gram 2 gram (mg/g-l)	Estimated Solution Conc./Gram 4 gram (mg/g-l)	Estimated Solution Conc./Gram 8 gram (mg/g-l)	Estimated Solution Conc./ml 2 gram (mg/g-l)	Estimated Solution Conc./ml 4 gram (mg/g-l)	Estimated Solution Conc./ml 8 gram (mg/g-l)
RHODAMINE IN ARS Co = 5.000 mg/l																			
ARS40-1	62.100	58.360	46.370	2.221	4.069	8.006	3.100	3.000	2.300	0.409	0.908	1.663	3.272	1.396	0.737	0.287	3.415	1.804	0.703
ARS40-2	57.800	53.480	44.960	2.221	4.069	8.006	3.000	2.800	2.100	0.409	0.908	1.663	3.272	1.351	0.688	0.262	3.305	1.684	0.642
ARS40-3	56.210	51.870	44.090	2.221	4.069	8.006	2.900	2.500	2.000	0.409	0.908	1.663	3.272	1.306	0.614	0.250	3.195	1.503	0.611
Avg	58.703	54.570	45.140	2.221	4.069	8.006	3.000	2.767	2.133	0.409	0.908	1.663	3.272	1.351	0.680	0.266	3.305	1.664	0.652
ARS60-1	52.550	40.260	35.430	2.091	3.981	8.294	2.800	1.900	1.700	0.214	0.448	0.853	1.777	1.339	0.477	0.205	6.248	2.227	0.956
ARS60-2	46.800	44.700	31.990	2.091	3.981	8.294	2.100	2.000	1.500	0.214	0.448	0.853	1.777	1.004	0.502	0.181	4.686	2.343	0.844
ARS60-3	45.890	39.130	30.900	2.091	3.981	8.294	2.000	1.850	1.450	0.214	0.448	0.853	1.777	0.956	0.465	0.175	4.463	2.169	0.816
Avg	48.413	41.363	32.773	2.091	3.981	8.294	2.300	1.917	1.550	0.214	0.448	0.853	1.777	1.100	0.482	0.187	5.133	2.247	0.872
ARS140-1	26.870	16.090	7.420	2.211	4.096	7.978	1.300	0.600	0.200	1.003	2.219	4.110	8.005	0.586	0.146	0.025	0.586	0.146	0.025
ARS140-2	24.490	14.630	6.900	2.211	4.096	7.978	1.200	0.450	0.190	1.003	2.219	4.110	8.005	0.543	0.110	0.024	0.541	0.109	0.024
ARS140-3	23.600	14.230	6.840	2.211	4.096	7.978	1.190	0.440	0.190	1.003	2.219	4.110	8.005	0.538	0.107	0.024	0.536	0.107	0.024
Avg	24.987	14.983	7.000	2.211	4.096	7.978	1.230	0.497	0.193	1.003	2.219	4.110	8.005	0.556	0.121	0.024	0.554	0.121	0.024
ARS200-1	15.450	5.060	1.500	2.082	4.145	8.201	0.500	0.160	0.050	1.429	2.975	5.924	11.720	0.240	0.039	0.006	0.168	0.027	0.004
ARS200-2	14.130	5.470	1.490	2.082	4.145	8.201	0.490	0.150	0.045	1.429	2.975	5.924	11.720	0.235	0.036	0.005	0.165	0.025	0.004
ARS200-3	13.560	5.250	1.450	2.082	4.145	8.201	0.460	0.140	0.045	1.429	2.975	5.924	11.720	0.221	0.034	0.005	0.155	0.024	0.004
Avg	14.373	5.527	1.480	2.082	4.145	8.201	0.483	0.150	0.047	1.429	2.975	5.924	11.720	0.232	0.036	0.006	0.162	0.025	0.004
ARS270-1	13.090	6.740	2.340	2.029	4.024	7.996	0.450	0.180	0.122	1.793	3.637	7.213	14.335	0.222	0.045	0.015	0.124	0.025	0.009
ARS270-2	12.660	6.550	2.530	2.029	4.024	7.996	0.430	0.170	0.125	1.793	3.637	7.213	14.335	0.212	0.042	0.016	0.118	0.024	0.009
ARS270-3	12.230	6.520	2.300	2.029	4.024	7.996	0.420	0.170	0.120	1.793	3.637	7.213	14.335	0.207	0.042	0.015	0.115	0.024	0.008
Avg	12.793	6.470	2.390	2.029	4.024	7.996	0.433	0.173	0.122	1.793	3.637	7.213	14.335	0.214	0.043	0.015	0.119	0.024	0.009
ARSPAN	3.520	1.340	46.530	2.176	4.062	8.051	0.133	0.095	0.019	2.251	4.899	9.144	18.124	0.061	0.023	0.002	0.027	0.010	0.001
ARSPAN	3.430	1.190	46.800	2.176	4.062	8.051	0.132	0.093	0.020	2.251	4.899	9.144	18.124	0.061	0.023	0.002	0.027	0.010	0.001
ARSPAN	3.290	1.170	47.930	2.176	4.062	8.051	0.130	0.090	0.019	2.251	4.899	9.144	18.124	0.060	0.022	0.002	0.027	0.010	0.001
Avg	3.413	1.233	47.107	2.176	4.062	8.051	0.132	0.093	0.019	2.251	4.899	9.144	18.124	0.061	0.023	0.002	0.027	0.010	0.001
RHODAMINE IN SS Co = 11.149 mg/l																			
11000-1	4.970	2.200	1.100	2.076	4.000	8.383	0.150	0.110	0.001	0.533	1.106	2.175	4.460	0.072	0.027	0.000	0.136	0.051	0.000
11000-2	5.100	2.300	1.100	2.076	4.000	8.383	0.170	0.110	0.001	0.533	1.106	2.175	4.460	0.082	0.027	0.000	0.154	0.051	0.000
11000-3	5.090	2.390	1.200	2.076	4.000	8.383	0.180	0.120	0.001	0.533	1.106	2.175	4.460	0.087	0.029	0.000	0.163	0.055	0.000
Avg	5.273	2.343	1.133	2.076	4.000	8.383	0.167	0.113	0.001	0.533	1.106	2.175	4.460	0.080	0.028	0.000	0.151	0.052	0.000

TABLE 14 (continued)

SUPERNATANT FLUORESCENT RESPONSE VALUES USED IN VARIABLE MASS EXPERIMENT

Soil	Intensity			Wt. Sample			Residual Solution Conc. (Cf)			BET Area	Total SA			Estimated Solution Conc./Gram			Estimated Solution Conc./m2		
Gradation	2 gram	4 gram	8 gram	2 gram	4 gram	8 gram	2 gram	4 gram	8 gram		2 gram	4 gram	8 gram	2 gram	4 gram	8 gram	2 gram	4 gram	8 gram
	(v-nm)	(v-nm)	(v-nm)	(g)	(g)	(g)	(mg/l)	(mg/l)	(mg/l)	(m2/g)	(m2)	(m2)	(m2)	(mg/g-l)	(mg/g-l)	(mg/g-l)	(mg/g-l)	(mg/g-l)	(mg/g-l)
110140-1	8.260	2.170	25.000	2.059	4.131	8.200	0.200	0.110	0.015	0.626	1.289	2.586	5.134	0.097	0.027	0.002	0.155	0.043	0.003
110140-2	8.550	2.250	23.200	2.059	4.131	8.200	0.210	0.110	0.014	0.626	1.289	2.586	5.134	0.102	0.027	0.002	0.163	0.043	0.003
110140-3	9.420	2.450	23.100	2.059	4.131	8.200	0.230	0.120	0.014	0.626	1.289	2.586	5.134	0.112	0.029	0.002	0.178	0.046	0.003
Avg	8.743	2.290	23.767	2.059	4.131	8.200	0.213	0.113	0.014	0.626	1.289	2.586	5.134	0.104	0.027	0.002	0.166	0.044	0.003

TABLE 15

ISOTHERM VALUES - VARIABLE MASS METHOD (VM)

Soil Gradation	MEASURED VALUES									COMPUTED ISOTHERM PARAMETERS							
	Spike Wt (g)	Soil Wt (g)	SA (m2)	Co (mg/l)	Avg Cr (mg/l)	Co-Cr (mg/l)	q (mg/m2)	q' (mg/g)	C	1/C	log C	C/q	C/q'	log q	log q'	1/q	1/q'
NAPHTHALENE in ARS																	
ARS60	8.077	2.263	0.485	6.655	3.237	3.418	0.057	0.012	3.237	0.309	0.510	56.853	265.298	-1.245	-1.914	17.565	81.967
	8.055	4.087	0.876	6.655	2.150	4.505	0.041	0.009	2.150	0.465	0.332	51.900	242.185	-1.383	-2.052	24.140	112.644
	8.084	8.088	1.733	6.655	1.873	4.781	0.022	0.005	1.873	0.534	0.273	84.005	391.999	-1.652	-2.321	44.843	209.252
ARS140	8.188	2.156	2.164	6.655	1.455	5.200	0.020	0.020	1.455	0.687	0.163	73.944	73.694	-1.706	-1.705	50.821	50.649
	8.147	4.383	4.398	6.655	0.250	6.405	0.012	0.012	0.250	4.000	-0.602	21.073	21.002	-1.926	-1.924	84.292	84.007
	8.108	8.158	8.186	6.655	0.062	6.593	0.007	0.007	0.062	16.216	-1.210	9.443	9.411	-2.185	-2.184	153.127	152.608
ARS200	8.064	2.089	2.986	6.655	1.087	5.568	0.015	0.021	1.087	0.920	0.036	72.269	50.569	-1.823	-1.668	66.905	46.536
	8.114	4.043	5.777	6.655	0.153	6.501	0.009	0.013	0.153	6.522	-0.814	16.793	11.751	-2.039	-1.884	109.521	76.636
	8.110	8.001	11.434	6.655	0.011	6.644	0.005	0.007	0.011	90.909	-1.959	2.335	1.634	-2.327	-2.172	212.234	148.509
ARS270	8.065	2.039	3.655	6.655	1.283	5.371	0.012	0.021	1.283	0.779	0.108	108.285	60.404	-1.926	-1.673	84.378	47.068
	8.015	4.013	7.195	6.655	0.983	5.671	0.006	0.011	0.983	1.017	-0.007	155.650	86.825	-2.199	-1.946	158.289	88.296
	8.338	8.041	14.414	6.655	0.088	6.566	0.004	0.007	0.088	11.321	-1.054	23.257	12.973	-2.420	-2.167	263.286	146.866
ARSPAN	8.074	2.091	4.708	6.655	0.101	6.554	0.011	0.025	0.101	9.901	-0.996	8.987	3.992	-1.949	-1.597	88.984	39.526
	8.277	4.005	9.017	6.655	0.016	6.639	0.006	0.014	0.016	63.830	-1.805	2.571	1.142	-2.215	-1.863	164.088	72.886
	8.063	8.178	18.411	6.655	0.001	6.654	0.003	0.007	0.001	1000.000	-3.000	0.343	0.152	-2.536	-2.183	343.176	152.435
p-XYLENE in ARS																	
ARS60	23.351	2.033	0.436	2.000	1.710	0.290	0.016	0.003	1.710	0.585	0.233	110.036	513.468	-1.809	-2.478	64.349	300.274
	22.052	4.054	0.869	2.000	1.357	0.643	0.016	0.003	1.357	0.737	0.132	83.082	387.692	-1.787	-2.456	61.240	285.768
	20.345	8.098	1.735	2.000	0.930	1.070	0.013	0.003	0.930	1.075	-0.032	74.144	345.980	-1.902	-2.571	79.724	372.022
ARS140	22.547	2.333	2.340	2.000	1.250	0.750	0.007	0.007	1.250	0.800	0.097	173.005	172.418	-2.141	-2.140	138.404	137.935
	22.095	4.024	4.037	2.000	0.255	1.745	0.010	0.010	0.255	3.922	-0.593	26.704	26.613	-2.020	-2.019	104.720	104.365
	20.251	8.374	8.403	2.000	0.016	1.984	0.005	0.005	0.016	63.830	-1.805	3.276	3.265	-2.320	-2.319	209.104	208.395
ARS200	22.468	2.133	3.049	2.000	1.587	0.413	0.003	0.004	1.587	0.630	0.200	520.860	364.467	-2.516	-2.361	328.273	229.706
	22.199	4.096	5.853	2.000	1.653	0.347	0.001	0.002	1.653	0.605	0.218	1257.493	879.920	-2.881	-2.726	760.581	532.210
	20.519	8.134	11.625	2.000	0.094	1.906	0.003	0.005	0.094	10.676	-1.028	27.836	19.478	-2.473	-2.318	297.180	207.949
ARS270	22.815	2.116	3.794	2.000	1.113	0.887	0.005	0.010	1.113	0.898	0.047	208.778	116.460	-2.273	-2.020	187.525	104.605
	21.710	4.169	7.473	2.000	0.098	1.902	0.006	0.010	0.098	10.169	-1.007	17.799	9.929	-2.258	-2.004	181.019	100.970
	20.214	8.090	14.504	2.000	0.018	1.982	0.003	0.005	0.018	56.604	-1.753	6.994	3.567	-2.559	-2.305	361.943	201.898
ARSPAN	22.656	2.037	4.585	2.000	0.027	1.973	0.010	0.022	0.027	36.585	-1.563	2.804	1.246	-2.011	-1.659	102.588	45.568
	21.646	4.119	9.273	2.000	0.021	1.979	0.005	0.010	0.021	47.619	-1.678	4.546	2.019	-2.335	-1.983	216.469	96.153

TABLE 15 (continued)

ISOTHERM VALUES - VARIABLE MASS METHOD (VM)

Soil Gradation	MEASURED VALUES									COMPUTED ISOTHERM PARAMETERS							
	Spike Wt (g)	Soil Wt (g)	SA (m2)	Co (mg/l)	Avg Cr (mg/l)	Co-Cr (mg/l)	q (mg/m2)	q* (mg/g)	C	1/C	log C	C/q	C/q*	log q	log q*	1/q	1/q*
	20.105	8.112	18.262	2.000	0.012	1.988	0.002	0.005	0.012	85.714	-1.933	5.330	2.367	-2.660	-2.307	456.836	202.921
NAPHTHALENE in SS																	
SS60	21.616	2.135	1.138	6.670	1.267	5.403	0.103	0.055	1.267	0.789	0.103	12.342	23.156	-0.989	-1.262	9.744	18.281
	20.993	4.097	2.183	6.670	0.183	6.487	0.062	0.033	0.183	5.455	-0.737	2.940	5.515	-1.205	-1.478	16.034	30.083
	20.659	8.417	4.486	6.670	0.067	6.603	0.030	0.016	0.067	14.925	-1.174	2.204	4.134	-1.517	-1.790	32.889	61.705
SS140	21.191	2.468	1.545	6.670	1.100	5.570	0.076	0.048	1.100	0.909	0.041	14.401	23.001	-1.117	-1.320	13.091	20.910
	20.080	4.072	2.549	6.670	0.153	6.517	0.051	0.032	0.153	6.522	-0.814	2.987	4.771	-1.290	-1.493	19.482	31.117
	20.554	8.076	5.056	6.670	0.093	6.577	0.027	0.017	0.093	10.714	-1.030	3.491	5.576	-1.573	-1.776	37.404	59.742
p-XYLENE in SS																	
SS60	22.874	2.011	1.072	11.349	1.400	9.949	0.212	0.113	1.400	0.714	0.146	6.592	12.368	-0.673	-0.946	4.709	8.835
	22.111	4.100	2.186	11.349	0.046	11.303	0.114	0.061	0.046	21.739	-1.337	0.402	0.755	-0.942	-1.215	8.745	16.407
	20.903	8.086	4.267	11.349	0.015	11.334	0.056	0.030	0.015	66.667	-1.824	0.270	0.507	-1.256	-1.529	18.010	33.790
SS140	22.733	2.207	1.382	11.349	0.821	10.528	0.173	0.108	0.821	1.219	-0.086	4.739	7.569	-0.762	-0.965	5.774	9.223
	21.840	4.018	2.515	11.349	0.051	11.298	0.098	0.061	0.051	19.737	-1.295	0.517	0.825	-1.008	-1.212	10.194	16.282
	20.240	8.050	5.040	11.349	0.014	11.335	0.046	0.028	0.014	71.429	-1.854	0.308	0.491	-1.342	-1.545	21.969	35.088
RHODAMINE in ARS																	
ARS40	8.152	2.221	0.908	5.000	3.000	2.000	0.018	0.007	3.000	0.333	0.477	167.025	408.673	-1.746	-2.134	55.675	136.224
	8.175	4.069	1.663	5.000	2.767	2.233	0.011	0.004	2.767	0.361	0.442	252.001	616.592	-1.959	-2.348	91.085	222.865
	8.108	8.006	3.272	5.000	2.133	2.867	0.007	0.003	2.133	0.469	0.329	300.300	734.769	-2.148	-2.537	140.766	344.423
ARS60	8.030	2.091	0.448	5.000	2.300	2.700	0.048	0.010	2.300	0.435	0.362	47.536	221.821	-1.315	-1.984	20.668	96.444
	8.026	3.981	0.853	5.000	1.917	3.083	0.029	0.006	1.917	0.522	0.283	66.066	308.286	-1.537	-2.206	34.469	160.845
	8.202	8.294	1.777	5.000	1.550	3.450	0.016	0.003	1.550	0.645	0.190	97.364	454.337	-1.798	-2.467	62.816	293.120
ARS140	8.086	2.211	2.219	5.000	1.230	3.770	0.014	0.014	1.230	0.813	0.090	89.515	89.212	-1.862	-1.861	72.777	72.530
	8.095	4.096	4.110	5.000	0.497	4.503	0.009	0.009	0.497	2.013	-0.304	55.992	55.802	-2.052	-2.051	112.736	112.354
	8.114	7.978	8.005	5.000	0.193	4.807	0.005	0.005	0.193	5.172	-0.714	39.683	39.549	-2.312	-2.311	205.258	204.562
ARS200	8.080	2.082	2.975	5.000	0.483	4.517	0.012	0.018	0.483	2.069	-0.316	39.401	27.570	-1.911	-1.756	81.519	57.042
	8.159	4.145	5.924	5.000	0.150	4.850	0.007	0.010	0.150	6.667	-0.824	22.456	15.714	-2.175	-2.020	149.710	104.758

TABLE 15 (continued)

ISOTHERM VALUES - VARIABLE MASS METHOD (VM)

Soil Gradation	MEASURED VALUES									COMPUTED ISOTHERM PARAMETERS							
	Spike Wt (g)	Soil Wt (g)	SA (m2)	Co (mg/l)	Avg Cr (mg/l)	Co-Cr (mg/l)	q (mg/m2)	q' (mg/g)	C	1/C	log C	C/q	C/q'	log q	log q'	1/q	1/q'
	8.052	8.201	11.720	5.000	0.047	4.953	0.003	0.005	0.047	21.429	-1.331	13.713	9.596	-2.468	-2.313	293.851	205.620
ARS270	8.396	2.029	3.637	5.000	0.433	4.567	0.011	0.019	0.433	2.308	-0.363	41.102	22.928	-1.977	-1.724	94.851	52.910
	8.223	4.024	7.213	5.000	0.173	4.827	0.006	0.010	0.173	5.769	-0.761	31.503	17.573	-2.259	-2.006	181.746	101.381
	8.156	7.996	14.335	5.000	0.122	4.878	0.003	0.005	0.122	8.174	-0.912	44.079	24.588	-2.557	-2.303	360.318	200.992
ARSPAN	8.092	2.176	4.899	5.000	0.133	4.867	0.008	0.018	0.133	7.519	-0.876	16.546	7.349	-2.095	-1.742	124.405	55.259
	8.005	4.062	9.144	5.000	0.095	4.905	0.004	0.010	0.095	10.526	-1.022	22.124	9.827	-2.367	-2.015	232.888	103.446
	8.017	8.051	18.124	5.000	0.019	4.981	0.002	0.005	0.019	52.356	-1.719	8.669	3.851	-2.657	-2.305	453.875	201.606
RHODAMINE in SS																	
SS60	8.231	2.076	1.106	11.149	0.167	10.982	0.042	0.044	0.167	6.000	-0.778	2.040	3.828	-1.088	-1.361	12.241	22.965
	8.390	4.080	2.175	11.149	0.113	11.036	0.043	0.023	0.113	8.824	-0.946	2.662	4.994	-1.371	-1.644	23.486	44.063
	8.383	8.383	4.468	11.149	0.001	11.148	0.021	0.011	0.001	789.474	-2.897	0.061	0.114	-1.680	-1.953	47.812	89.704
SS140	8.570	2.059	1.289	11.149	0.213	10.936	0.073	0.046	0.213	4.688	-0.671	2.934	4.687	-1.138	-1.342	13.754	21.968
	8.435	4.131	2.586	11.149	0.113	11.036	0.036	0.023	0.113	8.824	-0.946	3.149	5.029	-1.444	-1.647	27.785	44.378
	8.200	8.200	5.134	11.149	0.014	11.135	0.018	0.011	0.014	69.767	-1.844	0.806	1.287	-1.750	-1.953	56.230	89.810

TABLE 16

ISOTHERM VALUES - VARIABLE CONCENTRATION METHOD (VC)

MEASURED VALUES								COMPUTED ISOTHERM VALUES								
Co (mg/l)	Intensity (v-nm)	Cr (mg/l)	Wt. spk (g)	Wt. soil (g)	SA (m2/g)	q (mg/m2)	q' (mg/kg)	C	1/C	Log C	C/q	C/q'	Log q	Log q'	1/q	1/q'
NAPHTHALENE in ARS																
47.224	18.890	4.500	8.462	4.183	1.003	0.08617	86.430	4.500	0.222	0.653	52.221	0.052	-1.065	-1.063	11.605	0.012
47.224	18.690	4.300	8.462	4.183	1.003	0.08658	86.835	4.300	0.233	0.633	49.668	0.050	-1.063	-1.061	11.551	0.012
47.224	18.800	4.400	8.462	4.183	1.003	0.08637	86.633	4.400	0.227	0.643	50.942	0.051	-1.064	-1.062	11.578	0.012
6.620	3.060	1.150	8.688	4.588	1.003	0.01033	10.358	1.150	0.870	0.061	111.359	0.111	-1.986	-1.985	96.834	0.097
6.620	2.960	1.100	8.688	4.588	1.003	0.01042	10.453	1.100	0.909	0.041	105.553	0.105	-1.982	-1.981	95.957	0.096
6.620	2.960	1.100	8.688	4.588	1.003	0.01042	10.453	1.100	0.909	0.041	105.553	0.105	-1.982	-1.981	95.957	0.096
0.664	13.460	0.072	8.828	4.503	1.003	0.00116	1.160	0.072	13.889	-1.143	62.257	0.062	-2.937	-2.936	864.677	0.862
0.664	13.280	0.071	8.828	4.503	1.003	0.00116	1.162	0.071	14.085	-1.149	61.288	0.061	-2.936	-2.935	863.218	0.861
0.664	13.110	0.070	8.828	4.503	1.003	0.00116	1.164	0.070	14.286	-1.155	60.323	0.060	-2.935	-2.934	861.764	0.859
0.072	1.510	0.003	8.714	4.479	1.003	0.00013	0.134	0.003	333.333	-2.523	22.514	0.022	-3.875	-3.874	7504.520	7.482
0.072	1.470	0.003	8.714	4.479	1.003	0.00013	0.134	0.003	344.828	-2.538	21.731	0.022	-3.875	-3.873	7493.612	7.471
0.072	1.510	0.003	8.714	4.479	1.003	0.00013	0.134	0.003	333.333	-2.523	22.514	0.022	-3.875	-3.874	7504.520	7.482
0.007	0.600	0.001	8.238	4.275	1.003	0.00001	0.012	0.001	1111.111	-3.046	75.554	0.075	-4.924	-4.923	83948.74	83.698
0.007	0.480	0.001	8.238	4.275	1.003	0.00001	0.012	0.001	1250.000	-3.097	66.093	0.066	-4.917	-4.916	82616.22	82.369
0.007	0.530	0.001	8.238	4.275	1.003	0.00001	0.012	0.001	1176.471	-3.071	70.786	0.071	-4.921	-4.919	83277.15	83.028
0.001	ND	ND	9.039	4.045	1.003	0.00000	0.002	N/A	N/A	N/A	N/A	N/A	-5.763	-5.762	579868.0	578.134
0.001	ND	ND	9.039	4.045	1.003	0.00000	0.002	N/A	N/A	N/A	N/A	N/A	-5.763	-5.762	579868.0	578.134
0.001	ND	ND	9.039	4.045	1.003	0.00000	0.002	N/A	N/A	N/A	N/A	N/A	-5.763	-5.762	579868.0	578.134
p-XYLENE in ARS																
115.180	3.770	1.100	19.789	8.004	1.003	0.28120	282.048	1.100	0.909	0.041	3.912	0.004	-0.551	-0.550	3.556	0.004
115.180	3.620	1.030	19.789	8.004	1.003	0.28138	282.221	1.030	0.971	0.013	3.661	0.004	-0.551	-0.549	3.554	0.004
115.180	3.590	1.000	19.789	8.004	1.003	0.28145	282.296	1.000	1.000	0.000	3.553	0.004	-0.551	-0.549	3.553	0.004
11.389	2.300	0.460	19.676	8.143	1.003	0.02633	26.408	0.460	2.174	-0.337	17.471	0.017	-1.580	-1.578	37.980	0.038
11.389	2.370	0.465	19.676	8.143	1.003	0.02632	26.396	0.465	2.151	-0.333	17.669	0.018	-1.580	-1.578	37.998	0.038
11.389	2.340	0.463	19.676	8.143	1.003	0.02632	26.401	0.463	2.160	-0.334	17.590	0.018	-1.580	-1.578	37.991	0.038

TABLE 16 (continued)

ISOTHERM VALUES - VARIABLE CONCENTRATION METHOD (VC)

MEASURED VALUES								COMPUTED ISOTHERM VALUES								
Co (mg/l)	Intensity (v-nm)	Cr (mg/l)	Wt. spk (g)	Wt. soil (g)	SA (m2/g)	q (mg/m2)	q' (mg/kg)	C	1/C	Log C	C/q	C/q'	Log q	Log q'	1/q	1/q'
1.155	14.190	0.025	20.342	8.100	1.003	0.00283	2.837	0.025	40.000	-1.602	8.838	0.009	-2.548	-2.547	353.529	0.352
1.155	14.460	0.026	20.342	8.100	1.003	0.00283	2.835	0.026	38.462	-1.585	9.200	0.009	-2.549	-2.548	353.842	0.353
1.155	14.950	0.027	20.342	8.100	1.003	0.00282	2.833	0.027	37.736	-1.577	9.381	0.009	-2.549	-2.548	353.999	0.353
0.119	1.410	0.017	20.407	8.214	1.003	0.00025	0.254	0.017	60.606	-1.783	65.116	0.065	-3.596	-3.595	3946.436	3.935
0.119	1.300	0.015	20.407	8.214	1.003	0.00026	0.258	0.015	66.667	-1.824	58.341	0.058	-3.590	-3.589	3889.406	3.878
0.119	1.460	0.016	20.407	8.214	1.003	0.00026	0.257	0.016	64.516	-1.810	60.578	0.060	-3.592	-3.591	3908.232	3.897
0.013	0.230	0.010	20.624	8.286	1.003	0.00001	0.008	0.010	100.000	-2.000	1259.355	1.256	-5.100	-5.099	125935.5	125.559
0.013	0.580	0.010	20.624	8.286	1.003	0.00001	0.008	0.010	100.000	-2.000	1259.355	1.256	-5.100	-5.099	125935.5	125.559
0.013	0.510	0.010	20.624	8.286	1.003	0.00001	0.008	0.010	100.000	-2.000	1259.355	1.256	-5.100	-5.099	125935.5	125.559
0.001	ND	ND	20.042	8.080	1.003	0.00000	0.003	N/A	N/A	N/A	N/A	N/A	-5.493	-5.492	311056.8	310.126
0.001	ND	ND	20.042	8.080	1.003	0.00000	0.003	N/A	N/A	N/A	N/A	N/A	-5.493	-5.492	311056.8	310.126
0.001	ND	ND	20.042	8.080	1.003	0.00000	0.003	N/A	N/A	N/A	N/A	N/A	-5.493	-5.492	311056.8	310.126
NAPHTHALENE in SS																
47.224	42.970	14.500	21.683	2.176	0.626	0.52085	326.053	14.500	0.069	1.161	27.839	0.044	-0.283	-0.487	1.920	0.003
47.224	42.320	14.000	21.683	2.176	0.626	0.52881	331.035	14.000	0.071	1.146	26.475	0.042	-0.277	-0.480	1.891	0.003
47.224	41.990	12.000	21.683	2.176	0.626	0.56064	350.963	12.000	0.083	1.079	21.404	0.034	-0.251	-0.455	1.784	0.003
6.670	3.530	1.300	21.036	2.062	0.626	0.08751	54.783	1.300	0.769	0.114	14.855	0.024	-1.058	-1.261	11.427	0.018
6.670	3.320	1.200	21.036	2.062	0.626	0.08914	55.803	1.200	0.833	0.079	13.462	0.022	-1.050	-1.253	11.218	0.018
6.670	3.240	1.150	21.036	2.062	0.626	0.08996	56.313	1.150	0.870	0.061	12.784	0.020	-1.046	-1.249	11.116	0.018
0.677	16.990	0.025	21.744	2.025	0.626	0.01118	7.000	0.025	40.000	-1.602	2.236	0.004	-1.951	-2.155	89.427	0.143
0.677	18.090	0.030	21.744	2.025	0.626	0.01110	6.946	0.030	33.333	-1.523	2.704	0.004	-1.955	-2.158	90.118	0.144
0.677	17.740	0.028	21.744	2.025	0.626	0.01113	6.968	0.028	35.714	-1.553	2.516	0.004	-1.953	-2.157	89.840	0.144
0.069	1.430	0.002	21.093	2.226	0.626	0.00102	0.636	0.002	666.667	-2.824	1.477	0.002	-2.993	-3.197	984.615	1.573
0.069	1.530	0.002	21.093	2.226	0.626	0.00102	0.635	0.002	649.351	-2.812	1.517	0.002	-2.994	-3.197	985.202	1.574
0.069	ND	0.001	21.093	2.226	0.626	0.00102	0.641	0.001	1000.000	-3.000	0.977	0.002	-2.990	-3.193	977.332	1.561
p-XYLENE in SS																

TABLE 16 (continued)

ISOTHERM VALUES - VARIABLE CONCENTRATION METHOD (VC)

MEASURED VALUES								COMPUTED ISOTHERM VALUES								
Co (mg/l)	Intensity (v-nm)	Cr (mg/l)	Wt. spk (g)	Wt. soil (g)	SA (m2/g)	q (mg/m2)	q' (mg/kg)	C	1/C	Log C	C/q	C/q'	Log q	Log q'	1/q	1/q'
115.180	38.310	12.500	22.962	2.185	0.626	1.72389	1079.158	12.500	0.080	1.097	7.251	0.012	0.237	0.033	0.580	0.001
115.180	36.540	11.000	22.962	2.185	0.626	1.74908	1094.923	11.000	0.091	1.041	6.289	0.010	0.243	0.039	0.572	0.001
115.180	35.810	10.500	22.962	2.185	0.626	1.75747	1100.178	10.500	0.095	1.021	5.974	0.010	0.245	0.041	0.569	0.001
11.168	4.160	1.200	15.848	2.550	0.626	0.09895	61.943	1.200	0.833	0.079	12.127	0.019	-1.005	-1.208	10.106	0.016
11.168	4.330	1.300	15.848	2.550	0.626	0.09796	61.321	1.300	0.769	0.114	13.271	0.021	-1.009	-1.212	10.209	0.016
11.168	4.390	1.310	15.848	2.550	0.626	0.09786	61.259	1.310	0.763	0.117	13.387	0.021	-1.009	-1.213	10.219	0.016
1.146	33.790	0.049	22.387	2.011	0.626	0.01951	12.213	0.049	20.408	-1.310	2.512	0.004	-1.710	-1.913	51.255	0.082
1.146	34.450	0.050	22.387	2.011	0.626	0.01949	12.202	0.050	20.000	-1.301	2.565	0.004	-1.710	-1.914	51.302	0.082
1.146	36.110	0.051	22.387	2.011	0.626	0.01947	12.191	0.051	19.608	-1.292	2.619	0.004	-1.711	-1.914	51.349	0.082
0.114	ND	ND	22.442	2.122	0.626	0.00193	1.207	N/A	N/A	N/A	N/A	N/A	-2.715	-2.918	518.689	0.829
0.114	ND	ND	22.442	2.122	0.626	0.00193	1.207	N/A	N/A	N/A	N/A	N/A	-2.715	-2.918	518.689	0.829
0.114	ND	ND	22.442	2.122	0.626	0.00193	1.207	N/A	N/A	N/A	N/A	N/A	-2.715	-2.918	518.689	0.829

RHODAMINE in ARS

1039.580	0.280	800.000	7.996	4.045	1.003	0.47215	473.563	800.000	0.001	2.903	1694.388	1.689	-0.326	-0.325	2.118	0.002
1039.580	0.370	750.000	7.996	4.045	1.003	0.57068	572.395	750.000	0.001	2.875	1314.214	1.310	-0.244	-0.242	1.752	0.002
1039.580	0.370	750.000	7.996	4.045	1.003	0.57068	572.395	750.000	0.001	2.875	1314.214	1.310	-0.244	-0.242	1.752	0.002
88.841	70.790	4.500	8.233	4.232	1.003	0.16360	164.094	4.500	0.222	0.653	27.506	0.027	-0.786	-0.785	6.112	0.006
88.841	73.080	4.900	8.233	4.232	1.003	0.16283	163.316	4.900	0.204	0.690	30.093	0.030	-0.788	-0.787	6.141	0.006
88.841	79.860	5.300	8.233	4.232	1.003	0.16205	162.537	5.300	0.189	0.724	32.706	0.033	-0.790	-0.789	6.171	0.006
5.572	13.400	0.450	8.359	4.180	1.003	0.01021	10.242	0.450	2.222	-0.347	44.068	0.044	-1.991	-1.990	97.930	0.098
5.572	13.910	0.470	8.359	4.180	1.003	0.01017	10.202	0.470	2.128	-0.328	46.207	0.046	-1.993	-1.991	98.314	0.098
5.572	15.110	0.540	8.359	4.180	1.003	0.01003	10.062	0.540	1.852	-0.268	53.828	0.054	-1.999	-1.997	99.681	0.099
0.544	0.890	0.035	8.063	4.177	1.003	0.00098	0.983	0.035	28.571	-1.456	35.728	0.036	-3.009	-3.008	1020.811	1.018
0.544	0.870	0.034	8.063	4.177	1.003	0.00098	0.984	0.034	29.412	-1.469	34.640	0.035	-3.008	-3.007	1018.809	1.016
0.544	0.840	0.033	8.063	4.177	1.003	0.00098	0.986	0.033	30.303	-1.481	33.555	0.033	-3.007	-3.006	1016.815	1.014

TABLE 16 (continued)

ISOTHERM VALUES - VARIABLE CONCENTRATION METHOD (VC)

MEASURED VALUES								COMPUTED ISOTHERM VALUES								
Co (mg/l)	Intensity (v-nm)	Cr (mg/l)	Wt. spk (g)	Wt. soil (g)	SA (m2/g)	q (mg/m2)	q' (mg/kg)	C	1/C	Log C	C/q	C/q'	Log q	Log q'	1/q	1/q'
0.054	6.370	0.003	8.082	4.020	1.003	0.00010	0.102	0.003	357.143	-2.553	27.443	0.027	-3.991	-3.990	9801.09	9.772
0.054	6.820	0.003	8.082	4.020	1.003	0.00010	0.102	0.003	333.333	-2.523	29.519	0.029	-3.993	-3.992	9839.75	9.810
0.054	7.360	0.004	8.082	4.020	1.003	0.00010	0.100	0.004	256.410	-2.409	39.069	0.039	-4.001	-3.999	10017.58	9.988
0.007	ND	ND	8.760	4.167	1.003	0.00001	0.014	N/A	N/A	N/A	N/A	N/A	-4.846	-4.845	70155.9	69.946
0.007	ND	ND	8.760	4.167	1.003	0.00001	0.014	N/A	N/A	N/A	N/A	N/A	-4.846	-4.845	70155.9	69.946
0.007	ND	ND	8.760	4.167	1.003	0.00001	0.014	N/A	N/A	N/A	N/A	N/A	-4.846	-4.845	70155.9	69.946
RHODAMINE in SS																
1039.580	0.960	725.000	8.310	4.057	0.626	1.02924	644.302	725.000	0.001	2.860	704.406	1.125	0.013	-0.191	0.972	0.002
1039.580	0.870	750.000	8.310	4.057	0.626	0.94744	593.099	750.000	0.001	2.875	791.605	1.265	-0.023	-0.227	1.055	0.002
1039.580	0.910	715.000	8.310	4.057	0.626	1.06195	664.783	715.000	0.001	2.854	673.287	1.076	0.026	-0.177	0.942	0.002
503.000	19.930	275.000	8.304	4.100	0.626	0.73773	461.817	275.000	0.004	2.439	372.767	0.595	-0.132	-0.336	1.356	0.002
503.000	18.960	260.000	8.304	4.100	0.626	0.78626	492.200	260.000	0.004	2.415	330.679	0.528	-0.104	-0.308	1.272	0.002
503.000	18.500	255.000	8.304	4.100	0.626	0.80244	502.327	255.000	0.004	2.407	317.781	0.508	-0.096	-0.299	1.246	0.002
49.580	29.490	1.500	8.421	4.126	0.626	0.15675	98.127	1.500	0.667	0.176	9.569	0.015	-0.805	-1.008	6.379	0.010
49.580	26.880	1.400	8.421	4.126	0.626	0.15708	98.331	1.400	0.714	0.146	8.913	0.014	-0.804	-1.007	6.366	0.010
49.580	26.120	1.350	8.421	4.126	0.626	0.15724	98.433	1.350	0.741	0.130	8.586	0.014	-0.803	-1.007	6.360	0.010
5.690	39.850	0.019	8.469	4.192	0.626	0.01830	11.457	0.019	54.054	-1.733	1.011	0.002	-1.737	-1.941	54.638	0.087
5.690	41.410	0.019	8.469	4.192	0.626	0.01830	11.456	0.019	52.632	-1.721	1.038	0.002	-1.738	-1.941	54.642	0.087
5.690	44.390	0.020	8.469	4.192	0.626	0.01830	11.454	0.020	50.000	-1.699	1.093	0.002	-1.738	-1.941	54.652	0.087
0.669	10.420	0.010	8.058	4.085	0.626	0.00208	1.301	0.010	105.263	-2.022	4.569	0.007	-2.682	-2.886	481.00	0.768
0.669	10.520	0.010	8.058	4.085	0.626	0.00208	1.301	0.010	105.263	-2.022	4.572	0.007	-2.682	-2.886	481.22	0.769
0.669	11.280	0.010	8.058	4.085	0.626	0.00208	1.300	0.001	100.000	-2.000	4.816	0.001	-2.683	-2.886	481.58	0.769
0.074	ND	ND	8.576	4.107	0.626	0.00025	0.155	N/A	N/A	N/A	N/A	N/A	-3.608	-3.811	4051.5	6.472
0.074	ND	ND	8.576	4.107	0.626	0.00025	0.155	N/A	N/A	N/A	N/A	N/A	-3.608	-3.811	4051.5	6.472
0.074	ND	ND	8.576	4.107	0.626	0.00025	0.155	N/A	N/A	N/A	N/A	N/A	-3.608	-3.811	4051.5	6.472

TABLE 17

SUMMARY OF COEFFICIENTS AND ERRORS FOR VARIOUS ISOTHERM MODELS

	VARIABLE MASS						VARIABLE CONCENTRATION					
	LLVM (area)	LLVM (mass)	HLVM (area)	HLVM (mass)	FRVM (area)	FRVM (mass)	LLVC (area)	LLVC (mass)	LHVC (area)	LHVC (mass)	FRVC (area)	FRVC (mass)
NAPHTHALENE in ARS												
Slope	25.961	101.518	0.252	0.060	0.297	0.071	-0.068	-0.001	69.919	0.070	0.939	0.939
Constant	23.780	-4.091	104.083	95.841	-1.770	-1.902	62.633	0.062	-3066.49	-3.057	-1.818	1.183
R squared	0.315	0.706	0.485	0.091	0.679	0.104	0.000	0.000	0.956	0.956	0.976	0.976
Std. error	10.629	18.181	0.072	0.052	0.057	0.058	4.553	0.005	4.150	0.004	0.040	0.040
Y error	39.469	67.515	68.842	50.098	0.215	0.221	29.892	0.030	7325.400	7.300	0.224	0.224
p-XYLENE in ARS												
Slope	293.742	316.502	1.527	-1.153	0.110	-0.138	-481.670	-0.480	1051.392	1.048	1.773	1.773
Constant	-30.437	-24.036	204.031	233.348	-2.186	-2.341	420.266	0.419	-17222.7	-17.171	-0.649	2.352
R squared	0.390	0.733	0.056	0.069	0.089	0.194	0.155	0.155	0.631	0.631	0.852	0.852
Std. error	101.840	52.923	1.746	1.174	0.098	0.078	311.517	0.311	222.765	0.222	0.205	0.205
Y error	267.730	139.150	188.190	126.595	0.318	0.255	488.600	0.487	32581.0	32.484	0.652	0.652
NAPHTHALENE in SS												
Slope	9.640	16.863	1.840	3.305	0.379	0.380	1.554	0.002	1.178	0.002	0.660	0.660

TABLE 17 (continued)

SUMMARY OF COEFFICIENTS AND ERRORS FOR VARIOUS ISOTHERM MODELS

	VARIABLE MASS						VARIABLE CONCENTRATION					
	LLVM (area)	LLVM (mass)	HLVM (area)	HLVM (mass)	FRVM (area)	FRVM (mass)	LLVC (area)	LLVC (mass)	LHVC (area)	LHVC (mass)	FRVC (area)	FRVC (mass)
Constant	1.793	2.977	9.383	15.317	-1.053	-1.292	4.957	0.008	32.97	0.053	-1.035	1.762
R squared	0.947	0.987	0.832	0.923	0.824	0.863	0.821	0.821	0.940	0.940	0.993	0.993
Std. error	1.143	0.956	0.413	0.478	0.088	0.076	0.230	0.000	0.094	0.000	0.017	0.017
Y error	1.408	1.178	5.125	5.926	0.107	0.092	4.545	0.007	110.642	0.177	0.090	0.090
p-XYLENE in SS												
Slope	4.738	8.607	0.218	0.373	0.288	0.286	0.026	-0.000	2.357	0.004	0.804	0.804
Constant	0.285	0.387	4.975	8.650	-0.697	-0.938	7.443	0.012	4.28	0.007	-0.787	2.010
R squared	0.989	1.000	0.973	1.000	0.889	0.901	0.001	0.001	0.978	0.978	0.928	0.928
Std. error	0.254	0.054	0.018	0.004	0.051	0.047	0.319	0.001	0.134	0.000	0.085	0.085
Y error	0.334	0.070	1.276	0.289	0.099	0.092	4.868	0.008	3.722	0.006	0.246	0.246
RHODAMINE in ARS												
Slope	61.488	192.980	7.822	0.850	0.440	-0.032	1.842	0.002	30.450	0.030	0.714	0.714
Constant	16.381	-14.416	98.418	145.439	-1.896	-2.128	32.671	0.033	87.09	0.087	-1.911	1.091
R squared	0.598	0.735	0.694	0.016	0.707	0.007	0.988	0.988	0.973	0.973	0.927	0.927
Std. error	12.599	28.934	1.300	1.662	0.071	0.093	0.056	0.000	1.411	0.001	0.056	0.056

TABLE 17 (continued)

SUMMARY OF COEFFICIENTS AND ERRORS FOR VARIOUS ISOTHERM MODELS

	VARIABLE MASS						VARIABLE CONCENTRATION					
	LLVM (area)	LLVM (mass)	HLVM (area)	HLVM (mass)	FRVM (area)	FRVM (mass)	LLVC (area)	LLVC (mass)	LHVC (area)	LHVC (mass)	FRVC (area)	FRVC (mass)
Error Y	53.900	124.008	66.922	85.582	0.194	0.255	65.955	0.066	683.324	0.681	0.400	0.400
RHODAMINE in SS												
Slope	12.346	20.909	0.031	0.064	0.255	0.265	0.999	0.002	0.482	0.001	0.463	0.463
Constant	0.662	1.155	25.623	42.678	-1.069	-1.292	16.597	0.027	64.47	0.103	-1.192	1.568
R squared	0.677	0.680	0.294	0.432	0.661	0.730	0.985	0.985	0.404	0.404	0.925	0.925
Std. error	4.263	7.164	0.024	0.037	0.091	0.081	0.034	0.000	0.163	0.000	0.037	0.037
Error Y	0.793	1.334	16.971	25.884	0.177	0.156	37.798	0.060	154.633	0.247	0.300	0.300

TABLE 18

ISOTHERM DERIVED VALUES vs. OBSERVED DATA

	OBSERVED DATA			MODEL RESULTS (Best Fit Model)			% ERROR		
Co (mg/l)	Cr (mg/l)	q (mg/m2)	q' (mg/kg)	Cr (mg/l)	q (mg/m2)	q' (mg/kg)	Cr	q	q'
NAPHTHALENE in ARS MODELED by FRVC (surface area basis)									
47.22380	4.50000	0.08617	86.43023	6.10000	0.08307	83.31547	35.56	-3.60	-3.60
47.22380	4.30000	0.08658	86.83483						
47.22380	4.40000	0.08637	86.63253						
6.62020	1.15000	0.01033	10.35790	0.71700	0.01113	11.15921	-37.65	7.78	7.74
6.62020	1.10000	0.01042	10.45258						
6.62020	1.10000	0.01042	10.45258						
0.66370	0.07200	0.00116	1.15997	0.06500	0.00117	1.17119	-9.72	1.17	0.97
0.66370	0.07100	0.00116	1.16193						
0.66370	0.07000	0.00116	1.16389						
0.07170	0.00300	0.00013	0.13365	0.00620	0.00013	0.12893	106.67	-2.44	-3.53
0.07170	0.00290	0.00013	0.13385						
0.07170	0.00300	0.00013	0.13365						
0.00710	0.00090	0.00001	0.01195	0.00055	0.00001	0.01326	-38.89	-16.05	10.97
0.00710	0.00080	0.00001	0.01214						
0.00710	0.00085	0.00001	0.01204						
0.00077	ND	0.00000	0.00173	0.00001	0.00000	0.00031	N/A		
0.00077	ND	0.00000	0.00173						
0.00077	ND	0.00000	0.00173						
						avg	11.19	-2.63	2.51

p-XYLENE in ARS MODELED by FRVC (surface area basis)

TABLE 18 (continued)

ISOTHERM DERIVED VALUES vs. OBSERVED DATA

	OBSERVED DATA			MODEL RESULTS (Best Fit Model)			% ERROR		
Co (mg/l)	Cr (mg/l)	q (mg/m2)	q' (mg/kg)	Cr (mg/l)	q (mg/m2)	q' (mg/kg)	Cr	q	q'
115.17980	1.10000	0.28120	282.04827	1.01600	0.23079	231.48533	-7.64	-17.93	-17.93
115.17980	1.03000	0.28138	282.22134						
115.17980	1.00000	0.28145	282.29551						
11.38890	0.46000	0.02633	26.40843	0.26200	0.02088	20.93867	-43.04	-20.70	-20.71
11.38890	0.46500	0.02632	26.39635						
11.38890	0.46300	0.02632	26.40118						
1.15470	0.02500	0.00283	2.83711	0.07200	0.00211	2.12008	188.00	-25.41	-25.27
1.15470	0.02600	0.00283	2.83460						
1.15470	0.02650	0.00282	2.83334						
0.11880	0.01650	0.00025	0.25415	0.01860	0.00019	0.19237	12.73	-25.02	-24.31
0.11880	0.01500	0.00026	0.25788						
0.11880	0.01550	0.00026	0.25664						
0.01320	0.01000	0.00001	0.00796	0.00470	0.00002	0.01679	-53.00	151.87	110.75
0.01320	0.01000	0.00001	0.00796						
0.01320	0.01000	0.00001	0.00796						
0.00130	ND	0.00000	0.00322	0.00100	0.00000	0.00108	N/A		
0.00130	ND	0.00000	0.00322						
0.00130	ND	0.00000	0.00322						
						avg	19.41	12.56	4.51

NAPHTHALENE in SS MODELED by FRVC (surface area basis)

47.22380	14.50000	0.52085	326.05307	14.00000	0.52656	329.62401	-3.45	1.10	1.10
47.22380	14.00000	0.52881	331.03497						

TABLE 18 (continued)

ISOTHERM DERIVED VALUES vs. OBSERVED DATA

	OBSERVED DATA			MODEL RESULTS (Best Fit Model)			% ERROR		
Co (mg/l)	Cr (mg/l)	q (mg/m2)	q' (mg/kg)	Cr (mg/l)	q (mg/m2)	q' (mg/kg)	Cr	q	q'
47.22380	12.00000	0.56064	350.96255						
6.67000	1.30000	0.08751	54.78259	1.00000	0.09226	57.75297	-23.08	5.43	5.42
6.67000	1.20000	0.08914	55.80275						
6.67000	1.15000	0.08996	56.31283						
0.67700	0.02500	0.01118	7.00012	0.03950	0.01093	6.84429	58.00	-2.26	-2.23
0.67700	0.03000	0.01110	6.94644						
0.67700	0.02800	0.01113	6.96791						
0.06860	0.00150	0.00102	0.63578	0.00110	0.00103	0.64401	-26.67	1.42	1.29
0.06860	0.00154	0.00102	0.63540						
0.06860	0.00100	0.00102	0.64052						
0.00710	ND			0.00004	0.00011	0.07107	N/A		
0.00710	ND								
0.00710	ND								
0.00069	ND			0.00001	0.00003	0.01832	N/A		
0.00069	ND								
0.00069	ND								
						avg	0.96	1.14	1.12

p-XYLENE in SS MODELED by FRVC (surface area basis)

115.17980	12.50000	1.72389	1079.15774	17.50000	1.63081	1020.88524	40.00	-5.40	-5.40
115.17980	11.00000	1.74908	1094.92264						
115.17980	10.50000	1.75747	1100.17761						
11.16820	1.20000	0.09895	61.94284	0.60000	0.10830	67.79660	-50.00	9.45	9.45

TABLE 18 (continued)

ISOTHERM DERIVED VALUES vs. OBSERVED DATA

	OBSERVED DATA			MODEL RESULTS (Best Fit Model)			% ERROR		
Co (mg/l)	Cr (mg/l)	q (mg/m2)	q' (mg/kg)	Cr (mg/l)	q (mg/m2)	q' (mg/kg)	Cr	q	q'
11.16820	1.30000	0.09796	61.32144						
11.16820	1.31000	0.09786	61.25930						
1.14590	0.04900	0.01951	12.21336	0.08000	0.02143	13.41710	63.27	9.84	9.86
1.14590	0.05000	0.01949	12.20223						
1.14590	0.05100	0.01947	12.19110						
	ND				0.00030	0.18951	N/A		
	ND								
	ND								
						avg	17.76	4.63	4.64

RHODAMINE in ARS MODELED by LLVC (mass basis)

1039.58000	800.00000	0.47215	473.56331	791.00000	0.48832	489.78328	-1.13	3.43	3.43
1039.58000	750.00000	0.57068	572.39528						
1039.58000	750.00000	0.57068	572.39528						
88.84100	4.50000	0.16360	164.09383	7.50000	0.15578	156.25000	66.67	-4.78	-4.78
88.84100	4.90000	0.16283	163.31559						
88.84100	5.30000	0.16205	162.53735						
5.57200	0.45000	0.01021	10.24204	0.35200	0.01041	10.44386	-21.78	1.94	1.97
5.57200	0.47000	0.01017	10.20205						
5.57200	0.54000	0.01003	10.06207						
0.54400	0.03500	0.00098	0.98255	0.03300	0.00100	0.99800	-5.71	2.08	1.57
0.54400	0.03400	0.00098	0.98448						

TABLE 18 (continued)

ISOTHERM DERIVED VALUES vs. OBSERVED DATA

	OBSERVED DATA			MODEL RESULTS (Best Fit Model)			% ERROR		
Co (mg/l)	Cr (mg/l)	q (mg/m2)	q' (mg/kg)	Cr (mg/l)	q (mg/m2)	q' (mg/kg)	Cr	q	q'
0.54400	0.03300	0.00098	0.98641						
0.05370	0.00280	0.00010	0.10234	0.00045	0.00001	0.01364	-83.93	-90.20	-86.68
0.05370	0.00300	0.00010	0.10193						
0.05370	0.00390	0.00010	0.10012						
0.00680	ND	0.00001	0.01430	0.00001	0.00000	0.00030	N/A		
0.00680	ND	0.00001	0.01430						
0.00680	ND	0.00001	0.01430						
						avg	-9.18	-17.51	-16.90

RHODAMINE in SS MODELED by LLVC (mass basis)

1039.58000	725.00000	1.02924	644.30208	800.00000	0.78258	489.89590	10.34	-23.97	-23.96
1039.58000	750.00000	0.94744	593.09872						
1039.58000	715.00000	1.06195	664.78342						
503.00000	275.00000	0.73773	461.81692	275.00000	0.75351	471.69811	0.00	2.14	2.14
503.00000	260.00000	0.78626	492.19961						
503.00000	255.00000	0.80244	502.32718						
49.58000	1.50000	0.15675	98.12687	3.80000	0.14951	93.59606	153.33	-4.62	-4.62
49.58000	1.40000	0.15708	98.33096						
49.58000	1.35000	0.15724	98.43301						
5.69000	0.01850	0.01830	11.45731	0.36000	0.01705	10.67616	1845.95	-6.84	-6.82
5.69000	0.01900	0.01830	11.45630						
5.69000	0.02000	0.01830	11.45428						
0.66930	0.00950	0.00208	1.30146	0.04000	0.00193	1.20919	321.05	-7.17	-7.09

TABLE 18 (continued)

ISOTHERM DERIVED VALUES vs. OBSERVED DATA

	OBSERVED DATA			MODEL RESULTS (Best Fit Model)			% ERROR		
Co (mg/l)	Cr (mg/l)	q (mg/m2)	q' (mg/kg)	Cr (mg/l)	q (mg/m2)	q' (mg/kg)	Cr	q	q'
0.66900	0.00950	0.00208	1.30087						
0.66900	0.01000	0.00208	1.29988						
0.07400	ND			0.00400	0.00019	0.12118	N/A		
0.07400	ND								
0.07400	ND								
						avg	466.14	-8.09	-8.07

TABLE 19

GRAIN SIZE INFLUENCES ON SOLID SURFACE SCANS IN ARS

Gradation	Co (mg/l)	Cr (mg/l)	q (mg/m2)	q' (mg/kg)	Intensity (v-nm)	# part. Visible	TSA (mm2)	Eff. SA (mm2)	Visible (ug)	Fit. Fac.	CSA (mm2)	CV (mg)	% Cryptic
					2 GRAM SAMPLE @ FIELD CAPACITY								
ARS60	5.000	2.300	0.048	0.010	18.690	460.00	5161.000	1290.250	0.061932	0.191	374.173	0.000018	80.921
ARS140	5.000	1.230	0.014	0.014	47.790	3532.00	8759.000	2189.750	0.030657	1.000	3328.420	0.000047	0.000
ARS200	5.000	0.483	0.012	0.018	44.490	4768.00	10728.000	2682.000	0.032184	0.921	3754.800	0.000045	7.895
ARS270	5.000	0.433	0.011	0.019	29.760	9864.00	9469.000	2367.250	0.026040	0.724	2603.975	0.000029	27.632
ARSPAN	5.000	0.133	0.008	0.018	15.090	25958.00	7268.000	1817.000	0.014536	0.658	1817.000	0.000015	34.211
					8 GRAM SAMPLE @ FIELD CAPACITY								
ARS60	5.000	1.550	0.016	0.003	25.260	460.00	5161.000	1290.250	0.020644	0.267	1548.300	0.000025	73.333
ARS140	5.000	0.193	0.005	0.005	26.390	3532.00	8759.000	2189.750	0.010949	0.533	5255.400	0.000026	46.667
ARS200	5.000	0.047	0.003	0.005	36.670	4768.00	10728.000	2682.000	0.008046	1.000	12069.00	0.000036	0.000
ARS270	5.000	0.122	0.003	0.005	8.680	9864.00	9469.000	2367.250	0.007102	0.267	2840.700	0.000009	73.333
ARSPAN	5.000	0.019	0.002	0.005	6.080	25958.00	7268.000	1817.000	0.003634	0.356	2907.20	0.000006	64.444
					8 GRAM SAMPLE @ DRY CONDITIONS								
ARS60	5.000	1.550	0.016	0.003	33.237	460.00	5161.000	1290.250	0.020644	0.229	2064.400	0.000033	77.143
ARS140	5.000	0.193	0.005	0.005	38.380	3532.00	8759.000	2189.750	0.010949	0.500	7664.400	0.000038	50.000
ARS200	5.000	0.047	0.003	0.005	48.753	4768.00	10728.000	2682.000	0.008046	0.857	16092.000	0.000048	14.286
ARS270	5.000	0.122	0.003	0.005	49.197	9864.00	9469.000	2367.250	0.007102	1.000	16570.750	0.000050	0.000
ARSPAN	5.000	0.019	0.002	0.005	22.867	25958.00	7268.000	1817.000	0.003634	0.857	10902.000	0.000022	14.286

TSA = Total surface area
Eff. SA = Effective surface area
Fit. Fac. = Fitting factor
CSA = Corrected surface area
CV = Corrected visible
% Cryptic = % Shielded from detection
Cr is fluorometricly measured

TABLE 20

MOISTURE AND ORGANICS INFLUENCE ON SOLIDS SURFACE SCANS IN ARS140

Measured Values								Intensities at Moistures			Calculated Values			
Co (mg/l)	Cr (mg/l)	SA (m2/g)	Wt.Sand (g)	Tot. SA (m2)	Wt.spk so (g)	q (mg/m2)	q' (mg/Kg)	Sat. (v-nm)	F. C. (v-nm)	Dry (v-nm)	Eff. Part. #	TSA mm2	Eff. SA mm2	Apparent ug
							RHODAMINE IN ARS140							
1039.777	792.000	1.003	4.045	4.057	7.996	0.488	489.796	238.213	98.033	29.987	3532.00	8759.000	2189.750	1.069323
88.650	7.600	1.003	4.232	4.245	8.233	0.157	157.676	137.277	48.183	62.837	3532.00	8759.000	2189.750	0.344239
5.575	0.352	1.003	4.180	4.193	8.359	0.010	10.444	21.350	40.457	39.210	3532.00	8759.000	2189.750	0.022801
0.550	0.033	1.003	4.177	4.190	8.063	0.001	0.998	3.497	17.917	8.233	3532.00	8759.000	2189.750	0.002179
0.053	0.003	1.003	4.020	4.032	8.082	0.000	0.100	1.383	0.907	0.223	3532.00	8759.000	2189.750	0.000218
0.007	0.000	1.003	4.167	4.180	8.760	0.000	0.014	ND	0.280	ND	3532.00	8759.000	2189.750	0.000030
							RHODAMINE IN SS140							
1039.048	799.000	0.626	4.057	2.540	8.310	0.785	491.692	112.273	48.530	8.140	3532.00	5466.000	1366.500	1.073319
503.030	268.000	0.626	4.100	2.567	8.304	0.760	476.021	219.050	26.840	6.780	3532.00	5466.000	1366.500	1.039110
49.498	3.150	0.626	4.126	2.583	8.421	0.151	94.595	1.647	1.840	3.980	3532.00	5466.000	1366.500	0.206491
5.680	0.300	0.626	4.192	2.624	8.469	0.017	10.870	0.503	0.570	ND	3532.00	5466.000	1366.500	0.023727
0.671	0.034	0.626	4.085	2.557	8.058	0.002	1.256	ND	ND	ND	3532.00	5466.000	1366.500	0.002742
0.075	0.004	0.626	4.107	2.571	8.576	0.000	0.148	ND	ND	ND	3532.00	5466.000	1366.500	0.000323

Cr a result of Langmuir models

Sat. = Saturated soil moisture content

F.C. = Field capacity

TABLE 21

CALIBRATION CURVE DATA

Uncorrected Area (v-nm)	Corrected Area (v-nm)	Uncorrected Max. Wavelength (nm)	Corrected Max. Wavelength (nm)	Uncorrected Intensity (v)	Corrected Intensity (v)	Sensitivity	Concentration (mg/l)
			NAPHTHALENE				
114.753	113.592	332.996	332.996	3.389	3.359	1	47.2200
116.151	114.806	332.829	332.829	3.429	3.399	1	47.2200
116.604	115.442	332.662	332.662	3.451	3.421	1	47.2200
101.920	100.880	333.162	332.662	3.007	2.980	1	29.7900
101.240	100.200	333.329	333.329	2.988	2.960	1	29.7900
101.200	100.230	332.829	332.662	2.988	2.962	1	29.7900
28.850	28.600	333.000	333.000	0.858	0.846	1	9.8600
28.480	28.240	334.000	334.000	0.848	0.836	1	9.8600
28.120	27.880	334.000	334.000	0.833	0.821	1	9.8600
2.690	2.750	254.000	334.000	0.093	0.082	1	1.0800
2.620	2.690	332.000	336.000	0.085	0.080	1	1.0800
2.580	2.580	332.000	332.000	0.085	0.079	1	1.0800
0.465	0.403	251.500	328.162	0.109	0.012	1	0.0659
0.350	0.411	253.000	336.662	0.088	0.011	1	0.0659
0.453	0.453	251.500	323.996	0.071	0.011	1	0.0659
28.477	28.788	256.000	332.996	4.321	0.821	12	0.0659
29.151	29.401	254.500	332.996	4.347	0.839	12	0.0659
29.349	29.843	250.833	332.996	4.351	0.850	12	0.0659

TABLE 21 (continued)

CALIBRATION CURVE DATA

Uncorrected Area (v-nm)	Corrected Area (v-nm)	Uncorrected Max. Wavelength (nm)	Corrected Max. Wavelength (nm)	Uncorrected Intensity (v)	Corrected Intensity (v)	Sensitivity	Concentration (mg/l)
-0.872	2.618	256.000	330.496	4.331	0.082	12	0.0066
-0.748	2.620	257.167	330.162	4.335	0.084	12	0.0066
-0.129	2.872	255.500	328.662	4.327	0.089	12	0.0066
-2.427	0.268	256.000	305.997	4.324	0.023	12	0.0007
-2.297	0.276	255.834	306.997	4.337	0.017	12	0.0007
-2.658	0.343	255.834	305.997	4.332	0.025	12	0.0007
			p-XYLENE				
101.608	101.364	288.665	288.665	3.441	3.400	3	115.6048
97.280	97.158	288.832	288.665	3.279	3.234	3	115.6048
95.479	95.296	288.998	288.998	3.198	3.156	3	115.6048
100.174	100.052	288.665	288.665	3.348	3.305	3	94.1780
98.432	98.493	288.665	288.665	3.292	3.249	3	94.1780
96.666	96.605	288.498	288.498	3.225	3.183	3	94.1780
93.865	94.049	287.998	288.165	3.176	3.136	3	47.3765
91.929	91.990	288.165	288.165	3.101	3.061	3	47.3765
90.848	90.848	288.332	288.665	3.051	3.013	3	47.3765
58.309	58.309	288.332	288.165	1.956	1.918	3	24.1431

TABLE 21 (continued)

CALIBRATION CURVE DATA

Uncorrected Area (v-nm)	Corrected Area (v-nm)	Uncorrected Max. Wavelength (nm)	Corrected Max. Wavelength (nm)	Uncorrected Intensity (v)	Corrected Intensity (v)	Sensitivity	Concentration (mg/l)
56.456	56.395	288.498	288.498	1.877	1.842	3	24.1431
56.456	56.395	288.498	288.498	1.877	1.842	3	24.1431
34.611	34.489	288.998	288.498	1.173	1.140	3	9.4319
32.880	32.881	288.832	288.665	1.113	1.079	3	9.4319
31.947	31.886	288.998	288.498	1.077	1.043	3	9.4319
3.971	3.788	290.665	289.998	0.133	0.104	3	0.9758
4.201	3.895	292.998	292.331	0.134	0.103	3	0.9758
4.226	3.921	293.665	292.331	0.134	0.103	3	0.9758
1.763	1.580	297.831	300.164	0.062	0.037	3	0.0961
2.220	2.037	296.498	300.664	0.074	0.049	3	0.0961
2.260	2.077	297.998	303.164	0.076	0.050	3	0.0961
61.435	56.853	300.331	300.331	2.084	1.320	12	0.0961
60.193	55.979	299.164	301.164	2.059	1.295	12	0.0961
59.608	55.271	298.831	301.664	2.045	1.282	12	0.0961
-20.061	-18.468	250.000	340.000	0.667	0.007	12	0.0097
-15.779	-16.325	250.333	355.994	0.614	0.011	12	0.0097
-16.394	-16.635	250.500	348.161	0.626	0.008	12	0.0097
1.088	-0.498	298.998	333.995	0.698	0.075	12	0.0012
5.842	6.518	300.164	307.164	0.958	0.192	12	0.0012

TABLE 21 (continued)

CALIBRATION CURVE DATA

Uncorrected Area (v-nm)	Corrected Area (v-nm)	Uncorrected Max. Wavelength (nm)	Corrected Max. Wavelength (nm)	Uncorrected Intensity (v)	Corrected Intensity (v)	Sensitivity	Concentration (mg/l)
7.910	5.957	300.331	313.830	0.889	0.163	12	0.0012
-5.888	-7.535	250.333	344.162	0.670	0.081	12	0.0001
0.203	-1.749	301.997	334.829	0.677	0.108	12	0.0001
0.762	-1.252	302.831	332.996	0.687	0.117	12	0.0001
15.608	12.739	301.997	307.664	1.072	0.315	12	0.0000
21.069	18.016	302.664	309.164	1.229	0.454	12	0.0000
21.161	17.986	302.497	307.664	1.226	0.455	12	0.0000
			RHODAMINE				
10.785	8.818	618.179	618.179	0.208	0.188	1	300.6500
10.543	8.575	619.846	619.846	0.204	0.184	1	300.6500
6.104	4.820	617.679	617.679	0.122	0.107	1	300.6500
137.194	123.419	599.010	599.010	2.819	2.729	1	100.6100
129.721	116.544	599.510	599.510	2.665	2.579	1	100.6200
125.628	112.794	600.010	600.010	2.583	2.498	1	100.6200
198.207	183.063	595.676	595.676	4.315	4.219	1	49.8900
209.688	193.945	598.010	598.010	4.336	4.232	1	49.8900
198.207	183.063	595.676	595.676	4.315	4.219	1	49.8900
138.349	133.985	585.508	585.508	3.228	3.172	1	9.7900

TABLE 21 (continued)

CALIBRATION CURVE DATA

Uncorrected Area (v-nm)	Corrected Area (v-nm)	Uncorrected Max. Wavelength (nm)	Corrected Max. Wavelength (nm)	Uncorrected Intensity (v)	Corrected Intensity (v)	Sensitivity	Concentration (mg/l)
126.358	122.080	585.675	585.675	2.920	2.868	1	9.7900
121.728	117.535	585.675	585.675	2.799	2.749	1	9.7900
81.373	80.004	582.341	582.341	1.873	1.835	1	4.8500
73.651	72.454	582.341	582.341	1.688	1.651	1	4.8500
71.197	69.828	582.841	582.841	1.622	1.587	1	4.8500
20.759	20.673	578.507	578.507	0.475	0.461	1	1.0900
18.644	18.559	578.341	578.341	0.425	0.411	1	1.0900
17.783	17.783	579.007	579.007	0.406	0.393	1	1.0900
1.647	1.647	577.174	577.174	0.046	0.040	1	0.1100
1.589	1.503	574.507	574.507	0.040	0.035	1	0.1100
1.529	1.529	577.507	577.507	0.039	0.034	1	0.1100
0.034	0.120	576.174	577.341	0.009	0.004	1	0.0110
0.199	0.199	567.006	567.006	0.007	0.004	1	0.0110
0.029	0.029	563.172	563.172	0.007	0.002	1	0.0110
148.475	148.731	577.841	578.007	3.452	3.263	12	0.1100
146.270	146.697	577.507	578.007	3.414	3.217	12	0.1100
145.342	146.026	577.674	578.007	3.406	3.208	12	0.1100
11.419	11.590	578.341	579.174	0.388	0.264	12	0.0110
10.116	10.115	577.174	577.174	0.358	0.232	12	0.0110

TABLE 21 (continued)

CALIBRATION CURVE DATA

Uncorrected Area (v-nm)	Corrected Area (v-nm)	Uncorrected Max. Wavelength (nm)	Corrected Max. Wavelength (nm)	Uncorrected Intensity (v)	Corrected Intensity (v)	Sensitivity	Concentration (mg/l)
9.559	9.644	577.841	578.007	0.349	0.223	12	0.0110
0.117	0.458	694.355	573.674	0.652	0.019	12	0.0010
0.444	0.700	699.856	574.174	0.404	0.019	12	0.0010
0.111	0.281	699.689	573.007	0.265	0.016	12	0.0010
-0.550	-0.380	699.356	665.518	0.225	0.003	12	0.0001
-0.496	-0.326	699.356	613.678	0.265	0.004	12	0.0001
-0.438	-0.268	699.689	676.853	0.240	0.004	12	0.0001

APPENDIX C

EXAMPLE FLUORESCENT SCANS

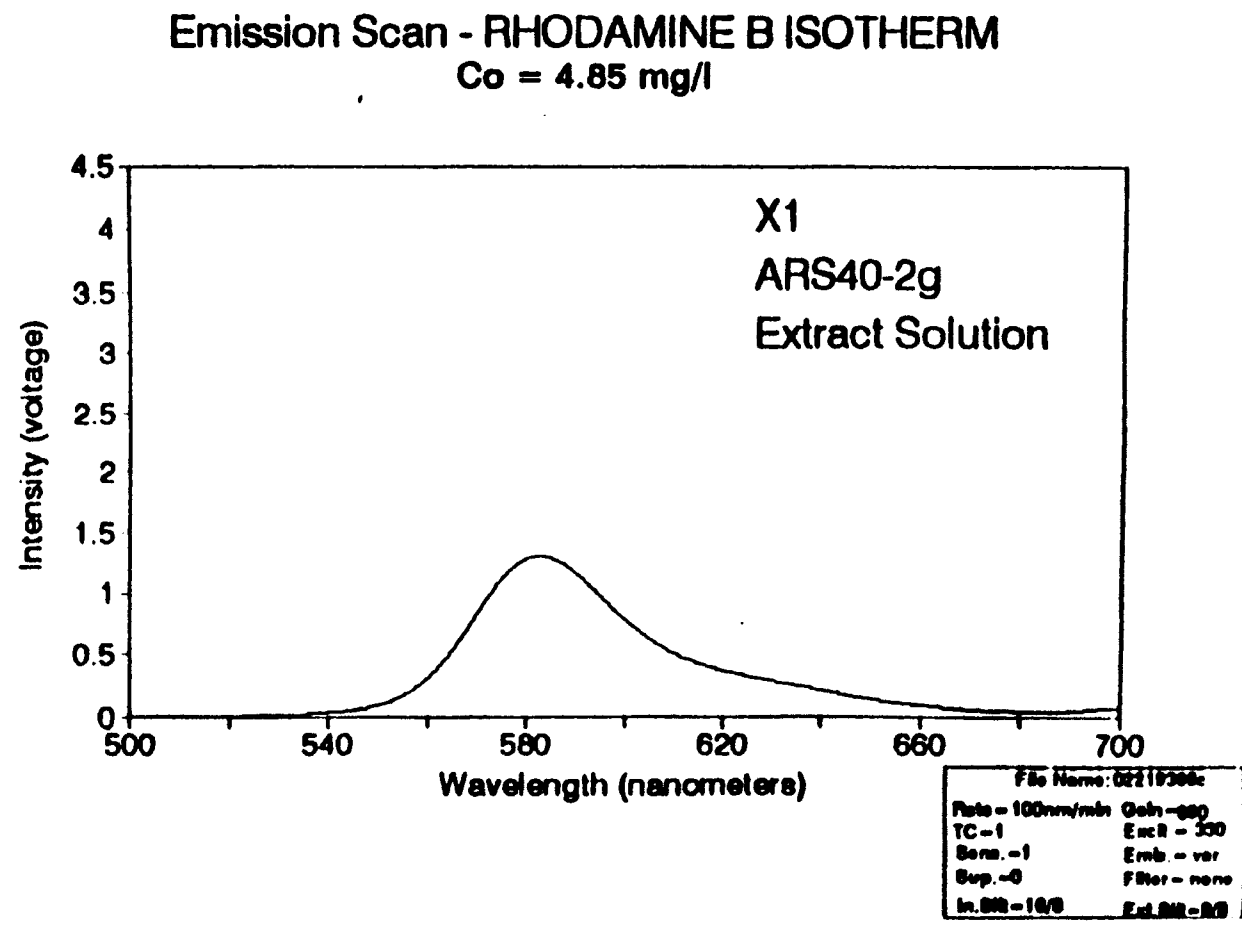

Figure C.1 Example Emission Scan of Rhodamine B Isotherm Result

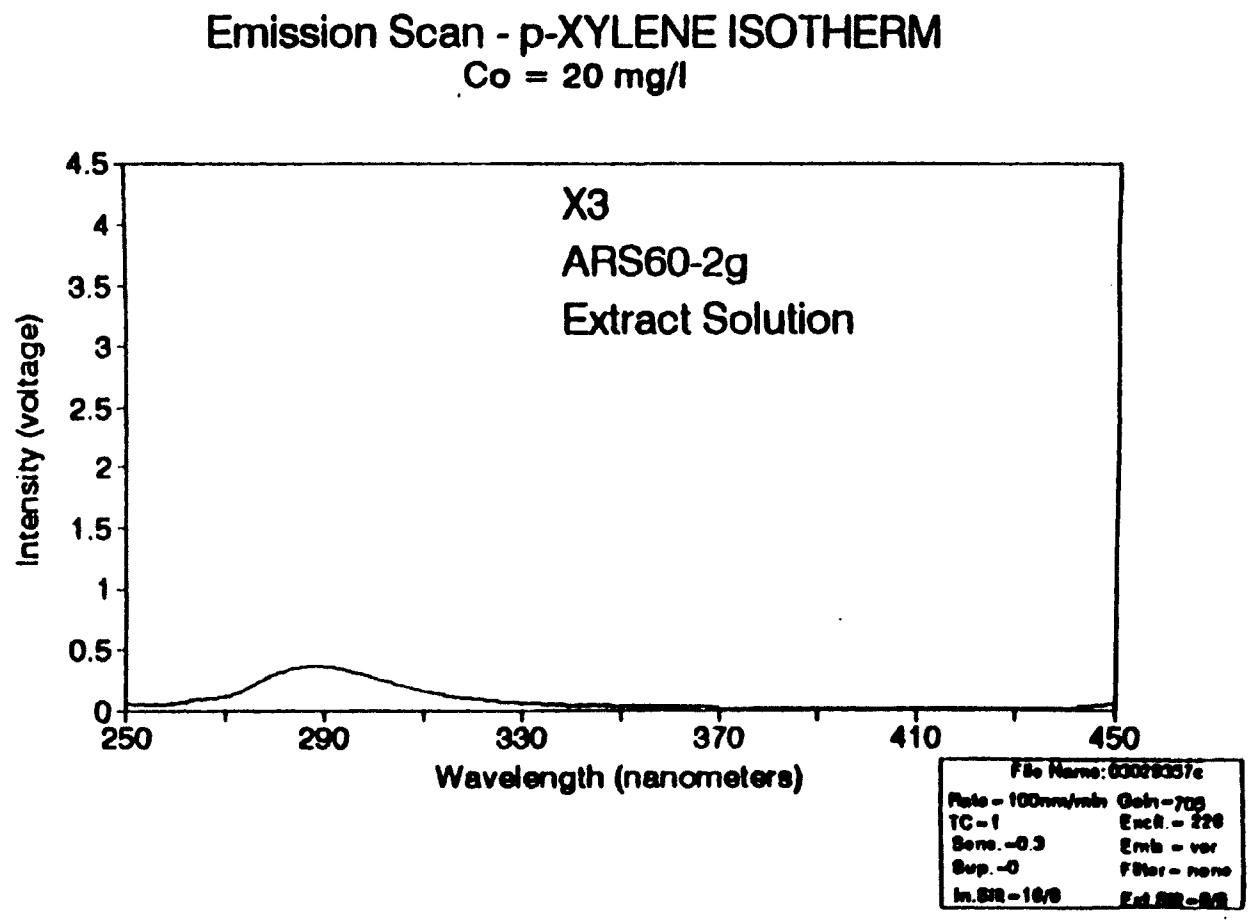

Figure C.2 Example Emission Scan of *p*-Xylene Isotherm Result

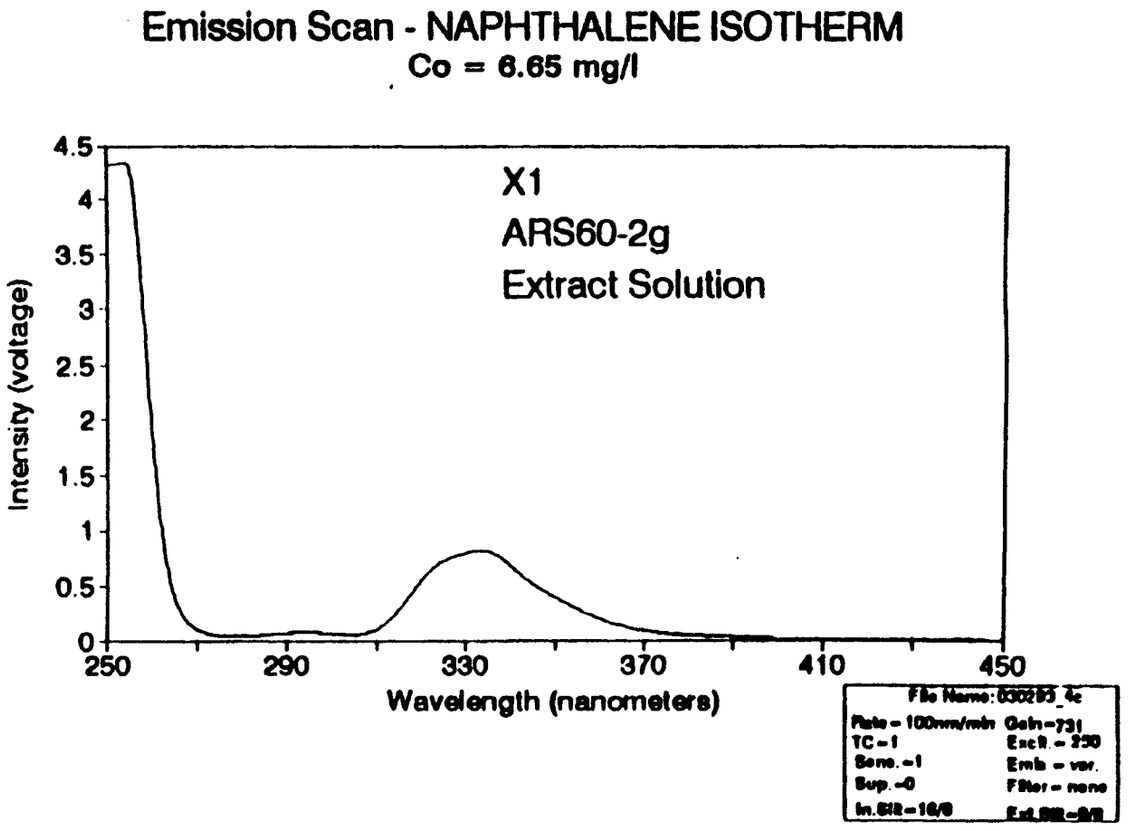

Figure C.3 Example Emission Scan of Naphthalene Isotherm Result

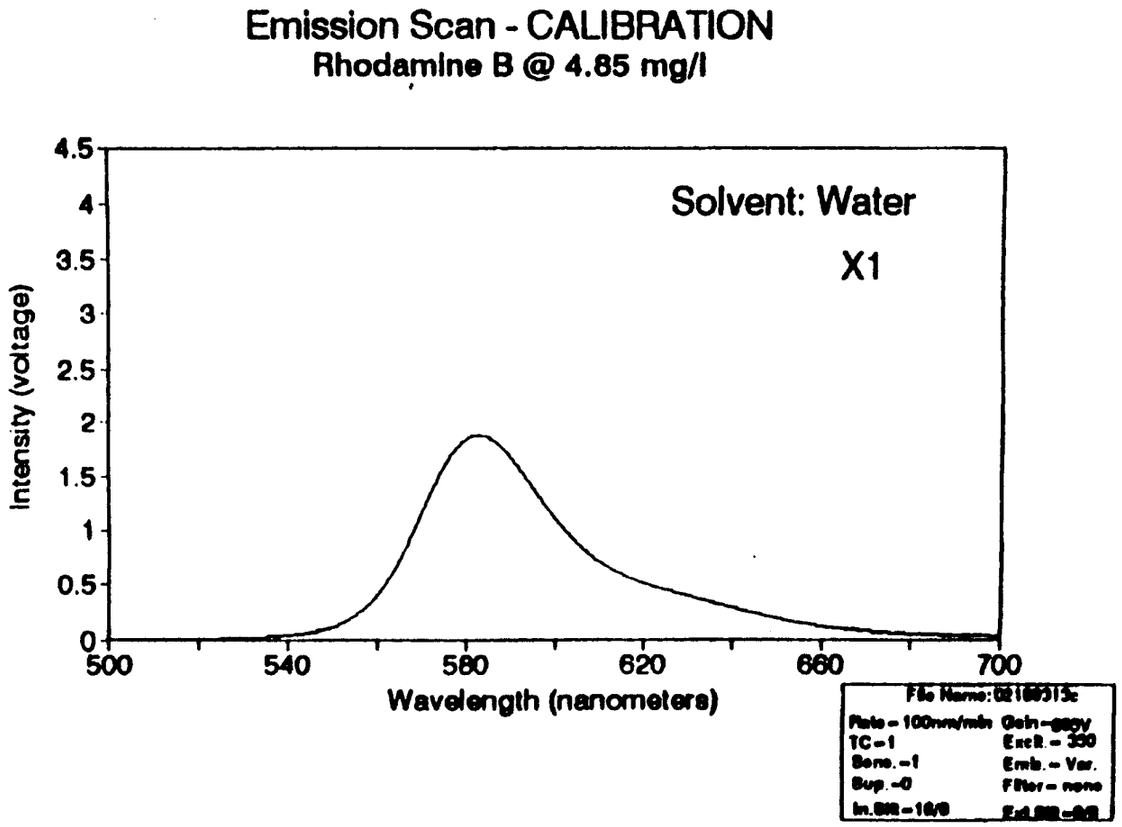

Figure C.4 Example Emission Scan of Rhodamine B Calibration Solution

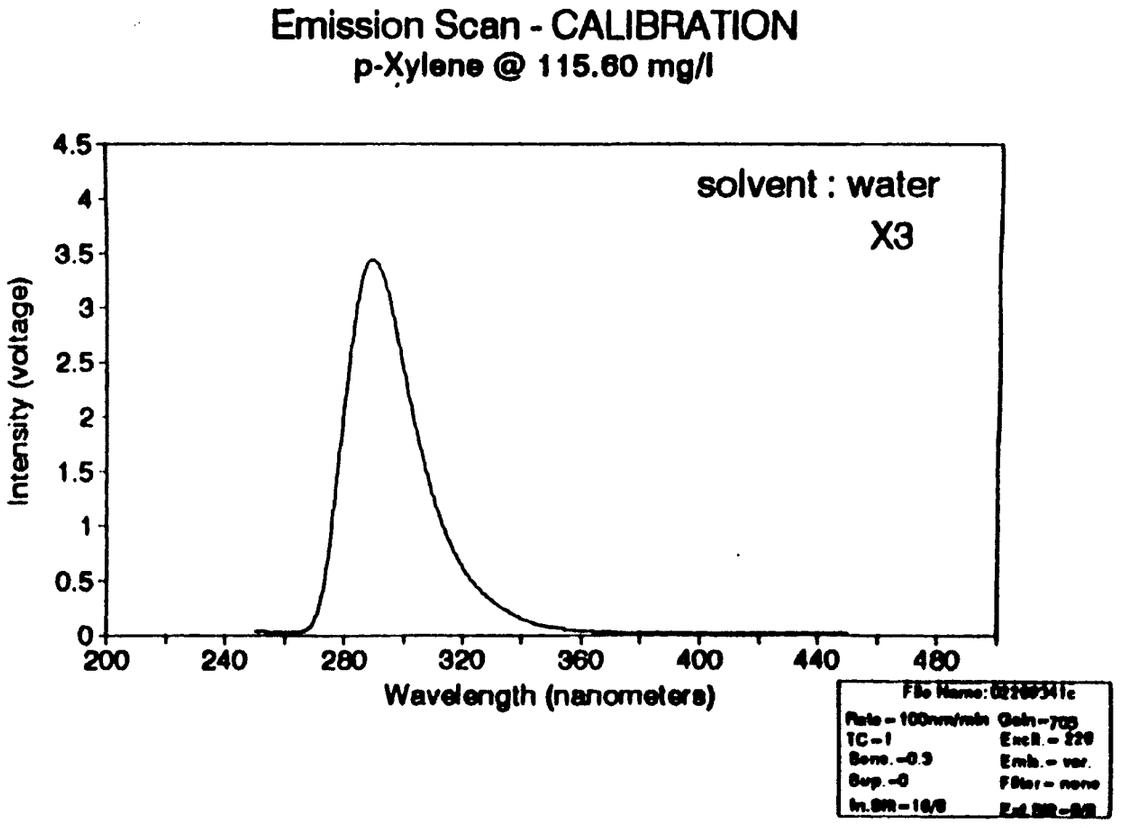

Figure C.5 Example Emission Scan of *p*-Xylene Calibration Solution

APPENDIX D

COMPUTER PROGRAM TO CALCULATE FLUORESCENT RESPONSE AREAS

```
clearall
paintcanvas border fill chr(199)
attribute 64
0,0,24,79
TEXT

                    AREA INTEGRATION PROGRAM FOR FL-750 DETECTOR

                                        by

                                   KENT P. KOLODZIEJ

                                       1/27/93


                                      VER 1.03


  WARNING:     Printer must be on before proceeding

endtext
lp=1
while lp<1000
lp=lp+1
endwhile
clearall
clear
f2=""

BB=1                    ;ARRAY SIZE     ----------------------STEP 1
CD=1                            ;
array aa[BB]
 AA[1]="052493_1"       ;---------------------------STEP 2
;AA[2]="052493_3"
;AA[3]="051993_3"
;AA[4]="051993_4"
;AA[5]="051993_5"
;AA[6]="051993_6"
;AA[7]="051933_7"
;AA[8]="051993_8"
;AA[9]="051993_9"
;AA[10]="05199310"
;AA[11]="05199311"
;AA[12]="05199312"
;AA[13]="03079313"
;AA[14]="03079341"
;AA[15]="03079342"
;AA[16]="03259313"
;AA[17]="03259314"
;AA[18]="03259315"
;AA[19]="03119316"
;AA[20]="03119317"
;AA[21]="03119318"
```

```
;AA[22]="03119319"
;AA[23]="03119320"
;AA[24]="03119321"
;AA[25]="03099328"
;AA[26]="03099329"
;AA[27]="03099330"
;AA[28]="03099331"
;AA[29]="03099332"
;AA[30]="03099333"
;AA[31]="030993_2"
;AA[32]="030993_3"
;AA[33]="030993_4"
;AA[34]="030993_5"
;AA[35]="030393_6"
;AA[36]="030393_7"
;AA[37]="030393_8"
;AA[38]="030393_9"
;AA[39]="03039310"
;AA[40]="03039311"
;AA[41]="03039312"
;AA[42]="03039313"
;AA[43]="03039314"
;AA[44]="03039315"
;AA[45]="030393_6"
;AA[46]="030393_7"
;AA[47]="030393_8"
;AA[48]="030393_9"
;AA[49]="03039310"
;AA[50]="03229311"
;AA[51]="03229312"
;AA[52]="03229313"
;AA[53]="03229314"
;AA[54]="03229315"
;AA[55]="03229316"
;AA[56]="03229317"
;AA[57]="03229318"
;AA[58]="03229319"
;AA[59]="03229320"
;AA[60]="03229321"
@1,1
??"ENTER DESCRIPTION OF TEST :  "
ACCEPT "A20" TO DESC
@2,1
??"ENTER SENSITIVITY SETTING :"
ACCEPT "A5" TO SENS

@16,1
??"ENTER BASELINE FILE :       "
ACCEPT "A8" TO F2


@18,1
??"ENTER BEGINING WAVELENGTH: "
ACCEPT "N" TO b
@20,1
??"ENTER ENDING WAVELENGTH: "
ACCEPT "N" TO c

WHILE CD<=ARRAYSIZE(AA)
BB=CD
```

```
@1,70
MESSAGE AA[BB]
MESSAGE BB
;-------------------IMPORT TABLES FROM 1ST FILE--------------
@22,48
??"IMPORTING DATA FROM FILE..."
{Tools} {ExportImport} {Import} {Quattro/PRO} {2} Quattro PRO}
{c:\\data\\} TYPEIN aa[BB]     ;---------------FILE ENTERED HERE
IF ISTABLE ("TEMP") THEN
TYPEIN "TEMP" ENTER {REPLACE}
ELSE
TYPEIN "TEMP" ENTER
ENDIF
@24,65
?? TIME()
EditKey Del Do_It! Menu
{Modify} {Restructure} ENTER TYPEIN "TEMP" ENTER Right CtrlBackspace  "waveleng"
 "th" Down CtrlBackspace  "intensity" Down CtrlBackspace  "b"
 "aseline" Down CtrlBackspace  "corr base" Down CtrlBackspace
 "line" Down ctrlbackspace "diff" Down ctrlbackspace "area" Down ctrlbackspace "
  down ctrlbackspace "area1" Up Up Up Right    ;          *2
 "n" Down  "n" Down  "n" down "n" Do_It!       ;           *3
If f2<>"" then                                ;
  Menu {Tools} {ExportImport}
  {Import} {Quattro/PRO} {2} Quattro PRO}
  {c:\\data\\} TYPEIN F2 ENTER                ;---------* BASELINE
  @24,65
  ??TIME()
 IF ISTABLE ("BASE") THEN
  TYPEIN "BASE" ENTER {REPLACE}
  EDITKEY DEL DO_IT!
  ELSE
  EDITKEY DEL DO_IT!
  TYPEIN "BASE" ENTER
 ENDIF
Endif                                         ;
 @24,65
 ??TIME()
CLEAR
Menu {Ask} {BASE} Right                       ;
Example  "x" Right Example  "a" Menu {Ask}{TEMP} Right Example
 "x" Right Right  "changeto " Example  "a" Do_It!
{Tools} {Copy} {JustFamily} ENTER TYPEIN "TEMP1" ENTER TYPEIN "TEMP" ENTER{REPLA
clear
;------------ZERO BASELINE IF NO BASELINE TABLE---------------------------
 IF F2="" THEN
  CLEARALL
  @24,35
  ??"NO BASELINE TABLE..ZEROING"
  {Ask}{temp} Right Right Right  "changeto 0" Do_It!
 ENDIF
@24,35                                                                    "
??"
CLEARALL
;---------------------END IMPORT TABLES-------------------------------------
     {VIEW}{temp}    ; ENTER TYPEIN "TEMP" ENTER
     editkey
;------------------------------------------- 1ST ITERATION   ----------------
scan for round(b,0)=round([wavelength],0)
  editkey
```

```
  a1=recno()                    ;
  if round(b,0)=round([wavelength],0) then
   a=recno()
  endif
   d=[intensity]-[baseline]   ;--BEGINNING DIFFERENCE
  if f2="" then                ;
   d=[intensity]               ;
   Y3=0
  endif                        ;
  while [wavelength]<c         ;
   f=[baseline]+d              ;-------BASELINE ADJUSTMET FROM BEGINNING WAVELENGT
   y1=[intensity]-f            ;---1ST Y VALUE
   x1=[wavelength]             ;---1ST X VALUE
   [CORR INT.]=Y1              ;--------1ST Y VALUE PLACE IN TABLE
   [CORR BASE]=f               ;
   [line]=[corr int.]          ;
   moveto record a+1           ;-------DOWN ONE RECORD
   y2= [intensity]-f           ;----2ND Y VALUE
   x2=[wavelength]             ;----2ND X VALUE
   moveto record a             ;-------BACKTO PREVIOUS RECORD
   [AREA1]=((x2-x1)*y1)+(.5*((x2-x1)*(y2-y1))) ;---AREA CALCULATION   ****1
   moveto record a+1           ;--------DOWN ONE RECORD
   a=recno()                   ;---------GET RECORD #
    @24,35
    ??"RUNNING...",a
  endwhile
  [corr base]=f                        ;
  [corr int.]=[intensity]-[corr base]  ;
;------------------------------------------- 2nd ITERATION -------------

;----------------------------------------ZEROING CORRECTED LINE
moveto record a1                          ;
while [wavelength]<c                      ;
    @24,35
    ??"THINKING...
    moveto [wavelength]
 scan for round(b,0)=round([wavelength],0)
    if round(b,0)=round([wavelength],0) then
     y1=[corr int.]              ;----BEGINNING WAVELENGTH
     a1=recno()                  ;---RECORD # OF BEGINNING
    endif
    moveto record a1
  scan for round(c,0)=round([wavelength],0)
    if round(c,0)=round([wavelength],0) then
     a2=recno()
    endif
    [diff]=a2                    ;
  endscan
    moveto record a2-3           ;
    y2=[corr int.]               ;
 endscan
    y3=(-y2)/(a1-a2)             ;---LINE INCREMENT/NM INTEGRATED
    [diff]=y3
endwhile
;-----------------------------------------------------------------

;-----------------------------------------CORRECT LINE VALUES-------
    moveto record a2-3        ;--------MOVE TO ENDING RECORD # FUZZY
if [corr int.]<>0 then        ;---------CHECK TO SEE IF CORR. INT. IS OFF ZERO
     y4=0
```

```
     Y2=0                        ;
     count=a1
     moveto record a1            ;---------MOVE TO BEGINNING RECORD
     a=recno()                   ;---------IDENTIFY BEGINNING RECORD
    while count<=a2-3            ;---------WHILE LESS THAN ENDING RECORD
      y1=[corr int.]-y4          ;---1ST Y VALUE
      [line]=[CORR INT.]-Y4      ;---------INPUT 2ND Y VALUE INTO TABLE..[LINE]
      y4=y4+y3                   ;---------INCREMENT ZEROING VALUE
      down                       ;---------DOWN ONE RECORD
      count=count+1
      @24,35
      ??"RUNNING 2ND ITERATION..",count
    endwhile
    [diff]=y4
endif
      do_it!

;-----------------------------------3rd INTERATION ----------------------
MOVETO RECORD A1
scan for round(b,0)=round([wavelength],0)
  editkey
  a1=recno()                     ;
  if round(b,0)=round([wavelength],0) then
   a=recno()
  endif
   y3=0                          ;
  while recno()<a2-3             ;
   y1=[line]                     ;---1ST Y VALUE
   x1=[wavelength]               ;---1ST X VALUE
   moveto record a+1             ;-------DOWN ONE RECORD
   y2= [line]                    ;----2ND Y VALUE
   x2=[wavelength]               ;----2ND X VALUE
    if isblank("line") then
     loop
    endif
   moveto record a                ;-------BACKTO PREVIOUS RECORD
   [AREA]=((x2-x1)*y1)+(.5*((x2-x1)*(y2-y1))) ;---AREA CALCULATION
   moveto record a+1              ;--------DOWN ONE RECORD
   a=recno()                      ;---------GET RECORD #
    @24,35
    ??"3rd ITERATION...            ",a
  endwhile
endscan
do_it!

;-----------------------------SCREEN DUMP CREATION -------------------
   SUM=csum("temp","AREA")
   sum2=csum("temp","area1")    ;            *4
   CLEARimage
   clear
   printer on
    @2,15
    ?"Input file is:                                          ",aa[bb]
    @4,15
    ?"Input baseline file is:                                 ",F2
    @16,15
    ?"Beginning Wavelength is :                               ",b
    @18,15
    ?"Ending Wavelength is:                                   ",c
```

```
   @19,15
   ?"Total # points evaluated is:                          ",λ2-a1
   @20,15
   ?"Total area under curve is (uncorr., baseline corr.): ",round(sum2,3)  ;
   @20,70                                          ;
   ??", ",round(sum,3)                                   ;
 clear                                             ;
  xy=cmax("temp","intensity")
    {view}{temp}
    scan for [intensity]=xy
     if [intensity]=xy then
      moveto [wavelength]
     xy=[wavelength]
     endif
      @21,15
      ?"Maximum original intensity occurs at wavelength:     ",round([wavelengt
     quitloop
    endscan
  xx=cmax("temp","line")
    {view}{temp}
    scan for [line]=xx
     if [line]=xx then
      moveto [wavelength]
      xx=[wavelength]
    endif
      @22,15
      ?"Maximum corrected intensity occurs at wavelength:    ",[wavelength]
     quitloop
    endscan
   @23,15
   ?"Corrected maximum intensity response (v)              ", cmax("temp","line"
   @24,15
   ?".                                                      "    ;
   @1,15
   ?".                                                      "    ;

;   report "temp" "1"                        ;
   PRINTER OFF
   printer on                               ;
   printer off                              ;
;-------------------------------COPY DATA TO MASTER FILE -----------------
  clear
   {view}{u:master}editkey
   moveto [input file] ins
      [input file]=aa[bb]
      [baseline file]=f2
      [beginning wave]=b
      [ending wave]=c
      [total pts]=a2-a1
      [total area un]=sum2
      [total area co]=sum
      [max int. wave un]=xy
      [max int. wave co]=xx
      [max int. un]=cmax("temp","intensity")
      [max int. co]=cmax("temp","line")
      [date]=today()
      [description]=desc
      [sensitivity]=sens
   do_it!
```

```
;-----------------------------EXPORT DATA ----------------------------------
   CLEAR
    @24,35
    ??"COPYING FILE TO \\TXT\\ DIRECTORY:"      ; ****2/18
   RUN "DEL *.TXT"
   {Tools} {ExportImport} {Export} {Ascii} {Delimited} {temp}
   TYPEIN aa[bb] ENTER
   RUN "COPY *.TXT \\TXT"                        ;******2/18
   RUN "DEL *.TXT"
    @24,65
    ??time()

QUITLOOP
endscan

clearall
clear
CD=CD+1
ENDWHILE
```

APPENDIX E

SURFACE CONTOURS AND FILTERING EFFECTS ON FL-750 SIGNAL RESPONSE

SURFACE CONTOURS AND FILTERING EFFECTS ON FL-750 SIGNAL RESPONSE

Introduction

The combination of sample preparation and instrumentation setup are key input parameters for signal response optimization by the FL-750 Spectrofluorescence Detector. The shape of the samples surface influences the output of detector readings. Flat, convex and concave surfaces are investigated in this report. Also the role of light filtering is examined. Flat surfaces in combination with proper filter was determined to be the optimum configuration.

Flat Surfaces and Filtering

Arkansas River sand retained on a No. 140 sieve was placed on the flat surface of a white sample holder. The sand was saturated with deionized water and subjected to a spectrofluorescent scan. Figure E.1 illustrates the light scattering effects of the sand and deionized water. Photomultiplier tube (PMT) overload occurs around the excitation wavelength of 305 nm. At 400 nm the PMT is no longer saturated, intensity is at it's maximum of 1.4 volts. Intensity gradually reduces until it reaches 580 nm where a second peak occurs saturating the PMT to an overloaded condition. This peak beginning at 580 nm and ending at 620 nm is due to second order light scatter from the excitation wavelength of 305 nm.

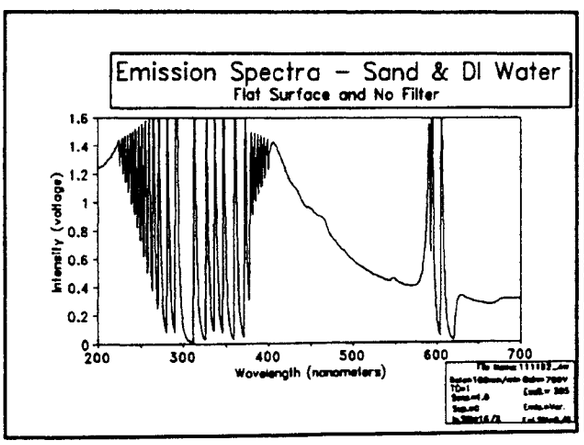

Figure E.1 Sand and Deionized Water. Flat Surface no Filter

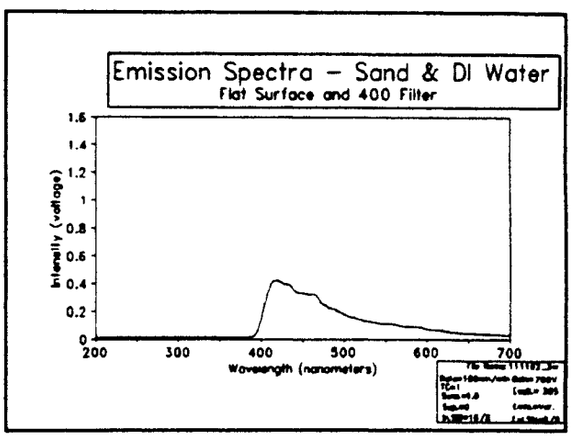

Figure E.2 Sand and Deionized Water. Flat Surface, 400 nm Filter

Some of the light scattering was eliminated through the addition of a 400 nm cutoff filter placed between the sample and the PMT. Figure E.2 illustrates the effects on the sample output readings once the filter was in place. Scatter around the excitation wavelength was eliminated as well as the secondary scatter which occurred at 610 nm.

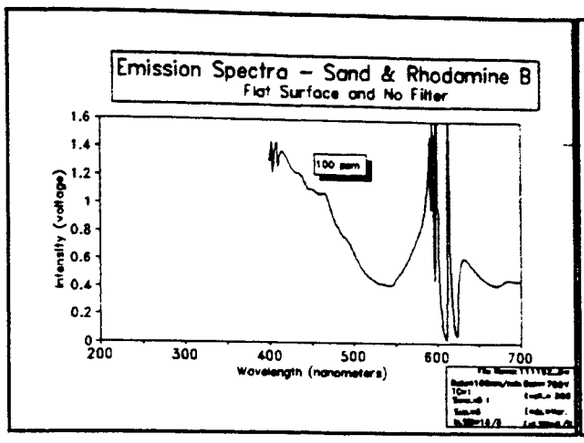

Figure E.3 Sand and Rhodamine on Flat Surface With No Filter

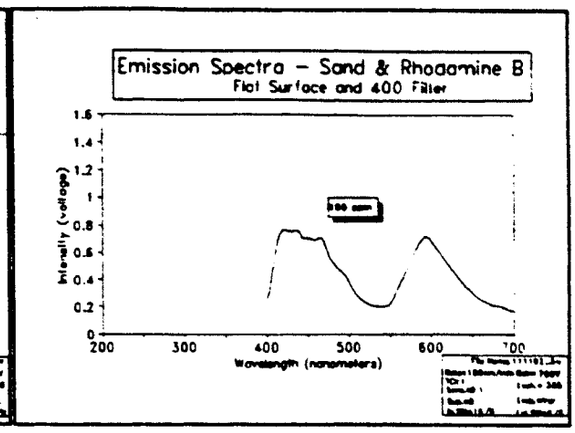

Figure E.4 Sand and Rhodamine on Flat Surface with 400 nm Filter

Next, the sample was spiked with 100 ppm solution of Rhodamine B and placed on a flat sample holder. Figure E.3 illustrates that the second order scatter masks the output expected from the 100 ppm spike. Figure E.4 is the same sample with the addition of a 400 nm filter in place to eliminate second order light scatter. A distinct peak due to rhodamine at 590 nm is now visible.

Concave Surface and Filtering

A new surface was constructed by grinding the porous membrane of a white soil holder into a concave shape. A sample of soil was then placed on the concave surface and wetted with deionized water. Figure E.5 illustrates the effects on the output of a concave surface with no filter. When Figure E.5 (concave surface) is compared to Figure E.1 (flat surface) a noticeable signal attenuation was observed. PMT overload is reduced in the 300 nm range as well as the 610 nm range. The slope of the line between 350 nm and 600 nm is also reduced in the concave sample.

Figure E.6 illustrates the effects on the concave surface signal response once a 400 nm cutoff filter was added to the instrument. The signal was dramatically reduced. There was no PMT overload and very little light scattering effects from excitation wavelength of 305 nm.

A soil sample spiked with 100 ppm Rhodamine B was placed on the concave surface and scanned. Sensitivity was increased 6 times by switching from a 1.0 setting to 0.1 setting. Figure E.7 illustrates the soil sample's signal response on a concave surface without a filter.

In Figure E.8, a 400 nm cutoff filter was installed to eliminate the second order scatter. A clear peak occurs at 590 nm but is somewhat diminished when compared to the peak from Figure E.4 which contained the same spike concentration. Therefore it appears that

although the concave surface helps to reduce light scattering effects, it also reduces signal response from the fluorescent material.

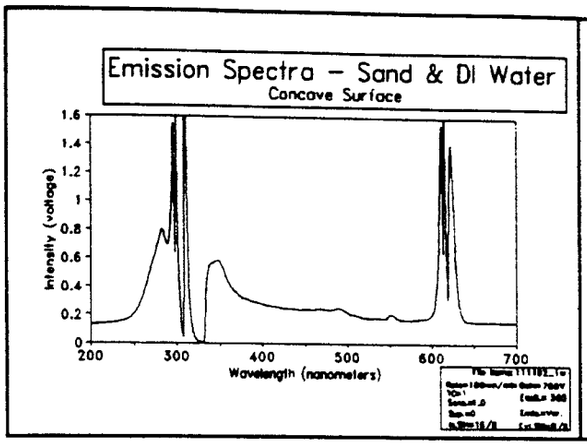

Figure E.5 Sand and Deionized Water With Concave Surface and no Filter

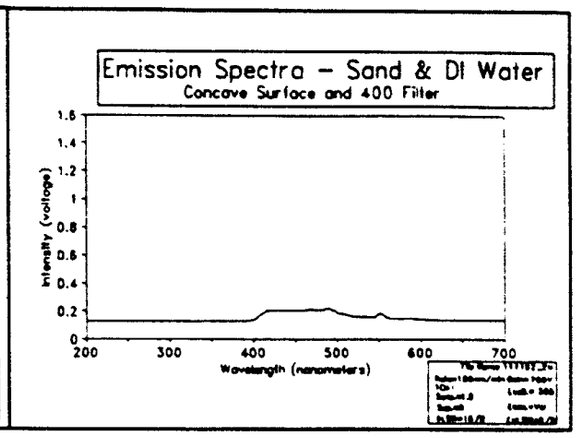

Figure E.6 Sand and Deionized Water With Concave Surface with 400 nm Filter

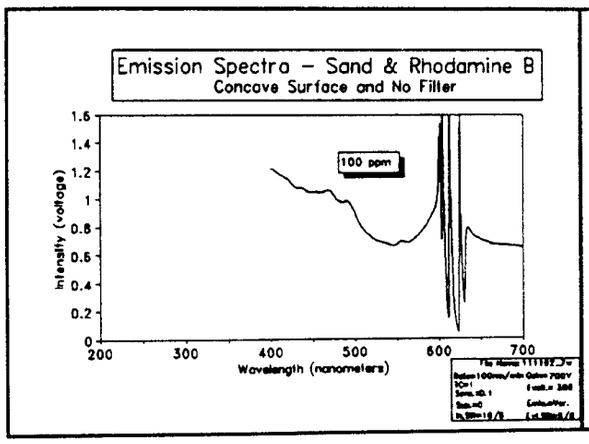

Figure E.7 Sand and Rhodamine on Concave Surface with No Filter

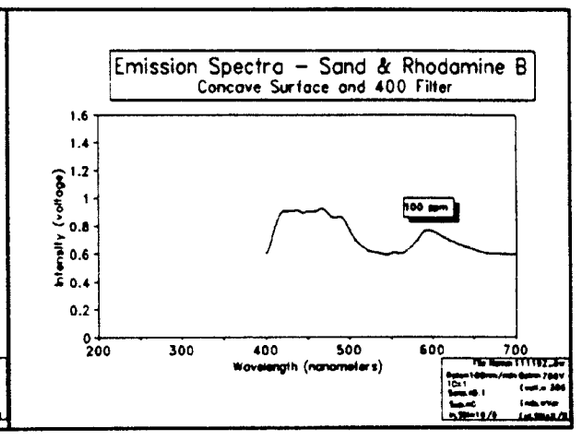

Figure E.8 Sand and Rhodamine on Concave Surface With 400 nm Filter

Convex Surfaces and Filtering

Figure E.9 illustrates the signal response due to a convex surface with no filter. Primary and second order light scattering effects are dramatically reduced. Background noise is virtually eliminated. Figure E.10 illustrates the effects of the addition of a 400 nm filter. The same dramatic reduction of light scatter and background noise is observed.

Finally, the soil was spiked with a 100 ppm solution of Rhodamine B and scanned. Figure E.11 illustrates the signal response of a spiked soil sample with a convex surface and no filter. Second order scatter has again saturated the PMT and masked any response of the fluorescent material.

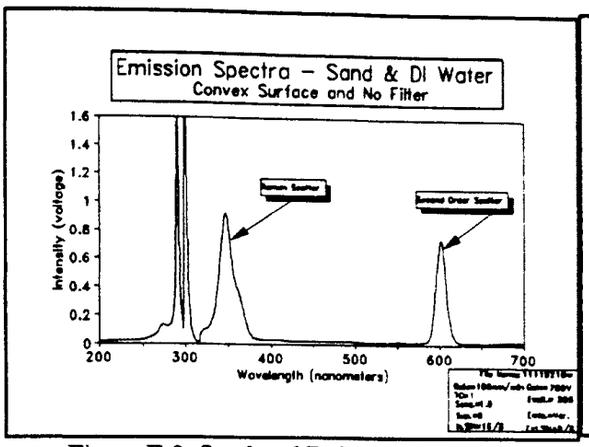

Figure E.9 Sand and Deionized Water on Convex Surface With No Filter

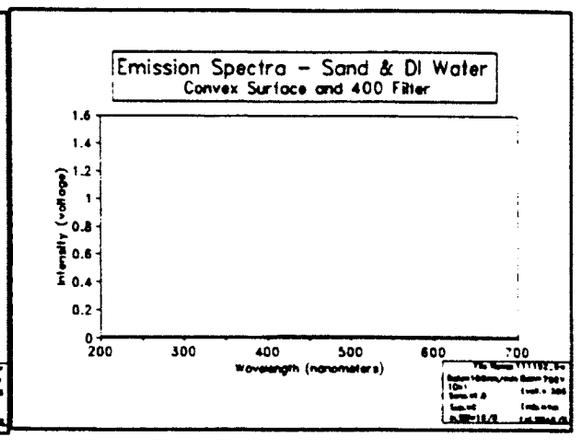

Figure E.10 Sand and Deionized Water on Convex Surface With No Filter

Figure E.12 illustrates the signal response of the same spiked soil with a filter. Almost no response is observed from the convex surface. A very slight peak can be discerned at 590 nm slightly above background noise.

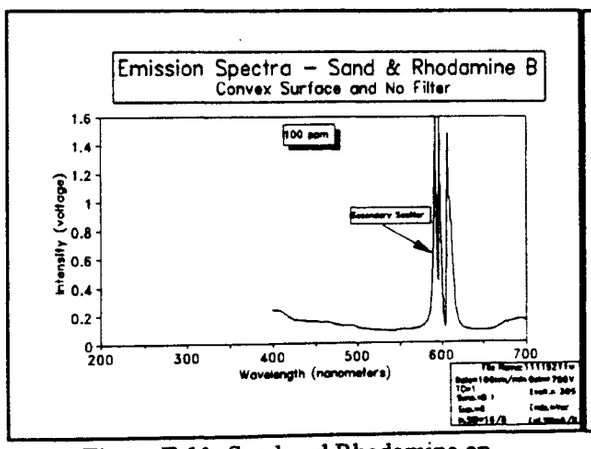

Figure E.11 Sand and Rhodamine on Convex Surface With No Filter

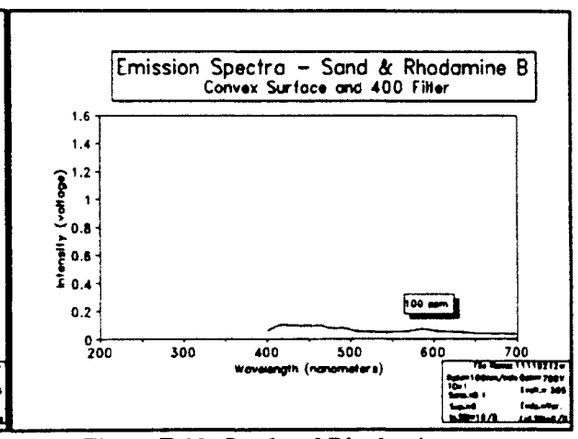

Figure E.12 Sand and Rhodamine on Convex Surface With 400 nm Filter

CONCLUSION

Light scattering from direct reflectance of the excitation wavelength can be reduced. Filters help to eliminate the second order light scatter. Filters also help to reduce the slope of the intensity curve coming from the excitation wavelength.

The shape of the samples surface is also critical to the signal response. A flat surface appears to be the best surface configuration. A concave surface slightly attenuate the signal response and will affect the instruments sensitivity. A convex surface dramatically alters the signal response by significantly attenuating the signal and is not a recommended surface configuration.

APPENDIX F

EQUIPMENT DETECTION LIMITS OF FLUORESCENT DYES IN AQUEOUS SOLUTIONS

EQUIPMENT DETECTION LIMITS OF FLUORESCENT DYES IN AQUEOUS SOLUTIONS

Introduction

This report is based upon an attempt to identify the liquid phase detection limits of the FL-750 Spectrofluorescence Detector. A qualitative and semi-quantitative analysis using fluorescent Dyes of know absorption and emission fluorescent spectra were used in the experiment. Serial dilutions were made from stock solutions of approximately 1000 ppm and reduced an order of magnitude until reaching a 1 ppt solution. These dilutions were then placed in a cuvette and subjected to spectrofluorescence analysis.

Method

Fluorescein Mercuric Acetate (FMA) and Rhodamine B were chosen as the fluorescent dyes to be used because of certain fluorescent characteristics they posses. Rhodamine B has long been used as a standard dye in many types of past experiments. Rhodamine B was also utilized as a calibration standard in experiments listed in various literature sources.

Fluorescein Mercuric Acetate was initially chosen because of its large separation between absorption and emission wavelengths. This large separation could possibly be used as an advantage to cut down on light scatter due to soils when the dye is placed in mixed media environments found with in soils.

Deionized water was used as a solvent to prepare serial dilutions. These dilutions were eventually used as spikes in soil matrixes. Table F.1 lists the gravemetrically determined serial dilution concentrations.

TABLE F.1
SERIAL DILUTIONS

Solution #	FMA Conc. in PPM	Rhodamine B Conc. in PPM
1	977.00	1018.00
2	98.00	100.00
3	11.00	11.00
4	1.00	1.00
5	0.11	0.11
6	0.012	0.013
7	0.0014	0.0014
8	0.00015	0.00016
9	0.000017	0.000017

Absorption and emission spectra were then created for each dye using a concentration of 0.1 ppm as a standard. Figure F.1 illustrates the absorption spectra of Fluorescein Mercuric Acetate. Maximum absorption occured at approximately 490 nm. FMA also

possessed a long absorption spectra of low intensity, roughly .1 volts, starting at 240 nm and ending at 410 nm as indicated in Figure F.1.

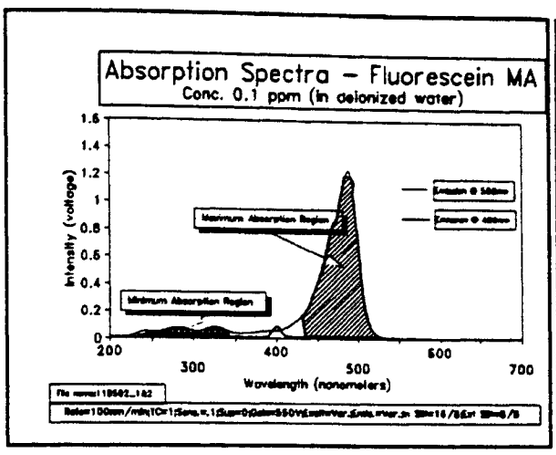

Figure F.1 Absorption Spectra of FMA

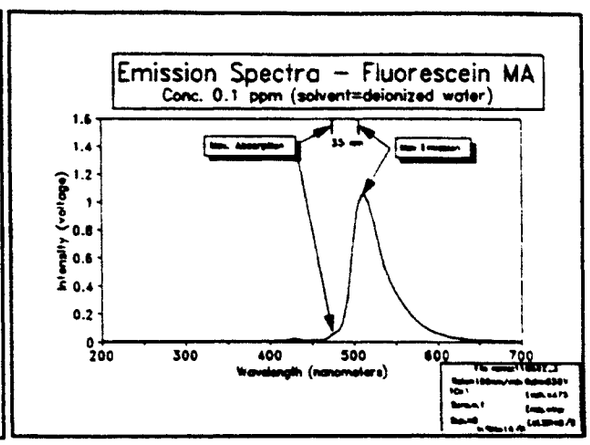

Figure F.2 Emission Spectra of FMA

Figure F.2 illustrates the maximum emission spectra of FMA occured at approximately 510 nm, when excited close to its maximum absorption, in this case 475 nm. An emission of 510 nm was expected to occur at various intensities over an excitation range from 240 nm to 490 nm.

Figure F.3 illustrates the emission of FMA occured at 510 nm when excited at 285 nm. This figure serves to illustrate the large separation distance that can be achieved between excitation and emission.

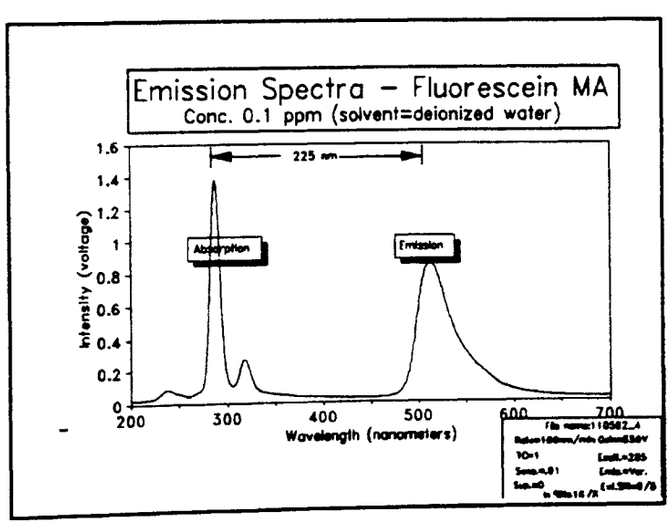

Figure F.3 Emission of FMA when Excited at 285 nm

Similar data were collected for rhodamine's emission and excitation spectra. Figure F.4 illustrates the maximum absorption occurring at 550 nm. Again a long region of low absorption precedes the large absorption region. This region of low absorption begins at approximately 250 nm and ends at approximately 475 nm.

Figure F.5 illustrates the maximum emission region occurring around 580 nm. This emission can be expected to occur when excited anywhere between 250 nm and 550 nm.

Figure F.6 illustrates the large separation which can be achieved between excitation and emission. Excitation impinges electromagnetic radiation upon the

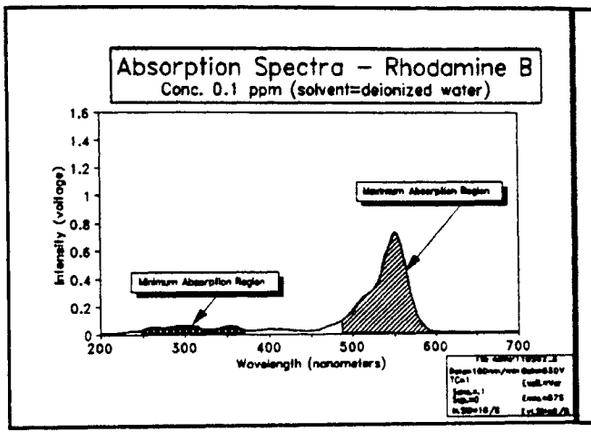

Figure F.4 Absorption Spectra of Rhodamine

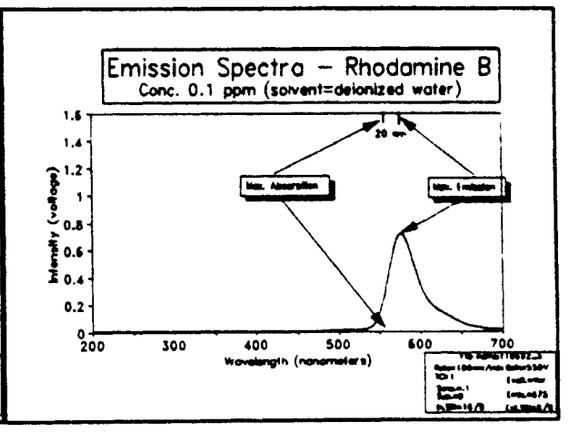

Figure F.5 Emission Spectra of Rhodamine

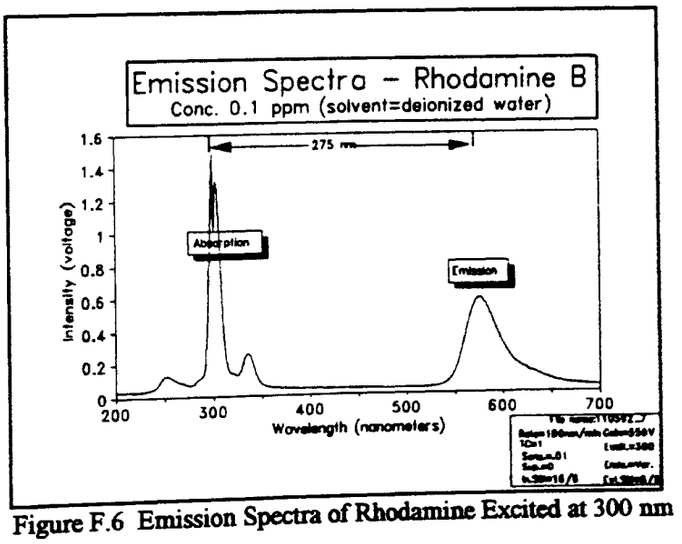

Figure F.6 Emission Spectra of Rhodamine Excited at 300 nm

the aqueous solution of 0.1 ppm Rhodamine B at 300 nm and a fluorescent emission of 580 nm occured simultaneously from the cuvette. Therefore a separation of 280 nm between excitation and emission is shown to produce satisfactory emission results. Next, detection limits of the two dyes using these large separation distances between excitation and emission were investigated. Aqueous solutions placed in cuvettes were first used to determine these limits.

Successively smaller solution concentrations were placed into cuvettes and readings were recorded until the most sensitive adjustments to the instruments were reached with no apparent emission intensity deflection. At this point if no noticeable raise beyond background noise was observed the detection limits of the instrument were assumed to be reached. The results were then compared to a baseline condition using deionized water, if no difference between the last concentration of FMA and the deionized water were detected, a "no detect" was assigned to the concentration. Therefore the last concentration before the current concentration would be considered the lowest detect level of the dye in cuvettes at a large separations.

Both FMA and Rhodamine B demonstrated detectabilities near the 1 ppb range with FMA possibly detectable in the 0.1 ppb region (further investigation warranted). Figure F.7 illustrates a peak occurring at 510 nm or FMA's emission signature. Instrument settings were adjusted to their most sensitive positions. Gain was at 820 volts to the photomultiplyer tube and sensitivity was adjusted to .003 (most sensitive). Excitation was placed at 285 nm.

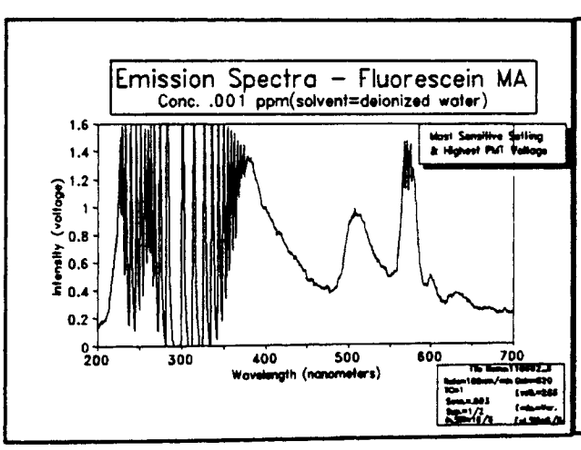

Figure F.7 Lowest Detection Limit of FMA

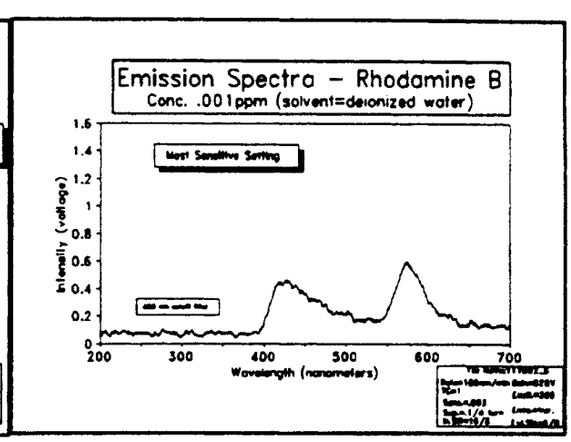

Figure F.8 Lowest Detection Limit of Rhodamine

Figure F.8 illustrates a peak occurring at 580 nm, Rhodamine B's emission signature, while maintaining the same instrument settings used in the FMA investigation. A 400 nm cutoff filter was used in the rhodamine B emission detection to eliminate the effects of secondary light scatter. The data is suppressed from 200 to 400 nm as can be seen in Figure F.8.

It is important to note that these detection limits were established for large separation distances between excitation and emission. It is also important to note that the absorption is very low at these distant points. It is therefore possible to attain better detection limits for the instrument if excitation were moved to their maximum absorption locations on the electromagnetic spectrum, 490 nm for FMA and 54 5nm for Rhodamine B.

Evidence presented through the comparison of Figure F.9 and F.10 demonstrated that an order of magnitude in detection limits can be gained by exciting the sample in a cuvette at it's maximum excitation wavelength. A sample of Rhodamine B with a concentration of .1 ppb was excited at it's maximum absorption of 545 nm and the emission was compared to a baseline emission of deionized water. Figure 9 is the baseline condition for deionized water. Figure 10 is the emission spectra of .1 ppb Rhodamine B solution.

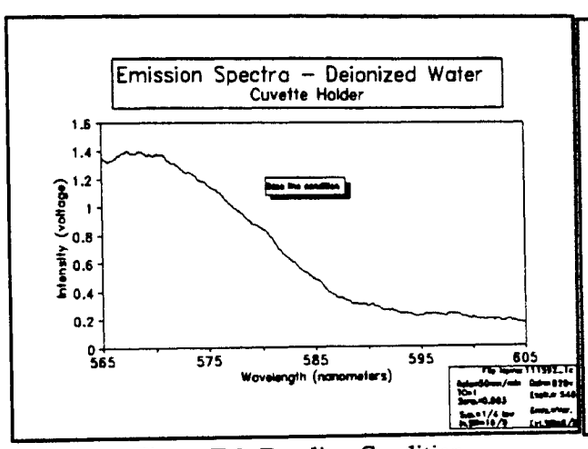

Figure F.9 Baseline Condition

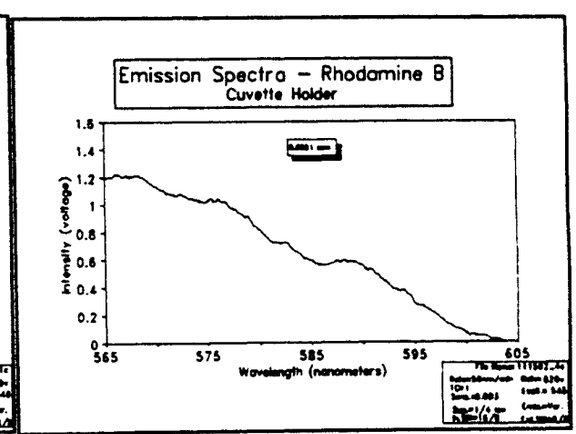

Figure F.10 Rhodamine at 0.1 ppb

Figure F.11 illustrates a composite value representing the numerical difference between Figures F.9 and F.10. Using the deionized water as the baseline, these intensity (voltages) values were subtracted from the values in the 0.1 ppb sample.

Therefore it may be more advantageous to excite the sample close to its maximum absorption value in order to review samples in the 0.1 ppb range using this instrument. However, this may not be possible when the fluorescent material is within a soil matrix subjected to high levels of light scattering.

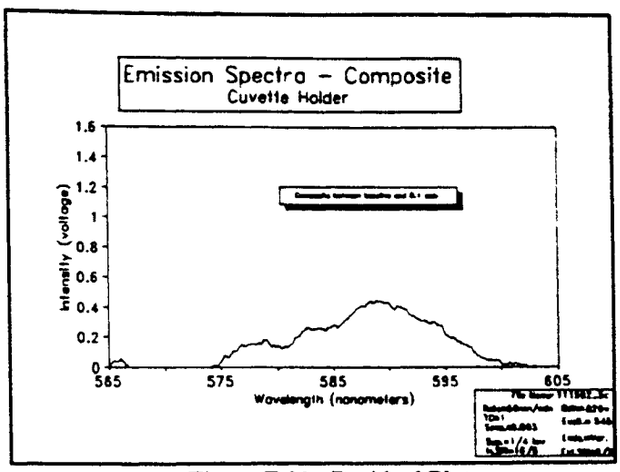

Figure F.11 Residual Plot

APPENDIX G

EQUIPMENT DETECTION LIMITS OF FLUORESCENT MATERIAL IN SOILS

EQUIPMENT DETECTION LIMITS OF FLUORESCENT MATERIAL IN SOILS

Introduction

A qualitative analysis of the detection limits for fluorescent materials in soil were investigated using a single grade of sand and various concentrations of fluorescent dyes. Numerous issues emerged concerning the influence of outside variables such as evaporation rate and beam focusing were duly noted and will be investigate at a later date. This report serves only to address the broad question of: can fluorescence be detected in a soil matrix and at roughly what concentration limits.

Method

Rhodamine B was used as the fluorescent dye to spike approximately 1 gram of soil. Rhodamine B in solution concentrations ranging from 100 ppm to 0.1 ppb were applied to the soil then subjected to scanning by the FL-750 instrument to detect any fluorescent emission coming from the soil matrix due to the dye. The sand was a single gradation, No. 145 , which originated from the banks of the Arkansas River in Tulsa.

Based upon previous evidence Rhodamine B can be excited at electromagnetic wavelength far less than it's expected emission of 580 nm - 590 nm without much loss in instrument sensitivity. The ability to fluoresce at 580 nm from an excitation of 305 nm can be used as means to cut down on Rayleigh scatter or direct reflectance from the sand particles. In addition, by placing a 400 nm cutoff filter between the light source and the sample, second order light scattering effects can be eliminated from the data.

The following figures illustrate the initial detection limits observed by placing Rhodamine B on a sample of No. 145 graded Arkansas River sand.

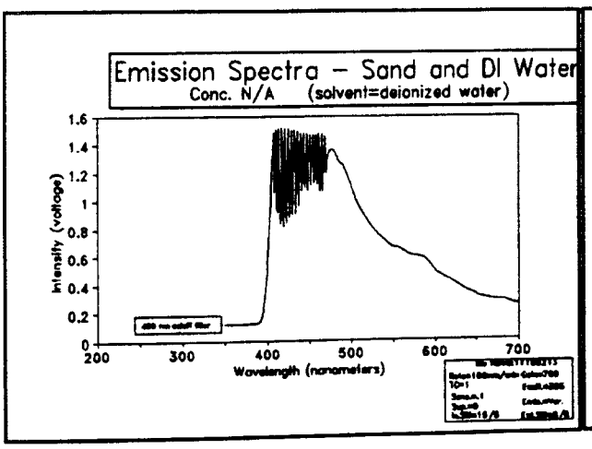

Figure G.1 Baseline Condition

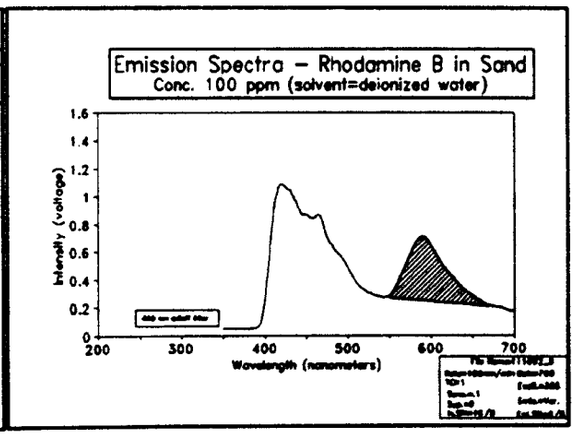

Figure G.2 Rhodamine @ 100 ppm in Sand

Figure G.1 illustrates the baseline condition where deionized water was placed on the soil matrix and scanned. Figure G.2 illustrates the effects of placing a 100 ppm concentration

solution of Rhodamine B on the same soil and immediately scanning the emission spectra. A noticeable peak occurs at the emission signature of 590 nm for Rhodamine B where one did not occur in the baseline condition.

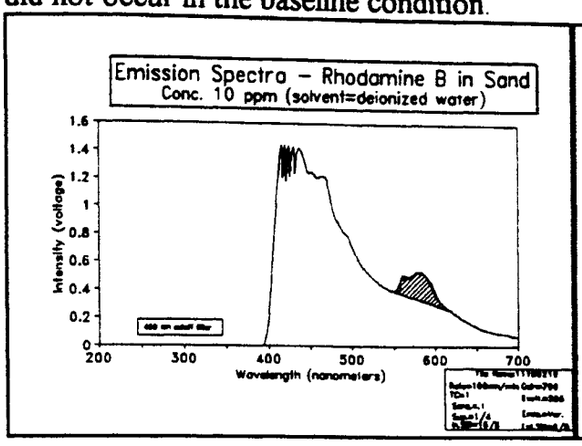

Figure G.3 Rhodamine @ 10 ppm in Sand

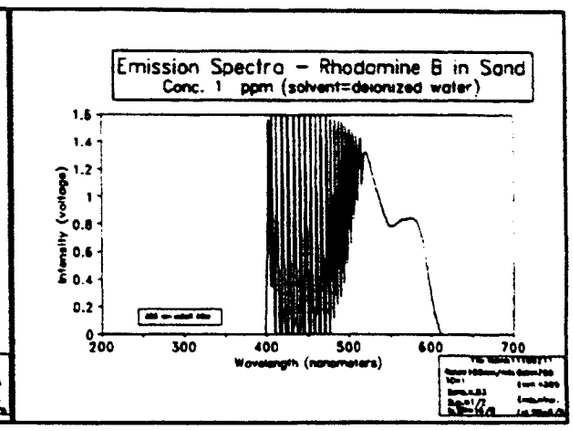

Figure G.4 Rhodamine @ 1ppm in Sand

Figure G.3 illustrates that Rhodamine B at 10 ppm appears as a less pronounced peak than at 100 ppm but still emits a noticeable peak at a wavelength of 580 nm. Figure G.4 illustrates that the sensitivity of the instrument was increased 10 times from .1 to .03 and the voltage suppressed 1/2 turn to detect a reading at Rhodamine B concentration of 1 ppm.

Further investigations of changing excitation wavelength relative to emission, sensitivities and voltages reveal basically the same conclusion. 1 ppm is approximately the detection limit of Rhodamine B in sand retained on a No. 145 sieve.

There does appear to be an advantage in tuning the instrument to where the baseline condition of the background matrix is flat or nearly flat. It is more difficult to detect a difference in concentrations if your baseline is steeply sloped. That is to say, it is more difficult to discern a gaussian shape which represents an increase in concentration if it occurs on a steeply sloped baseline curve.

Figure G.5 illustrates a flat background baseline condition. When a 10 ppm Rhodamine B solution is applied to the soil a gaussian curve is readily apparent as Figure G.6 illustrates.

However, when an adjustment is made to the instrument, such as a change in excitation wavelength, the baseline condition may change from flat to steeply sloping as in Figure G.7. In Figure G.8 it is difficult to differentiate between the baseline and the 10 ppm sample.

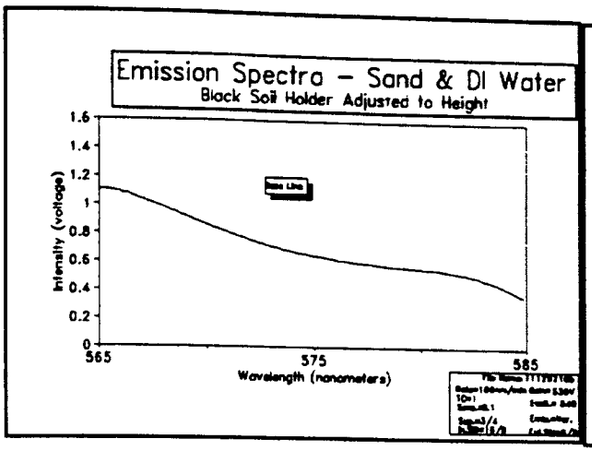

Figure G.5 Baseline Condition-Flat Slope

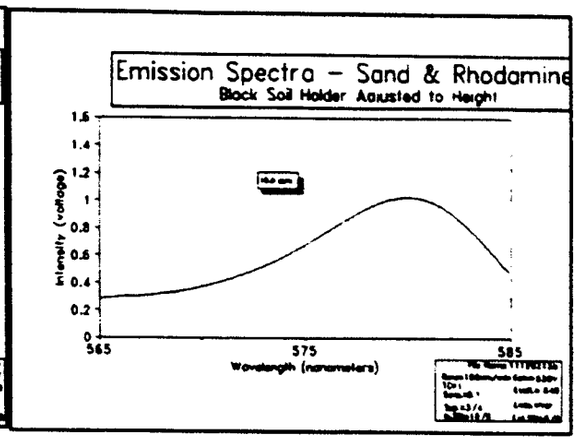

Figure G.6 Sand & Rhodamine @ 10 ppm Flat slope

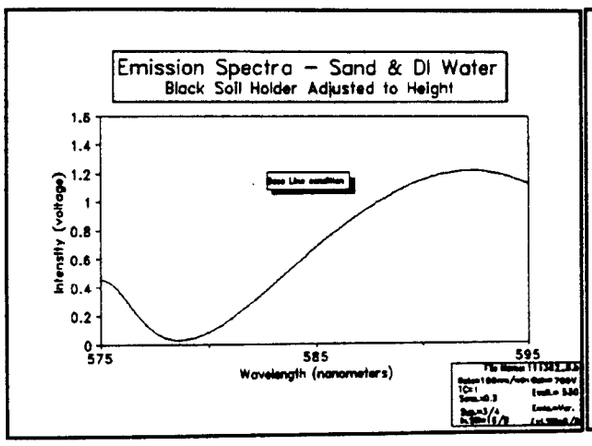

Figure G.7 Baseline Condition-Steep Slope

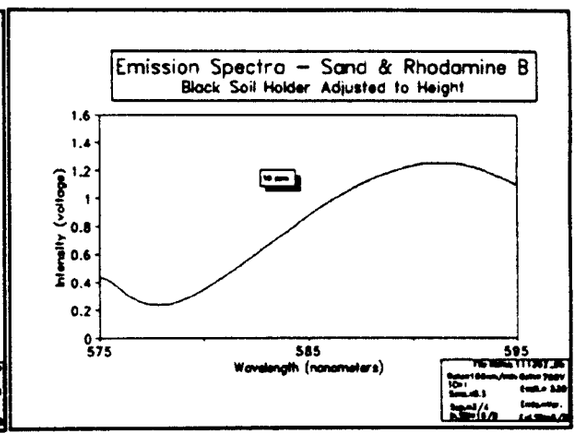

Figure G.8 Sand & Rhodamine @ 10 ppm - Steep Slope

APPENDIX H

OPTIMIZATION TECHNIQUES OF THE FL-750 FOR THE DETECTION OF FLUORESCENT MATERIAL IN SOILS

OPTIMIZATION TECHNIQUES OF THE FL-750 FOR THE DETECTION OF FLUORESCENT MATERIAL IN SOILS

Introduction

Many variables must be taken into account when optimizing the FL-750 Spectrofluorescence Detector. Settings such as focal length, voltage, sensitivity, suppression, scan rate and excitation wavelength are all equipment variables affecting signal response. In addition, variables related to the sample itself will affect the response of the detector. Moisture content, dye concentration and grain size are a few of the sample variables affecting the signal response. This report identifies optimization techniques used to arrive at equipment settings which allow for the most sensitive readings possible from the FL-750. Sample variables such as moisture content and grain size were kept constant while equipment settings were altered.

Focal Length

A preliminary test was conducted to compare the effects of focal length on signal response emanating from a spiked sand sample versus an unspiked sand. The spike consisted of 100 ppm Rhodamine B in sand while the unspiked sample consisted of deionized water in sand. The sand originated from the banks of the Arkansas River and was screened to a constant particle size (Tyler sieve No. 140). The sample holder was constructed of anodized aluminum and had the capability of varying the samples distance from the xenon lamp.

Rhodamine B in another test revealed that when excited at 305 nm a fluorescent emission simultaneously occurs at 590 nm. In this test the excitation and emission wavelengths were held constant while the distance of the sample from the excitation lamp was varied by 1 mm. The same method was applied to the unspiked sample. Figure H.1 illustrates a comparison of the two results

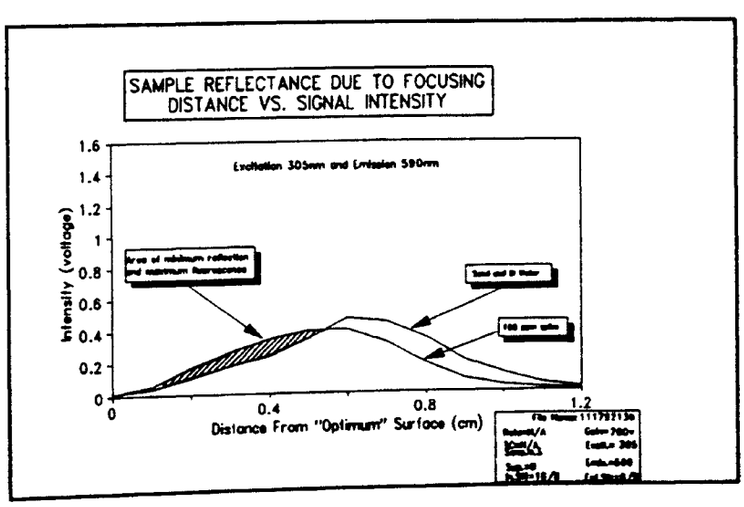

Figure H.1 Focal Lengths Effects on Signal Response

As illustrated in Figure H.5 (focal length 2 mm), the maximum fluorescent response occured at 590 nm an had begun to influence the signal response. In Figure H.9, the background noise was slightly greater than the fluorescent signal response. As illustrated in Figure H.11 (5 mm focal length), the samples background noise at 615 nm dominated the signal response. If fluorescent response were to occur at 615 nm, it would have been masked by this background sample noise. Figure H.7 (3 mm focal length) was considered the optimum focal length because no background noise affected the signal response from the fluorescent material at 590 nm.

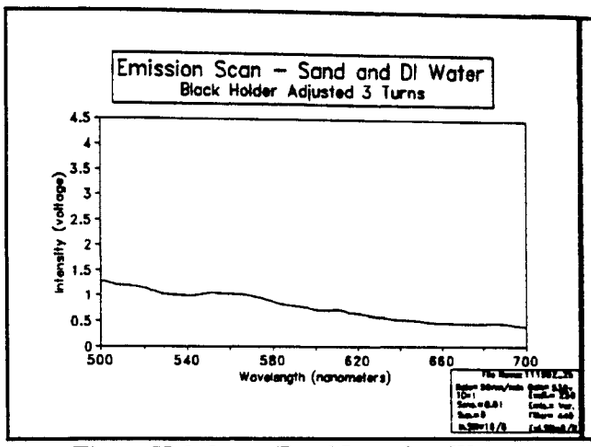

Figure H.6 3 mm Focal Length - Water

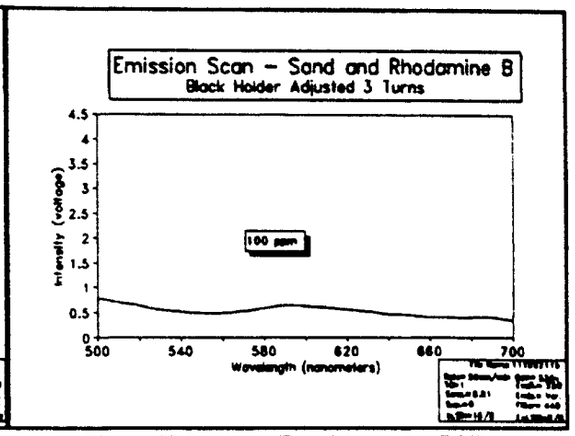

Figure H.7 3 mm Focal Length - RhB

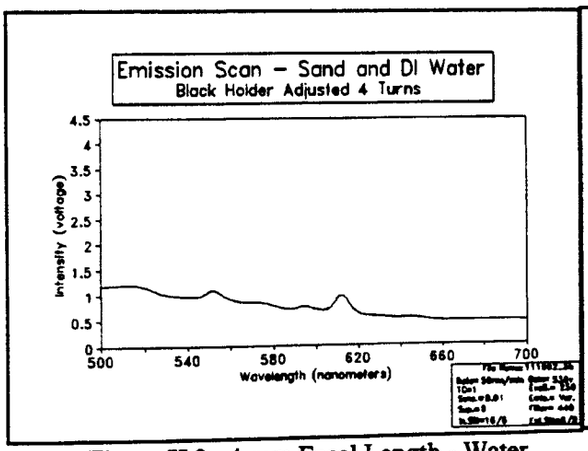

Figure H.8 4 mm Focal Length - Water

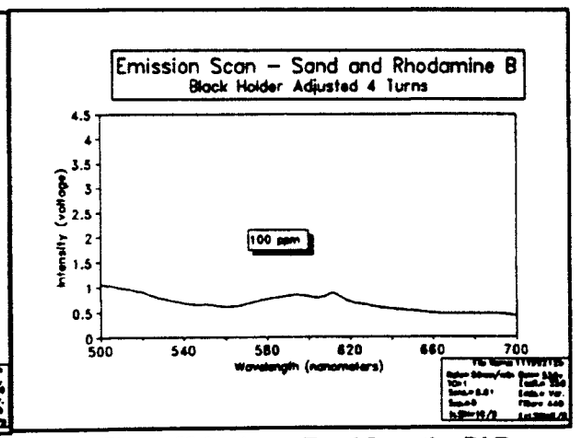

Figure H.9 4 mm Focal Length - RhB

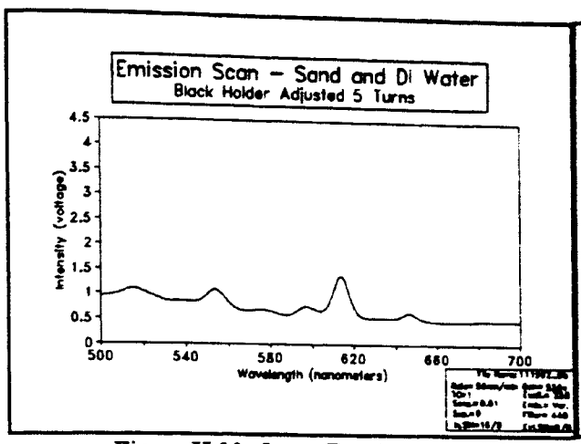

Figure H.10 5 mm Focal length - Water

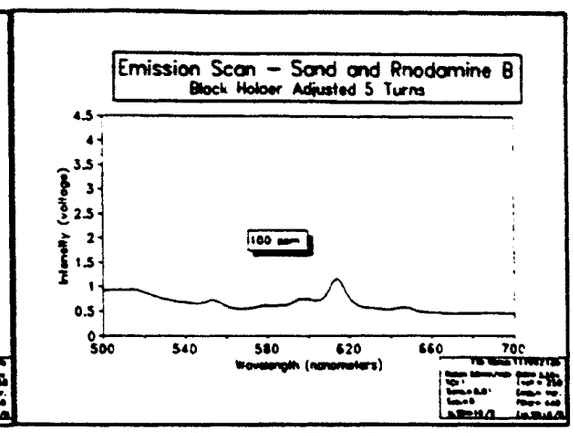

Figure H.11 5 mm Focal Length - RhB

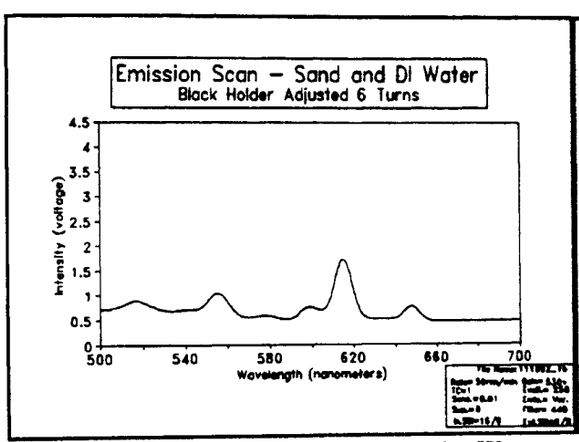

Figure H.12 6 mm Focal Length - Water

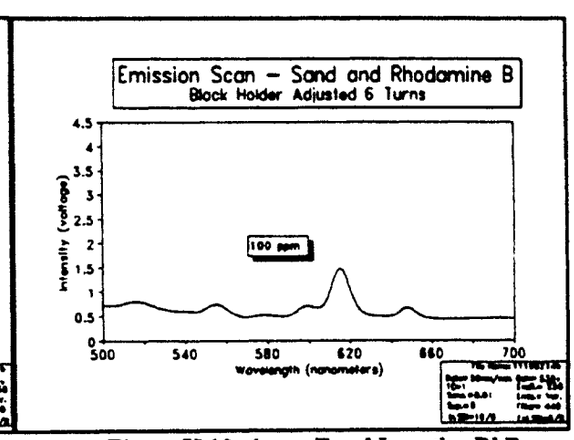

Figure H.13 6 mm Focal Length - RhB

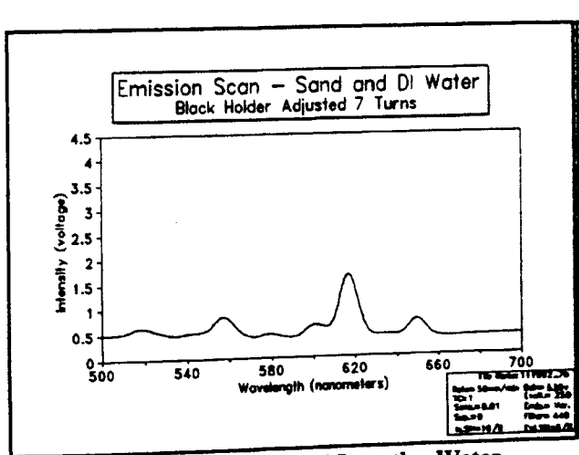

Figure H.14 Focal Length - Water

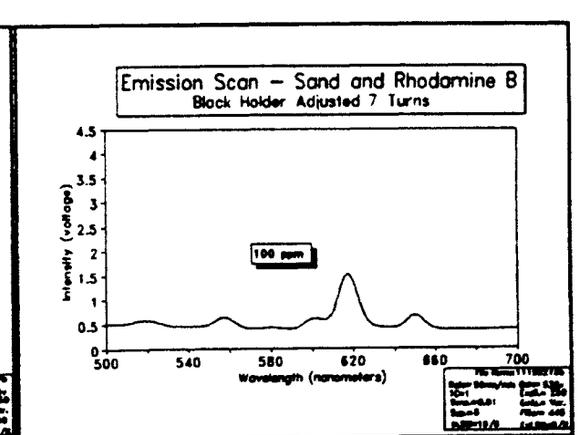

Figure H.15 Focal Length - RhB

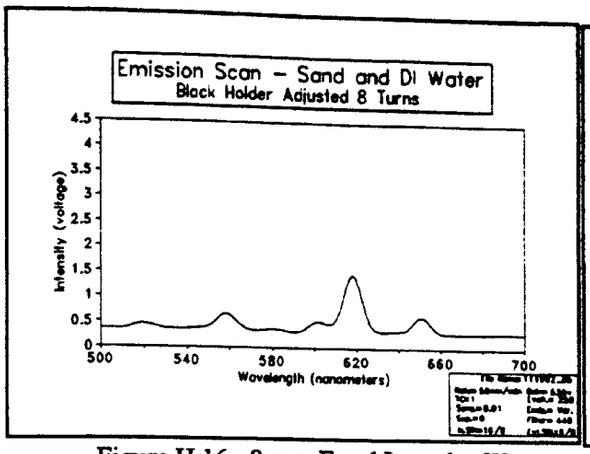

Figure H.16 8 mm Focal Length - Water

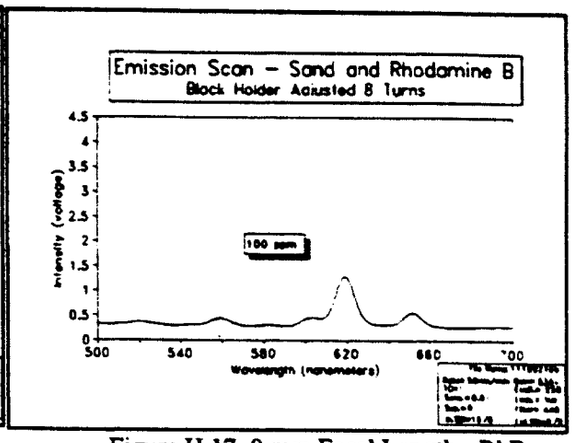

Figure H.17 8 mm Focal Length - RhB

Determination of Excitation Wavelength

All equipment settings were held constant and the excitation wavelength was increased by 20 nm between 250 nm and 350 nm. Figure H.18 illustrates the signal response coming from a clean sample of soil excited at 250 nm. The peak at 615 nm is a result of a third order Rayleigh light scatter. The peak at 645 nm was the result of third order Raman scatter. When the excitation was increased 20 nm, as in Figure H.19, the third order Rayleigh peak decreased by 20 nm to 595 nm. These peaks continue to lower in emission wavelength with an equal increase in excitation wavelength (a phenomenon not found in the literature).

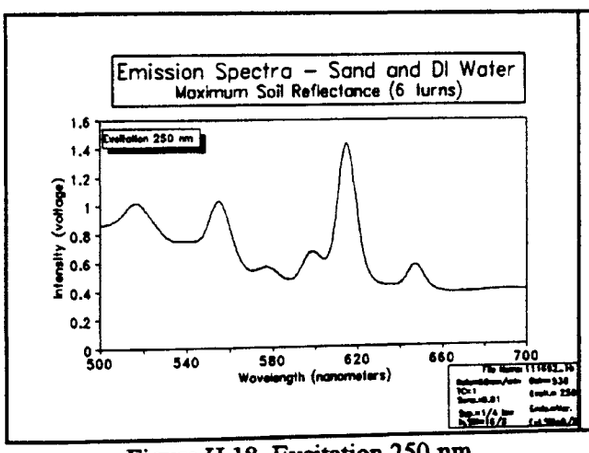

Figure H.18 Excitation 250 nm

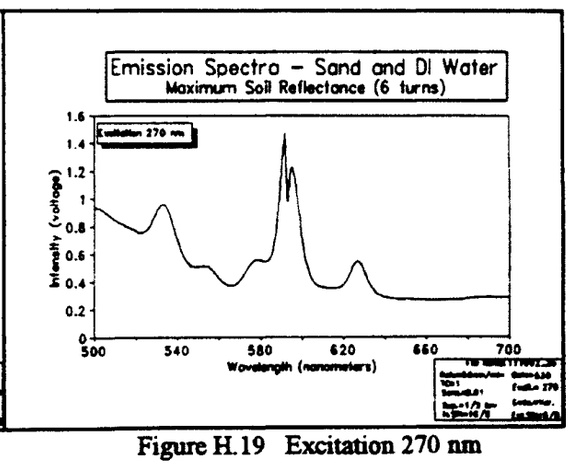

Figure H.19 Excitation 270 nm

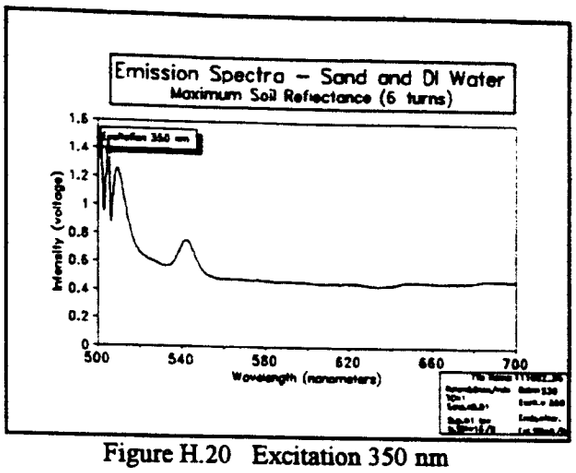

Figure H.20 Excitation 350 nm

Finally, in order to clear the background noise due to these third order light scattering effects, an excitation of 350 nm was achieved as illustrated in Figure H.20. The background noise from an excitation of 350 nm resulted in signal peaks at 500 nm and 540 nm. These peaks no longer interfered with the expected emission wavelength of 590 nm from the Rhodamine B fluorescent spike.

Further confirmation for choosing the optimum excitation wavelength of 350 nm was achieved by exciting a spiked soil sample at increasing maximum absorption wavelengths of 250 nm, 300 nm, 350 nm, and 450 nm. The optimum focal length was held constant at 3 mm.

Signal responses to these increasing excitation wavelengths are illustrated in Figures H.21 through H.25. The maximum signal response to the Rhodamine B spike was shown to be at 350 nm which also corresponded to a low light scattering from 500 nm to 560 nm and is illustrated in Figure H.23. Figures H.21 and H.22 illustrate an increasing signal response to the Rhodamine B spike at 590 nm with a slight increase of direct light scatter occurring at 500 nm.

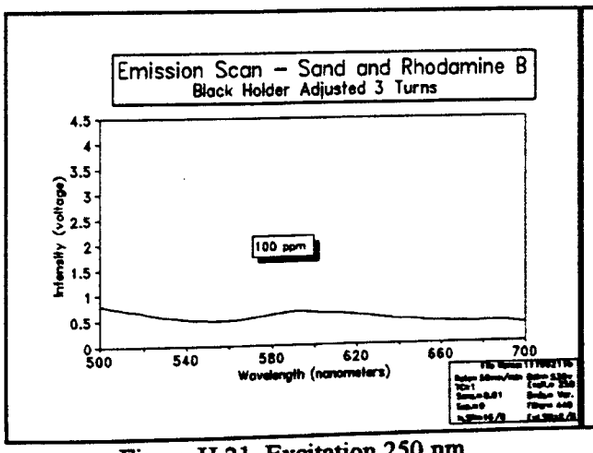

Figure H.21 Excitation 250 nm

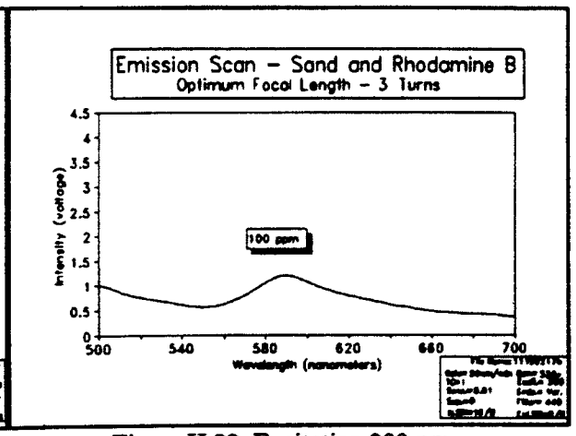

Figure H.22 Excitation 300 nm

Figure H.23 illustrates good signal response at 590 nm with a relatively low direct reflectance signal occurring at 500 nm. Figure H.24 illustrates a relative decrease in signal intensity at 590 nm and an increase in direct light scatter signal at 500 nm. Figure H.25 illustrates a diminished signal response at 590 nm and an unacceptable signal response from direct light scattering at 500 nm.

Therefore, the strongest signal response from the Rhodamine B and the lowest direct light scatter occurs at an excitation of 350 nm. Figure H.23 was considered the optimum excitation resulting in approximately 1 volt direct light scatter response and approximately a 0.75 volt relative deflection peak as a response to the Rhodamine B spike at 590 nm.

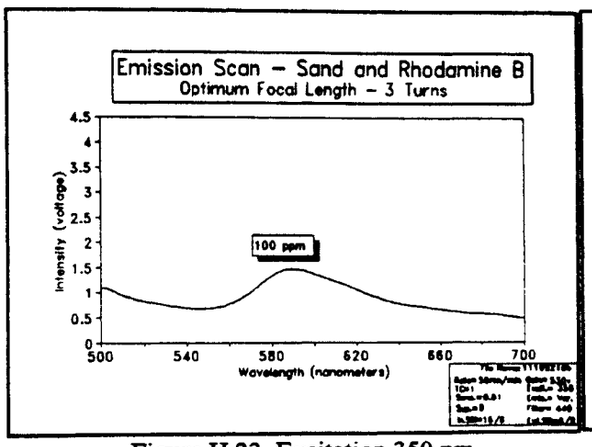

Figure H.23 Excitation 350 nm

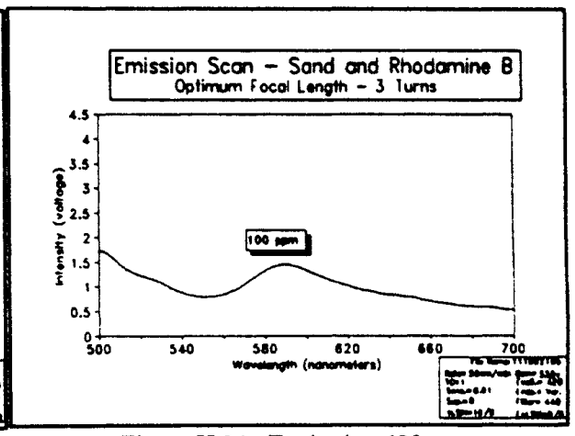

Figure H.24 Excitation 420 nm

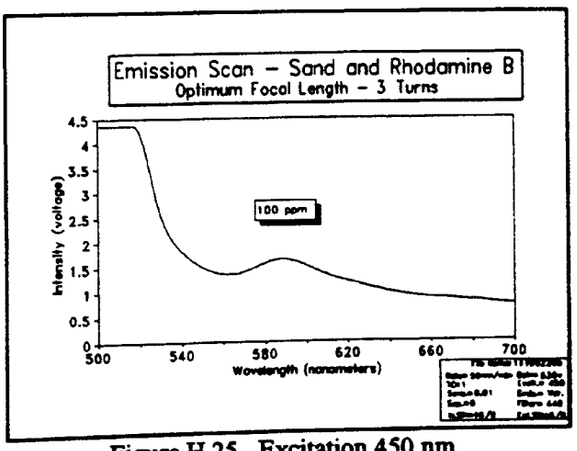

Figure H.25 Excitation 450 nm

Voltage to the PMT

Signal responses to a 100 ppm Rhodamine B soil spike were compared to increasing applied voltages to the PMT. Voltages to the PMT were varied while maintaining an optimum focal length of 3 mm and an optimum excitation of 350 nm. Voltages were varied from 200 to 900 volts in this test.

Figure H.26 illustrates signal response to the Rhodamine B spike appeared to be very slight when 400 volts was applied to the PMT. Figure 27 illustrates an increase in signal response due to fluorescence when 600 volts is applied to the PMT. As voltage was increased from 400 to 600, the maximum voltage deflection due to fluorescent intensity also increased from 0.1 to 2.3 volts, respectively. In Figure H.28, the maximum signal response of 2.5 volts was achieved with 700 volts applied to the PMT. Further increases of the voltage applied to the PMT resulted in no further increase in signal response over the background noise. Figure H.29 illustrates that an applied voltage to the PMT of 900 volts actually decreases the fluorescent signal deflection from a high 2.5 volts to 1.9 volts (sensitivity also was decreased from 0.03 to 0.3 to accommodate the complete range of signal response).

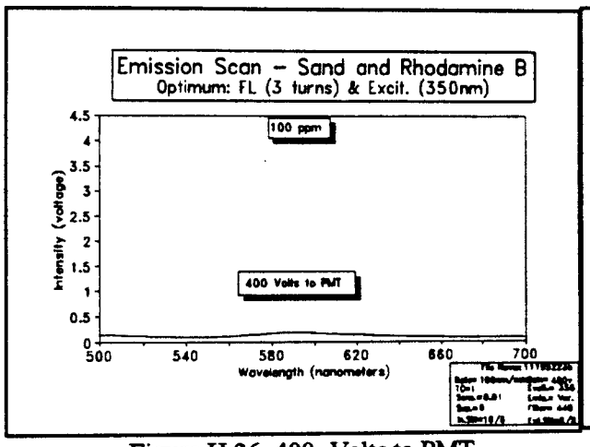

Figure H.26 400 Volts to PMT

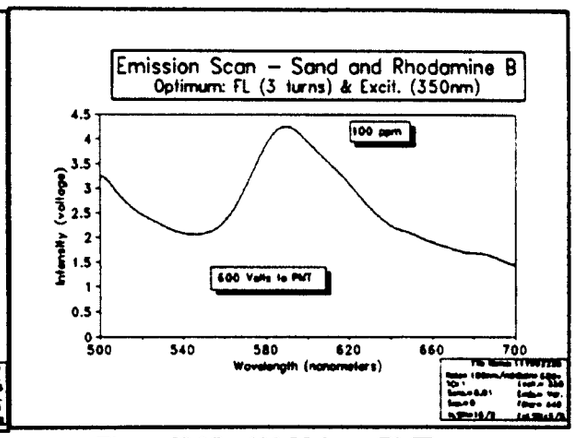

Figure H.27 600 Volts to PMT

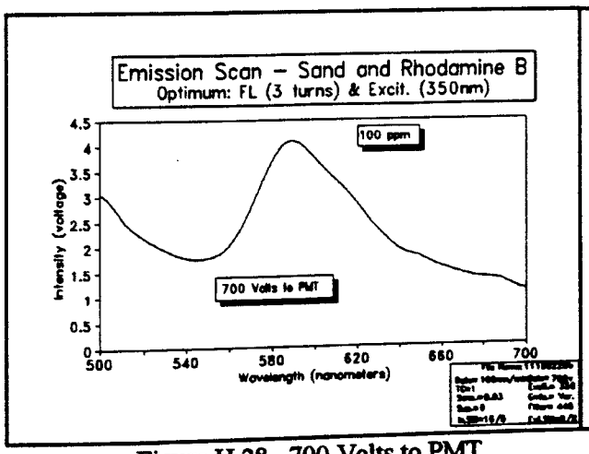

Figure H.28 700 Volts to PMT

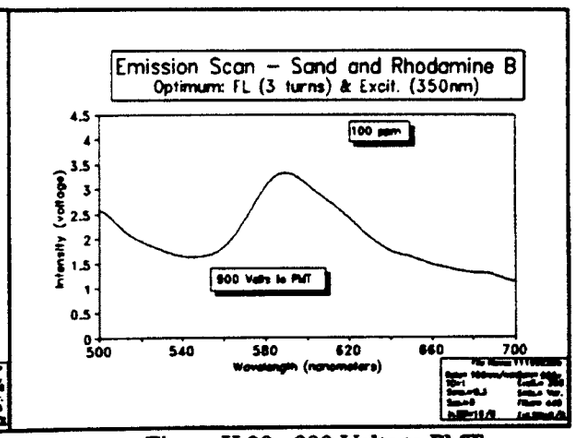

Figure H.29 900 Volts to PMT

Conclusion

Optimization of the FL-750 Spectrofluorometer detection limits was achieved through successively building upon the results from individual optimum equipment setting experiments. By first optimizing the focal length (3 mm) and eliminating it as a variable, optimization of the excitation wavelength proceeded. Once the optimum excitation wavelength was established (350 nm) at the optimum focal length (3 mm), an optimum applied PMT voltage was established (700 volts).

The determination of optimum equipment settings based upon previously established optimums worked as a means to best determine the overall equipment configuration setup for a specific dye and soil type. Different fluorescent dyes and different soils will require a similar equipment setup procedure.

A summary of findings from this procedure include the following optimized values obtained for Arkansas river sand retained on a No. 145 sieve and spiked with Rhodamine B:

* Focal length ..... 3 mm
* Excitation optimum.....350 nm
* Voltage setting .....700 volts
* Sensitivity setting..... 0.03
* Suppression 0
* Cutoff filter ..... 440 nm

APPENDIX I

FL-750 DETECTION LIMITS BASED UPON OPTIMUM EQUIPMENT SETTINGS

FL-750 DETECTION LIMITS BASED UPON OPTIMUM EQUIPMENT SETTINGS

Introduction

Optimum equipment settings established in previous experiments were used to scan Arkansas River sand (Tyler No. 140 sieve) spiked with various concentrations of Rhodamine B fluorescent dye. The dye concentrations applied to the soil ranged from 1000 ppm to 100 ppb.

The results indicate detection was possible down to the 0.10 ppm range. Concentrations below 0.10 ppm were not detectable due to the background noise of the soil itself masking the fluorescent signal response. A plot of the data resulted in a linear correlation between concentration and fluorescent signal response.

Method

Approximately 0.05 grams of various florescent dye concentration solutions were applied to 0.25 grams of sand sample. Each sample was allowed to dry then scanned. The optimum instrument settings established through previous experimentation include:

* Focal length ..... 3 mm
* Excitation optimum ..... 350 nm
* Voltage setting ..... 700 volts
* Sensitivity setting 0.03
* Suppression 0
* Cutoff filter ..... 440 nm

These settings allowed the instrument to perform at optimum sensitivity.

Data

The data demonstrated a direct correlation between the maximum signal response and maximum chemical concentrations at saturated soil moisture conditions. The signal intensity response to a concentration was determined by comparing a baseline condition, where no contaminant was present in the soil, to the response of a fluorescent dye present in the soil.

A line with a mild slope is characteristic of the baseline condition existing in a non-spiked soil. Figure I.1 illustrates the baseline condition for this particular soil type. The flat region extending from 540 nm to 600 nm is the area of interest. This region was where emissions from the rhodamine spike were expected to occur. This region, which has a slope of approximately 0.5v/40 nm, was referred to as the baseline condition. The response signals deflection off this baseline to its emission peak was an indication of rhodamines concentration in the soil.

Departure from this baseline is due to the influence of the fluorescent dye existing within the soil matrix. Figure I.2 illustrates the signal response to a 1000 ppm Rhodamine B spike. From Figure I.2 the response can be visualized as the maximum signal deflection off the baseline.

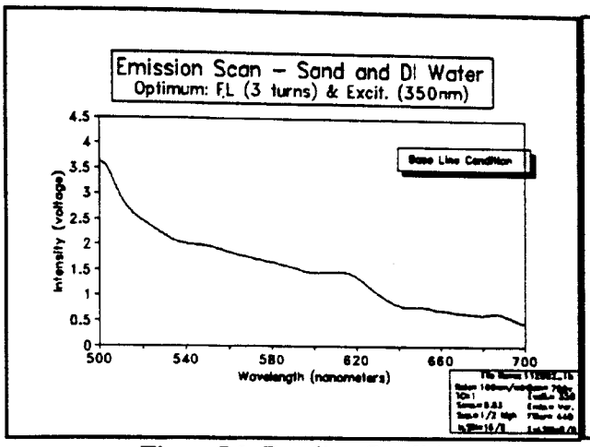

Figure I.1 Baseline Condition

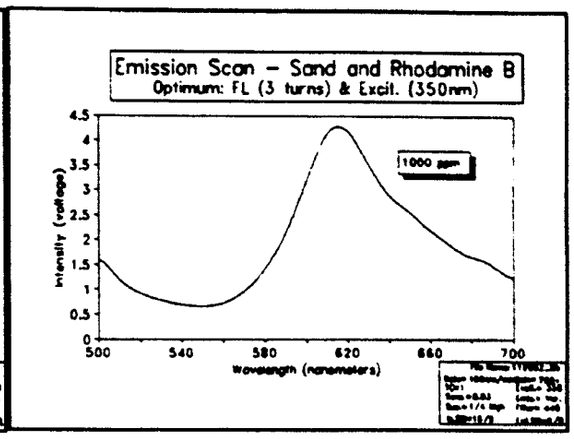

Figure I.2 1000 ppm RhB

Figures I.3 through I.6 illustrate the effect of decreased dye concentrations on signal response relative to the baseline condition. It is important to note the initial signal response beginning at 500 nm is reduced with increased dye concentrations. This is probably due to the fact that Rhodamine B is a red dye and reduces direct reflectance from the sample by darkly coating the soil particles.

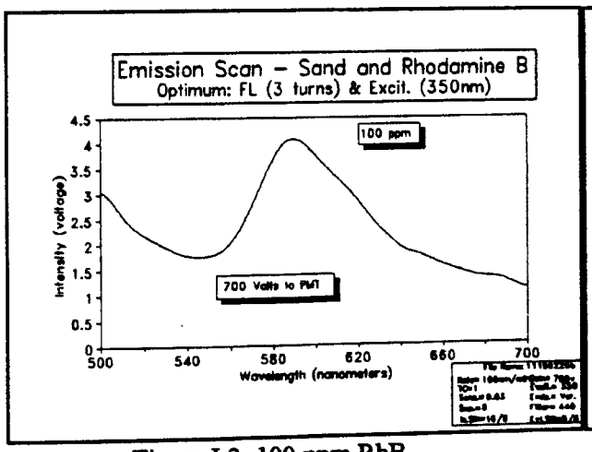

Figure I.3 100 ppm RhB

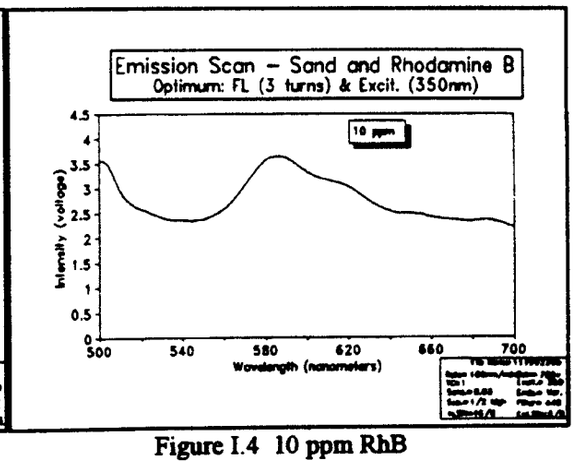

Figure I.4 10 ppm RhB

An example of this reduced reflectance can be observed by comparing the 1000 ppm spike to the 0.1 ppm spike data. In Figure I.2 (1000 ppm) the signal response at 500 nm due to

direct reflectance is 1.5 volts where as in Figure I.6 (0.10 ppm) the signal response at 500 nm is 3.7 volts. Therefore the reflectance from the soil is much higher with a lower spike concentration due to less soil staining.

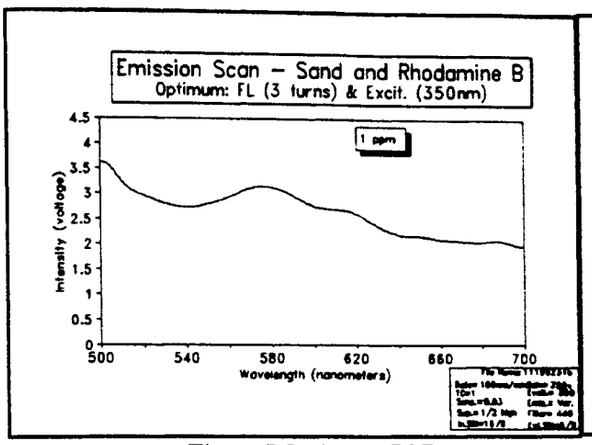

Figure I.5 1 ppm RhB

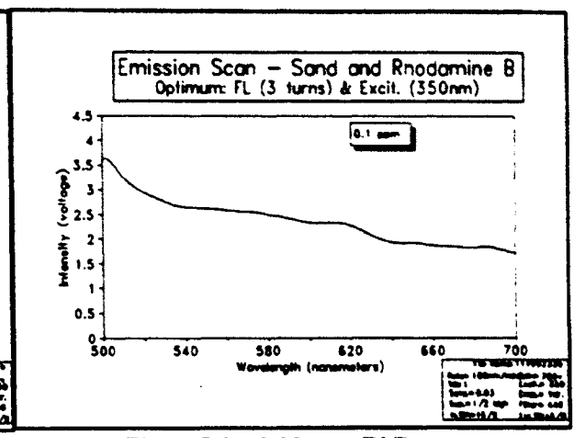

Figure I.6 0.10 ppm RhB

Results

Plotting the signal response to the log of the Rhodamine B concentrations a linear relationship is observed. From this plot a sample concentration can be obtained directly if the signal response intensity is know. Figure I.7 illustrates this graphical relationship between signal intensity and concentration. A high degree of confidence in this method existed between the concentrations of 0.10 to 2000 ppm under saturated soil moistures.

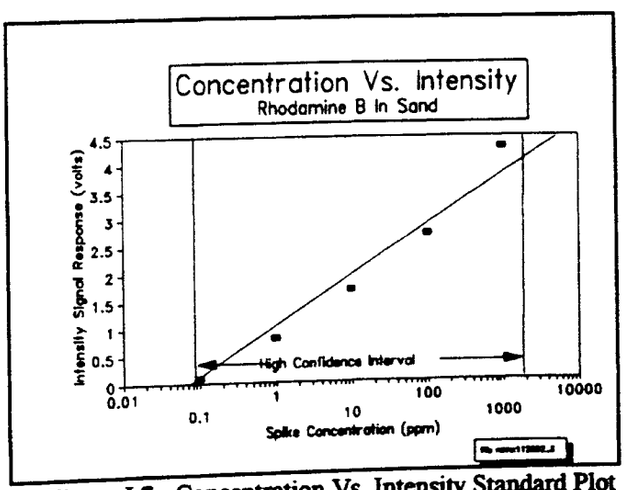

Figure I.7 Concentration Vs. Intensity Standard Plot

Conclusion

Once an instrument is properly calibrated and a favorable fluorescent material is chosen, detection limits from a spiked sand sample can be as low as 0.1 ppm. Lower detection limits are possible if all background signals could be eliminated. This is possible by utilizing a phosphorescent dye or a high intensity excitation light source such as a laser.

APPENDIX J

SOLUBILITY OF KODAK FLUORESCENT DYES

SOLUBILITY OF KODAK FLUORESCENT DYES

Four fluorescent chemical dyes were purchased as a means to spike soils in the immunoassay experiment. Table J.1 lists the chemicals (powder form) and some of their characteristics.

TABLE J.1
FLUORESCENT DYE CHARACTERISTICS[a]

Name	Spectral data Ads.	Emis.	Solubility in water	Incompatibility	Best Solvent[b]
8-anilino-napthalenesul	268	450	appreciable	oxidizers	isobutyl alcohol
Fluorescein Mercuric	293	499	N/A	oxidizer/acetylene	soap and water
9-Isothiocyanatoacrid	300	490	decomposes	oxidizer/water	isobutyl alcohol
Rhodamine B	554	627	appreciable	oxidizer	water

a Kodak MSDS sheets

b Observed

Additional information concerning solubility of each chemical is provided below as a preliminary investigation into the characteristics of these four fluorescent dyes.

8-anilino-1-napthalenesulfonic acid magnesium salt

8-anilino-1-napthalenesulfonic acid magnesium salt (light green powder) was placed in 500 ml of deionized water which resulted in light green liquid phase. The majority of the solids did not dissolve into solution but remained clumped together then settled to the bottom of the container. When a liquid sample was taken from the container and scanned in the 268 nm range, no visible fluorescence was observed at any excitation wavelength. A small amount of acetone was placed into the container with no visible effect on its ability to dissolve the fluorescent dye. Soap was also investigated as a solvent and did not work.

8-anilino-1-napthalenesufonic acid magnesium salt did dissolve in isobutyl alcohol. The solution had a pale green appearance. When this solution was subjected to the spectrofluorescence detector it did fluoresce. Beginning at an excitation of 418nm and continuing through 440 nm the emissions were light blue in appearance, which did not correspond to the literatures absorption (268 nm) and emission (450) spectra.

8-anilino-1-napthalenesulfonic acid magnesium salt did not dissolve in toluene or cyclohexane. Toluene did not have any affect on the powder where cyclohexane did have some ability to dissolve but did not totally dissolve the powder. Cyclohexane, once mixed with the powder and allowed to settle, created a mat of lint-like particles on the bottom of the container.

Fluorescein Mercuric Acetate

Fluorescein Mercuric Acetate (bright orange powder) was placed in a small beaker of deionized water. It was observed not to readily dissolve and remained in discrete particles. A small amount was then placed in a beaker containing isobutyl alcohol with the same outcome. However, when soap was added to the beaker with deionized water and the chemical, the powder was observed to dissolve. A light orange color solution was observed in the as a result of the mixture.

The Fluorescein Mercuric Acetate and soap mixture was then subjected to the spectrofluorometer scan. A noticeable light green emission (490 nm) occurred when excited at 293 nm, as predicted by the literature. A more intense green emission began when excited at 451 nm through 523 nm with a peak emission at 507 nm. The soap in deionized water mixture by itself demonstrated no fluorescence at these wavelengths.

9-Isothiocyanatoacridine

9-Isothiocyanatoacridine was mixed with water and did not dissolve. Soap was added to the water/powder mixture with no indication of dissolving.

9-Isothiocyanatoacridine was dissolved in isobutyl alcohol and formed a bright yellow solution. When this solution was subjected to the spectrofluorescence detector, light blue (cyan-485 nm) emissions began to appear at an excitation of 265 nm and disappeared at 291 nm. Light blue emissions reappeared at an excitation of 310 nm, raised and lowered in intensity until an excitation of 447 nm was reached.

Rhodamine B

Rhodamine B was readily soluble in water and turns a deep purple color in high concentrations. When a dilute sample is placed in the spectroflurometer and excited at the recommended wavelength (554 nm) it's emission color is orange-red (627 nm) as predicted by the literature.

APPENDIX K

SDI SOIL DESCRIPTION

SDI SOIL DESCRIPTION

Eight soil samples from various locations around the United states were shipped from Strategic Diagnostics, Inc. (SDI) to Amoco Production Co.. The purpose of this report is to roughly characterizes these soils. Soil properties such as moisture content and organic matter were investigated. The result of this analysis provided information which will be useful in choosing one of these soils for further experimentation. Table K.1 consists of information relating to each soil sample. Information such as origin and soil classifications were provided by SDI.

TABLE K.1
GENERAL SOIL CHARACTERISTICS OF EIGHT SOILS

Inventory #	Soil series	Arrival weight (g)	Classification	Sample Location	Source
108	Cecil Sand Clay	1121.7	Sandy Clay/Sandy Clay Loam (red clay)	Piedmont region of Georgia (Bledsoe Res. Farm)	Univ. GA, Dept. of Agronomy
109	Davidson Clay Loam	1034.5	Clay Loam (dark red clay)	Piedmont upland of Georgia	Univ. GA, Dept.. of Agronomy
110	Shelbyville Sand (high OM)	1011.9	High organic sand	Pocomoke (?)/ southern DE	Univ. DE Plant & Soil Science
121	Wooster Silt Loam	1074.1	Silt Loam	Wayne Co., OH (Wooster Township)	Wayne Co. Extension Service
123	Opal Clay	1644.1	Shale derived soil/clay texture	Jones County, SD	SD State Univ.
126	Drummer	739.2	unknown	unknown	unknown
127	Cisne	994.7	unknown	unknown	unknown
128	Musatine	981.3	unknown	unknown	unknown

The eight soil samples were shipped through UPS and arrived at Amoco October 5, 1992. Soil samples ranged in weight from 1644.1 grams to 739.2 grams. The majority of the samples are from known locations. Generally, the source of the information provided with the samples came from a university or a government agency. Additional information about the soil is available upon request. In the case of "unknowns," attempts were made to determine soil classifications and origins.

Moisture Content

Moisture content for each sample was estimated using the Denver Instrument IR-100 moisture analyzer. Approximately 2 grams of soil was placed in the analyzer and dried at

105 C until a constant weight was sensed by the analyzer. The following equation is used by the analyzer to determine the soil moisture content:

$$\% \text{ Moisture} = \frac{\text{Wt. of Moist Soil - Wt. of Dry Soil (g)}}{\text{Wt. of Dry Soil (g)}} \qquad \text{(K1)}$$

Table K.2 contains soil moisture contents for each sample as shipped by SDI. Additional information on volatile solids is also included in the table. The combination of this information provides a rough overview for each soil.

TABLE K.2
PHYSICAL CHARACTERISTICS

Inventory #	Shipped moisture content (%)	Volatile Solids (VS)
108	21.13	7.21
109	15.28	4.32
110	21.09	11.99
121	15.10	4.11
123	29.48	9.02
126	17.62	9.28
127	11.08	3.73
128	20.35	7.88

Not surprisingly, the clays contained the highest moisture content. Sample number 123 contained the greatest moisture content of 29.48% and had volatile solids (VS) of 9.02%. Sample number 123, when referenced to Table K.1, was listed as Opal clay. Sample number 110 contained the highest percentage of volatile solids (11.99%) and had a high moisture content (21.09%). Referring to sample number 110 in Table K.1, Shelbyville sand was identified as soil high in organic matter.

Determination of Volatile Solids

The percentage of volatile solids contained in each soil sample was determined through a process of first driving off residual water then exposing the sample to high temperatures for a period of time. Each sample was carefully weighed then dried at a temperature of 105 C to a constant weight. The samples then were placed in a muffle oven where all organic matter was allowed to burn off until reaching a constant weight.

The following paragraphs describe the laboratory procedure carried out to determine the percentage of volatile solids in each sample. Care was taken in handling of the soil

samples so as not to reintroduce moisture once they were dried. Tongs were used to handle the crucibles and sample containers. Eight empty crucibles were placed into the muffle oven overnight (550 C) and then stored in a desiccater until needed for the experiment.

Approximately 2 grams of each soil type was placed in the IR-100 moisture analyzer until a constant weight was achieved. The time required to arrive at a constant weight varied from 15 minutes to 35 minutes depending upon the initial moisture content of the soil sample. After weighing a crucible, the soil sample was then placed into the crucible and again weighed. Each sample in the crucible was stored a desiccater until into the muffle oven. Both soil and crucibles were exposed to the atmosphere for no more than 10 minutes. The crucible arrangement within the muffle oven is illustrated in Figure K.1.

The samples were first placed in the muffle oven for 1 hour and 15 minutes, and allowed to cooled in a desiccater, then weighed. This was identified as the "1st burn" in Figure K.1. The samples were then returned to the muffle oven for a "2nd burn" which lasted approximately 1 hour and 30 minutes. The samples were allowed to cool and then weighed. The arrangement of the crucibles in the muffle oven was not considered to be critical. Approximately 1/2 inch was left between each crucible allowing for full heat circulation.

Cooling was relatively quick and generally occurred within 30 minutes. Samples were removed from the desiccater and weighed. Organic matter in this case was considered to be the material which had burned off when the soil was exposed to a temperature of 550 C for an extended period of time. The following equation was used in determining the percentage of organic matter for each soil sample:

$$\% \text{ OM} = \frac{(\text{Tot. Dry Wt.} - \text{Wt. Crucible}) - (\text{Tot. Burned Wt.} - \text{Wt. Crucible})}{\text{Tot. Dry Wt.} - \text{Wt. Crucible}} \qquad \text{(K2)}$$

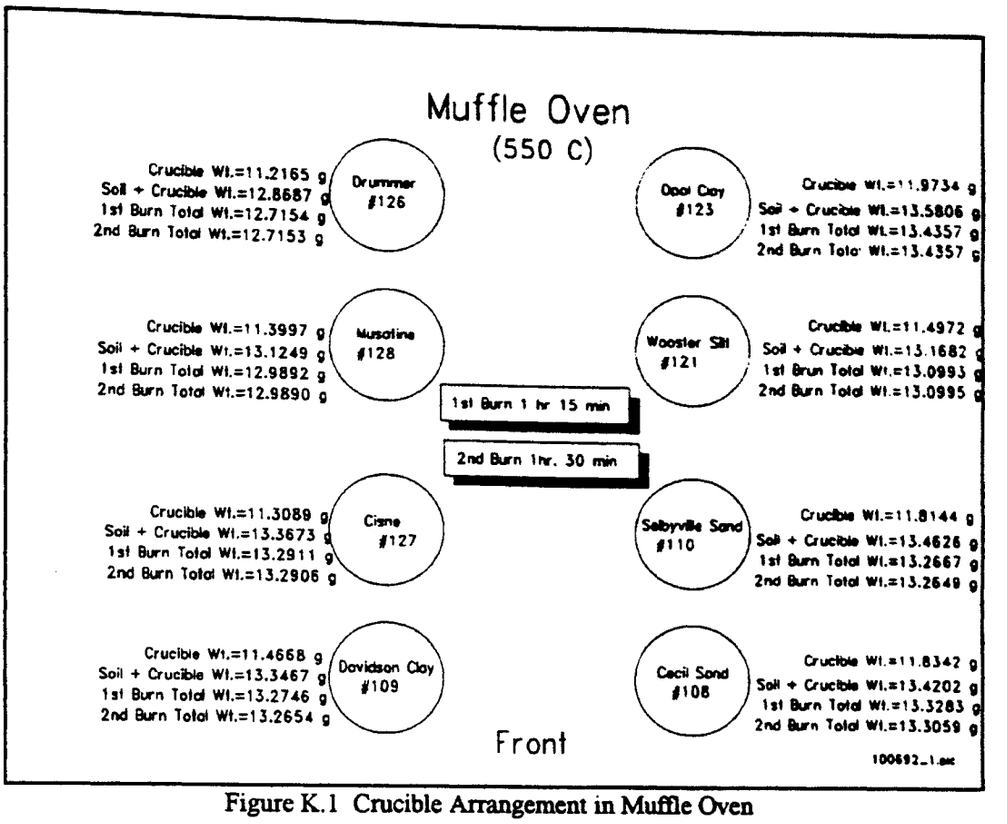

Figure K.1 Crucible Arrangement in Muffle Oven

The data listed in Table K.3 are the results of the volatile solids analysis. The weight of each crucible is provided. Also provided are total weights before and after each burn. Finally, the percentage of organic matter is provided in the last column and is calculated as described above.

The results indicated that after the 1st burn the percent of organic matter ranged from a low of 3.70% for sample No. 127 (Cisne) to a high of 11.89% for sample No. 110 (Shelbyville Sand). After the 2nd burn, no significant change in weight occurred between the two burns and it was assumed most organic matter had been burnt away by the 2nd burn.

Figure K.2 graphically illustrates the relative differences of each soil's organic matter content. In addition it illustrates the differences in total organic matter after each burn. Sample No. 108 demonstrates the greatest difference between the 1st and the 2nd burn. Sample No. 108 went from an organic matter of 5.79% in the first burn to 7.21% in the 2nd burn. All others, however, did not demonstrate any significant change between the two burns. Further exposure of the samples to the muffle oven was therefore unnecessary.

TABLE K.3
ESTIMATION OF ORGANIC MATTER USING MUFFLE OVEN

Sample #	Crucible Wt.	Soil + Crucible Wt.	1st Burn Total Wt.	2nd Burn Total Wt.	Organic matter (1st burn)	Organic matter (2nd Burn)
	(g)	(g)	(g)	(g)	(%)	(%)
108	11.8342	13.4202	13.3283	13.3059	5.79	7.21
109	11.4668	13.3467	13.2746	13.2654	3.84	4.32
110	11.8144	13.4626	13.2667	13.2649	11.89	11.99
121	11.4972	13.1682	13.0993	13.0995	4.12	4.11
123	11.9734	13.5806	13.4357	13.4357	9.02	9.02
126	11.2165	12.8687	12.7154	12.7153	9.28	9.28
127	11.3089	13.3673	13.2911	13.2906	3.70	3.73
128	11.3997	13.1249	12.9892	12.989	7.87	7.88

CONCLUSION

Eight soil samples which arrived from Strategic Diagnostics, Inc. were analyzed. The results of this analysis will be useful in the screening process to choose a soil which will be used in a fluorescent spike study.

The results indicated that the Shelbyville sand, a rich black soil, contained the highest organic matter of 11.99%. The Opal clay and the Cecil sand contained the highest moisture content at 29.48% and 21.13%, respectively. The Opal clay was a highly cohesive clay with a texture like sculpting clay. The Cisne sand was shown to contain the lowest organic matter of 3.70%.

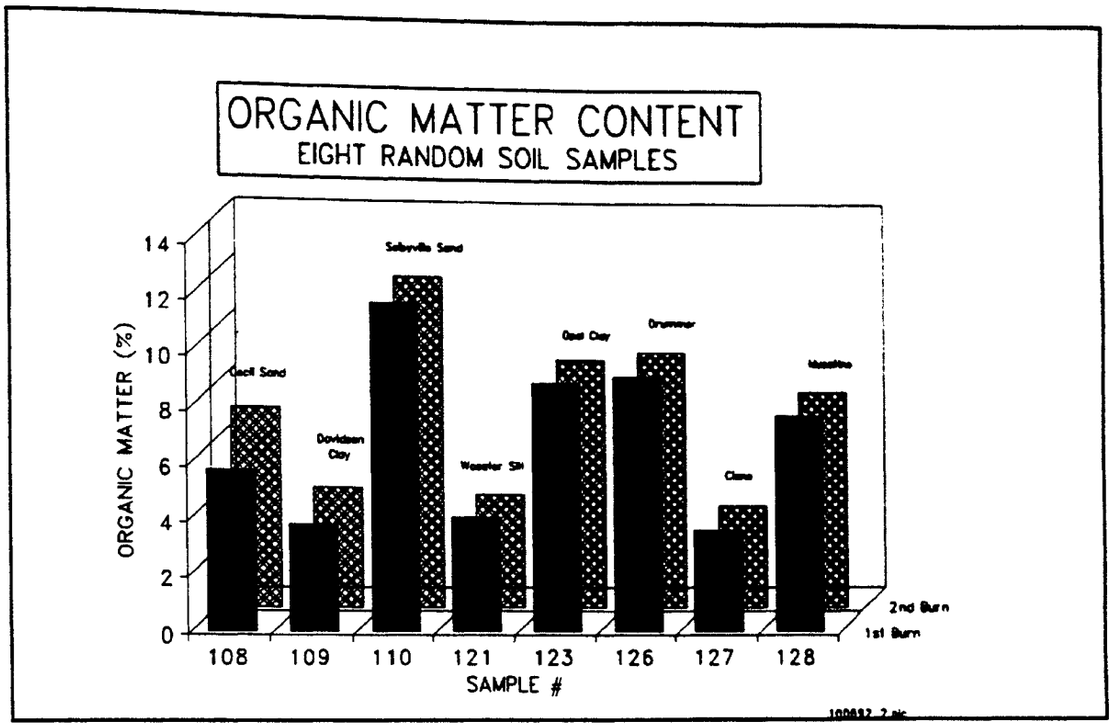

Figure K.2 Relative Organic Matter Contents in Double Burn Experiment

APPENDIX L

ARKANSAS RIVER SAND CHARACTERIZATION

ARKANSAS RIVER SAND CHARACTERIZATION

Introduction

Arkansas River sand was graded into discrete particle sizes through a wet and dry sieving process. Volumetric calculations were then used to determine the sand's bulk density within each gradation. The moisture capacity of each grade was also estimated. These parameters will be utilized in future fluorescent spiking experiments.

Method

Grains per Gram of Sample

Sand was collected from the banks of the Arkansas River in Tulsa, Oklahoma. The sand was wet sieved using Tyler sieves Nos. 10, 40, 60, 140, 200, and 270. These sieves correspond to actual mesh sizes of 2.0 mm, 0.425 mm, 0.250 mm, 0.106 mm, 0.075 mm, and 0.053 mm, respectively. Therefore in a series of nested sieves, sand retained on each of these sieves correspond to a population of sand particles small enough to pass through the preceding sieve but large enough to be held by the retaining sieve. Each volume of sand retained on a sieve contained its own gradation but was known to be not larger than the preceding sieve and not smaller than the sieve which retained it. Efforts were made to determine the mean particle size for the population of sand retained on each sieve using the Malvern Particle Sizer.

10 ml volumetrics were used to derive the total surface area from the bulk density which could be expected from a population of sand retained on each sieve. By first estimating the bulk density of each gradation and assuming a spherical particle shape, the number of particles could then be estimated within the volumetric.

Bulk density of each particle population was estimated utilizing Equation L.1. Starting with a 10 ml volumetric, a dry sand sample of known sieve size was added and weighed. Deionized water was then added and weighed. The sample was then subjected to a Type 16700 vibratory Maxi Mixer for approximately 1 minute to ensure complete grain wetting and elimination of air pockets held within the sample. Deionized water was then added to the 10 ml mark. Excess water droplets in the neck of the volumetric were eliminated by wiping with a paper towel. Bulk density is expressed by the equation:

$$\frac{\text{Mass}_{\text{dry sand (g)}}}{\text{Volume}_{\text{total}} - \text{Volume}_{\text{liquid}}\ (\text{cm}^3)} = \rho_{\text{sand}} \qquad \text{(L.1)}$$

Making a simplifying assumption that all sand grains are spherical, Equation L.2 was used to estimate the volume of one sphere. By multiplying the volume of one sphere times it's bulk density, the mass of one sphere was determined.

$$\frac{4}{3}\pi r^3 = \text{Volume of Sphere} \qquad \text{(L.2)}$$

Assuming all spheres in one sieve gradation are of nearly equal size, the total number of spheres held in the volumetric were determined by dividing the total mass of the sand by the mass of an individual sand grain (Equation 3).

$$\frac{\text{Total Mass}_{sand}\ (g)}{\text{Mass Individual Grain}_{sand}\ (g)} = \text{No.Particles} \qquad \text{(L.3)}$$

An example calculation is provided with data from Table L.4 (test 1 of 10) as follows:

$$\rho = \frac{5.13\ (g)_{sand}}{10\ (cc)_{water} - 8.02\ (cc)_{water}} = 2.59\ \left(\frac{g}{cc}\right)$$

$$\text{Mass of One Sphere} = \frac{4}{3}\pi\ (0.0061)^3 \bullet 2.59 = 0.0000025\ \left(\frac{g}{grain}\right)$$

or 406,896 grains per gram of sand.

Moisture Holding Capacity

Moisture holding capacity for each sand grade was estimated using two different fluid elimination methods, gravity drainage and pipette withdrawal. The first method, gravity drainage, was similar to estimating container capacity. This method used a 27 ml glass vial filled with approximately 5 grams of one sand grade. Deionized water was then added to the halfway mark, more than enough to cover the sand. The sample was then subjected to the vibratory mixer for 1 minute to ensure proper wetting and mixing. The sample was allowed to settled. The vial was then wedged in a 250 ml beaker with the vial opening resting approximately 130 degrees from vertical. The position of the vial allowed the fluid to drain without any loss of sand sample. The vial was allowed to drain in this manner for eight hours then capped and stored for further testing.

The second method of fluid extraction involved elimination of the fluid using a pipette. A 1 ml Eppendorf pipette was used to withdraw the liquid from the vial. The pipette tip was placed into the sand for the final extraction and all moveable liquid was withdrawn. Inevitably some sand was drawn into the pipette tip, therefore this technique was determined to be inferior to the gravity drainage technique because of the mass balancing problems it created.

Each sample preparation technique was repeated for all sand grades. The sample was then subjected to the Denver Instrument moisture analyzer to determine it's moisture content. Three measurements were taken for each grade. Moisture capacity and drying times were recorded and are also presented in Table L.1.

Data

Table L.1 demonstrates several characteristics of the Arkansas River sand at various gradations. Average particle diameters were measured by the Malvern particle sizer indicate that most of the particles in a particular gradation have a tendency to be sized closer to the upper sieve size and not the retaining sieve. For example, particles which were retained on the sieve No. 270 (0.053 mm) and passing sieve No. 200 (0.075 mm) had an average size of .073 mm (as measured by the Malvern).

The average bulk densities for each particle grade ranged from a low of 2.59 g/cc for the pan material, to a high of 2.62 g/cc corresponding to those particles retained on the No. 270 mesh sieve. The average number of particles per gram of sample ranged from 1006 grains/gram for the No. 40 sieve to 8,106,169 grains/gram for the pan material.

The moisture holding capacity (gravity drainage technique) for each grade increased as particle size decreased. Beginning from a low of 17% at No. 40 sieve size to a high of 24% for the pan material. Also recorded are the drying times necessary to bring the sample from maximum moisture content to completely dry conditions.

TABLE L.1
PARTICLE ANALYSIS SUMMARY SHEET

Sieve #	40	60	140	200	270	>270
Sieve Size (mm)	0.425	0.250	0.106	0.075	0.053	pan
Average Part. Dia.(mm)	0.900	0.338	0.122	0.105	0.073	0.045
Rho Avg. (g/cc)	2.60	2.61	2.60	2.60	2.62	2.59
Rho Std. Dev.	0.0129	0.0185	0.0167	0.0232	0.0188	0.0213
Rho Variance	0.0002	0.0003	0.0003	0.0005	0.0004	0.0005
# Part./gram	1006	19066	404459	635782	1871878	8106169
Moisture Capacity %	17.237	19.600	21.667	22.340	22.310	24.063
Drying Time (min)	17.333	18.500	17.933	19.733	18.000	22.067

Results

The results indicate that the bulk density of various gradations of Arkansas River sand, ranging from coarse sand to silt, and averaged 2.60 g/cc. Figure L.1 illustrates the

relationship between grain density and sieve size. The consistency of the grain densities between gradations was an indication that the volumetric method of estimating bulk density was both accurate and precise.

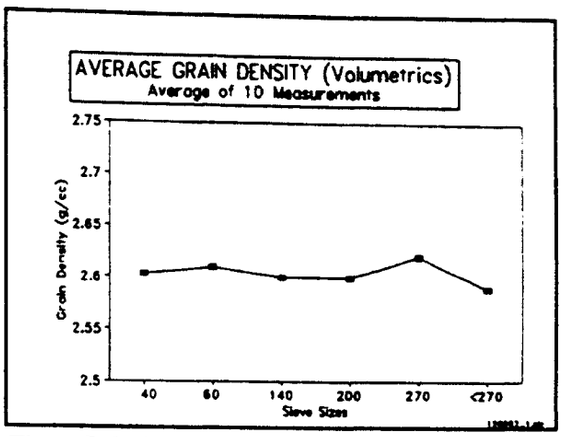

Figure L.1 Average Bulk Density at Each Gradation

Conclusion

Six grades of sand were extracted from a single soil sample originating from the banks of the Arkansas River. This soil was found to range from coarse sand to silt according to ASTM standards. Average bulk densities for each grade were derived from ten measurements made from within each gradation. Within the six gradations, bulk densities were found to ranged from 2.59 g/cc to 2.62 g/cc with an average of 2.60 g/cc and a standard deviation of .009 g/cc. Moisture holding capacity increased with decreasing particle size.

TABLE L.2

SAND RETAINED ON SIEVE #40

Test #	1	2	3	4	5	6	7	8	9	10	
Sieve #	40	40	40	40	40	40	40	40	40	40	
Sieve Size (mm)	0.4250	0.4250	0.4250	0.4250	0.4250	0.4250	0.4250	0.4250	0.4250	0.4250	
Wt. Vile (g)	39.5637	39.8449	31.5707	32.9060	9.5533	9.7168	9.6586	9.8174	9.8375	37.2349	
Wt. sand (g)	8.1424	5.4502	6.3390	7.0652	6.9481	7.5600	8.3270	6.1781	6.9809	7.2451	
Wt. liquid (g)	6.8475	7.9016	7.5767	7.3080	7.3233	7.0884	6.8095	7.6175	7.3114	7.2352	
Total WT. (g)	54.5536	53.1967	45.4864	47.2792	23.8247	24.3652	24.7951	23.6130	24.1298	51.7152	
Total Vol (ml)	10.0000	10.0000	10.0000	10.0000	10.0000	10.0000	10.0000	10.0000	10.0000	10.0000	AVG
Rho (g/cc)	2.5828	2.5973	2.6159	2.6245	2.5958	2.5965	2.6099	2.5931	2.5965	2.6205	2.603282
Part. Dia (mm)	0.9000	0.9000	0.9000	0.9000	0.9000	0.9000	0.9000	0.9000	0.9000	0.9000	
Part. Rad. (cm)	0.0450	0.0450	0.0450	0.0450	0.0450	0.0450	0.0450	0.0450	0.0450	0.0450	
Grain SA (cm2)	0.0254	0.0254	0.0254	0.0254	0.0254	0.0254	0.0254	0.0254	0.0254	0.0254	
Grain Vol. (cc)	0.0004	0.0004	0.0004	0.0004	0.0004	0.0004	0.0004	0.0004	0.0004	0.0004	
Grain Wt. (g)	0.0010	0.0010	0.0010	0.0010	0.0010	0.0010	0.0010	0.0010	0.0010	0.0010	
# Part/Vile	8259.0281	5497.4606	6348.6448	7052.5944	7012.5109	7627.9100	8358.5818	6241.7556	7043.6869	7243.3183	
SA grains (cm2)	210.1667	139.8933	161.5533	179.4667	178.4467	194.1067	212.7000	158.8333	179.2400	184.3200	
SA/gram (cm2/g)	25.8114	25.6676	25.4856	25.4015	25.6828	25.6755	25.5434	25.7091	25.6758	25.4406	25.60933
#Part/gram	1014.3236	1008.6714	1001.5215	998.2158	1009.2703	1008.9828	1003.7927	1010.3034	1008.9941	999.7541	1006.383
	STATISTICAL DATA										
Avg. Rho. (g/cc)	2.603281671576	2.603281671576	2.603281671576	2.603281671576	2.603281671576	2.603281671576	2.603281671576	2.603281671576	2.603281671576	2.603281671576	
Std Dev. Rho	0.012862379798	0.012862379798	0.012862379798	0.012862379798	0.012862379798	0.012862379798	0.012862379798	0.012862379798	0.012862379798	0.012862379798	
Var. Rho.	0.000165440814	0.000165440814	0.000165440814	0.000165440814	0.000165440814	0.000165440814	0.000165440814	0.000165440814	0.000165440814	0.000165440814	

120992_1

TABLE L.3

SAND RETAINED ON SIEVE #60

Test #	1	2	3	4	5	6	7	8	9	10	
Sieve #	60	60	60	60	60	60	60	60	60	60	
Sieve Size (mm)	0.2500	0.2500	0.2500	0.2500	0.2500	0.2500	0.2500	0.2500	0.2500	0.2500	
Wt. Vile (g)	39.5692	39.8450	31.5706	32.9050	9.5526	9.7165	9.6582	9.8385	9.8385	37.2357	
Wt. sand (g)	5.9924	8.1071	7.6351	5.2371	5.0572	6.1226	6.0204	4.3472	4.3472	5.1681	
Wt. liquid (g)	7.6934	6.8913	7.1148	8.0057	8.0400	7.6319	7.6821	8.3284	8.3284	8.0244	
Total WT. (g)	53.2550	54.8434	46.3205	46.1478	22.6498	23.4710	23.3607	22.5141	22.5141	50.4282	
Total Vol (ml)	10.0000	10.0000	10.0000	10.0000	10.0000	10.0000	10.0000	10.0000	10.0000	10.0000	AVG
Rho (g/cc)	2.5979	2.6079	2.6463	2.6260	2.5802	2.5854	2.5974	2.6006	2.6006	2.6160	2.605836
Particle Dia(mm)	0.3375	0.3375	0.3375	0.3375	0.3375	0.3375	0.3375	0.3375	0.3375	0.3375	
Part. Rad. (cm)	0.0169	0.0169	0.0169	0.0169	0.0169	0.0169	0.0169	0.0169	0.0169	0.0169	
Grain SA (cm2)	0.0036	0.0036	0.0036	0.0036	0.0036	0.0036	0.0036	0.0036	0.0036	0.0036	
Grain Vol. (cc)	0.00002	0.00002	0.00002	0.00002	0.00002	0.00002	0.00002	0.00002	0.00002	0.00002	
Grain Wt. (g)	0.00005	0.00005	0.00005	0.00005	0.00005	0.00005	0.00005	0.00005	0.00005	0.00005	
# Part/Vile	114591.4814	154439.6680	143336.2274	99076.4725	97372.4545	117646.7906	115152.8634	83044.7933	83044.7933	98147.4597	
SA grains (cm2)	410.0622	552.6578	512.9244	354.5422	348.4444	420.9956	412.0711	297.1733	297.1733	351.2178	
SA/gram (cm2/g)	68.4304	68.1696	67.1798	67.6982	68.9007	68.7609	68.4458	68.3597	68.3597	67.9588	68.22636
#Part/gram	19122.8025	19049.9276	18773.3268	18918.1937	19254.2226	19215.1685	19127.1117	19103.0533	19103.0533	18991.0141	19065.79
	STATISTICAL DATA										
Avg. Rho. (g/cc)	2.605835604733	2.605835604733	2.605835604733	2.605835604733	2.605835604733	2.605835604733	2.605835604733	2.605835604733	2.605835604733	2.60583560473	
Std Dev. Rho	0.018475226028	0.018475226028	0.018475226028	0.018475226028	0.018475226028	0.018475226028	0.018475226028	0.018475226028	0.018475226028	0.01847522603	
Var. Rho.	0.000341333977	0.000341333977	0.000341333977	0.000341333977	0.000341333977	0.000341333977	0.000341333977	0.000341333977	0.000341333977	0.00034133398	

120992_1

TABLE L.4

SAND RETAINED ON SIEVE #140

Test #	1	2	3	4	5	6	7	8	9	10	
Sieve #	140	140	140	140	140	140	140	140	140	140	
Sieve Size (mm)	0.1060	0.1060	0.1060	0.1060	0.1060	0.1060	0.1060	0.1060	0.1060	0.1060	
Wt. Vile (g)	39.5673	39.8452	31.5709	32.9063	9.5532	9.7165	9.6578	9.8172	9.8402	37.2350	
Wt. sand (g)	5.1276	4.6964	6.8312	5.2616	7.0167	5.9412	4.8238	5.2930	6.3350	5.3323	
Wt. liquid (g)	8.0163	8.1846	7.3960	7.9961	7.2951	7.7163	8.1391	7.9465	7.5590	7.9679	
Total WT. (g)	52.7112	52.7262	45.7981	46.1640	23.8650	23.3740	22.6207	23.0567	23.7342	50.5352	
Total Vol (ml)	10.0000	10.0000	10.0000	10.0000	10.0000	10.0000	10.0000	10.0000	10.0000	10.0000	AVG
Rho (g/cc)	2.5849	2.5870	2.6233	2.6257	2.5941	2.6016	2.5922	2.5776	2.5952	2.6240	2.600553
Melvern Part. Dia(mm)	0.1220	0.1220	0.1220	0.1220	0.1220	0.1220	0.1220	0.1220	0.1220	0.1220	
Part. Rad. (cm)	0.0061	0.0061	0.0061	0.0061	0.0061	0.0061	0.0061	0.0061	0.0061	0.0061	
Grain SA (cm2)	0.0005	0.0005	0.0005	0.0005	0.0005	0.0005	0.0005	0.0005	0.0005	0.0005	
Grain Vol. (cc)	0.0000010	0.0000010	0.0000010	0.0000010	0.0000010	0.0000010	0.0000010	0.0000010	0.0000010	0.0000010	
Grain Wt. (g)	0.0000025	0.0000025	0.0000025	0.0000025	0.0000025	0.0000025	0.0000025	0.0000025	0.0000025	0.0000025	
# Part/Vile	2086401.4650	1909388.1229	2738816.0582	2107647.2731	2844939.9216	2401933.2689	1957243.7799	2159815.1980	2567377.1114	2137307.2627	
SA grains (cm2)	975.5902	892.8197	1280.6557	985.5246	1330.2787	1123.1311	915.1967	1009.9180	1200.4918	999.3934	
SA/gram (cm2/g)	190.2625	190.1072	187.4716	187.3051	189.5875	189.0411	189.7253	190.8026	189.5015	187.4226	189.1227
#Part/gram	406896.2994	406564.2030	400927.5176	400571.5511	405452.6945	404284.1966	405747.2905	408051.2371	405268.6837	400822.7712	404458.6
	STATISTICAL DATA										
Avg. Rho. (g/cc)	2.600553021018	2.600553021018	2.600553021018	2.600553021018	2.600553021018	2.600553021018	2.600553021018	2.600553021018	2.600553021018	2.600553021018	
Std Dev. Rho	0.016742248673	0.016742248673	0.016742248673	0.016742248673	0.016742248673	0.016742248673	0.016742248673	0.016742248673	0.016742248673	0.016742248673	
Var. Rho.	0.000280302891	0.000280302891	0.000280302891	0.000280302891	0.000280302891	0.000280302891	0.000280302891	0.000280302891	0.000280302891	0.000280302891	

120992_1

TABLE L.5

SAND RETAINED ON SIEVE #200

Test #	1	2	3	4	5	6	7	8	9	10	
Sieve #	#200	#200	#200	#200	#200	#200	#200	#200	#200	#200	
Sieve Size (mm)	0.0750	0.0750	0.0750	0.0750	0.0750	0.0750	0.0750	0.0750	0.0750	0.0750	
Wt. Vile (g)	39.5658	39.8444	31.5683	32.9060	9.5534	9.7175	9.6579	9.8175	9.8380	37.2369	
Wt. sand (g)	7.1058	4.9152	5.9714	4.8035	5.1008	5.1255	6.2861	4.4541	4.1462	4.6087	
Wt. liquid (g)	7.2616	8.0929	7.7073	8.1684	8.0181	8.0323	7.5953	8.2618	8.3837	8.2488	
Total WT. (g)	53.9332	52.8525	45.2470	45.8779	22.6723	22.8753	23.5393	22.5334	22.3679	50.0944	
Total Vol (ml)	10.0000	10.0000	10.0000	10.0000	10.0000	10.0000	10.0000	10.0000	10.0000	10.0000	AVG
Rho (g/cc)	2.5949	2.5773	2.6045	2.6226	2.5737	2.6048	2.6141	2.5625	2.5652	2.6317	2.595134
Melvern Part. Dia(mm)	0.1050	0.1050	0.1050	0.1050	0.1050	0.1050	0.1050	0.1050	0.1050	0.1050	
Part. Rad. (cm)	0.0053	0.0053	0.0053	0.0053	0.0053	0.0053	0.0053	0.0053	0.0053	0.0053	
Grain SA (cm2)	0.0003	0.0003	0.0003	0.0003	0.0003	0.0003	0.0003	0.0003	0.0003	0.0003	
Grain Vol. (cc)	0.0000006	0.0000006	0.0000006	0.0000006	0.0000006	0.0000006	0.0000006	0.0000006	0.0000006	0.0000006	
Grain Wt. (g)	0.0000016	0.0000016	0.0000016	0.0000016	0.0000016	0.0000016	0.0000016	0.0000016	0.0000016	0.0000016	
# Part/Vile	4517835.0104	3146349.3823	3782515.4574	3021788.8567	3269755.0421	3246327.7644	3967293.9854	2867696.7628	2666585.1327	2889144.2705	
SA grains (cm2)	1564.8000	1089.7714	1310.1143	1046.6286	1132.5143	1124.4000	1374.1143	993.2571	923.6000	1000.6857	
SA/gram (cm2/g)	220.2145	221.7146	219.3982	217.8887	222.0268	219.3737	218.5957	222.9984	222.7582	217.1297	220.2098
#Part/gram	635795.4080	640126.4205	633438.6337	629080.6405	641027.8862	633368.0157	631121.6788	643833.0443	643139.5332	626889.2031	635782
	STATISTICAL DATA										
Avg. Rho. (g/cc)	2.595134416474	2.595134416474	2.595134416474	2.595134416474	2.595134416474	2.595134416474	2.595134416474	2.595134416474	2.595134416474	2.59513441647	
Std Dev. Rho	0.023175800442	0.023175800442	0.023175800442	0.023175800442	0.023175800442	0.023175800442	0.023175800442	0.023175800442	0.023175800442	0.02317580044	
Var. Rho.	0.000537117726	0.000537117726	0.000537117726	0.000537117726	0.000537117726	0.000537117726	0.000537117726	0.000537117726	0.000537117726	0.00053711773	

120992_1

TABLE L.6

SAND RETAINED ON SIEVE #270

Test #	1	2	3	4	5	6	7	8	9	10	
Sieve #	#270	#270	#270	#270	#270	#270	#270	#270	#270	#270	
Sieve Size (mm)	0.0530	0.0530	0.0530	0.0530	0.0530	0.0530	0.0530	0.0530	0.0530	0.0530	
Wt. Vile (g)	39.5703	39.8460	31.5695	32.9062	9.5542	9.7167	9.6582	9.8176	9.8381	37.2368	
Wt. sand (g)	6.6950	5.1534	5.4042	5.1072	5.0039	5.3919	4.3265	4.7846	5.2061	3.6644	
Wt. liquid (g)	7.4410	8.0298	7.9433	8.0708	8.0708	7.9370	8.3386	8.1767	8.0069	8.6227	
Total WT. (g)	53.7063	53.0292	44.9170	46.0842	22.6289	23.0456	22.3233	22.7789	23.0511	49.5239	
Total Vol (ml)	10.0000	10.0000	10.0000	10.0000	10.0000	10.0000	10.0000	10.0000	10.0000	10.0000	AVG
Rho (g/cc)	2.6163	2.6157	2.6276	2.6473	2.5938	2.6136	2.6041	2.6241	2.6121	2.6606	2.621514
Melvern Part. Dia(mm)	0.0730	0.0730	0.0730	0.0730	0.0730	0.0730	0.0730	0.0730	0.0730	0.0730	
Part. Rad. (cm)	0.0037	0.0037	0.0037	0.0037	0.0037	0.0037	0.0037	0.0037	0.0037	0.0037	
Grain SA (cm2)	0.0002	0.0002	0.0002	0.0002	0.0002	0.0002	0.0002	0.0002	0.0002	0.0002	
Grain Vol. (cc)	0.0000002	0.0000002	0.0000002	0.0000002	0.0000002	0.0000002	0.0000002	0.0000002	0.0000002	0.0000002	
Grain Wt. (g)	0.0000005	0.0000005	0.0000005	0.0000005	0.0000005	0.0000005	0.0000005	0.0000005	0.0000005	0.0000005	
# Part/Vile	12563281.2768	9672597.4098	10097264.7917	9471309.9802	9471309.9802	10128194.3236	8156559.4034	8951399.2779	9785023.8034	6761784.7998	
SA grains (cm2)	2103.2877	1619.3425	1690.4384	1585.6438	1585.6438	1695.6164	1365.5342	1498.6027	1638.1644	1132.0274	
SA/gram (cm2/g)	314.1580	314.2280	312.8009	310.4722	316.8816	314.4748	315.6210	313.2138	314.6625	308.9257	313.5438
#Part/gram	1876516.9943	1876935.1127	1868410.6420	1854501.4842	1892785.6232	1878409.1551	1885255.8427	1870877.2474	1879530.5129	1845263.8358	1872849
	STATISTICAL DATA										
Avg. Rho. (g/cc)	2.621514402088	2.621514402088	2.621514402088	2.621514402088	2.621514402088	2.621514402088	2.621514402088	2.621514402088	2.621514402088	2.62151440209	
Std Dev. Rho	0.018762532488	0.018762532488	0.018762532488	0.018762532488	0.018762532488	0.018762532488	0.018762532488	0.018762532488	0.018762532488	0.01876253249	
Var. Rho.	0.000352032625	0.000352032625	0.000352032625	0.000352032625	0.000352032625	0.000352032625	0.000352032625	0.000352032625	0.000352032625	0.00035203263	

120992_1

TABEL L.7

SAND PASSING SIEVE #270 AND RETAINED IN PAN

Test #	1	2	3	4	5	6	7	8	9	10	
Sieve #	<270	<270	<270	<270	<270	<270	<270	<270	<270	<270	
Sieve Size (mm)	pan	pan	pan	pan	pan	pan	pan	pan	pan	pan	
Wt. Vile (g)	39.5698	39.8462	31.5703	32.9056	9.5543	9.7169	9.6551	9.8181	9.8386	37.2373	
Wt. sand (g)	4.2273	5.3408	6.4792	5.7664	5.6602	6.5254	3.5214	5.2405	4.0645	4.1319	
Wt. liquid (g)	8.3573	7.9315	7.4700	7.7837	7.8087	7.4929	8.6311	7.9685	8.4152	8.4327	
Total WT. (g)	52.1544	53.1185	45.5195	46.4557	23.0232	23.7352	21.8076	23.0271	22.3183	49.8019	
Total Vol (ml)	10.0000	10.0000	10.0000	10.0000	10.0000	10.0000	10.0000	10.0000	10.0000	10.0000	AVG
Rho (g/cc)	2.5734	2.5820	2.5609	2.6018	2.5830	2.6028	2.5724	2.5796	2.5647	2.6363	2.585696
Melvern Part. Dia(mm)	0.0450	0.0450	0.0450	0.0450	0.0450	0.0450	0.0450	0.0450	0.0450	0.0450	
Part. Rad. (cm)	0.0023	0.0023	0.0023	0.0023	0.0023	0.0023	0.0023	0.0023	0.0023	0.0023	
Grain SA (cm2)	0.0001	0.0001	0.0001	0.0001	0.0001	0.0001	0.0001	0.0001	0.0001	0.0001	
Grain Vol. (cc)	0.00000005	0.00000005	0.00000005	0.00000005	0.00000005	0.00000005	0.00000005	0.00000005	0.00000005	0.00000005	
Grain Wt. (g)	0.00000012	0.00000012	0.00000012	0.00000012	0.00000012	0.00000012	0.00000012	0.00000012	0.00000012	0.00000013	
# Part/Vile	34428816.4632	43353020.5479	53025449.3528	46450712.8065	45926745.9157	52545495.6807	28690331.0747	42577549.5495	33215309.1440	32848532.3204	
SA grains (cm2)	2190.2667	2758.0000	3373.3333	2955.0667	2921.7333	3342.8000	1825.2000	2708.6667	2113.0667	2089.7333	
SA/gram (cm2/g)	518.1243	516.4020	520.6404	512.4630	516.1891	512.2751	518.3166	516.8718	519.8835	505.7560	515.6922
#Part/gram	8144398.6618	8117327.0948	8183950.0791	8055409.4073	8113979.3498	8052455.8925	8147421.7853	8124711.2965	8172052.9325	7949982.4101	8106169
	STATISTICAL DATA										
Avg. Rho. (g/cc)	2.585696193412	2.585696193412	2.585696193412	2.585696193412	2.585696193412	2.585696193412	2.585696193412	2.585696193412	2.585696193412	2.585696193412	
Std Dev. Rho	0.021338731115	0.021338731115	0.021338731115	0.021338731115	0.021338731115	0.021338731115	0.021338731115	0.021338731115	0.021338731115	0.021338731115	
Var. Rho.	0.000455341446	0.000455341446	0.000455341446	0.000455341446	0.000455341446	0.000455341446	0.000455341446	0.000455341446	0.000455341446	0.000455341446	

120992_1

APPENDIX M

IMMUNOASSAY DEVELOPMENT

Immunoassays

Theory and Current Applications

Immunoassays often are used in the pharmaceutical industry to identify toxins in humans and are used in the agricultural industry to identify pesticides in soils. The success and acceptability achieved by immunoassay analysis of soil bound pesticides in the agrochemical industry can be attributed to many factors. Cheung *et al.*, (1988) point out many of these factors which apply to immunoassays performed on extract solutions. Speed of analysis, ease of automation, specificity, sensitivity, and cost effectiveness are all advantages attributable to an immunoassay when compared to traditional analytical methods. These same advantages can be expected to apply to solid phase PAH specific FIA's.

Immunoassays promise the ability to identify polycyclic aromatic hydrocarbons (PAH) in groundwaters as well as on soil surfaces. Fluoroimmunoassays are special adaptations which utilizes the phenomenon of fluorescence as an identifying (and quantifiable) label.

A detailed account describing the development of a fluoroimmunoassay involves the science of biochemistry which is beyond the scope of this paper. However, a brief explanation of the process is required to understand the necessity of studying properties of fluorescent chemicals in soils.

Antibody Production

The production of antibodies designed to attach to a soil bound PAH, such as naphthalene, involves several steps, as illustrated in Figure M.1. Immunoassays require the mass production of antibodies, usually by mice, which attach with specificity to an invading foreign body (PAH) within the mouse. Injected foreign chemicals need to be of a sufficient size for the mouse's immune system to produce antibodies. Therefore, in the production of antibodies for a PAH-specific immunoassay, the PAH must be coupled to a high molecular weight protein called Bovine Serum Albumin (BSA) to create an immune system response. This allows the immune system of the mouse to recognize the PAH/BSA conjugate as a foreign body. The mouse subsequently produces antibodies specific for the PAH/BSA conjugate. Antibodies also are produced specific to the PAH because of its attachment to the larger BSA protein molecule.

The mouse receives booster injections of the PAH/BSA conjugate 7,21,42 and 49 days after the initial injection. Then the mouse is bled and the red blood cells removed. Antibodies in the remaining serum can be used directly for an immunoassay but are limited in quantity. This method of antibody production requires an abundant supply of mice to manufacture large quantities of antibodies.

This method stimulates the mouse to produce many different antibodies to a specific antigen. The term "polyclonal" is used to describe the host of antibodies which are produced. Polyclonal antibodies obtained from this serum recognize a variety of antigenic determinants with varying degrees of specificity and affinity. Polyclonal production of antibodies has several disadvantages. The major disadvantage is that the animal producing the antibodies eventually dies thus terminating the source of PAH specific antibodies.

Further screening and testing for specificity are performed to identify a monoclonal antibody from the polyclonal antibody population. "Monoclonal" antibodies, once isolated, are cloned into an endless supply. Monoclonal antibodies with specificity for one antigen (PAH) are produced by fusing spleen cells from an immunized mouse with myloma cells to produce hybrid cells (hybridomas) capable of producing antibodies. Single cells are screened for the desired affinity toward a specific antigen. From this single, very specific hybridoma cell, many are cloned. In this manner, highly specific antibodies are reproduced continuously without depending upon an individual mouse to sustain the production of antibodies. These cells are cultured continuously into a virtually endless supply of very specific antibodies.

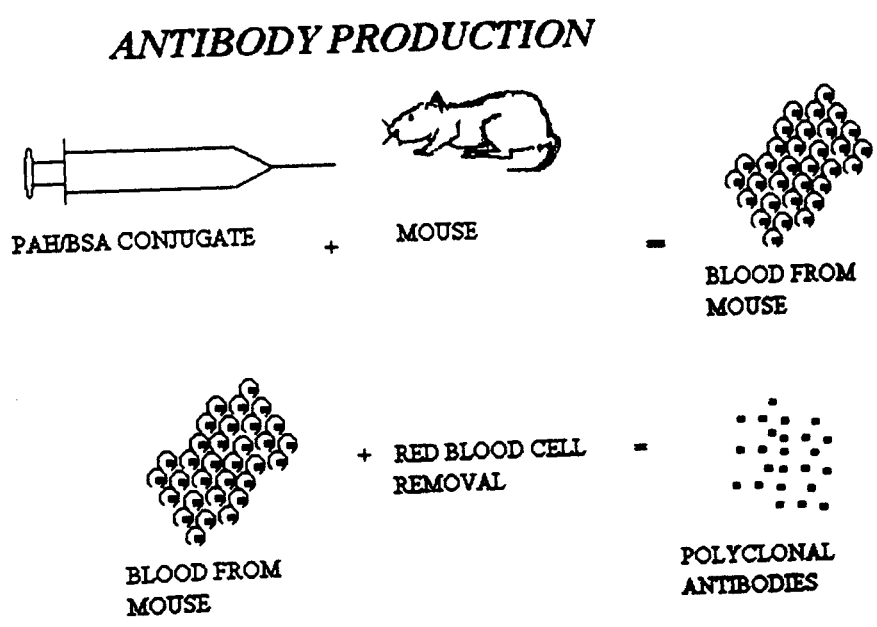

Figure M.1 Polyclonal Antibody Production Procedure in Mice

Different Types of Immunoassays

The most common immunoassay techniques outlined by Hall *et al.* (1990) include direct and indirect enzyme-linked immunosorbent assays (ELISA) as well as radioimmunoassays (RIA). Each of these techniques involves the principle of competitive inhibition as a method to determine herbicide concentrations in plant extracts.

An indirect ELISA involves exposing the extract solution to a 96-well chemically-prepared microtiter plate. Each well is washed several times and a chromogenic chemical is added. The resultant color intensity is measured quantitatively using a spectrophotometer. This type of test is based upon competitive inhibition and produces color intensities which are inversely proportional to the concentration of the free contaminant. A direct ELISA follows the same general protocol but is simpler and more rapid. The intensity of the color reaction also is inversely proportional to the concentration of the contaminant. The concepts of competitive inhibition and of color intensities which are inversely proportional to concentrations could create confusion in the hands of an inexperienced operator. RIA's require an even simpler procedure but necessitate a license to handle radioisotopes and therefore are not likely field techniques. The PAH-specific monoclonal fluoroimmunoassay (FIA) proposed by Amoco, in contrast with ELISA or RIA, has the potential to eliminate the solute extraction step, as well as, to provide a direct correlation between intensity responses and soil concentrations.

Schwalbe *et al.* (1984) found that, in comparison to the more widely used ELISA, an FIA for the herbicide Diclofop-methyl was equally effective in estimating plant extract concentrations. Detection limits of 45 ng/ml were reliable and were consistent with the more traditional GC analysis of the same extract solutions. The FIA characteristics for solution phases analysis hopefully will transfer to solids surface analysis. A limiting factor in solids analysis is the detectability of the fluorescent label from within the soil.

Fluorescent Label

One way to ensure optimum FIA detectability in soil matrices is to choose carefully the fluorescent label that will be covalently bonded to the antibody. A critical step in the development of a FIA is choosing a fluorescent label which posseses optimum fluorescent characteristics after exposure to common soil environments. For example, quenching of the fluorescent label by soil organic matter would not be an acceptable label response.

The fluorescent label is the key indicator system for the FIA technique. The label, as illustrated in Figure M.2, allows the antibody (once attached to the target analyte) to be located and quantified within a soil matrix. The label,

serving as a beacon, must posses the right combination of a high quantum yield and a large Stokes shift. A sufficient number of photons must be released at the right wavelength to overcome interferences from Raman or Rayleigh light scattering. The label should have a low affinity for soils once bonded to the antibody keeping background FIA adsorption to a minimum.

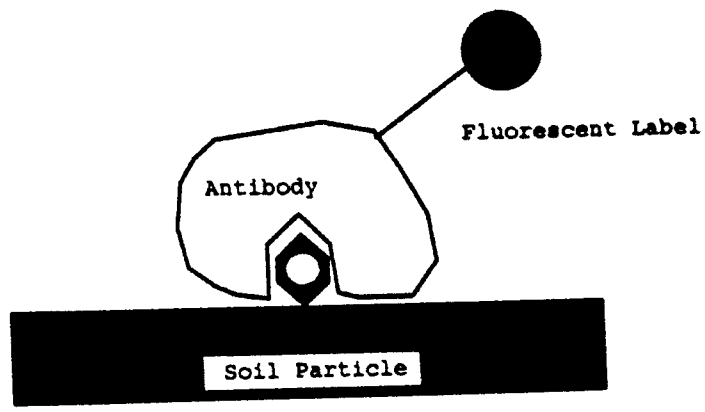

Figure M.2 PAH-Specific Fluoroimmunoassay with Covalently Attached Fluorescent Label

VITA

Kent P. Kolodziej

Candidate for the Degree of

Master of Science

Thesis: INVESTIGATION BY SOLID-PHASE FLUOROMETRY OF RHODAMINE B ADSORPTION ONTO SOIL SURFACES

Major Field: Civil Engineering

Biographical:

Personal Data: Born in Gary, Indiana, May 8, 1957, the son of Peter F. and Betty J. Kolodziej.

Education: Graduated from Crown Point Senior High School, Crown Point, Indiana, in June 1975; received Bachelor of Science degree in Civil Engineering from Purdue University in May, 1980; completed requirements for the Master of Science degree at Oklahoma State University in December, 1994.

Professional Experience: Engineer, Gearhart Industries, August 1980, to March, 1987.